

Fibre Fractionation in Hydrocyclones

by

Tazim Rehmat

B.A.Sc., University of British Columbia, 1992.

**A THESIS SUBMITTED IN PARTIAL FULFILLMENT OF THE
REQUIREMENTS FOR THE DEGREE OF MASTER OF APPLIED SCIENCE**

in

**THE FACULTY OF GRADUATE STUDIES
Department of Chemical and Biological Engineering**

**We accept this thesis as conforming
to the required standard**

**THE UNIVERSITY OF BRITISH COLUMBIA
January, 2001**

© Tazim Rehmat, 2001

In presenting this thesis in partial fulfillment of the requirements for an advanced degree at the University of British Columbia, I agree that the Library shall make it freely available for reference and study. I further agree that permission for extensive copying of this thesis for scholarly purposes may be granted by the head of my department or by his or her representatives. It is understood that copying or publication of this thesis for financial gain shall not be allowed without my written permission.

Department of Chemical Engineering
The University of British Columbia
2216 Main Mall
Vancouver, B.C. V6T 1Z4

January, 2001

Abstract

Literature on fibre fractionation in hydrocyclones is reviewed.

A force balance on an idealized particle moving in an idealized centrifugal field is used to show that the radial velocity of a fibre or other type of particle moving inside a hydrocyclone is slower for particles having higher values of specific surface. Thus, in theory, the rejects stream is more likely to contain material having lower specific surface than the feed and the accepts stream is more likely to contain material having higher specific surface material. It is also shown that fibre coarseness is inversely related to specific surface.

Fractionation of various pulps are described showing evidence of fractionation by length and coarseness. Sheet property measurements, showing that sheets made from hydrocyclone accepts are always stronger than those made from hydrocyclone rejects, are also presented.

Multistage fractionation of mechanical and chemical pulps has been investigated to show the degree of separation achievable. This was quantified by the measurement of fibre (length, coarseness, microscopy, width, shape factor) and paper (tensile, tear, burst, roughness) properties. For tests performed with mechanical pulp, it was shown that the hydrocyclone tested in these experiments resulted in rejects fibres which were coarser and shorter than fibres reporting to the accepts. In these tests fibre fines reported to the rejects. A different hydrocyclone was tested to fractionate chemical pulp. In these tests it was found that fibre fines and earlywood fibres reported to the accepts and latewood fibres reported to the rejects.

Refining of fractionated chemical pulp was performed. These tests illustrated that earlywood fibres develop at lower refining intensity than latewood fibres. It was also demonstrated that latewood fibres could be upgraded to usable fibre through refining.

Table of Contents

	Page Number
Abstract	ii
List of Tables	v
List of Figures	vi
Nomenclature	xv
Acknowledgments	xvi
1 Introduction	1
1.1 Thesis Objectives	3
1.2 Organization of Thesis	3
2 Literature Review	4
2.1 Overview	4
2.2 Studies of Fractionation in Hydrocyclones to Date	4
2.3 Summary	45
3 Materials and Methods	46
3.1 Overview	46
3.2 Hydrocyclones	46
3.3 Pulps Tested	47
3.4 Hydrocyclone Test Facility	48
3.4.1 UBC Pulp and Paper Centre Hydrocyclone Test Facility	48
3.4.2 STFI Hydrocyclone Test Facility	50
3.5 Fibre Analysis	51
3.6 Pulp and Sheet Strength Characterization	54
3.7 Photomicrographs	56
3.8 Refiner	56
4 Theoretical Analysis	57
5 Results and Discussion	72
5.1 Overview	72
5.2 Fractionation of TMP	72
5.2.1 Fractionating TMP_A in Hydrocyclone A	72
5.2.2 Fractionating TMP_A in Hydrocyclone B	77
5.3 Fractionation of Other Pulp Types with Hydrocyclone A	81
5.3.1 Fractionation of CTMP_A and CTMP_B	86
5.3.2 Fractionation of Recycled Fibre	95
5.3.3 Fractionation of CTMP from a Latency Chest	100
5.4 Varying Reject Ratio of Hydrocyclone A	101
5.4.2 Reject Ratio Variations when Fractionating CTMP_B	101
5.4.2 Reject Ratio Variations for Fractionation of BCTMP	105
5.5 Consistency Effects on Fractionation	114
5.6 Multistage Fractionation	116
5.6.1 Multistage Fractionation of CTMP_A With Hydrocyclone A	116

5.6.2	Multistage Fractionation of TMP_B With Hydrocyclone A with Varying Reject Ratios	119
5.6.3	Multistage Fractionation of Chemical Softwood and Refining of Accepts and Rejects	125
5.6.3.1	Preliminary Experiments Testing Operation of Hydrocyclone C	125
5.6.3.2	Three Stage Fractionation of Hydrocyclone Accepts and Rejects	140
5.6.3.3	Refining of Initial Feed and Fractionated Accepts (AA3) and Rejects (RR3)	160
6	Conclusions	195
6.1	Objectives	195
6.2	Literature Review and Theoretical Analysis	195
6.3	Experimental Studies on Fractionation	196
6.4	Multistage Fractionation Experiments	198
6.5	Refining of Accepts and Rejects Fibres	199
6.6	Suggestions for Further Research	199
	References	201

List of Tables

	Page Number
Table 1 Paavilainen's Hydrocyclone Fibre Fractionations	32
Table 2 Demuner's Hydrocyclone Fibre Fractionations	38
Table 3 Kure et. al.'s Hydrocyclone Fibre Fractionation Data for Newsprint Pulp	40
Table 4 Kure et. al.'s Hydrocyclone Fibre Fractionation Data for a Super Calender Magazine Pulp	41
Table 5 Pulp Specifications	48
Table 6 CPPA Standard Methods	54
Table 7 SCAN-Test Standard Testing Procedures	55
Table 8 Whole Pulp Characterization of Feed, Accepts and Rejects for CTMP_B Fractionation Experiment (Hydrocyclone A Tested with Pulp Consistency 1%)	91
Table 9 Pulp and Paper Properties for TMP_B 6 Stage Fractionation (Hydrocyclone A Tested with Underflow Diameters of 3 and 5 mm)	123
Table 10 Operating Conditions and Performance Parameters for Three Stage Accepts Fractionation	144
Table 11 Average Length Weighted Length, Width, and Shape Factor Measurements for Streams Resulting from Three Stage Accepts Fractionation	144
Table 12 Operating Conditions and Performance Parameters for Three Stage Rejects Fractionation	150
Table 13 Average Length Weighted Length, Width, and Shape Factor Measurements for Streams Resulting from Three Stage Rejects Fractionation	150
Table 14 Pulp and Fibre Characteristics for Feed, Accepts, and Rejects	156
Table 15 Paper Properties for Feed, Accepts, and Rejects for Three Stage Fractionation Experiment	156
Table 16 Earlywood and Latewood Fibre Content for Initial Feed, AA3, and RR3	159
Table 17 Average Length Weighted Fibre Lengths of Initial Feed, Accepts, and Rejects from Refining Trials	162
Table 18 Average Length Weighted Fibre Widths of Initial Feed, Accepts, and Rejects from Refining Trials	162
Table 19 Average Length Weighted Fibre Shape Factors of Initial Feed, Accepts, and Rejects from Refining Trials	163
Table 20 Average Length, Width and Shape Factor Measurements of Feed, Accepts, Fines Removed Accepts and 70:30 Mixture of Accepts and Rejects. Samples Refined at SEL of 2 Ws/m	181

List of Figures

	Page Number
Figure 1 Bauer McNett Fractions for Deinked Ledger Stock for Feed, Accepts and Rejects	22
Figure 2 Bauer McNett Fractions for Recycled Corrugated Boxes for Feed and Rejects	22
Figure 3 Data of Kure et al for Newsprint Pulp	42
Figure 4 Data of Kure et al for SC-A Magazine Pulp	42
Figure 5 UBC Fractionation Flow Loop	49
Figure 6 Photograph of UBC Test Facility and Sampling Procedure	50
Figure 7 STFI Fractionation Flow Loop	50
Figure 8 Experimental Method and Sampling Procedure	51
Figure 9 Different Average Fibre Length Measures vs. Feed Flowrate. Hydrocyclone A tested with TMP Pulp Having a Consistency of 0.75%	53
Figure 10 Vortex Flow Pattern Inside a Hydrocyclone	58
Figure 11 Axial and Radial Flow Patterns Inside a Hydrocyclone	58
Figure 12 Idealized Spherical Model Representing Pulp Fines	61
Figure 13 Straight Circular Cylinder Model Representing a Pulp Fibre	65
Figure 14 Fibre Coarseness vs. Specific Surface for Wheat Straw and Aspen Pulps	71
Figure 15 Pressure Drop versus Feed Flowrate for TMP_A Fractionated in Hydrocyclone A (Pulp Consistency Tested: 0.65%)	75
Figure 16 Reject Ratio versus Feed Flowrate Relationship for Fractionation of TMP_A in Hydrocyclone A	75
Figure 17 Thickening Ratio versus Feed Flowrate (TMP_A Fractionated in Hydrocyclone A at Consistency of 0.65%)	76
Figure 18 Mass Fraction Fibres Rejected Fractionating TMP_A in Hydrocyclone A	76
Figure 19 Fibre Length Results for TMP_A Fractionation in Hydrocyclone A	79
Figure 20 Fibre Coarseness Measurements for Fractionation of TMP_A in Hydrocyclone A	79
Figure 21 Burst Index Values for Accepts and Rejects for Fractionation of TMP_A in Hydrocyclone A	80
Figure 22 Tear Index Values for Accepts and Rejects for Fractionation of TMP_A in Hydrocyclone A	80

Figure 23	Pressure Drop versus Feed Flowrate for TMP_A Fractionated in Hydrocyclone B (Pulp Consistency Tested: 0.60%)	82
Figure 24	Reject Ratio versus Feed Flowrate Relationship for Fractionation of TMP_A in Hydrocyclone B	82
Figure 25	Thickening Ratio versus Feed Flowrate (TMP_A Fractionated in Hydrocyclone B at Consistency of 0.60%)	83
Figure 26	Mass Fraction Fibres Rejected Fractionating TMP_A in Hydrocyclone B	83
Figure 27	Fibre Length Results for TMP_A Fractionation in Hydrocyclone B	84
Figure 28	Fibre Coarseness Measurements for Fractionation of TMP_A in Hydrocyclone B	84
Figure 29	Burst Index Values for Fractionation of TMP_A in Hydrocyclone B	85
Figure 30	Figure 30 Tear Index Results for TMP_A Fractionation in Hydrocyclone B	85
Figure 31	Arithmetic Average Length Values for Accepts and Rejects Stream for CTMP_A (Pulp Consistency: 0.65%)	87
Figure 32	Fibre Coarseness Measurements for CTMP_A Fractionation	87
Figure 33	Burst Index Values for CTMP_A Fractionation Having a Consistency of 0.65%	89
Figure 34	Arithmetic Average Fibre Length Measurements for CTMP_A Fractionation (Pulp Consistency: 0.68%)	89
Figure 35	Accepts and Rejects Freeness Values for CTMP_B Fractionation (Pulp Consistency: 0.68%)	90
Figure 36	Feed Flowrate versus Pressure Drop for CTMP_B Fractionation (Pulp Consistency 1%)	92
Figure 37	Feed, Accepts, and Rejects Fibre Length Measurements for Various Flowrates (CTMP_B Fractionation at Consistency of 1%)	93
Figure 38	Feed, Accepts, and Rejects Freeness Measurements for Various Flowrates (CTMP_B Fractionation at Consistency of 1%)	93
Figure 39	Weighted Percent Fibre Retained in Bauer McNett Classifier (CTMP_B Fractionated at Flowrate of 47 kg/min. and Consistency of 1%)	94
Figure 40	Length Weighted Average Fibre Distribution Feed, Accepts, and Rejects or CTMP_B Fractionated at 1% Consistency and Flowrate of 47 kg/min.	94
Figure 41	Coarseness Distribution Obtained from Bauer McNett Fractions (CTMP_B Fractionated at Flowrate of 47 kg/min. and Consistency of 1%)	95

Figure 42	Pressure Drop versus Feed Flowrate Relationship for Hydrocyclone A Fractionating Recycled Pulp Having a Consistency of 1%	97
Figure 43	Fibre Length Measurements for Recycled Pulp Fractionation	97
Figure 44	Burst Index Values for Feed, Accepts, and Rejects for Recycled Fibre Fractionation Study	98
Figure 45	Tear Index Values for Feed, Accepts, and Rejects for Recycled Fibre Fractionation	98
Figure 46	Photomicrographs of Feed, Accepts, and Rejects for Recycled Fibre Fractionation Study. Samples Collected at a Feed Flowrate of 49 kg/min. In the photomicrographs above chemical fibres are stained yellow, mechanical fibres are stained dark green to blue green, and sulphite pulps are stained a yellowish green	99
Figure 47	Arithmetic Average Fibre Lengths for CTMP_C Fractionation (Pulp Obtained from Latency Chest having Consistency of 0.6%)	102
Figure 48	Fibre Coarseness Measurements for Latency Chest CTMP_C Fractionation	102
Figure 49	Burst Index Values for Feed, Accepts, and Rejects from Latency Chest CTMP_C Fractionation	103
Figure 50	Tear Index Values for Samples Collected at Various Flowrates from Fractionating CTMP_C at 0.6%	103
Figure 51	Drainage Index of Feed, Accepts, and Rejects from CTMP_C Fractionation Study	104
Figure 52	Reject Ratio Values for Operation of Hydrocyclone A with Underflow Sizes of 3, 5, and 6 mm (Experiment Testing CTMP_B with 0.7% Consistency)	106
Figure 53	Mass Fraction Fibres Rejected for Operation of Hydrocyclone A with Underflow Sizes of 3, 5, and 6 mm (Experiment Testing CTMP_B with 0.7% Consistency)	106
Figure 54	Length Weighted Av. Fibre Length of Accepts Stream for Experiment Varying Hydrocyclone Underflow Opening	107
Figure 55	Length Weighted Av. Fibre Length of Rejects Stream for Experiment Varying Hydrocyclone Underflow Opening	107
Figure 56	Freeness of Accepts Stream for Experiment Varying Hydrocyclone Underflow Opening	108
Figure 57	Rejects Freeness Measurements for Experiment Varying Underflow Opening of Hydrocyclone A	108
Figure 58	Figure 58 Reject Ratio Relationship for Fractionation of BCTMP in Hydrocyclone A Using Underflow Tip Sizes of 5 and 6 mm	109

Figure 59	Thickening Ratio for BCTMP Fractionation in Hydrocyclone A Having Underflow Tip Sizes of 5 and 6 mm	111
Figure 60	Mass Fraction Fibres Rejected for BCTMP Fractionation in Hydrocyclone A Having Underflow Tip Sizes of 5 and 6 mm	111
Figure 61	Length Weighted Fibre Measurements for Feed, Accepts, and Rejects for BCTMP Fractionation (Underflow Tip Size: 5 mm)	112
Figure 62	Length Weighted Fibre Measurements for Feed, Accepts, and Rejects for BCTMP Fractionation (Underflow Tip Size: 6 mm)	112
Figure 63	Freeness Measurements for Feed, Accepts, and Rejects for BCTMP Fractionation (Underflow Tip Size: 5 mm)	113
Figure 64	Freeness Measurements for Feed, Accepts, and Rejects for BCTMP Fractionation (Underflow Tip Size: 6 mm)	113
Figure 65	Length Weighted Fibre Lengths of Accepts for Fractionation at Varying Consistencies	115
Figure 66	Length Measurements of Feed, Accepts, and Rejects for 6 Stage Fractionation of CTMP_A (Pulp Consistency Tested: 0.8%)	117
Figure 67	Coarseness Measurements of Feed, Accepts, and Rejects for 6 Stage Fractionation of CTMP_A (Pulp Consistency Tested: 0.8%)	118
Figure 68	Burst Index Values of Feed, Accepts, and Rejects for 6 Stage Fractionation of CTMP_A (Pulp Consistency Tested: 0.8%)	118
Figure 69	Tear Index Values of Feed, Accepts, and Rejects for 6 Stage Fractionation of CTMP_A (Pulp Consistency Tested: 0.8%)	119
Figure 70	Photomicrographs of Accepts and Rejects from Stage 1 and TMP_B Fractionation Experiment	121
Figure 71	Photomicrographs of Accepts and Rejects from Stage 6 and TMP_B Fractionation Experiment	122
Figure 72	Bauer McNett Fibre Weight Distribution of Feed, Accepts 1 and 6, and Rejects for Underflow Opening of 3 mm	123
Figure 73	Bauer McNett Fibre Weight Distribution of Feed, Accepts 1 and 6, and Rejects for Underflow Opening of 5 mm	124
Figure 74	Feed Flowrate versus Pressure Drop for Hydrocyclone C	130
Figure 75	Volumetric Reject Ratio Relationship for Hydrocyclone C	130
Figure 76	Thickening Ratio versus Feed Flowrate for Hydrocyclone C	131

Figure 77	Mass Fraction of Fibre Rejected with Hydrocyclone C Operated at Various Flowrates	131
Figure 78	Length Distribution for Hydrocyclone C Operating at a Feed Flowrate of 150 kg/min. and Pressure Drop of 42 kPa	132
Figure 79	Fibre Width Distribution for Hydrocyclone C Operating at a Feed Flowrate of 150 kg/min. and Pressure Drop of 42 kPa	132
Figure 80	Shape Factor Distribution for Hydrocyclone C Operating at a Feed Flowrate of 150 kg/min. and Pressure Drop of 42 kPa	133
Figure 81	Length Distribution for Hydrocyclone C Operating at a Feed Flowrate of 200 kg/min. and Pressure Drop of 75 kPa	133
Figure 82	Fibre Width Distribution for Hydrocyclone C Operating at a Feed Flowrate of 200 kg/min. and Pressure Drop of 75 kPa	134
Figure 83	Shape Factor Distribution for Hydrocyclone C Operating at a Feed Flowrate of 200 kg/min. and Pressure Drop of 75 kPa	134
Figure 84	Length Distribution for Hydrocyclone C Operating at a Feed Flowrate of 270 kg/min. and Pressure Drop of 130.5 kPa	135
Figure 85	Fibre Width Distribution for Hydrocyclone C Operating at a Feed Flowrate of 270 kg/min. and Pressure Drop of 130.5 kPa	135
Figure 86	Shape Factor Distribution for Hydrocyclone C Operating at a Feed Flowrate of 270 kg/min. and Pressure Drop of 130.5 kPa	136
Figure 87	Length Distribution for Hydrocyclone C Operating at a Feed Flowrate of 400 kg/min. and Pressure Drop of 230 kPa	136
Figure 88	Fibre Width Distribution for Hydrocyclone C Operating at a Feed Flowrate of 400 kg/min. and Pressure Drop of 230 kPa	137
Figure 89	Shape Factor Distribution for Hydrocyclone C Operating at a Feed Flowrate of 400 kg/min. and Pressure Drop of 230 kPa	137
Figure 90	Freeness Measurements for Feed, Accepts and Rejects From Scandinavian Softwood Fractionation Using Hydrocyclone C	138
Figure 91	Length Weighted Average Fibre Length Measurements for Feed, Accepts and Rejects From Scandinavian Softwood Fractionation Using Hydrocyclone C	138

Figure 92	Average Fibre Width Measurements for Feed, Accepts and Rejects From Scandinavian Softwood Fractionation Using Hydrocyclone C	139
Figure 93	Average Fibre Shape Factor Measurements for Feed, Accepts and Rejects From Scandinavian Softwood Fractionation Using Hydrocyclone C	139
Figure 94	Three Stage Scheme for Fractionation of Accepts	143
Figure 95	Three Stage Scheme for Fractionation of Rejects	143
Figure 96	Length Distribution for Feed, Accepts and Rejects for 1 st Stage of Multistage Fractionation of Accepts	145
Figure 97	Length Distribution for Feed, Accepts and Rejects for 2 nd Stage of Multistage Fractionation of Accepts	145
Figure 98	Length Distribution for Feed, Accepts and Rejects for 3 rd Stage of Multistage Fractionation of Accepts	146
Figure 99	Width Distribution for Feed, Accepts and Rejects for 1 st Stage of Multistage Fractionation of Accepts	146
Figure 100	Width Distribution for Feed, Accepts and Rejects for 2 nd Stage of Multistage Fractionation of Accepts	147
Figure 101	Width Distribution for Feed, Accepts and Rejects for 3 rd Stage of Multistage Fractionation of Accepts	147
Figure 102	Length Distribution for Feed, Accepts and Rejects for 2 nd Stage of Multistage Fractionation of Rejects	151
Figure 103	Length Distribution for Feed, Accepts and Rejects for 3 rd Stage of Multistage Fractionation of Rejects	151
Figure 104	Width Distribution for Feed, Accepts and Rejects for 2 nd Stage of Multistage Fractionation of Rejects	152
Figure 105	Width Distribution for Feed, Accepts and Rejects for 3 rd Stage of Multistage Fractionation of Rejects	152
Figure 106	Multistage Fractionation Schemes and Photomicrographs of Initial Feed, AA3 and RR3	155
Figure 107	Length Distribution for Initial Feed, AA3 and RR3 from Three Stage Fractionation Study Using Hydrocyclone C	157
Figure 108	Width Distribution for Initial Feed, AA3 and RR3 from Three Stage Fractionation Study Using Hydrocyclone C	157
Figure 109	Shape Factor Distribution for Initial Feed, AA3 and RR3 from Three Stage Fractionation Study Using Hydrocyclone C	158
Figure 110	Earlywood and Latewood Fibre Characterization	158
Figure 111	Length Distribution of Initial Feed. Pulps Refined at SEL = 2.0 Ws/m and Energy Consumption of 50 and 100 kWh/ton	164
Figure 112	Length Distribution of AA3. Pulps Refined at SEL = 2.0 Ws/m and Energy Consumption of 50 and 100 kWh/ton	164
Figure 113	Length Distribution of RR3. Pulps Refined at SEL = 2.0 Ws/m and Energy Consumption of 50 and 100 kWh/ton	165
Figure 114	Length Distribution of Initial Feed. Pulps Refined at	165

	SEL = 3.5 Ws/m and Energy Consumption of 50 and 100 kWh/ton	
Figure 115	Length Distribution of AA3. Pulps Refined at SEL = 3.5 Ws/m and Energy Consumption of 50 and 100 kWh/ton	166
Figure 116	Length Distribution of RR3. Pulps Refined at SEL = 3.5 Ws/m and Energy Consumption of 50 and 100 kWh/ton	166
Figure 117	Width Distribution of Initial Feed. Pulps Refined at SEL = 2.0 Ws/m and Energy Consumption of 50 and 100 kWh/ton	167
Figure 118	Width Distribution of AA3. Pulps Refined at SEL = 2.0 Ws/m and Energy Consumption of 50 and 100 kWh/ton	167
Figure 119	Width Distribution of RR3. Pulps Refined at SEL = 2.0 Ws/m and Energy Consumption of 50 and 100 kWh/ton	168
Figure 120	Width Distribution of Initial Feed. Pulps Refined at SEL = 3.5 Ws/m and Energy Consumption of 50 and 100 kWh/ton	168
Figure 121	Width Distribution of AA3. Pulps Refined at SEL = 3.5 Ws/m and Energy Consumption of 50 and 100 kWh/ton	169
Figure 122	Width Distribution of RR3. Pulps Refined at SEL = 3.5 Ws/m and Energy Consumption of 50 and 100 kWh/ton	169
Figure 123	Freeness Values for Feed, and Fractionated Accepts and Rejects versus Refining Energy for SEL of 2 and 3.5 Ws/m	171
Figure 124	Tensile Index of Feed, and Fractionated Accepts and Rejects versus Refining Energy Measured for SEL's of 2 and 3.5 Ws/m	172
Figure 125	Light Scattering Coefficient Measurements of Feed, and Fractionated Accepts and Rejects versus Refining Energy for SEL's of 2 and 3.5 Ws/m	172
Figure 126	Sheet Density Structure Measurements of Feed, and Fractionated Accepts and Rejects versus Refining Energy for SEL's of 2 and 3.5 Ws/m	173
Figure 127	Tear Index Measurements of Feed, and Fractionated Accepts and Rejects versus Refining Energy for SEL's of 2 and 3.5 Ws/m	173
Figure 128	Burst Index Measurements of Feed, and Fractionated Accepts and Rejects versus Refining Energy for SEL's of 2 and 3.5 Ws/m	174
Figure 129	Sheet Roughness Measurements of Feed, and Fractionated Accepts and Rejects versus Refining Energy for SEL's of 2 and 3.5 Ws/m	174
Figure 130	Fines Content of Feed, and Fractionated Accepts and Rejects versus Refining Energy for SEL's of 2 and 3.5 Ws/m	175
Figure 131	Water Retention Value (WRV) of Feed, and Fractionated	175

	Accepts and Rejects versus Refining Energy for SEL's of 2 and 3.5 Ws/m	
Figure 132	Length Distribution of Accepts and 70:30 Mixture of Accepts and Rejects. Samples Refined at SEL of 2 Ws/m	179
Figure 133	Length Distribution of Fines Removed Accepts. Samples Refined at SEL of 2 Ws/m	179
Figure 134	Width Distribution of Accepts and 70:30 Mixture of Accepts and Rejects. Samples Refined at SEL of 2 Ws/m	180
Figure 135	Width Distribution of Fines Removed Accepts. Samples Refined at SEL of 2 Ws/m	180
Figure 136	Freeness Measurements of Feed, Accepts, Fines Removed Accepts and 70:30 Mixture of Accepts and Rejects. Samples Refined at SEL of 2 Ws/m	182
Figure 137	Tensile Strength of Feed, Accepts, Fines Removed Accepts and 70:30 Mixture of Accepts and Rejects. Samples Refined at SEL of 2 Ws/m	183
Figure 138	Light Scattering Measurements of Feed, Accepts, Fines Removed Accepts and 70:30 Mixture of Accepts and Rejects. Samples Refined at SEL of 2 Ws/m	183
Figure 139	Sheet Density of Handsheets Prepared from Feed, Accepts, Fines Removed Accepts and 70:30 Mixture of Accepts and Rejects. Samples Refined at SEL of 2 Ws/m	184
Figure 140	Tear Index Measurements of Feed, Accepts, Fines Removed Accepts and 70:30 Mixture of Accepts and Rejects. Samples Refined at SEL of 2 Ws/m	184
Figure 141	Burst Index Measurements of Feed, Accepts, Fines Removed Accepts and 70:30 Mixture of Accepts and Rejects. Samples Refined at SEL of 2 Ws/m	185
Figure 142	Sheet Roughness Measurements of Feed, Accepts, Fines Removed Accepts and 70:30 Mixture of Accepts and Rejects. Samples Refined at SEL of 2 Ws/m	185
Figure 143	Fines Content of Feed, Accepts, Fines Removed Accepts and 70:30 Mixture of Accepts and Rejects. Samples Refined at SEL of 2 Ws/m	186
Figure 144	Water Retention Value (WRV) of Feed, Accepts, Fines Removed Accepts and 70:30 Mixture of Accepts and Rejects. Samples Refined at SEL of 2 Ws/m	187
Figure 145	Photomicrographs of Unrefined and Refined Feeds. Escher Wyss Refiner Operated at SEL = 2.0 Ws/m and Energy Consumption of 50 and 100 kWh/ton	190
Figure 146	Photomicrographs of Unrefined and Refined Accepts	191

	(AA3). Escher Wyss Refiner Operated at SEL = 2.0 Ws/m and Energy Consumption of 50 and 100 kWh/ton	
Figure 147	Photomicrographs of Unrefined and Refined Rejects (RR3). Escher Wyss Refiner Operated at SEL = 2.0 Ws/m and Energy Consumption of 50 and 100 kWh/ton	192
Figure 148	Photomicrographs of Unrefined and Refined 70:30 Mixture of AA3 and RR3. Escher Wyss Refiner Operated at SEL = 2.0 Ws/m and Energy Consumption of 50 and 100 kWh/ton	193
Figure 149	Photomicrographs of Unrefined and Refined Fines Removed AA3. Escher Wyss Refiner Operated at SEL = 2.0 Ws/m and Energy Consumption of 50 and 100 kWh/ton	194

Nomenclature

TMP	Thermomechanical Pulp
CTMP	Chemithermomechanical Pulp
BCTMP	Bleached Chemithermomechanical Pulp
FQA	Fibre Quality Analyzer
CSF	Canadian Standard Freeness
CPPA	Canadian Pulp and Paper Association
SCAN	Scandinavian Pulp and Paper Testing
TAPPI	Technical Association of the Pulp and Paper Industry
WRV	Water Retention Value
PAPRICAN	The Pulp and Paper Research Institute of Canada
STFI	Swedish Pulp and Paper Research Institute
SEL	Specific Edge Load
CEL	Cutting Edge Load
RPM	Revolutions Per Minute
l_n	Arithmetic Average Fibre Length
l_{lw}	Length Weighted Average Fibre Length
l_{ww}	Weight Weighted Average Fibre Length
W_n	Arithmetic Average Fibre Width
W_{lw}	Length Weighted Average Fibre Width
SF_n	Arithmetic Average Fibre Shape Factor
SF_{lw}	Length Weighted Average Fibre Shape Factor
C_D	Drag Coefficient

Acknowledgements

Financial support for this project came from a grant from the Mechanical Wood-Pulps Network of NSERC's National Centres of Excellence. Additional support came from a grant from Forest Renewal British Columbia, PAPRICAN, and the Pulp and Paper Centre.

A number of individuals have greatly assisted me with this work. I am very grateful for their time and assistance.

I would like to thank my supervisor, Dr. Richard Branion, for his helpful suggestions and advice during the course of my studies. I appreciate all the opportunities you have given me over the years I have known you.

I would also like to thank Peter Taylor, Tim Patterson, Lisa Brandly, Brenda Dutka, Georgina White, John Senger, Sheau-ling Ho, Brian MacMillan and Ken Wong for all their help and encouragement. I would also like to thank all the staff and students of the Pulp and Paper Centre. I also gratefully acknowledge the helpful discussions with Dr. Elida Sevilla, Dr. James Olson, Jan Backman, Norm Webster, Dr. Raj Seth, and Dr. Richard Kerekes. Sincere thanks also to the late Dr. Alkis Karnis whose suggestions were always very helpful. I also appreciate the considerable support of James Drummond, Norm Roberts, John Hoffman and Gordon Robertson.

I am also grateful to Dr. Ulla-Britt Mohlin and Helena Vollmer for allowing me to perform part of my work at the Swedish Pulp and Paper Institute (STFI). My sincere appreciation to Karl-Johan Grundström, Lars Thomsson, Lars Norburg, Hannes Vomhoff, Hans Wallin, Ulla Gyllenberg, Ranjit Chowdury, Joanna Hornatowski, Helén Sigertun, and Anette Lindé for all your assistance during my stay at STFI.

Most of all I am grateful to my parents, and my brothers, Karim and Amyn. It has been your encouragement and support that has helped me to achieve.

Chapter 1

Introduction

The fractionation of pulp into separate streams containing pulp fibres of different characteristics can be useful in papermaking. Screens and hydrocyclones are currently the most common type of equipment found in pulp and paper mills capable of fractionating pulp. In this thesis only the use of hydrocyclones for fractionating pulp fibres will be considered.

Hydrocyclones, also known as centrifugal cleaners, are widely used by pulp and paper mills for removing contaminants (dirt, plastic) and unsatisfactorily pulped fibres (shives) from the product stream. More recently some pulp and paper mills have installed hydrocyclones to fractionate pulp fibres [45]. The objective here is to separate thick-walled fibres from thin-walled fibres since thick-walled fibres negatively affect paper properties (smoothness, bonded area, and strength). After fractionation these mills reject refine the separated thick-walled fibres to develop the desirable fibre characteristics required in papermaking.

Bliss [5,6,7,8] summarizes some other reasons for fractionation of fibres using hydrocyclones. Some of his objectives for fractionating include:

1. Production of stronger paper sheets at the same freeness.
2. Producing pulps that give equivalent sheet strengths at higher freeness with reduction in the amount of fines.
3. Reduction in refining power requirements. This can result by realizing that fractionated streams require different amounts of energy input for fibre development.
4. Separation of chemical pulps from mechanical pulps and separation of hardwood fibres from softwood fibres.

Bliss [5,6] further suggests that after a successful fractionation, the longer and stronger fibre fraction might be refined to produce sheets having higher strengths than the unfractionated pulp but at the same freeness as the unfractionated pulp. If this were possible then the so upgraded pulp (refined fraction) could be used to replace another, more expensive furnish component without an overall adverse effect on drainage.

If the sheet strength of paper made from the unfractionated pulp was adequate, fractionation, and subsequent refining could result in one of the exit streams from the hydrocyclone having equal sheet strength potential but at higher freeness and with a lower fines content. Thus papermachine drainage and first pass retention might be improved.

In his paper [3,4], Bliss presents four fractionation schemes. In the first of these the accepts from the fractionation stage are sent to papermachine A while the rejects go to papermachine B. For this scheme to be useful two, or more papermachines, which can produce marketable products from each of the accepts and rejects streams from the fractionation, must be available.

In the second scheme the accepts and rejects from the hydrocyclone go to different layers of a multilayer sheet (e.g. liner and filler for paperboard). For this scheme to be useful ply bonding between the different layers must be acceptable.

In the third scheme the rejects are discarded and the accepts proceed to papermaking. This is the conventional way of using hydrocyclones to get rid of dirt, shives, etc.

In the fourth scheme, Bliss [3,4,5,6] proposes the accepts stream goes directly to the papermachine and the rejects are upgraded by refining. The upgraded rejects are then mixed with the accepts and proceed to a papermachine. Such a scheme was contemplated as a way of reducing refining energy requirements because only the fraction of the pulp that needed refining would be refined. Bliss provides an energy balance to show that, if it is assumed that the refiner motor draws constant power, there are no savings in energy. This assumption seems arguable but that argument is better left to those with a greater knowledge of refiner energetics than we have. Bliss [3] notes that these fractionation schemes have some limitations and often are impractical from a process or economic standpoint.

Another reason for fibre fractionation is to study the characterization of pulps for prediction of their papermaking potential. To do this a laboratory fractionating device would be

required which would be capable of separating fibres into fractions having different properties, such as specific surface, coarseness, fibre length distribution, etc. Some studies on fractionating pulp for this reason have been published by Wood and Karnis [83,84,85].

1.1 Thesis Objectives

To show via a theoretical analysis and by reviewing relevant literature that a hydrocyclone can separate pulp suspensions into fractions having different specific surfaces. To relate specific surface to other fibre properties (coarseness, specific volume, freeness).

To experimentally determine how varying hydrocyclone operating parameters (flowrate, pulp consistency, reject rate) can affect the characteristics of the fibres of the separated streams.

To determine what fibre properties should be characterized when fractionating different types of pulps (mechanical, recycled, Kraft).

To develop a fractionation scheme that produces streams of different characteristics and to then refine these different streams to study how each stream responds to subsequent refining.

1.2 Organization of Thesis

Chapter 2 presents a chronological literature review on the uses of hydrocyclones for fractionating pulp.

Chapter 3 details the experimental equipment used. Experimental procedures and analytical methods are also outlined.

Chapter 4 describes theoretical analysis of fibre separation in a hydrocyclone.

Chapter 5 presents the results and discussion of the experiments performed.

Chapter 6 draws conclusions on the work performed and suggests recommendations for future work.

Chapter 2

Literature Review

2.1 Overview

Section 2.2 presents a chronological literature review on fibre fractionation.

Section 2.3 summarizes the key findings of the literature reviewed to date.

2.2 Studies of Fractionation in Hydrocyclones to Date

This review concentrates on literature, in chronological order of appearance, that deals with separating pulp into streams, both of which might be useful in making paper, that have different fibre properties.

The first patent for a hydrocyclone was granted to E. Bretney in 1891. The first patent for hydrocyclone processing of pulp was granted to J. MacNaughton in 1906. More information about the history of the hydrocyclone can be found in a review by Bliss [8].

In a 1956 paper Boadway and Freeman [9] described a centrifugal pulp cleaner for removing shives. In it, it was recognized that the ability of the cleaner to separate undesirables from the pulp depended on the size of the particles to be separated and on the dimensions of the hydrocyclone. In a later paper Broadway [10], in discussing the theory of particle separation in a hydrocyclone, pointed out that if fibres were to be considered as cylindrical rods, the fibre property governing fibre separation in a hydrocyclone would be fibre diameter. Since it can be shown that fibre coarseness is related to fibre diameter then a hydrocyclone should, in theory, be able to fractionate based on differences in fibre coarseness.

McCulloch [48] studied the effects of Vorjects, primarily used for shive removal, on groundwood pulp quality. He found at various rejects rates that the burst strength,

breaking length and tear strength of handsheets made from the feed, accepts and rejects streams were greatest for the accepts stream, lower for the feed stream and much lower for the rejects stream.

Boadway [12] described the use of hydrocyclones in separating coarse, stiff fibres and shives from groundwood. He believed that a hydrocyclone tended to fractionate fibres via a mechanism based on differences in their fibre diameters rather than on differences in their lengths. Photomicrographs showed clearly that shives were preferentially rejected by a hydrocyclone and that the material in the rejects was coarser and less fibrillated than material in the accepts or in the feed to the hydrocyclone. He noted that the rejects tended to be free of fines, possibly because of the type of cleaner used involved the injection of elutriation water the result of which was that the fines would make several passes through the separation zone and thus have a greater probability of being accepted.

One of the purposes of Boadway's investigation was to develop a fibre classifier based on the use of a series of hydrocyclones of progressively smaller diameters. The accepts from stage 1 would be the feed for stage 2 etc. The rejects from each stage and the accepts from the final stage would then provide $(n+1)$ fractions of pulp having different properties with n being the number of stages.

In Boadway's work, when a single stage hydrocyclone was operated with the accepts being recycled continuously to the feed tank the level of coarse material appearing in the rejects decreased with time. The assessment of coarseness was subjective based on the appearance of stock in the photomicrographs and on visual observations made on handsheets.

Boadway also noted that smaller diameter hydrocyclones were capable of rejecting material that could not be rejected by larger diameter hydrocyclones. He worked at consistencies of the order of 0.1% to avoid interfibre interferences as the fibres moved inside of the hydrocyclone.

Also in 1963 a patent was granted to A.W. Pesch [61] for a process using hydrocyclones which could separate pulp suspensions into fractions having a greater content of springwood fibres in the accepts and a greater content of summerwood fibres in the rejects than what prevailed in the feed stream to the hydrocyclone. He observed that, under the influence of gravity, summerwood fibres from southern pine species sedimented three times faster than springwood fibres. The springwood fibres were more flexible, tending to be thin, collapsed ribbons having diameters around 40 - 45 μm and a thickness of 10 - 12 μm (i.e. thickness = twice the cell wall thickness of 5 - 6 μm). The more rigid summerwood fibres did not collapse but retained their tubular nature with diameters of 25 - 35 μm and cell wall thickness of 10 - 15 μm . The best pulp consistencies for such separations were in the range of 0.1 - 0.2%. Bliss [3] notes that these consistencies are too low for economical hydrocyclone operation.

Further studies in this area of springwood/summerwood separation were carried out by Jones et al. [38]. They used fibres resulting from the Kraft pulping of various species of pine which grow in the southern USA. The most impressive results were obtained using longleaf pine (*Pinus palustris*) and slash pine (*Pinus caribea*). Effective separations of springwood from summerwood fibres could be made for other species but there were less differences in the papermaking characteristics between summerwood and springwood fibres from those species.

Jones's springwood/summerwood separations were achieved in a Bauer (600N) 3 inch diameter, centrifugal cleaner. Other cleaners were tested but the 600N gave the best separations. Smaller diameter cleaners were more effective in achieving fibre separation than larger ones. The relative amounts of springwood and summerwood fibres in the feed, accepts and rejects streams were measured by making microscope slides from samples taken from each of these streams and counting the numbers of springwood and summerwood fibres in each. The rejects and accepts streams were collected on screens with an attempt made to retain their fines contents by using recycled white water from the screens.

Jones adopted as the criteria for the acceptability of a separation that 70% of the springwood fibres were in the accepts stream and 70% of the summerwood fibres were in the rejects stream. The reason for this was that increasing the springwood content of a pulp, that was subsequently made into a sheet of paper, to more than 70% resulted in little further change in burst strength and breaking length. As the springwood content increased the tearing strength decreased.

Feed, accepts and rejects stream samples were refined in a Valley beater to various freeness levels. Handsheets were made and their burst factors, tear factors, densities, opacities, smoothness, porosities and breaking length measured. Print quality tests were also done. Some tests were also done on a pilot plant scale to confirm the results obtained with handsheets.

The parameters which were found to affect the springwood/summerwood fibre separation were pulp consistency, temperature, reject nozzle opening diameter, pressure drop between the feed and accepts stream and prior mechanical treatment of the fibres.

As pulp consistency rose from 0.05 - 0.25% (the range studied by Jones et al.) the fraction of springwood fibres in the accepts decreased and the fraction of summerwood fibres in the rejects also decreased. The ratio of the mass flow rate of the accepts stream to the feed stream increased as the consistency increased while the ratio of the mass flow rate of the rejects stream to the feed stream tended to decrease. An empirical equation was presented which relates the % of springwood fibres in the accepts stream to % consistency. However this equation is only valid over the rather modest range of consistencies studied by Jones et al. The % springwood fibres in the accepts stream ranged from 85 at a feed pulp consistency of 0.05% to 63 at a feed pulp consistency of 0.25%. The % summerwood fibres in the rejects stream ranged from 74 at a feed pulp consistency of 0.05% to 65 at a feed pulp consistency of 0.25%. The ratio of the mass flow of accepts to feed covered the range 31 - 42% while the ratio of the mass flow rate of rejects to feed covered the range 69 - 58%.

It was noted that the rejects had higher freeness values than the accepts. This observation is consistent with the views expressed below that hydrocyclones can separate fibres based on differences in specific surface, tending to reject fibres of low specific surface. The theory of El-Hosseiny and Yan [20] indicates that as specific surface increases freeness decreases. It was also observed that little springwood/summerwood fibre separation occurred at feed pulp consistencies greater than 0.25%.

Jones et al. note that *“for high purity in both fractions the accepts to rejects ratio must be nearly the same as the ratio of springwood to summerwood in the original pulp. This ratio is about 50 : 50 for southern pine. If one fraction is only a small percentage of total feed, this fraction may be quite pure, but the larger fraction will have about the same fibre composition as the feed pulp.”* This may not be strictly true, perhaps there is an optimum ratio of accepts to rejects flow split that gives best separation and that this optimum may not necessarily be the ratio of springwood fibres to summerwood fibres in the feed. What the optimum is depends on the desired objective of the separation.

As already noted mechanical damage done to the fibres during processing can affect the ability of a hydrocyclone to separate springwood from summerwood fibres. Jones et al. observed that never dried pulps separated better than pulps which had been dried and reslurried. Some samples were refined in a laboratory Jordan refiner. When these were passed through the hydrocyclone the more refined fibres tended to concentrate in the accepts stream. In this case the separation achieved was more on the basis of degree of refining of the fibres, as measured by freeness, than by springwood/summerwood differences. Again recall that El-Hosseiny and Yan [20] have demonstrated that Canadian Standard Freeness (CSF) can be inversely related to specific surface. As the specific surface of pulp increases the value of the CSF decreases. The ratio of mass flow of accepts to rejects was also affected by refining, the lower the freeness the greater the accepts to rejects ratio. Bleaching of pulp was also noted to affect (adversely) separation.

The ratios of the mass flow rate of rejects to feed and of accepts to feed depended on temperature, pressure drop between the feed inlet and the accepts outlet; (the rejects outlet is at atmospheric pressure) and the diameter of the opening in the rejects nozzle. As noted above they also depended on consistency and the degree of refining of the pulp.

Over the range 27 - 41 °C the % of springwood fibres in the accepts stream tended to increase with increasing temperature but the % of summerwood fibres in the rejects was insensitive to temperature changes. As the temperature rose the mass flow rate ratio of rejects to feed increased at a constant pressure drop of 241 kPa.

As might be expected as the reject nozzle opening diameter increased the amount of fibre rejected increased at constant pressure drop.

Burst factors, breaking lengths, apparent densities, and smoothness were better for sheets made from the accepts than for sheets made from the feed pulp which in turn were better than sheets made from the rejects. Tear factors and porosities were higher for sheets made from the rejects than for sheets made from the feed which in turn had higher values than sheets made from the accepts. Opacities were about the same for all three sources of pulp.

Jones et al. observed that the fines in the springwood rich accepts tended to consist of macerated fibre debris. This material significantly lowered the freeness values of the accepts pulp streams. This complicates the analysis of the effects of refining because the presence of these fines means that refining to a certain level of freeness requires less energy than if the fines were not there. Thus the strength potential of the non-fines fibres may not be fully developed. These sorts of fines did contribute positively to sheet strength and fibre bonding. Fines in the summerwood rich rejects seemed to consist of short, cut fibres which had little influence on sheet strength and pulp freeness.

Stephens and Pearson [74] investigated the effectiveness of 76 mm (3 inch), 102 mm (4 inch), and 305 mm (12 inch) diameter hydrocyclones in removing shives and dirt from Eucalypt groundwood. Their studies were conducted over a consistency range of 0.5 - 1.8%. They found that operation at consistencies above 1.2% resulted in worse separation efficiencies in terms of dirt and shive removal. In their experiments they observed that the wet and dry strengths (burst factor, breaking length and tear factor) of handsheets made from pulp in the accepts from the 75 mm and 102 mm hydrocyclones were greater than those of the feed and noted that not all of the differences could be attributed to differences in shive or dirt counts. The wet and dry strength values for the handsheets made from the pulp in the rejects stream were usually lower than those for sheets made from the feed stream. With the 305 mm hydrocyclone the accepts burst factors in 21 out of 23 tests were higher than for the feed. Improvements ranged from -1.1% to +17.0%, and averaged 5.1%. Similarly in 20 out of 23 tests the breaking lengths of the accepts were higher than for the feed. Improvements ranged from -0.9% to +13.0% and averaged 4.8%. Stephens and Pearson [74] interpret this finding to mean that a hydrocyclone fractionates fibres on the basis of differences in fibre flexibility, the less flexible material having a higher probability of being rejected.

Marton and Robie [47] investigated the sedimentation behaviour of mechanical pulp (stone and refiner groundwoods, spruce, balsam fir mixtures) fibre suspensions. The settling velocities of several Bauer McNett classifier fractions were measured as were fibre properties such as specific surface, fibre coarseness, fibre length and handsheet strengths. Their work had nothing whatsoever, directly, to do with hydrocyclones but is of interest to this review because fibres settling (sedimenting) under the influence of gravity have many things in common with fibres moving under the influence of the centrifugal forces found in a hydrocyclone. They observed that fibre length correlated well with fibre coarseness. If a fibre is considered to be a circular cylinder or a flat ribbon in theory fibre coarseness shouldn't be a function of fibre length [32]. Multiple regression analysis showed that most of the relation between settling velocity and fibre properties could be attributed to coarseness and a lesser, but still statistically significant,

amount to fibre specific surface. The influence of fibre length was statistically insignificant.

However, Marton and Robie also state "*These results should by no means be construed to mean that settling rate is independent of fibre length*". Chapter 4 of this thesis presents some theoretical evidence that shows there is a relationship between fibre coarseness and fibre specific surface, thus it would appear from Marton and Robie's work that fibre settling velocity is primarily a function of fibre coarseness. Later in this thesis, experimental evidence is provided showing that hydrocyclones can separate fibres into fractions having different fibre lengths.

Corson and Tait [16] used multiple regression analysis on some experimental data obtained in a Bauer 606-110-P, Centri-Cleaner which had a cyclone diameter of 6 inches. Six independent variables were varied; these included inlet pulp consistency, inlet pulp freeness (CSF), reject tip outlet diameter, the pressure drop across the cleaner, the inlet shive content of the pulp and a parameter (b) which characterizes the fibre length distribution of the pulp entering the cleaner. The dependent variables considered were weight % rejection of fibre, volumetric ratio of reject flow to feed flow, accepts consistency, accepts freeness, accepts parameter b value, accepts shive content, rejects consistency, rejects parameter b value and rejects shive content. The test data were obtained using refiner mechanical pulps of *Pinus radiata* from which latency had been removed. The tests were done at 50 °C.

The fibre length distributions could be represented by a modified Rosin-Rammler equation [16]. Thus

$$W = ae^{-bx} \quad (1)$$

where

W = fraction of fibres having length > x

x = fibre length

a, b = constants for a particular fibre sample

The parameter b , which affects the fibre length distribution, was shown, for the accepts stream to be a function of the pressure drop across the hydrocyclone and the feed freeness of the pulp. Parameter b for the rejects stream depended upon the inlet consistency and the inlet fibre length distribution or upon the inlet consistency, reject tip diameter and inlet freeness, depending on whether or not the inlet fibre length distribution was included as an independent variable in the regression analysis. In any event passage through a hydrocyclone was shown to affect the fibre length distributions of the accepts and rejects streams. Accepts freeness values were lower than feed freenesses.

Seifert and Long [71] have noted, in a paper comparing a variety of ways of fractionating pulp fibres, that in a 76.2 mm diameter cleaner operating with a 25% reject ratio, long fibres were concentrated in the accepts and short fibres in the rejects.

Hill et al. [30] studied the separation of shives in screens and hydrocyclones using an optical shive analyzer to provide the data. The slope of a plot of shive removal efficiency against rejects ratio gave the number of shives per kg of rejects divided by the number of shives per kg of feed. The higher the value was above one the better the rejection of shives. Two hydrocyclone cleaners were tested in this manner. One cleaner was smaller than the other. For the small cleaner when the ratio of shives in the rejects to shives in the feed was plotted against shive length, shive removal effectiveness decreased as shive length increased for both TMP and stone groundwood. In the case of the larger cleaner the ratio increased as shive length increased up to a maximum value and then decreased as shive length was further increased.

Wood and Karnis [83], in an investigation directed at minimizing the linting of newsprint, used a hydrocyclone to separate fibres into fractions having different values of specific surface. For TMP they found that lint consisted mostly of short, stiff fibres

which had smooth surfaces, low values of specific surface and hence a low level of interfibre bonding potential. They collected enough lint samples from a printing press to show that, after processing it by solvent exchange, it had an average specific surface, as measured by the Robertson Mason [68] water permeability test, of around $2.5 \text{ m}^2/\text{g}$ (range $0.7 - 4.0 \text{ m}^2/\text{g}$). Material that would have a tendency to lint was defined as having fibre lengths in the range $0.2 - 1.5 \text{ mm}$ and specific surfaces in the range $0.7 - 4.0 \text{ m}^2/\text{g}$. It was also observed that lint had an extraordinary amount of latewood (summerwood) fibres in it as compared to the whole pulp which the lint originated.

Knowing that a hydrocyclone could separate fibres into fractions having different levels of specific surface, Wood and Karnis built a fractionating device (the Domtar Specific Surface Fractionator) which used a hydrocyclone to do the fractionating. The hydrocyclone used had a cyclone diameter of 51 mm and reject tip openings of 7.9 or 4.0 mm . This device is also discussed in a later paper by the same authors [66]. Pulp was processed in the Fractionator at a consistency of 0.015% . The pressure drop across that hydrocyclone was 138 kPa (20 psi). Using this device they were able to measure specific surface distributions. They also pointed out that there was an inverse relationship between freeness and specific surface.

By sequentially passing the rejects from the hydrocyclone through the hydrocyclone again, fractions having different values of specific surface could be collected. The ratio of feed pulp specific surface to the specific surface of the 4th stage rejects had a value of about $8:1$, thus indicating that low specific surface material tended to be found in the rejects. The ratio of average fibre length (Forgac's L factor) in the feed to that in the rejects was around 0.9 indicating that this value didn't change much and that the rejects tended to have higher values of L factor.

TMP material, that was in the rejects from the hydrocyclone, tended to consist of stiff fibres having low values of specific surface with little evidence of surface fibrillation or fibre delamination. When papers containing chemical pulp fibres were disintegrated and

passed through the hydrocyclone the chemical pulp fibres tended not to report to the rejects stream. These findings are similar to the work of Jones et al. discussed above who observed that the more flexible a fibre was the more likely it was to be accepted by a hydrocyclone.

Wood and Karnis defined a pulp linting propensity index (PLPI) as the weight fraction of a pulp having a specific surface less than $2.5 \text{ m}^2/\text{g}$ and noted that a hydrocyclone has the ability to remove material that has a high value of PLPI. The small diameter cleaner used in their study was more effective in rejecting a material with a high value of PLPI than a commercial cleaner, designed for shive rejection, but they thought that the latter should be able to reject some of this material. Such commercial cleaners usually have a reject ratio of less than 10%. If this were increased to 20 - 30%, rejection of high PLPI material should be improved. To confirm this a mill trial was undertaken. This showed that increasing the reject ratio of the hydrocyclone following the screens (which had a reject ratio of 10%) from 3% to 14% resulted in rejects stream which could be more effectively refined in a rejects refiner resulting in a pulp, after reject refining, that had a lower value of PLPI. There was no direct evidence of a decrease in PLPI solely as a result of this change in cleaner rejects ratio. However there was a definite change in the specific surface distribution which resulted from such a change. Thus the weight fraction having a specific surface less than some particular value was highest for neither screened nor cleaned pulp, intermediate for a pulp which was screened (reject ratio = 10%) and cleaned (reject ratio = 3%) and lowest for a pulp which had been screened (reject ratio = 10%) and cleaned (reject ratio = 14%).

In another paper Wood and Karnis [84] have further discussed the distribution of specific surface in papermaking pulps. Their premise was that hydrocyclones separate pulps into fractions having different values of specific surface.

Wood and Karnis believed that for pulps that had not been mechanically refined, that is for pulps with little development of external specific surface, fibre fractionation in a

hydrocyclone was dependent on differences in coarseness or in specific volume. Data were provided to support this belief using an unbeaten, softwood, semibleached, Kraft pulp. For such pulps there was an increase in coarseness in the rejects stream from the hydrocyclone compared to the feed stream. The specific volume of the rejected pulp was lower than the feed pulp. The specific surfaces of the rejects were more or less the same as for the feed. The hydrocyclone used was the one associated with the Domtar Fractionator described in Wood and Karnis [83].

When their softwood, semibleached, Kraft pulp was beaten (from 700 CSF to 467 CSF) the rejects had lower specific surfaces than the feed. The specific volumes decreased slightly in the rejects and the coarseness of the rejects was the same as the feed. Thus their conclusion was that for mechanically treated chemical pulp fibres that the hydrocyclone fractionated on the basis of fibre specific surface differences. A similar conclusion was drawn on the basis of experiments done using softwood, refiner mechanical pulps refined to CSF = 557 and 152. For these pulps coarseness was not reported, the rejects specific surfaces were lower than the feed to the hydrocyclone and the specific volumes were more or less the same in the rejects as in the feed.

Specific surface distributions were presented for semibleached; softwood Kraft pulps refined to various degrees and for stone groundwood and refiner mechanical pulps having various energy inputs. These distributions were based on the assumptions that the measured specific value was the median for the particular sample being measured and that the specific surfaces were additive. Thus the specific surface of the accepts from the hydrocyclone could be calculated from knowledge of the specific surfaces of the feed and rejects streams and the ratio of the mass flow rate of fibre in the rejects stream to the mass flow rate in the feed.

To determine if the hydrocyclone rejects and feed streams displayed differences in fibre lengths, samples were taken from these streams and passed through a Bauer McNett fibre classifier. Not a great deal of difference was detected between the feed stream and the

rejects stream when the feed stream (refiner mechanical pulp) had consistencies of 0.052% and 0.31%. There was less of the fraction retained on the 14 mesh screen in the rejects samples than in the feed samples for both consistencies. There was also less of the -200 mesh fines in the rejects stream than in the feed. There was even less difference between the Bauer McNett distributions of the rejects streams as a function of hydrocyclone feed consistency. At the lower consistency there was less of the -200 mesh material in the rejects stream than at the higher consistency.

Bauer McNett distributions of fibre length for a bleached softwood pulp beaten in a Valley beater were not very different as the freeness changed from CSF = 668 to 428, but their specific surface distributions were. Wood and Karnis then did experiments to see whether fractionation of such pulps was based on fibre length differences or upon specific surface differences. In one of these experiments semibleached softwood Kraft pulp was beaten to two levels of freeness. These refined pulps were fractionated using Bauer McNett classifier. Samples of these pulps were also put through the Domtar Fractionator. The rejects streams from the hydrocyclone after 1, 2, and 3 passes were also fractionated by the Bauer McNett classifier. As the number of passes through the hydrocyclone increased the fraction of pulp retained on a 14 mesh screen decreased, the fraction through the 14 mesh screened but retained on a 200 mesh screen increased and the fraction which passed a 200 mesh screen stayed more or less the same. Not much difference was seen between the pulps with respect to their differing freenesses as far as the Bauer McNett distributions went. There were distinct differences between the pulps with respect to freeness differences detectable in the specific surface distributions. The specific surface distributions of the retained on 14 mesh fraction and the through 14 mesh retained on 200 mesh fraction were superimposable at the low end of the specific surface range but diverged at the high end. This was true for both levels of freeness but the values of specific surface were much higher for the lower freeness pulp.

A similar test was done using a refiner mechanical pulp and four passes through the Domtar Fractionator. As the number of passes through the hydrocyclone increased the

fraction retained on a 28 mesh screen decreased slightly, the fraction through the 28 mesh screen retained on a 200 mesh screen increased and the fraction passing the 200 mesh screen decreased. In going from 2 passes through the hydrocyclone to 3 and 4 passes the diameter of the opening in the rejects nozzle was reduced from 7.9 mm to 4.0 mm which may have influenced the distributions in the rejects stream.

From these experiments it can be concluded that passage of a pulp suspension through a hydrocyclone has an effect on the fibre length distribution in the rejects stream such that it is different from that of the feed stream. However Wood and Karnis' data indicate that passage through their hydrocyclone had little, if any, effect on mean fibre length as expressed by Forgacs' [23] L factor.

Data was provided to show that specific surface as measured by the Robertson Mason [68] technique was additive provided that the fibre lengths of the component pulps of a mixture were not too dissimilar.

To see if fibre length had any effect on specific surface the pulp fraction retained on the 48 mesh screen of a Bauer McNett classifier was formed into air dried handsheets. These handsheets were then cut up using guillotine paper cutter, reslurried, reformed into handsheets, further cut up, et. The cutting served to reduce the fibre length without affecting the specific surface. A plot of specific surface vs. fibre length showed that as fibre length decreased specific surface increased slightly.

Specific surface balances around a Domtar Fractionator hydrocyclone (diameter = 51 mm) and two commercial cleaners (diameters = 152 and 305 mm) showed that indeed specific surface was an additive property. Thus the specific surface of the feed was calculated from material balances around the cleaner in question and the specific surfaces as measured in the accepts and rejects streams. These calculated values closely matched measured values of specific surface in the feed stream.

Wood and Karnis noted that consistency over the range 0.05 - 0.30% didn't have much effect on the fibre length distribution in the rejects stream from the Domtar Fractionator hydrocyclone. It did however affect the specific surface distributions. More selectivity was observed at lower consistencies.

There was not much of an effect of pressure drop (flowrate) on the specific surface distribution if the pressure drop was above a particular value. Below that selectivity based on specific surface decreased no doubt as a result of the lessened centrifugal forces available to act upon the fibres.

The diameter of the reject nozzle opening also affected the specific surface distribution curves in a significant way as well as affecting the reject ratio. Larger tip openings were observed to provide a more selective separation. Small tip openings seemed to result in changes to the specific volume of the rejects stream pulp compared to the feed stream pulp.

House [35] investigated the performance of a Bauer 606-110 P hydrocyclone which had a diameter of 150 mm. Several types of pulp were employed in the study in which consistencies ranged from 0.05 - 0.8%. No significant differences were observed in the fibre length distributions of the feed, accepts and rejects streams for a variety of conditions, leading House to conclude that no classification according to fibre length had occurred. House also measured specific surface and specific volume for the various pulps he used both for the hydrocyclone feed and for the hydrocyclone rejects. The standard deviations on these measurements were high but in all cases the mean specific surfaces of the rejects pulps were lower than those of the feed pulps. No significant differences in specific volume between feed and rejects were noted, nor were any differences in pulp density.

Karnis [42] compared the fractionating abilities of pulp screens and hydrocyclones particularly with respect to their responses to refining treatment of pulp. He concluded

that screens tend to separate on the basis of fibre length and/or flexibility whereas hydrocyclones separate on the basis of specific surface and/or specific volume. He observed that the specific surfaces of the rejects from the third pass through a hydrocyclone fractionator had specific surfaces that were much below the specific surfaces of the feed to the fractionator. The feed to the fractionator consisted of fractions of pulp passing the 14 mesh screen and retained on the 28 mesh screen of a Bauer McNett fibre classifier. The same conclusion resulted when the -28 +48 fraction from the Bauer McNett was used as the feed

It was noted that as the reject ratio (ratio of rejects flow to feed flow) increased the specific surface area distribution curve of the rejects stream approached that of the feed stream. As the rejects ratio decreased the specific surface area distribution curve of the accepts approached that of the feed stream. As the value of the rejects ratio increased the specific surface of the fibres in the rejects tended to increase as did the specific surface of the fibres in the accepts. For fibres having specific surfaces less than $2.5 \text{ m}^2/\text{g}$ the ratio of the concentration of specific surface in the accepts to that in the rejects decreased as the reject ratio increased over the range 10 - 65%. For fibres having specific surfaces in the range $2.5 - 4.0 \text{ m}^2/\text{g}$ that ratio increased as the reject ratio increased.

Bliss [3,4] investigated the fractionation of secondary fibres using hydrocyclones. In his paper [4] scanning electron microscope photos are presented which show the very different characteristics of cleaner accepts and rejects for TMP. The rejects are much coarser in appearance than the accepts. With a feed freeness of 135 ml the accepts had a freenesses of 25 ml and the rejects 275 ml. Since freeness is inversely related to specific surface this result is in accord with Wood and Karnis [84] premise that hydrocyclones separate on the basis of specific surface.

Bliss notes that the rejects stream contained the less refined, longer, stiffer and lower specific surface area fibres, while the accepts tended to contain the extreme fines, well refined fibres, shorter fibres and other material which was high in specific surface area.

After fractionation in a hydrocyclone the rejects stream had a higher freeness and handsheets made from it were slightly lower in burst index, breaking length, tear index and corrected fold than the accepts or feed pulps.

Bliss demonstrated that refining the rejects stream to a freeness level comparable to the feed freeness resulted in handsheets that could have higher burst, breaking length and fold than the feed pulp but lower tear.

In one of his experiments some deinked ledger stock was passed through a 76 mm hydrocyclone cleaner. Note that the deinking process tends to remove not only ink but fines and filler particles as well. The feed flowrate was 238 l/min., the feed consistency was 0.69% and its freeness was 504 ml. The accepts flow rate was 193 l/min., consistency was 0.27% and freeness was 140 ml. The accepts contained light weight contaminants, flexible, well refined, high specific surface area fibres, fines and springwood. The rejects flowrate was 45 l/min., consistency was 2.82% and freeness was 645 ml. The rejects stream contained heavy contaminants, stiff, whole, unrefined, low specific surface area fibres and summerwood. After fractionation the rejects stream was refined and recombined with the accepts in proportion to the flow split in the hydrocyclone. A plot of freeness vs. specific refining energy showed no difference between the recombined accepts and refined rejects and the original feed pulp. Thus it was demonstrated that rejects could be upgraded to become usable fibre. Paper strength tests on the recombined accepts and refined rejects confirmed this.

Handsheet test showed that the breaking length and burst strengths of sheets made from the accepts were greater than those made from the feed and that those made from the feed had greater strengths than those made from the rejects. Tear index values were highest for the feed and lowest for the accepts.

Figure 1 provides the Bauer McNett distributions for the feed, accepts and rejects streams in Bliss' fractionation of deinked ledger stock. Note that most of those fines still remaining in the feed pulp stock after the deinking process, reported to the accepts.

In another experiment Bliss [3] investigated the ability of the same hydrocyclone as used for the deinking stock to fractionate a repulped corrugated box stock. In one such test the feed flowrate was 225 l/min., its consistency was 1.03% and its freeness was 370 ml. The rejects flowrate was 61 l/min., consistency was 3.06% and freeness was 560 ml. The accepts flowrate was 164 l/min., consistency was 0.28% and freeness was 20 ml. Figure 2 presents the Bauer McNett distributions for the feed and rejects streams. For this kind of pulp again it was clear that a separation occurred based on differences in freeness (specific surface). Burst and tear were greatest for sheets made from the accepts and lowest for sheets made from the rejects. Tear values were highest in the feed and lowest in the accepts but there wasn't much difference. Not much separation based on differences in fibre length was noted, although the rejects had less fines than the feed.

Some tests were done in order to evaluate the effects of changes in hydrocyclone geometry on fibre fractionation. The inlet area for flow of pulp into the hydrocyclone was found to significantly affect the cyclone's fractionating ability; large inlet areas resulted in less fractionation than small inlet areas but the small inlet areas had higher pressure drops associated with them. For rectangular inlets the length, and widths were not individually important, within reason, only their product. Use of smaller than usual reject nozzle diameters failed to improve fractionation and resulted in reduced capacity. Interactions between pressure drop (an indirect measure of flowrate) and hydrocyclone geometry were observed.

A 3 level, 4 factor, statistical experimental design was employed to assess the effects of the flow split (i.e. the volumetric ratio of the accepts flowrate to the feed flowrate), pressure drop, feed stock consistency, and feed temperature on feed flow rate, rejects freeness, accepts freeness and pulp split (i.e. the mass ratio of accepts pulp flowrate to

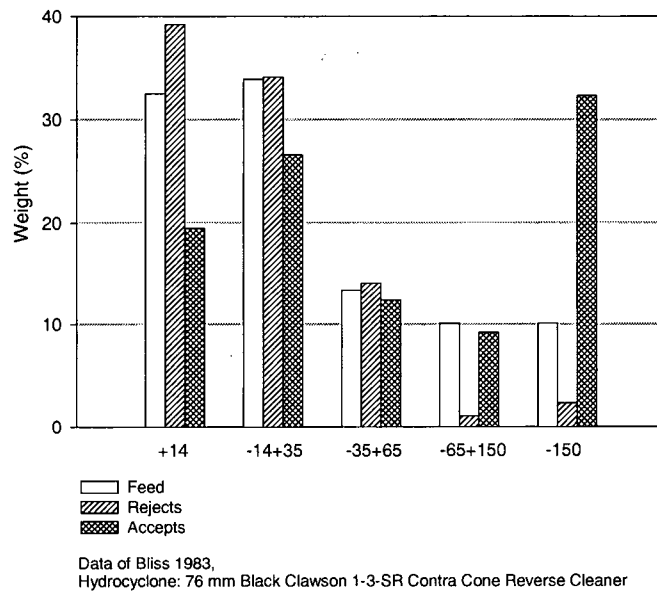


Figure 1: Bauer McNett Fractions for Deinked Ledger Stock for Feed, Accepts and Rejects [3]

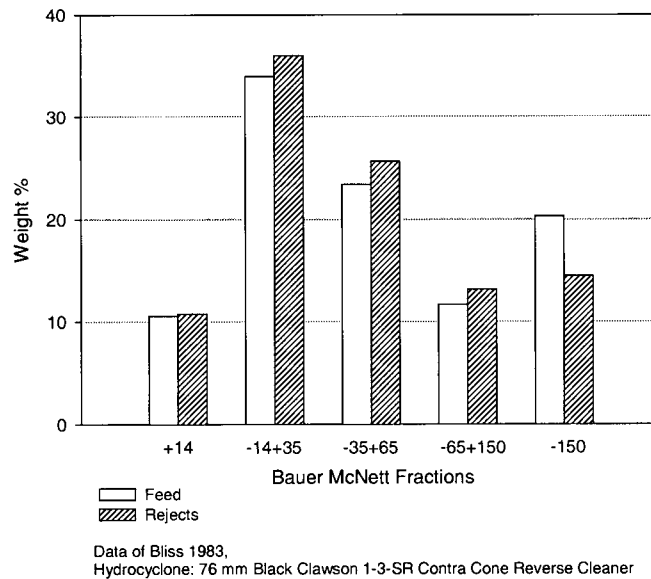


Figure 2: Bauer McNett Fractions for Recycled Corrugated Boxes for Feed and

feed pulp flowrate). Regression equations were fitted to the data, rejecting those relationships which were not statistically significant. Thus it was found that feed flowrate was dependent upon flow split, and pressure drop. Rejects freeness was affected by flow split, pressure drop and the product of flow split and feed consistency. Accepts freeness was influenced by flow split, pressure drop, feed consistency and temperature. Pulp split depended upon flow split, temperature, pressure drop, the product of flow split and pressure drop, the product of flow split and consistency and the product of pressure drop and consistency. Various sheet strength parameters were also related to the above listed independent variable plus two others, the refined feed and the refined rejects freeness values. The regression equations developed by Bliss in his thesis [3] are further discussed in another paper [6].

Underflow freeness could be used as a parameter for assessing fractionation. Given a constant value for flow split, as pressure drop increased the rejects freeness increased. At constant flow split and constant pressure drop the rejects freeness increased as feed consistency decreased. At constant pressure drop and constant consistency the rejects freeness increased as the flow split value decreased. The equations generated by Bliss' statistical model permit calculation of all of these parameters.

Ricker and House [67] defined a critical flowrate through a hydrocyclone, below which no fluid solid separation occurs. They believed, as a result of their studies, that this critical flowrate was primarily dependent upon fibre length.

Mukoyoshi, Ohtake and Ohsawa [51,52] observed that a Bauer Centri-Cleaner 600 could be used to separate vessel elements from tropical, and other, hardwood Kraft pulps. Vessel elements with large projected areas and low length to diameter ratios tended to be concentrated in the hydrocyclone rejects stream. Separation efficiencies based on concentration in the rejects tended to be low for vessel elements having high values of length to diameter ratio. Separation efficiency was noted to decrease as the consistency of the feed pulp increased.

Mukoyoshi and Ohsawa [51,52] continued their studies on a Bauer 600 Centri-Cleaner for separating vessel element from wood fibres using bleached Kraft pulp. They based their analysis of the mechanism by which this separation occurs on the sedimentation velocities of fibres suspended in water. They observed that particles with large projected areas and small values of length to diameter ratio tended to settle faster. The % rejected by their hydrocyclone was a more or less linear function of the settling velocity of pulp fibres. Settling velocities under the influence of gravity ranged from 0.105 to 0.241 mm/s for fibres and from 0.142 to 0.761 mm/s for vessel elements. The settling velocities of the vessel elements were linearly proportional to their projected areas. The settling velocities of the fibres were linearly proportional to the product of the apparent density (based on water retention values of pulp [38]) of the fibres and their diameter. For model fibres (cylinders) settling velocity for a fibre having a particular diameter was only slightly affected by fibre length, but was strongly affected by fibre diameter.

Ohtake, Usuda, and Kadoya [55] published a paper on flow visualization techniques for studying hydrocyclone fluid mechanics, in it they mention that a hydrocyclone can be used for the separation of vessel elements from pulp fibres. They observed that the existence of a flow towards the conical apex of the hydrocyclone in the liquid phase at the outer edge of the air core. As a result of its presence they commented that large tracheids that were located near the wall of the hydrocyclone might move upward towards the vortex finder exit while small fibres and/or fibre fragments might tend to be rejected. No evidence is given for this conjecture.

In a paper [6] on the effect of fibre fractionation on multilayer sheet formation Bliss noted that in general the rejects stream from a hydrocyclone contained the less refined, longer and stiffer, low specific surface area fibres plus other material that was higher in specific surface. The rejects (underflow) stream contained pulp that was much higher in freeness which produced paper that was somewhat lower in burst, breaking length, tear and corrected fold than the accepts. If the rejects pulp was refined the resulting pulp produced

paper that was significantly higher in burst, breaking length and corrected fold and slightly lower in tear than the feed pulp when compared on the basis of equal freeness.

Bliss [6] also pointed out that hydrocyclone fractionation has certain advantages over screen fractionation, e.g. the ease of adjustment to a wide range of flow and pulp splits. The flow split (volumetric rejects ratio), pulp consistency and pressure drop can all be controlled by valves, whereas to achieve similar results in a screen fractionation, the screen may have to be changed. The disadvantage of hydrocyclone fractionation is that the consistency range over which successful fractionation can be achieved is limited to consistencies $< 1.5\%$. The energy consumed in pumping through hydrocyclones (ca. 10 - 20 kWh/ton) is somewhat higher than for screen fractionation.

Mohlin [50] defined an index of fibre bonding ability to be the tensile index, of handsheets, produced under standard conditions, from pulp that passed a 16 mesh screen but was retained on a 30 mesh screen in a Bauer McNett fibre classifier. Studies done on hydrocyclone cleaners in a TMP mill showed that the screened pulp entering the cleaners had a fibre bonding index value of 8.0. The rejects index value was 5.3 while the accepts index value was 8.9. Thus the cleaners were capable of separating out material which had poorer bonding potential.

Wood et al. [84] have described how a hydrocyclone can be used to characterize the fines generated in mechanical pulping process. As noted above in their earlier work they conclude that a hydrocyclone can separate on the basis of specific surface differences. In the paper now under discussion they extend this concept to the fractionation of the fines component of mechanical pulps. Since mechanical pulp fines drain very slowly, measurement of specific surface by the Robertson and Mason [68] water permeability method become impractical. As an alternative the use of a turbidity measurement was proposed. Such turbidity measurements, at 0.03% consistency, gave a straight line on log log paper when plotted against specific filtration resistance which in turn is a measure of specific surface.

If the operating conditions in a hydrocyclone are maintained constant then, for a pulp having a larger proportion of low specific surface material, the rejects stream will contain more material having low specific surface and will have a higher consistency and a higher ratio of rejects consistency to feed consistency (thickening factor) than would be the case for a pulp having a lesser proportion of low specific surface material. Wood et al. [83,85] concluded then that reject rate or thickening factor could be used as a criterion which to rank pulps with respect to their content of low specific surface material. To demonstrate this point samples were obtained from three mills, one of which had greater linting problems than the others. The pass 100 mesh fractions of the pulps obtained from a Bauer McNett classifier were used as feed to a 25 mm diameter hydrocyclone which had interchangeable reject nozzle openings of 3.92 and 1.78 mm. With the larger tip opening the thickening factors for all three pulps were the same, but with the smaller tip there were significant differences. The mill with the linting problem had a fines fraction which displayed a much higher thickening factor. This indicates that mill's fines had more low specific surface material than the other mill's fines. A further demonstration showed that larch fibre fines had higher reject rates than spruce fibre fines. The larch fibre fines were less successful in contributing, in a positive way, to sheet strength and optical properties than were the spruce fibre fines.

Microscopic examination of the rejects and accepts streams from such a hydrocyclone separation suggested that a better separation could be achieved by multiple passes through the hydrocyclone. The procedure adopted was to pass the fines sample through the hydrocyclone using the 3.92 mm reject nozzle (tip) opening. Next the collected accepts and rejects streams from the first pass were separately passed through the hydrocyclone with the 3.92 mm tip in place. This produced four fractions. Finally each of these four fractions was put through the hydrocyclone using the 1.78 mm tip, giving rise to eight fractions. Turbidities, corrected to a common consistency of 0.03%, were measured for all of the fractions.

Photomicrographs of the fractions having the lowest and highest turbidities exhibited big differences. The lowest turbidity sample contained intact fibre fragments having little evidence of surface fibrillation which were in the length range of 10 - 200 μm . Ray cells were evident. The highest turbidity sample contained material of high specific surface including fibre fragments with well fibrillated surfaces, and bits of fibre as small as 0.5 μm . From the samples collected using the hydrocyclone as a fractionating device and using turbidity as being indicative of specific surface, Wood et al. were able to construct turbidity distribution plots. In such plots the fraction of the pulp fines which had a turbidity less than a certain value were plotted against turbidity. This is a representation of a specific surface distribution plot.

Another paper on the subject of fibre fractionation in hydrocyclones has been written by Gavelin and Backman [28]. In it they note the earlier work done by Mohlin [50] with respect to separation of fibre having lower values of fibre bonding index by a hydrocyclone cleaner. Thus a hydrocyclone has the capability of rejecting stiff coarse fibres while accepting soft pliable ones. Gavelin and Backman reported that they were using an optical instrument to determine fibre coarseness in a study of hydrocyclone performance but do not report any results obtained by its use. In the interests of practicality they measured drainage time, under standard conditions in a handsheet machine, as an indicator of freeness or specific surface. They also measured sheet density, air permeability and tensile strength of the sheet for both the feed and rejects streams to and from a hydrocyclone cleaner. The ratios of each of these characteristics in the rejects to the corresponding characteristics in the feed were used as indicators of fibre coarseness. Thus a suspension of coarse fibres should drain faster than a suspension of fibres having a lower value of coarseness. Sheets made from the coarser fibres should be less dense, have greater air permeability and be weaker in tensile strength. In their opinion the ratio of tensile indices should be the most indicative of fractionating efficiency.

Their procedure was tested using a softwood Kraft pulp. In such a pulp all of the fibres should have more or less the same stiffness (coarseness) and the ratios of rejects properties to feed properties should be close to 1.0. For this test drainage times were not given but the density ratio was 0.96; the air permeability ratio was 0.89 as was the tensile ratio. Thus not much fractionation was achieved with these chemical pulp fibres. For newsprint grade groundwood pulp however there was a significant degree of fractionation. The drainage time ratio was 0.41, the density ratio was 0.81, the air permeability ratio was 0.15 and the tensile strength ratio was 0.69. The drainage time ratio of 0.49 indicated that rejects drained faster than the feed, thus the rejects would have had higher freeness and lower specific surface than the feed.

Further testing was done which showed that operating the same hydrocyclone at different pressure drops had an effect on the drainage time and tensile ratios and possibly a slight affect on the air permeability ratio. Changing the pressure drop from 100 kPa to 150 kPa changed the drainage time ratio from 0.28 to 0.19. This reduction in drainage time means that at the higher pressure drop the rejected pulp was easier to drain than the hydrocyclone feed pulp. This can be interpreted to mean that at the higher pressure drop more low specific surface material went to the rejects.

This procedure for evaluating hydrocyclone fractionation was applied to systems of cleaners for TMP and groundwood pulps. Equations were developed to calculate the fractionation efficiency for various combinations of cleaners in cascade. The results indicated that hydrocyclones can singly or in combination could fractionate pulp. Gavelin and Backman [28] leave the reader with the impression that they believe that the criterion for separation was fibre coarseness.

Rehmat [62] observed, using TMP, that the fibre length distributions in the feed stream to, and the accepts and rejects streams from, a 76 mm diameter commercial hydrocyclone were different from one another. The mean fibre lengths of the rejects fibres were less than those of the accepts at feed consistencies of 0.25, 0.5, and 0.75%.

Wood and Karnis [85], in a paper that is mostly concerned with linting, presented some photomicrographs (also presented in Wood et al. [82]) of the rejects and accepts from a three stage, hydrocyclone fractionation. The rejects appeared to consist mostly of coarse material, much of which was ray cells. The accepts appeared to consist of material that exhibits a greater degree of fibrillation and of debris. Subjectively speaking, it seems that these photos indicate that the hydrocyclone rejected material, which was longer in fibre length than the material accepted. In this work the hydrocyclone feed was material that had been previously screened to pass 100 mesh.

Another important article on the fractionation of pulps in hydrocyclones has been written by Paavilainen [58]. Her study involved the fractionation of softwood Kraft fibres using hydrocyclones, a Johnson fractionator and a Jacquelin apparatus. At the outset she noted that softwood fibres as raw material for pulping have widely varying properties. The fibre lengths of springwood fibres were said to be somewhat shorter than those of summerwood fibres. The cell wall thicknesses of these two categories of fibres are quite different as noted above in the review of the work of Jones et al. [38].

In the experimental work involving hydrocyclones Paavilainen used both bleached and unbleached, softwood Kraft pulps which had been screened in the pulp mill. She later rescreened them to remove shives, thus her pulps could be regarded as fines free. Summerwood comprised 25% of the pulp; its kappa number was 32. The hydrocyclone employed was a Bauer 601, which had a diameter of 75 mm.

Some tests were done using a single stage hydrocyclone treatment. In these test the pulp consistency was 0.10% and the stock temperature was 7%. In Paavilainen's work reject ratios of approximately 20, 50, and 80% were achieved by reject nozzle tip size/cleaner pressure drop combinations of 4.6 mm/150 kPa, 6.2 mm/100 kPa and 11.2mm/180 kPa. The separation efficiencies for these tests were assessed by measuring fibre length and coarseness using a Kajaani FS100 analyzer. Handsheets were formed and measurements

of tensile index, air resistance, tear index and relative bonded area were made. Table 1 provides a summary of the results.

The data displayed in Table 1 indicate that in all instances the accepts fraction had equal or higher fibre length, and lower coarseness than the feed, which in turn had higher fibre length and lower coarseness than the rejects fraction. The differences between rejects and accepts mean fibre lengths and coarsenesses were not large. As the reject ratio increased the difference between feed fibre length and rejects fibre length decreased as expected. The maximum difference between accepts and rejects fibre length was observed at the lowest reject ratio. Conversely as the rejects ratio decreased one would expect that the difference between accepts and feed fibre length would diminish, however these differences did not change by much as the rejects ratio was varied and showed no pattern. Note that the mean fibre lengths of the rejects were lower than those of the accepts and the coarsenesses were higher even though there was more summerwood fibre, which was longer than springwood, found in the rejects stream.

As the rejects ratio increased the rejects coarseness tended to approach the feed coarseness. As the rejects ratio decreased the accepts coarseness approached the feed coarseness. The maximum differences between rejects and accepts coarseness occurred at the highest reject ratio.

Handsheets made from the accepts fractions had a greater % relative bonded areas than sheets made from the corresponding rejects fractions. The % relative bonded area data of Table 1 imply that sheets made from the accepts fraction had greater levels of interfibre bonding and therefore should be stronger than sheets made from the rejects fraction. This is illustrated by the tensile index data which showed that the accepts always produced stronger sheets. The tensile index values for the accepts sheets were higher and those for the rejects were lower than those of the unfractionated pulp. The highest tensile index values were found for sheets made from the least coarse pulp, which was the accepts at a reject ratio of 80%. The lowest tensile index values were noted for sheets made from the

coarsest pulp, which was the rejects stream at a reject ratio of 20%. The volume of air passing through the sheets per unit time was always lower for sheets made from the accepts implying that their air resistance was higher and that they formed a less permeable, less porous, denser sheet. The unbeaten accepts (at an 80% reject ratio) had higher tear index values than the rejects. After beating to various degrees in a PFI mill however the tear index of this type of pulp decreased. For all the other cases (feed, 20% rejects, 50% rejects) as the number of revolutions, to which the pulp was exposed in the PFI mill, increased the tear index values rose to a maximum then declined. As the number of PFI mill revolutions increased the rejects developed higher tear indices than the accepts. The lower the ratio of rejects to feed the higher was the tear index of sheets made from the rejects streams.

Paavilainen [58] noted in comparing the behaviour of bleached and unbleached pulps that the bleaching process had no effect on the ability of the hydrocyclone to separate springwood from summerwood fibres. She also observed in order to get a summerwood rich rejects stream and a springwood rich accepts stream the reject ratio had to be less than 50% if the summerwood content of the feed was below 30%.

Paavilainen also investigated the effects of multistage cleaning on fibre fractionation by passing a pulp through a hydrocyclone cleaner, collecting the accepts and rejects streams in separate containers, then passing the rejects stream through the cleaner again at a different pressure drop. Finally the rejects were again collected and passed through the cleaner yet again at the same pressure drop as in the previous passage. In these multistage trials, it was demonstrated that the summerwood content of the pulp, which was 20% in the unfractionated pulp, rose to approximately 40%, 60% and 70% in the rejects after one, two and three stages of cleaning. The accepts from a single pass through the hydrocyclone contained about 6% summerwood fibre. This value didn't change appreciably upon further passes through the hydrocyclone. Since summerwood fibres tend to be coarser than springwood fibres the hydrocyclone in Paavilainen's experiments was rejecting on the basis of differences in fibre coarseness.

Table 1
Paavilainen's Hydrocyclone Fibre Fractionations

	% REJECTED OR ACCEPTED	FIBRE LENGTH (mm)	COARSENESS (mg/mm)	RELATIVE BONDED AREA (%)
Original Pulp	-	2.60	0.192	12.6
Reject Target 20%				
Rejects	21.3	2.44	0.202	8.3
Accepts	78.7	2.65	0.190	18.5
Reject Target 50%				
Rejects	55.2	2.50	0.198	9.9
Accepts	44.8	2.60	0.185	13.4
Reject Target 80%				
Rejects	80.6	2.52	0.199	10.0
Accepts	19.4	2.66	0.164	25.8

Cell wall thickness and fibre widths on the fibres in the feed, rejects and accepts streams were also measured. The mean cell wall thickness of the feed fibres was 5.6 μm . The cell wall thicknesses of the accepts were 4.7 - 4.0 μm ; those of the rejects were 6.6, 8.0 and 9.2 μm after one, two and three stages of cleaning. The mean fibre width of the feed fibres was 43.6 μm ; the accepts fibres had widths of 44.0 - 50.5 μm and the rejects had widths of 41.2, 39.0 and 36.7 μm after one, two and three stages of cleaning.

Paper strength tests done on handsheets made from samples of feed, accepts and rejects from multistage cleaning showed that the accepts had a higher tensile index than the feed and that the rejects had lower tensile index than the feed. The sheets made from the rejects of the third stage had lower tensile index than those from a single stage. At high levels of refining (in a PFI mill) the third stage rejects had higher tear index than the first stage which in turn was higher than that of the feed. The lowest tear index was for the accepts at these higher refining levels.

When Bendsten smoothness was plotted against tensile index different relationships could be seen for each of the unfractionated feed, stage 1 accepts, stage 1 rejects and stage 3 rejects. For a given value of tensile index the smoothness values (ml/min.) were lowest for the accepts, next lowest was the feed, then the stage 1 rejects and the highest values were for the stage 3 rejects. Plots of light scattering coefficient against apparent sheet density resulted in linear, but distinctly different, relations for the feed pulp, the stage 1 accepts, stage 1 rejects and stage 3 rejects.

Karnis [42] proposed the use of a fractionation index as a means of characterizing the fractionating abilities of various fibre fractionating devices including hydrocyclones. He defined this fractionation index as

$$FI = 1 - X_I/X_{II} \quad (2)$$

where FI = fractionation index

X_I = average value of fibre property in stream I

X_{II} = average value of fibre property in stream II

X_I and X_{II} are chosen so that X_I is always $< X_{II}$ thus $0 \leq FI \leq 1$ and this determines which fraction is fraction_I and which is fraction_{II}. To get the average value of a fibre property in stream I or II plot the distribution of that property, i.e. plot the weight (or number) fraction of fibres having property value $>$ than the particular value of the property vs. the

particular property value. The average value of the property is the value of the property associated with the 50% weight (or number) fraction > than whatever the property that is being considered. Karnis recommends using the FI value as the dependent variable in assessing changes in the independent variables associated with the particular fractionation device being studied.

Karnis plotted, on probability paper, the distribution of surface areas in the rejects and accepts from a hydrocyclone (diameter = 305 mm, cone angle = 5°) for a 100 CSF TMP at 0.6% feed consistency. As expected, based on Karnis and Wood's earlier work, the high specific surface fraction was the accepts. As the reject ratio went from 23% to 45% the distribution plot of the low specific surface fraction moved to the right (towards regions of higher specific surface). If the reject ratio were increased to 100%, of course, as Karnis points out, the distribution of specific surface in the rejects would be the same as in the feed. He also found that if he plotted the fractionation index (based on specific surface area distributions) against average specific surface all the data from three different cyclones, with more or less constant values of cone angle ($4.5 - 5.5^\circ$), but varying diameters (76, 152 and 305 mm), each having a particular reject ratio (31%, 20% and 23% respectively), fell on the same curve. He interpreted this finding to mean that hydrocyclone diameter had little effect on fractionation index. He did conclude however that cone angle had an important effect on fractionation index because a plot of fractionation index vs. average specific surface for a hydrocyclone having a cone angle of 5° had a much higher index value at a particular value of average specific surface than a hydrocyclone with a cone angle of 10° .

Karnis also considered the distributions of fibre length (Bauer McNett) in a hydrocyclone having a diameter of 76 mm. As the rejects tip opening increased (range 5.0 mm - 30 mm) the reject ratio increased and generally the fraction of long fibres in the rejects stream increased. Karnis suggested this was the result of a wall effect. Thus long fibres, that would be rejected in a hydrocyclone with high reject ratios and hence higher fluid velocities down the wall, had a higher probability of being accepted if these near wall

velocities were lower due to the lower reject ratio observed with a smaller reject tip opening. However, for reject ratios < 16%, in this hydrocyclone, reject ratio had very little effect on fibre length distribution. Karnis states that *in general long fibres have lower specific surfaces*.

In a three stage hydrocyclone fractionation in which the rejects from the first stage were the feed to the second stage and the rejects from the second stage were feed to the third stage Karnis found that the first stage rejects tended to have lower fibre lengths than the second stage rejects which in turn had lower fibre lengths than the third stage rejects. The reject ratios in all three stages were about the same (60%, 61%, and 58%). The average specific surfaces in the rejects stream were 4.5 m²/g for stage one, 3.7 m²/g for stage two and 2.6 m²/g for stage three. These findings are consistent with Karnis' view that long fibres have low specific surface.

Sandberg, Nilsson and Nikko [69] have reported on the use of Noss hydrocyclones in a two stage system for fibre fractionation in a TMP mill environment. Photomicrographs in their paper show that the accepts stream contained fines and long fibres while the rejects stream appeared to have more coarse material and a lesser amount of fines. The feed stream freeness, mean fibre length and shive content were 84 ml, 1.28 mm and 0.02 respectively. For the accepts stream these values were 50 ml, 1.06 mm, and 0.01. For the rejects stream the values were 573 ml, 1.35 mm and 0.04. Paper sheet properties were also measured on sheets made from the feed, accepts and rejects streams. For the feed pulp the results were tensile 32 kNm/kg, tear 6.3 mNm²/g, light scattering coefficient 46 m²/kg and roughness 86 ml/min. For the accepts stream these values (in the same order) were 44, 6.7, 60 and 50; for the rejects stream they were 6.1, 1.7, 30 and 293.

Bliss [8] has published a very useful monograph on "Stock Cleaning Technology" which includes, among many other topics, a chapter that reviews literature on fibre fractionation in hydrocyclones.

Hoydahl and Dalqvist [36] have noted that the surface smoothness of paper sheet is important to print quality and that the presence of thick-walled fibres in the sheet surface is detrimental. Thus the separation of such fibres for further refining should result in reducing their fibre wall thickness. Return of these thinner walled fibres to the furnish should then result in a smoother sheet.

Hoydahl and Dahlqvist [36] have said that hydrocyclones to some extent tend to accept fibres that should be rejected because of their negative contribution to surface smoothness. They referred to such fibres as low energy material. They noted that fractionating hydrocyclones of a special design exist to separate such material. They present a plot which shows that fibre wall thickness of the feed pulp and the pulp rejected by one of these fractionating hydrocyclones were significantly different. There were many more very thick fibres in the rejects than there were in the feed. Fibre wall thickness distributions for rejects ratios of 4% and 14% were not very different. They also show that fibre perimeters for the feed and rejects were the same. Refining of thick-walled fibres reduced their fibre wall thickness.

Vollmer [77] has discussed fibre fractionation as a means of improving the strength characteristics of multiply paper and board. In this work the STFI Fibre Master was used to measure the fibre length, and fibre thickness distributions. Vollmer noted that in order to use a hydrocyclone, or any other fibre fractionation device for that matter, for fractionation the distribution of fibre properties, e.g. fibre thickness, should be broad, since if the distribution in the pulp to be fractionated was narrow there would be little probability of achieving much separation.

Vollmer fractionated a pulp via a hydrocyclone and sent the rejects to the core and the accepts to the surface layers of a three ply sheet. This led to improved surface smoothness when compared to a sheet made from the same pulp but not fractionated.

Demuner [19] investigated, amongst other devices, the use of a Noss Radiclone AM80-F for the fractionation of an ECF, Eucalypt market pulp at a hydrocyclone feed consistency of 0.5%. Eucalypt pulps have a rather narrow distribution of fibre properties and thus represent a challenge to any fibre fractionation process. The feed pulp was directed to stage 1 of a 2 stage system. The rejects from stage 1 became the feed to stage 2 while the accepts from stages 1 and 2 were combined to become the accepts from the system. The rejects from the system were the rejects from stage 2. The combined accepts flow represented 30% of the system feed flow while the rejects stream was 70% of the feed flow rate.

Demuner reported the results shown in Table 2 for hydrocyclone fibre fractionation. Average fibre length was lower in the accepts than it was in the rejects. Demuner did not observe significant differences in coarseness among feed, accepts, and rejects. Fines were concentrated in the accepts. There were some chemical composition differences as well between feed, accepts and rejects. Perhaps this means that different types of fibres were separated during the fractionation.

Refining the accepts and rejects streams in a PFI mill showed for the accepts fraction, that for a particular number of PFI mill revolutions the tensile index of the accepts was significantly greater than the tensile index of the feed pulp. Refining of the rejects resulted in a lower, but not by much, tensile index than that observed for the feed pulp.

Demuner plotted values of air resistance (Gurley), apparent sheet density, light scattering coefficient, Bendsten roughness, dynamic drainage time and water retention value versus tensile index. The air resistance of the accepts pulp was greater than that of the feed pulp and the air resistance of the rejects pulp was lower at a particular value of tensile index. The apparent sheet density of the accepts pulp was greater than that of the feed pulp while the feed and rejects apparent densities were approximately the same at a particular value of tensile index. Demuner concluded that the hydrocyclone he used was indeed capable

of separating a stream of Eucalypt fibres into two outlet streams containing fibres that have different characteristics.

Table 2
Demuner's Hydrocyclone Fibre Fractionations

Property	Feed Pulp	Accepts Pulp	Rejects Pulp
Weighted Average Fibre Length mm	0.67	0.64	0.69
Fibre Coarseness mg/100m	7.8	7.8	7.9
Number of Fibres per Gram millions	22.7	24.2	21.6
Fines Content from Dynamic Drainage Jar %	10.9	19.5	7.1
Pentosans Content %	16.6	16.8	15.3
Carboxyl Content meq/100g	5.8	5.9	5.7

Kure et al. [45] published a paper on fractionation of two pulps, a newsprint pulp and a super-calendar magazine pulp (SC-A) using Noss Radiclone hydrocyclones in a two stage fractionating system. The accepts from stage 1 were the system accepts. The rejects from stage 1 became the feed to stage 2 and the rejects from stage 2 became the system rejects. The accepts from stage 2 were mixed with the incoming, unfractionated feed to be the feed to stage 1. The incoming unfractionated feed consistency was 1%, the consistency of the combined incoming feed and accepts from stage 2 was 0.6%. The system reject ratio was varied. The incoming feed mass flow rate of fibres ranged from 3.5 - 4.0 oven dry kilograms per minute. The objective of the work was to separate thick walled fibres from the thin walled fibres, then refine the thick walled fibres so that print quality and smoothness of the resulting paper sheet would be improved. Their data is reproduced in Tables 3 and 4.

The findings of Kure et al. fractionating studies are summarized as follows;

1. the rejects mean fibre length was greater than the accepts mean fibre length. This finding seems to be typical of what's observed using the Noss Radiclone fractionating hydrocyclone. (Also see work of Demuner and Sandberg et al. [19,69]).

2. the CSF values for the rejects were higher than for the rejects (this is in accord with the idea that hydrocyclones tend to reject material of low specific surface).
3. the fibre wall thicknesses were greater for the rejects than for the accepts as measured on the +50 mesh Bauer McNett fraction (this is in accord with findings that hydrocyclones tend to reject coarse material).
4. fibre perimeters were not significantly different between rejects and accepts.
5. the % of fibres having microscopically observable breaks in the fibre circumference (indicative of fibre damage) was higher in the accepts than in the rejects, indicating that fibre flexibility plays a role in fibre fractionation.
6. shive content was substantially higher in the rejects than in the accepts.
7. scattering coefficients, for sheets made from the various hydrocyclone fractions, were higher for the accepts than for the rejects.
8. considering the Bauer McNett distributions (see Figures 3 and 4) of the feed, accepts and rejects it was found that the pass 200 mesh fraction (fines) was higher for the accepts than for the rejects. The +30 mesh fraction (long fibres) was higher for the rejects than for the accepts; this was also true for the -30 +50 and -50 +100 fractions.

For the studies with the newsprint pulp (data of Table 3) as the system reject ratio rose the difference between the rejects and accepts CSF values increased, for the SC-A pulp the opposite was observed. For both pulps as the reject ratio increased the difference between the rejects and accepts fibre lengths increased. As the reject ratio increased the difference between the amount of fines in the accepts and in the rejects increased for both types of pulp. With one exception, as the reject ratio increased the difference between rejects and accepts fibre wall thickness tended to decrease for both types of pulp.

Refining of the rejects stream resulted in decreasing the mean fibre wall thickness. Increasing the specific energy of refining (kWh/ton) resulted in decreasing fibre wall thickness at both low (3.5%) and high (21%) refining consistencies. At a given specific energy low consistency refining produced slightly thinner fibres than refining at high consistency.

Table 3
Kure et al.'s Hydrocyclone Fibre Fractionation Data for a Newsprint Pulp [45]

	Feed	Accepts	Rejects	Accepts	Rejects	Accepts	Rejects
System Reject Ratio %		10	10	17	17	25	25
CSF ml	130	141	596	129	632	120	652
Mean Fibre Length mm	1.36	1.34	1.51	1.27	1.49	1.31	1.63
Fibre Wall Thickness μm	2.78 \pm 0.12	2.46 \pm 0.10	2.99 \pm 0.13	2.58 \pm 0.12	3.04 \pm 0.15	2.57 \pm 0.10	2.95 \pm 0.15
Fibre Perimeter μm	94.7 \pm 3.1	95.9 \pm 3.1	93.9 \pm 3.2	96.3 \pm 3.5	94.2 \pm 3.0	92.7 \pm 2.9	94.2 \pm 3.0
Fibres With Broken Circumference %	28.5	32.4	29.0	33.8	24.0	31.0	28.7
Shive Weight %	0.14	0.05	0.57	0.03	0.83	0.06	0.41
Bauer McNett +30 %	49.6	47.6	50.7	44.1	46.6	44.3	52.5
Bauer McNett -30+50 %	17.6	16.5	22.2	17.7	24.8	16.2	23.1
Bauer McNett -50+100 %	10.8	10.9	11.9	12.0	13.5	11.5	12.6
Bauer McNett -100+200 %	5.0	5.3	4.5	5.9	4.5	5.9	4.1
Bauer McNett -200 %	17.0	19.7	10.7	20.3	10.6	22.1	7.7
Scattering Coefficient	24.6	28.4	24.5	25.8	23.6	26.1	24.1

Refining of the rejects caused the fibre wall thickness distribution to shift towards lower values. Almost all of the thickest fibres disappeared during refining. Refining the rejects resulted in improved tensile index, improved Parker Print Surf and increased light scattering coefficient. All of these variables changed linearly with increasing refining specific energy. The light scattering coefficient and the Parker Print Surf were unaffected by refining consistency, but at a given specific energy the tensile index was higher for low consistency refining.

Table 4
Kure et al.'s Hydrocyclone Fibre Fractionation Data for a Super Calender
Magazine Pulp [45]

	Feed	Accepts	Rejects	Accepts	Rejects	Accepts	Rejects
System Reject Ratio %		5	5	10	10	15	15
CSF ml	32	31	425	29	398	26	349
Mean Fibre Length mm	1.27	1.26	1.43	1.24	1.43	1.20	1.50
Fibre Wall Thickness μm	2.01 \pm 0.09	2.06 \pm 0.09	2.40 \pm 0.11	1.96 \pm 0.10	2.34 \pm 0.10	2.00 \pm 0.08	2.19 \pm 0.09
Fibre Perimeter μm	81.8 \pm 3.0	84.1 \pm 3.1	79.0 \pm 2.6	79.7 \pm 3.0	83.8 \pm 2.8	89.2 \pm 3.0	83.8 \pm 2.8
Fibres With Broken Circumference %	28.5	32.4	29.0	33.8	24.0	31.0	28.7
Shive Weight %	0.01	0.00	0.08	0.05	0.08	0.01	0.07
Bauer McNett +30 %	40.9	39.1	43.9	37.8	48.1	36.9	51.6
Bauer McNett -30+50 %	13.7	12.5	22.1	12.7	19.2	12.4	18.4
Bauer McNett -50+100 %	9.2	9.4	12.4	8.9	11.0	9.1	10.6
Bauer McNett -100+200 %	5.5	5.7	4.5	4.8	4.9	4.6	4.6
Bauer McNett -200 %	30.7	33.3	17.1	35.8	16.8	37.0	14.8
Scattering Coefficient	31.8	32.2	25.4	31.7	28.3	31.8	25.6

Li et al. [46] studied the fractionation of Eucalypt Kraft pulp in a hydrocyclone. They proposed that fibre fractionation in a hydrocyclone is governed by drag forces, centrifugal forces and flocculation effects, the latter, in turn, being dependent upon consistency. In their work they decided to avoid any complicating effects of the presence of fines by working only with a prescreened (Bauer McNett fibre classifier), long fibre, pulp fraction from which the fines had been removed. To avoid flocculation effects they chose to work

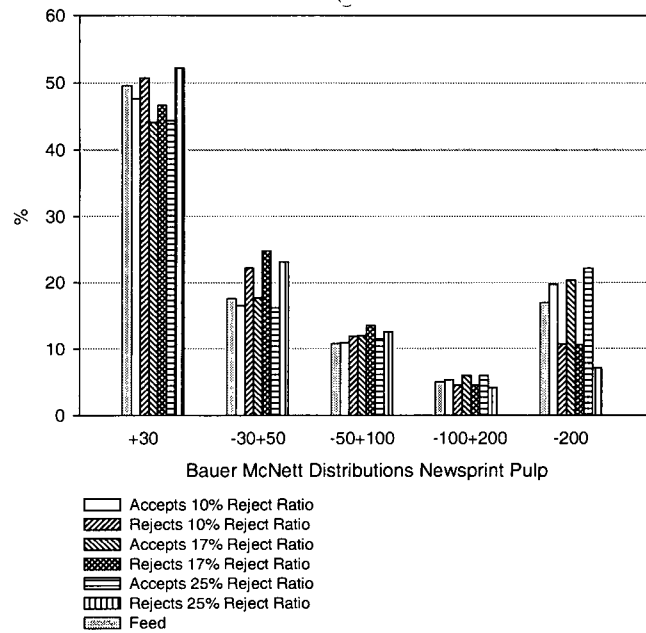


Figure 3: Data of Kure et al. for Newsprint Pulp [45]

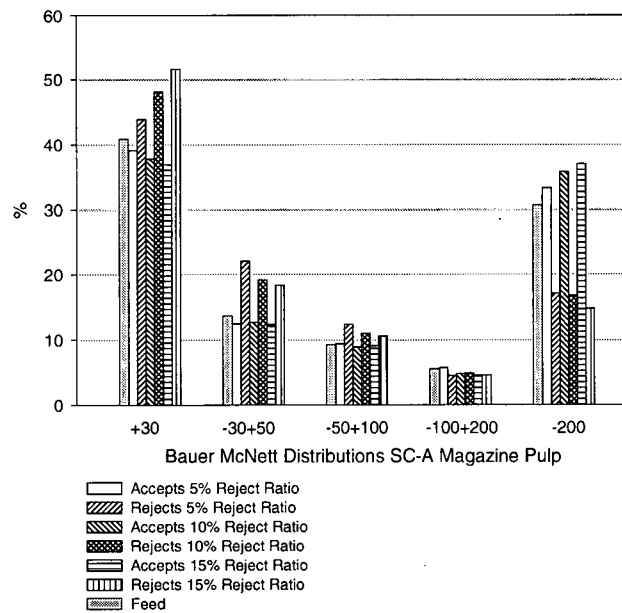


Figure 4: Data of Kure et al. for SC-A Magazine Pulp [45]

at a pulp consistency of 0.05%. Their objective was to shed some light on the mechanism of fibre fractionation and the motion of pulp fibres hydrocyclones.

Li et al. [46] used an AKW (Ambeger Kaolinwerke) hydrocyclone having a diameter of 40 mm (1.5 inches); a $16 \times 3 \text{ mm}^2$ feed inlet, a 6 mm diameter rejects tip opening and a 13 mm diameter vortex finder (accepts outlet). The operating pressure drop was 310 kPa (45 psi) and the feed flow rate was $2.5 \text{ m}^3/\text{hr}$. The mass flowrate of fibres in the rejects was approximately equal to the mass flow rate of fibres in the accepts. Fibre lengths were measured using a Kajaani FS-200; other fibre properties were measured by confocal microscopy.

Since the apparent density of a fibre moving under the influence of centrifugal and drag forces in a hydrocyclone affects the fibre trajectory, Li et al. [46], as did Rehmat and Branion [64], calculated an apparent density for a water swollen fibre which was modeled as a straight circular cylinder. Li et al.'s apparent density was a function of water density, fibre coarseness (which is a function of dry fibre density), dry fibre diameter, dry fibre lumen diameter and wet fibre diameter. The appropriate fibre dimensions for use in calculating an apparent fibre density, and ultimately fibre trajectory in a hydrocyclone, were estimated using confocal microscopy. As these authors note this is not a simple task. Rehmat and Branion's model used wet fibre specific surface and specific volume as parameters to be estimated in the calculation of wet fibre trajectories in a hydrocyclone. These parameters are somewhat more accessible but still require some specialized equipment [71].

As a correlating parameter Li et al. recommended, and used in their research an apparent density factor (AD) which is a function of dry fibre diameter and dry lumen diameter. AD can also be related to fibre thickness and to Runkel ratio, which latter is defined as twice the fibre wall thickness divided by the lumen diameter.

Li et al.'s experimental data indicated that the rejects from their hydrocyclone were slightly longer (mean fibre length 0.92 mm) than the accepts (0.88 mm). Rejects fibre coarseness in the rejects was 0.081 mg/m while that of the accepts was 0.073 mg/m. Fibre wall cross-sectional area in the rejects was $90 \mu\text{m}^2$; that of the accepts was $66 \mu\text{m}^2$. Accepts sheet bulk was $1.86 \text{ cm}^2/\text{g}$, reject sheet bulk was $1.95 \text{ cm}^2/\text{g}$. Accepts tensile index was 31.3 Nm/g, rejects tensile index was 23.8 Nm/g. Accepts tear index was 6.11 Nm^2/g , the rejects value was 4.9. Thus Li et al.'s results are similar to those noted by others in that hydrocyclones tended to reject long, coarse, thick fibres and that sheets made from the rejects were less dense and weaker than sheets made from the accepts.

From the confocal microscope images it was observed that 35% of the fibre in the accepts were collapsed compared to only 17% in the rejects. Plots of the distribution functions of AD showed that the rejects tended to have higher values of AD than the accepts for all fibres and for collapsed and uncollapsed fibre individually.

Li et al. [46] also have calculated grade efficiency curves in terms of AD, that is they have plotted the fraction of material having a certain value of AD that is rejected against AD.

Ho et al. [32] presented a paper in which they reported some revisions to a theory explaining why hydrocyclones fractionate on the basis of specific surface differences. Experimentally they observed that with a feed stream containing a 50:50 (mass basis) mixture of nylon fibres having a common length but different coarseness values a Bauer 600 3 inch Centri Cleaner produced an accepts stream that was more concentrated in the lower coarseness fibres and a rejects stream that was more concentrated in the higher coarseness fibres. Using a 50:50 (mass basis) of nylon fibres having the same coarseness but different fibre lengths they found that the longer fibres tended to report to the accepts stream and the shorter fibres to the rejects stream.

2.3 Summary

The above review of literature indicates that yes indeed, hydrocyclones can fractionate a stream of pulp, ranging from consistencies of close to zero to somewhat above 1%, into rejects and accepts streams containing fibres having different properties.

There is general agreement that hydrocyclones tend to reject coarse, stiff, dense, thick-walled, low specific surface fibres. Conversely they tend to accept fine, flexible, light, thin-walled, high specific surface area fibres.

Some hydrocyclones tend to reject short fibres, others tend to reject long fibres. This observation may be specific to certain pulp types as well as certain hydrocyclone geometries and hydrocyclone operating conditions.

The hydrocyclone design parameters affecting fractionation include hydrocyclone diameter, cone angle, reject nozzle diameter, feed entrance dimensions, accept nozzle diameter and the number of stages.

The hydrocyclone operating parameters affecting fractionation include feed flowrate (pressure drop), feed pulp consistency, pulp temperature and reject ratio.

Fractionation is more readily accomplished with pulps, such as mechanical pulps, which have relatively wide distributions of fibre properties although some fractionation has been observed in hydrocyclones treating chemical pulps in which the fibre property distributions are narrow.

Chapter 3

Materials and Methods

3.1 Overview

Section 3.2 summarizes operating parameters used to describe the hydrocyclones used in the experiments

Section 3.3 describes the various pulps tested

Section 3.4 illustrates and describes the fractionation pilot plants where the experiments were performed

Sections 3.5 – 3.7 summarizes the fibre analysis instruments, paper and pulp testing procedures, and photomicroscopy techniques respectively

Section 3.8 describes the refiner used for our fibre beating trials

3.2 Hydrocyclones

The fractionating capabilities of three commercial hydrocyclones were investigated. In this thesis, these hydrocyclones will be referred to as Hydrocyclones A, B, and C.

There are various parameters which describe the operation and performance of different types of hydrocyclones. The parameters are as follows:

1. Consistency: this is the mass fraction of pulp fibres in water expressed as %.
2. Pressure Drop: The pressure drop is a measure of the difference in feed pressure and accept pressure. The pressure drop is a measure of the capacity of the hydrocyclone. Most manufacturers recommend an operating pressure drop at which optimum efficiency occurs. The pressure drop is also indicative of the energy consumed by the hydrocyclone.
3. Reject Rate: Reject rate can be defined in terms of a volume reject rate or mass reject rate. R_v (volumetric reject rate) = reject flowrate/feed flowrate and R_m (mass reject rate) is calculated by dividing the mass of fibres and contaminants in the rejects by the mass in the feed. The volumetric reject rate reflects the flow split inside of a hydrocyclone.

4. **Thickening Ratio:** The thickening ratio is the ratio of the reject consistency to the feed consistency. It is often used as an indication of the fibre loss through the rejects stream of a hydrocyclone.

3.3 Pulps Tested

Several types of pulp have been used in the experiments performed. They include two sources of thermomechanical pulp (TMP), chemithermomechanical pulp (CTMP) from three different mills, recycled pulp, bleached chemithermomechanical pulp (BCTMP) and a fully bleached Kraft pulp. Table 5 characterizes some properties of these pulps. With the exception of BCTMP, all the fibre length ranges of the pulps listed in Table 5 are expressed as arithmetic average fibre lengths, l_n . Table 5 records the average fibre length of BCTMP fibres as a length weighted average, l_{lw} . The differences between these fibre length measurements is discussed later in this chapter.

With the exception of one source of CTMP pulp, all other pulps were obtained in a dry state and were re-slurried.

Table 5
Pulp Specifications

Pulp	Source	Wood Species	Average Fibre Length (mm)
Thermomechanical Pulp (TMP_A)	Eastern Canada	Spruce	$l_n = 0.75 - 0.80$
Thermomechanical Pulp (TMP_B)	Western Canada	Northern Softwood	$l_n = 0.58 - 0.59$
Chemithermomechanical Pulp (CTMP_A)	Eastern Canada	10% Aspen 45% Spruce 45% Balsam Fir	$l_n = 0.55 - 0.60$
Chemithermomechanical Pulp (CTMP_B)	Western Canada	Northern Softwood	$l_n = 0.52 - 0.55$
Chemithermomechanical Pulp (CTMP_C)	Western Canada (Pulp obtained from Latency Chest)	Northern Softwood	$l_n = 0.62 - 0.64$
Recycled Pulp	Western Canada	ONP, OMP, Phone Books	$l_n = 0.40 - 0.42$
Bleached Chemithermomechanical Pulp (BCTMP)	Western Canada	Northern Softwood	$l_{hw} = 2.15 - 2.17$
Bleached Softwood Sulphate Pulp	Sweden	Swedish Softwood	$l_n = 1.06 - 1.07$

3.4 Hydrocyclone Test Facility

Two hydrocyclone test facilities were used for the experiments performed in this thesis. These facilities are described below.

3.4.1 UBC Pulp and Paper Centre Hydrocyclone Test Facility

The UBC Hydrocyclone Test Rig is diagrammed in Figure 5. A pulp suspension of desired consistency was prepared in the slurry tank. The tank was equipped with an agitator to ensure that a constant consistency was maintained throughout the experiment. The pulp slurry in the tank was pumped to the hydrocyclone. The flow into the cleaner was controlled by a valve in the feed line. Another valve in the accepts line could be used to control the accepts flow rate. Feed and accepts line pressures were monitored using electronic pressure sensors. Samples from the accepts and rejects streams were collected over 10 second

intervals and then weighed on an electronic scale to determine the mass flowrates of each stream. When not being sampled both accepts and rejects streams emptied into a trough and were re-circulated back to the storage tank. Samples were collected from the accepts and rejects streams at various pressure drops and analyzed for consistency, fibre length distribution and coarseness. Handsheets were prepared from such samples to characterize sheet strength. Figure 6 illustrates the test facility and sampling procedures.

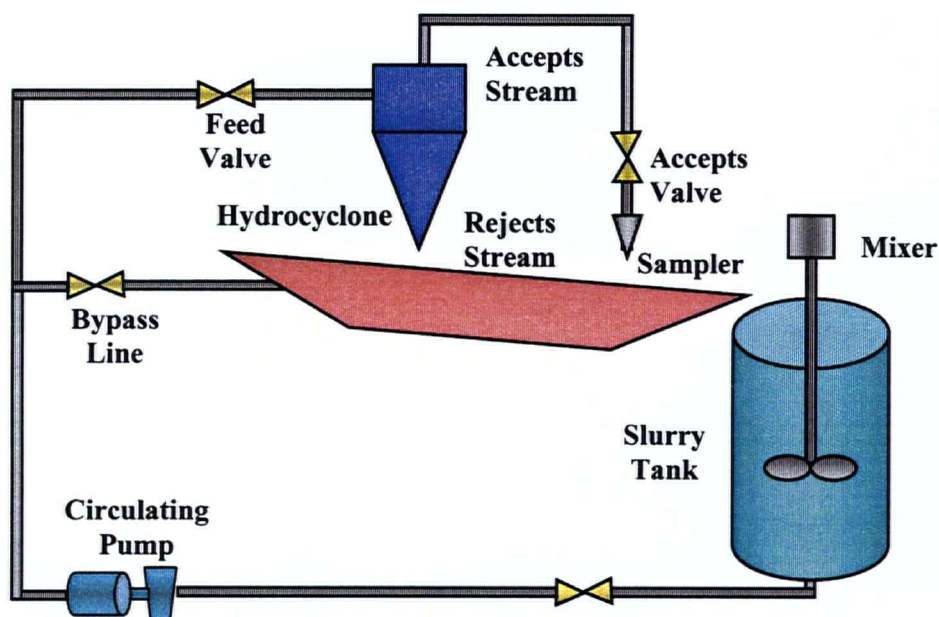


Figure 5 UBC Fractionation Flow Loop

Hydrocyclone A and B were tested at UBC.

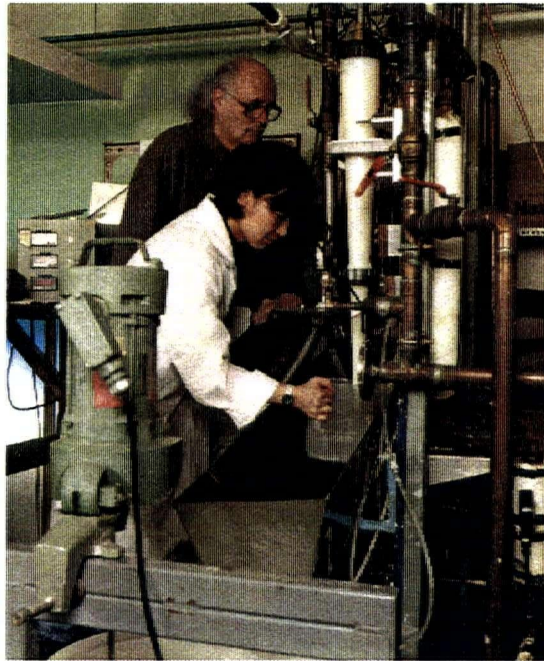


Figure 6 Photograph of UBC Test Facility and Sampling Procedure

3.4.2 STFI Hydrocyclone Test Facility

An experimental study was performed at the fractionation pilot plant located at the Swedish Pulp and Paper Centre (STFI). A general flowsheet of the facility is depicted in Figure 7. The fractionation system is incorporated into STFI's EuroFEX pilot plant which consists of mixing chests, fractionating equipment, thickeners, refiners, and a paper machine.

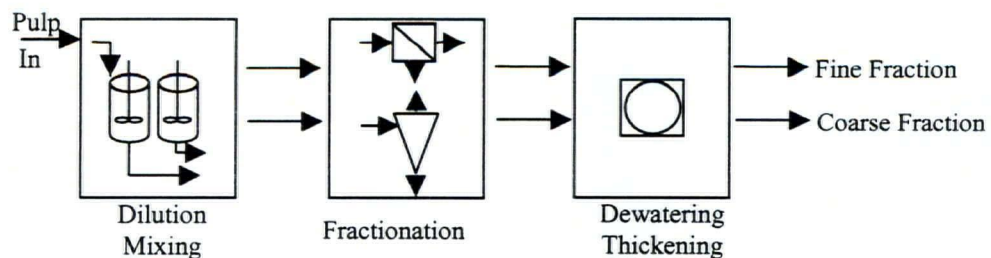


Figure 7 STFI Fractionation Flow Loop [77]

The fractionation experiments were performed in a staged system of commercial cleaners designed for pulp fractionation. For our tests, the fractionated streams were diverted to

separated chests and then re-fractionated. These chests are equipped with mixers to obtain the right pulp consistency. Accepts and rejects samples were manually collected.

Some photographs of the pilot plant and sample collection procedures are shown in Figure 8. The commercial hydrocyclone tested at the facility was obtained from a hydrocyclone manufacturer; in this report this hydrocyclone will be identified as Hydrocyclone C.

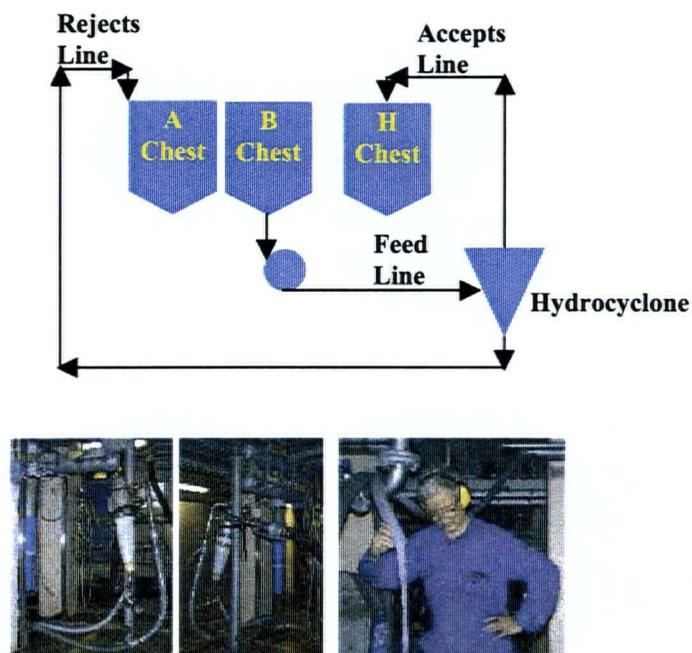


Figure 8 Experimental Method and Sampling Procedure

3.5 Fibre Analysis

Fibre length can be measured by classification with screens to obtain weight averages or by optical analyzers to obtain number averages. For our experiments we followed the procedures outlined in TAPPI Standard Methods (T233) to obtain weighted average fibre lengths. This method describes using the Bauer-McNett Classifier for measuring weighted average fibre length.

For tests performed at the UBC Fractionation Pilot Plant, two different fibre length analyzers were used for fibre length and coarseness measurements, these were the Kajaani FS-200 and the Fibre Quality Analyser (FQA). The FQA is designed with a unique sampling flow cell

which reduces some operating difficulties (fibre blockage) when analyzing [57]. Therefore the analyser chosen for measurement depended on the nature of the sample being tested. Long fibre fraction measurements were always performed in the FQA.

For tests performed at the STFI Pilot Plant, fibre analysis was performed on the STFI FiberMaster and the Kajaani FS-200. The STFI FibreMaster is capable of measuring length, width, and shape factor distribution. The shape factor is the ratio of the projected length of the fibre to the real length of the fibre in the projection plane the analyzer measures the fibre property. Its measure ranges from 0 – 100%, where 100% represents a completely straight fibre. The Kajaani was used to obtain a fibre coarseness value.

The Kajaani FS-200 and FQA analyzers used in our experiments are capable of reporting length averages as an arithmetic (l_n), a length weighted (l_{lw}) or weight weighted average (l_{ww}). The STFI FibreMaster can report fibre lengths as arithmetic and length weighted averages. These fibre averages or means are calculated [39] as follows:

$$l_n = \sum_i n_i l_i / \sum_i n_i \quad (3)$$

$$l_{lw} = \sum_i n_i l_i^2 / \sum_i n_i l_i \quad (4)$$

$$l_{ww} = \sum_i n_i l_i^3 / \sum_i n_i l_i^2 \quad (5)$$

where n_i is the number of fibres having length l_i .

Most often the length weighted average, l_{lw} , has been reported in the literature reviewed. The reason for this is that the arithmetic average mean, l_n , is sensitive to the number of fines in the sample whereas the l_{lw} is less sensitive. In most of our experiments we have reported fibre length in terms of the l_{lw} . In some of our experiments summarized in this thesis, we have expressed average fibre length as l_n . In the cases where l_n has been reported, we found that while there were differences in magnitude amongst the various average fibre lengths the trends shown for each type of average fibre length, when plotted vs. feed flowrate, are similar. This is illustrated in Figure 9.

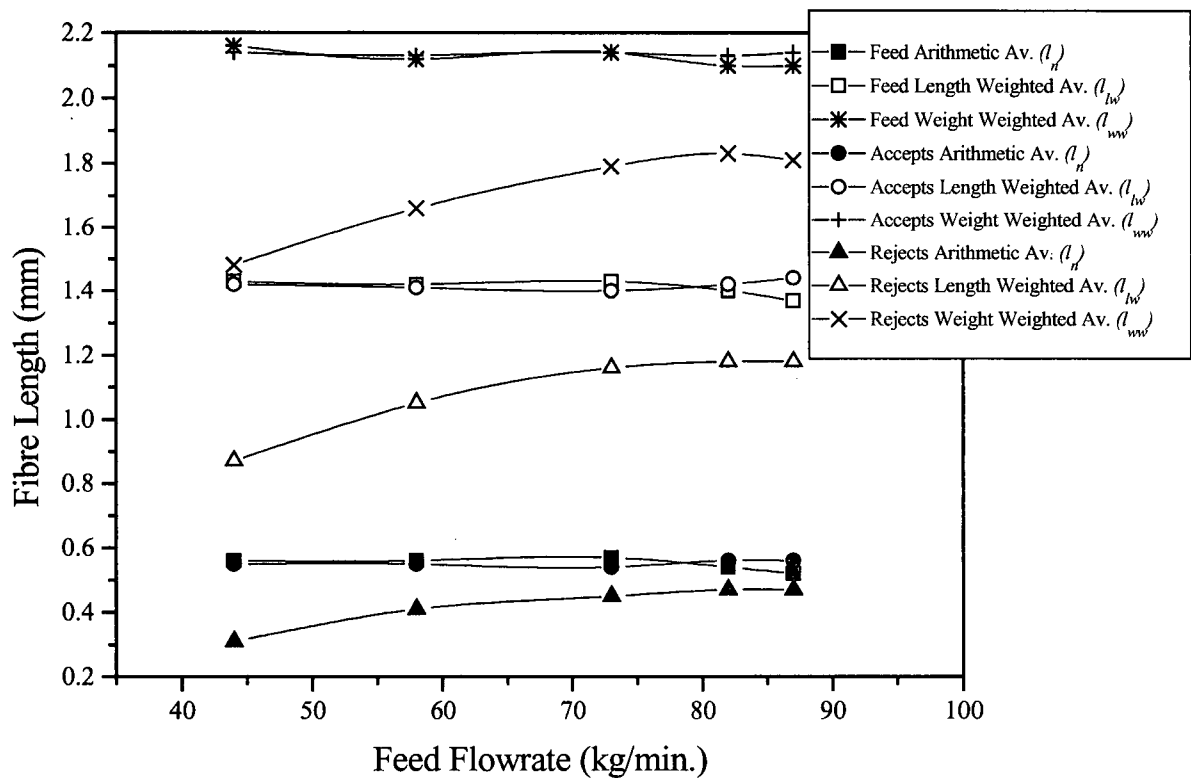


Figure 9 Different Average Fibre Length Measures vs. Feed Flowrate. Hydrocyclone A tested with TMP Pulp Having a Consistency of 0.75%

Shape and width averages measured by the STFI FiberMaster are reported as both arithmetic and length weighted averages (W_n , W_{lw} , SF_n , and SF_{lw}). As with average fibre length measurements, the arithmetic averages of these properties are more sensitive to the fines content of samples than the length weighted average.

The Kajaani FS200 and FQA analyzers used test small masses (~ 5 - 10 mg) of pulp fibres. To minimize errors in measurement we followed a procedure outline by Seth et al. [72] that describes a technique for sample preparation prior to testing for length and coarseness in a fibre analyzer. The method suggests consistent results for length and coarseness can be obtained when samples are debris-free. This method is recommended for chemical wood pulps however, we applied the technique for mechanical wood pulps as well.

3.6 Pulp and Sheet Strength Characterization

Paper strength tests were performed on the handsheets made from the feed, accepts, and rejects streams of the hydrocyclone. The procedures outlined in the CPPA Standard Testing Methods for performance of burst and tear on handsheets were followed for the tests performed in the UBC facility. Test handsheets were prepared as outlined in the standard methods. Table 6 summarizes all the tests methods used for our experimental analysis.

Pulp drainage was characterized by performing the Canadian Standard Freeness (CSF) test. This pulp property is a measure of the rate a pulp sample may be dewatered. In one of the experiments summarized later, a drainage index was measured to infer the freeness behaviour of the pulp tested. This was accomplished by measuring the time the pulp stock drained in a standard handsheet preparation machine. This time was then divided by the sheet basis weight to account for any concentration differences between the samples and the result was defined as the drainage index.

Table 6 CPPA Standard Methods

Procedure	Test	Standard Number
Fibre Treatment	Freeness	C.1
	Forming Handsheets for Physical Tests of Pulp	C.5
	Pulp Disintegration	C.10
Physical Testing	Bursting Strength of Paper	D.8
	Internal Tearing Resistance of Paper, Paperboard, and Pulp Handsheets	D.9

For the facility at STFI, SCAN-test standard procedures were followed. Table 7 summarizes all test procedures used for tests performed at STFI's fractionation pilot plant.

In addition to the tests presented in Table 7, for some of the experiments performed at STFI, our samples were characterized for fines content and water retention value (WRV). Fines content was measured by following TAPPI Standard Method T261. This method describes a device called the Britt Dynamic Jar which is used for determination of fines content in a pulp sample. The WRV is the water retained by a wet pulp sample after centrifuging under specified condition. WRV is express as gram water per gram oven-dry pulp. There is no standard method for the determination of WRV. The method for measurement for our samples involved by centrifuging pulp samples in tubes fitted with screens. The samples were centrifuged at 3000 g forces at 23 °C for a fixed amount of time. A similar technique to that used for our samples is in a paper by Ellis et al [21].

Table 7 SCAN-Test Standard Testing Procedures

SCAN-Test Series	Test	Standard Number
C-Series Test Methods for Chemical and Mechanical Pulp and Wood Chips	Pulp – Preparation of laboratory sheets for optical properties and for physical testing	CM 11:95 CM 26:99 C28:76
	Drainability of pulp by the Canadian freeness method	C 21:65
P-Series Test Methods for Paper and Board	Papers and Boards – Thickness and apparent sheet-density or apparent bulk-density	P 7:96 FP 402 I
	Papers and Boards – Light scattering and light absorption coefficients	P 8:93
	Papers and Boards – Tearing resistance	C:28:76
	Roughness of paper and paperboard determined with the Bendtsen tester	P 21:67
	Paper – Bursting strength and bursting energy absorption	P 24:99 C 28:76
	Paper and Board – Tensile strength, stretch and tensile energy absorption – constant rate of elongation	P 67:93

3.7 Photomicrographs

For some of the experiments qualitative analysis of the fibre samples was performed. For this type of analysis photomicrographs were prepared following appropriate standard methods for characterisation (CPPA Standard Method B.2P and SCAN-test Method G 4:90). Fibre characterisation was performed using a scanning electron microscope (SEM). Analysis of fibres was performed at microscopy facilities located at PAPRICAN (The Pulp and Paper Research Institute of Canada) and STFI (Swedish Pulp and Paper Research Institute).

3.8 Refiner

For one set of experiments refining of fractionated pulp samples was performed. The Escher Wyss Laboratory Refiner was used for these experiments. This is a small, low-angle conical refiner and is similar to a commercial refiner in that the refiner's stator and rotor have a bar and groove pattern.

The refiner tests 500 g (oven-dried basis) pulp samples having a consistency of 3.5%. In our experiments we varied two refining variables. The first variable was the intensity of treatment as measured by the specific edge load (SEL). The second variable was the energy consumption; this variable depends on treatment time and the gap between the stator and rotor. The SEL is calculated from the power input the refiner is operated at and from the cutting edge length, CEL. The CEL is dependent on the speed of the refiner (revolutions per minute, RPM) and on parameters characteristic of the bar pattern of the refiner plates [44]. The energy consumption is dependent on the operating conditions of the refiner (power input, refining time) and the pulp sample size tested. Details on calculation of SEL and power consumption are presented in the operating instructions of the Escher Wyss Refiner [22].

This refiner was used to analyze trends in sheet and fibre properties due to varying refining conditions (SEL and energy consumption). This particular refiner was chosen for our experiments because it is reported to produce properties of refined pulp which are comparable to industrial units [22,78].

Chapter 4

Theoretical Analysis

There are four types of hydrocyclones found in the pulp and paper industry. They are referred to as:

1. Forward Cleaners
2. Core Bleed Cleaners
3. Reverse Cleaners
4. Flow Through Cleaners

Each are designed to remove specific contaminants (shives, plastic particles, low and high density contaminants, and ink) from pulp prior to papermaking. Only forward type cleaners or hydrocyclones are considered in this thesis. In a pulp mill, the role of a forward cleaner is to remove contaminants which have specific gravities greater than 1.0. The specific gravities that have been observed to be separated are in the range of 1 to 5. These hydrocyclones operate at pressure drops in the range of 140 to 200 kPa. In a forward cleaner the centrifugal force on the high specific gravity particle tends to force the particle away from the axis of rotation towards the wall of the hydrocyclone where it becomes entrained in a flow that is moving along the wall of the hydrocyclone towards the exit at the apex of the cone (rejects). Most of the desirable fibres are dragged inward and upward to leave the hydrocyclone via the vortex finder [13,75].

Figure 10 illustrates the flow patterns which exist inside of a hydrocyclone. The flow is three dimensional having velocity components in the axial, radial and tangential directions. Aside from a region near the inlet the flow is symmetric about the central axis of the hydrocyclone. Figure 11 diagrams the fluid velocity pattern in a cross section view through the centre of a hydrocyclone. A particle such as a fibre in an operating hydrocyclone may be subjected to some or all of several forces. These forces include centrifugal, drag, lift, and buoyant forces.

Under the influence of the centrifugal forces, generated by the tangential component of velocity, a particle that is more dense than the fluid in which it is suspended will tend to

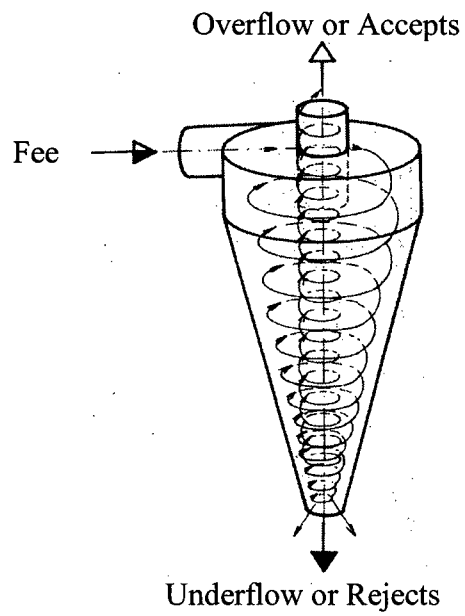


Figure 10 Vortex Flow Pattern Inside a Hydrocyclone [75]

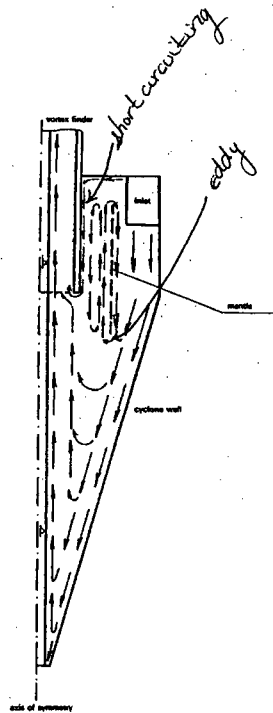


Figure 11 Axial and Radial Flow Patterns Inside a Hydrocyclone [75]

move toward the wall of the hydrocyclone. Conversely a particle which is less dense than the suspending fluid will move inward. Drag forces act in a direction opposite to that of the particle motion. Particles which move into the region near the wall are dragged towards the reject opening at the tip of the conical by the fluid stream that is moving in that direction. Particles which do not make it into the wall region are dragged inward and eventually move towards the vortex finder located at the opposite end of the hydrocyclone and through which the accepts stream flows.

One of the objectives of this thesis is to provide some theoretical evidence which shows how fibre properties (coarseness, specific surface, specific volume, and length) can affect fibre fractionation inside a hydrocyclone. We start by examining particle flow inside of a hydrocyclone. Equation 6 [32] is the result of a force balance on a particle in a centrifugal field which includes centrifugal, buoyant and drag forces,

$$m \frac{dv_{rp}}{dt} = (m - \frac{m\rho}{\rho_p})a - (C_D)(A_p) \frac{\rho v_{rp}^2}{2} \quad (6)$$

Where

m = particle mass

v_{rp} = particle radial velocity

t = time

ρ_p = particle density

ρ = fluid density

a = particle acceleration

C_D = drag coefficient

A_p = projected area of particle on a plane perpendicular to the particle velocity vector

Our theoretical analysis is simplified by omitting the effects of gravity, since its magnitude is insignificant in comparison with other forces involved [13,75]. Also omitted are the effects of the radial and axial components of the fluid velocity in a hydrocyclone and any lift force effects.

In a centrifugal field the particle acceleration is defined as

$$a = r\omega^2 \quad (7)$$

Where

r = radial distance from the axis of rotation

ω = angular velocity

Combining equations 6 and 7 give

$$m \frac{dv_{rp}}{dt} = m \frac{(\rho_p - \rho)}{\rho_p} r\omega^2 - C_D A_p \frac{\rho v_{rp}^2}{2} \quad (8)$$

It has been shown by calculation and by measurement [13,75] that a particle moving in a relatively non-viscous medium like water inside of a hydrocyclone rapidly accelerates to a velocity at which the forces acting on the particle balance one another. The particle then continues to move at constant velocity. If this were the case then one could set the left hand side of equation 4 to zero. This may not be the case for particle movement through a fibre suspension or even for the movement of a single fibre, however in this analysis we will assume this is true. With this assumption Equation 8 simplifies to

$$m \frac{(\rho_p - \rho)}{\rho_p} r\omega^2 = C_D A_p \frac{\rho v_{rp}^2}{2} \quad (9)$$

The next step of this theoretical analysis is to determine how the specific surface of a particle suspended in a fluid is involved in the particle's motion in a centrifugal field. This particle characteristic is important for our theoretical analysis since much of the earlier work in fractionation has concentrated on fractionation based on fibre specific surface [84]. The first

particle geometry considered is a sphere. For this particle we can adopt the Robertson and Mason [68] concept developed for flow through a porous medium consisting of solids which swell in the permeating fluid. With this concept a spherical particle can be described as a swollen solid having a dry density of ρ_f that carries with it some immobilized water that has a density of ρ . This water can be in the fibre lumens or in the fibre walls or even entrapped on the fibre surfaces a result of fibrillar projections from the surface. Our spherical model can be used to represent the behaviour of pulp fines.

Figure 12 is an idealized diagram of a swollen spherical particle. In this figure d_f represents the diameter of the fibre component of the water/fibre composite as it would be in the dry state and d_p represents the effective diameter of the fibre in its swollen state. The volume of water in the fibre (wherever its location in the swollen fibre) would be $(\pi/6)(d_p^3 - d_f^3)$, the volume of the dry fibre would be $(\pi/6)(d_f^3)$.

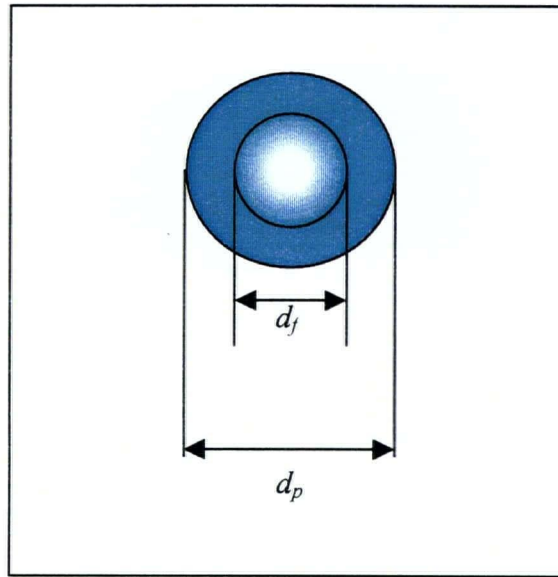


Figure 12 Idealized Spherical Model Representing Pulp Fines

The mass of this particle is

$$m = \frac{\pi}{6}(d_p^3 - d_f^3)\rho + \frac{\pi}{6}d_f^3\rho_f \quad (10)$$

Its projected area is

$$A_p = \frac{\pi}{4} d_p^2 \quad (11)$$

The apparent density of this particle is

$$\rho_p = \frac{\frac{\pi}{6}(d_p^3 - d_f^3)\rho + \frac{\pi}{6}d_f^3\rho_f}{\frac{\pi}{6}d_p^3} = \rho + \left(\frac{d_f}{d_p}\right)^3(\rho_f - \rho) \quad (12)$$

Combining equations 9, 10, 11 and 12 and simplifying gives

$$v_{rp}^2 = \frac{4r\omega^2 d_f^3}{3C_D \rho d_p^2} \left\{ \rho \frac{d_p^3}{d_f^3} + (\rho_f - \rho) \right\} \left\{ \frac{\frac{d_f^3}{d_p^3}(\rho_f - \rho)}{\rho + \left(\frac{d_f}{d_p}\right)^3(\rho_f - \rho)} \right\} \quad (13)$$

The specific surface (surface area per unit dry mass of solids) of a spherical particle is

$$\sigma = \frac{6d_p^2}{\rho_f d_f^3} \quad (14)$$

Its specific volume (volume of composite particle per unit dry mass of solids) is

$$\alpha = \frac{d_p^3}{\rho_f d_f^3} \quad (15)$$

Combining equations 13, 14 and 15 leads to

$$v_{rp}^2 = \frac{8r\omega^2 (\rho_f - \rho)}{C_D \rho \rho_f \sigma} \quad (16)$$

Also,

$$\omega = \frac{v_{\theta}}{r} \quad (17)$$

Where v_{θ} = the tangential fluid velocity. Then equation 15 can be written as

$$v_{rp}^2 = \frac{8v_{\theta}^2(\rho_f - \rho)}{r C_D \rho \rho_f \sigma} \quad (18)$$

White [79] provides semi-empirical, semi-theoretical equation (Equation 19) for the drag coefficient (C_D) of a sphere valid over a Reynolds number (N_{Re}) range of $0 < N_{Re} < 2 \times 10^5$. Measured values of Reynolds numbers have been reported in this range for studies performed in laboratory hydrocyclones [18].

$$C_D = \frac{24}{N_{Re}} + \frac{6}{1 + \sqrt{N_{Re}}} + 0.4 \quad (19)$$

Where

$$N_{Re} = \frac{d_p v_{rp} \rho}{\mu} \quad (20)$$

And μ = liquid viscosity.

Combining equations 14 and 15 gives

$$d_p = \frac{6\alpha}{\sigma} \quad (21)$$

Substituting equations 20 and 21 into 19 results in

$$C_D = \frac{4\mu\sigma}{\alpha\rho v} + \frac{6\sqrt{\mu\sigma}}{\sqrt{\mu\sigma} + \sqrt{6\alpha\rho v_{rp}}} + 0.4 \quad (22)$$

For low Reynolds number equation 22 reduces to

$$C_D = \frac{4\mu\sigma}{\alpha\rho v} \quad (23)$$

Substituting equation 23 into equation 19 gives

$$v_{rp} = \frac{2r\omega^2 (\rho_f - \rho) \alpha}{\mu \rho_f \sigma^2} \quad (24)$$

If we consider high Reynolds numbers, equation 22 simplifies to

$$C_D = 0.4 \quad (25)$$

Substituting equation 25 into equation 16 gives

$$v_{rp}^2 = \frac{20r\omega^2 (\rho_f - \rho)}{\rho \rho_f \sigma} \quad (26)$$

Both equations 24 and 26 indicate that as specific surface (σ) increases the value of the particle velocity (v_{rp}) in the radial direction decreases. So high specific surface area particles move towards the hydrocyclone wall at a slower rate than low specific surface particles. Therefore low specific surface particles have a higher probability of being rejected and high specific surface area particles have a higher probability of being accepted.

The literature review in this thesis has provided several examples [45,69,42,84] of fibre fines reporting in the accepts after fractionating TMP pulp fibres. The review characterizes the fines component of pulp as high specific surface area material [84]. Equations 24 and 26 illustrate that pulp fines will have low radial velocities inside a hydrocyclone and therefore fines are likely to exit through the overflow or accepts stream of a hydrocyclone. Our analysis for fines does provide some agreement with what has been physically observed by several researchers.

A similar analysis can be performed on a fibre subjected to the forces inside of a hydrocyclone. We have represented a fibre to have the geometry of the straight circular cylindrical particle illustrated in Figure 13. This is a rather simplistic model and it should be noted that this geometry is not a realistic geometric model for a wood pulp fibre. However, it does serve to provide some information on fibre separation inside of a hydrocyclone.

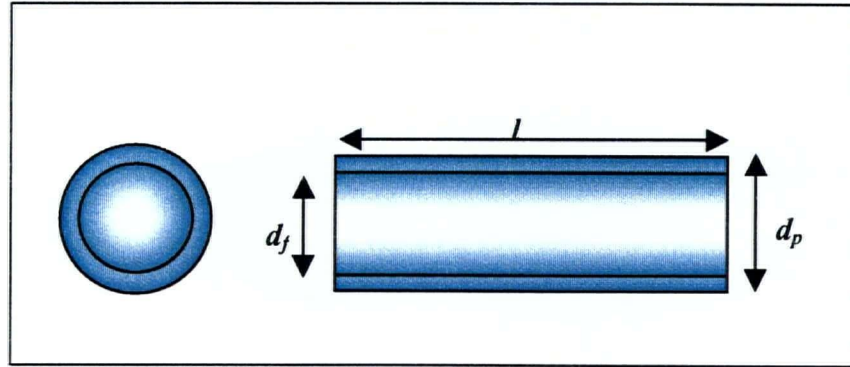


Figure 13 Straight Circular Cylinder Model Representing a Pulp Fibre

The mass of a cylindrical particle is given by

$$m = \frac{\pi l}{4} \{ \rho d_p^2 + (\rho_f - \rho) d_f^2 \} \quad (27)$$

Where l represents the fibre length.

If the fibre is moving so that its length axis is perpendicular to a radius from the centre of rotation of the hydrocyclone its projected area in the flow direction is

$$A_p = d_p l \quad (28)$$

The apparent density is given by

$$\rho_p = \rho + \frac{d_f^2}{d_p^2} (\rho_f - \rho) \quad (29)$$

The specific surface of a cylindrical particle, ignoring the contributions from the cylinder ends, is

$$\sigma = \frac{4d_p}{d_f^2 \rho_f} \quad (30)$$

The specific volume is given by

$$\alpha = \frac{d_p^2}{d_f^2 \rho_f} \quad (31)$$

Combining equations 9, 27, 28, 29, 30 and 31 gives

$$v_{rp}^2 = \frac{2\pi r \omega^2 (\rho_f - \rho)}{C_D \rho \rho_f \sigma} \quad (32)$$

White [79] records an empirical equation for the drag coefficient for flow across a cylinder which is

$$C_D = 1 + \frac{10}{N_{Re}^{2/3}} \quad (33)$$

Combining equations 30 and 31 we can show that particle diameter can be defined as

$$d_p = \frac{4\alpha}{\sigma} \quad (34)$$

Substituting equation 34 into 33 gives

$$C_D = 1 + \frac{10.0(\mu\sigma)^{2/3}}{(4\alpha\rho v)^{2/3}} \quad (35)$$

For high values of Reynolds number, equation 35 reduces to

$$C_D = 1 \quad (36)$$

Introducing equation 36 into equation 32 results in

$$v_{rp}^2 = \frac{2\pi r \omega^2 (\rho_f - \rho)}{\rho \rho_f \sigma} \quad (37)$$

If we consider low values of Reynolds numbers, equation 31 becomes

$$C_D = \frac{3.97(\mu\sigma)^{2/3}}{(\alpha\rho\nu)^{2/3}} \quad (38)$$

Combining equations 32 and 38

$$v_{rp}^{4/3} = \frac{2\pi r \omega^2 \alpha^{2/3} (\rho_f - \rho)}{3.97 \mu^{2/3} \rho^{1/3} \rho_f \sigma^{2/3}} \quad (39)$$

Once again equations 37 and 39 show, for a cylinder oriented with its length axis perpendicular to a radius from the centre of rotation, that as specific surface becomes larger the particle velocity in the radial direction becomes smaller.

If our cylindrical particle is oriented such that its length axis is oriented along the radius instead of perpendicular to it, then the projected area is

$$A_p = \frac{\pi d_p^2}{4} \quad (40)$$

Equation 40 results in a radial particle velocity relation of

$$v_{rp}^2 = \frac{2l \omega^2 (\rho_f - \rho)}{C_D \rho \rho_f \alpha} \quad (41)$$

Happel and Brenner [29] have derived an equation for the drag force per unit length on a solid cylinder (diameter = d_p) moving at the core of a fluid cylinder (diameter = d_a). At radius = $d_a/2$, the shear stress in the fluid = 0. If we assume our cylindrical particle orientation follows accordingly to the observations of Happel and Brenner, the drag force on the cylinder is

$$F_D = \frac{2\pi l \mu v_{rp}}{\ln\left(\frac{d_a}{d_p}\right) + \frac{3}{4}} \quad (42)$$

By definition

$$F_D = C_D A_p \frac{\rho v_{rp}^2}{2} = C_D \frac{\pi}{4} d_p^2 \frac{\rho v_{rp}^2}{2} \quad (43)$$

From equations 42 and 43

$$C_D = \frac{16\mu l}{\rho v_{rp} d_p^2 \left[\ln\left(\frac{d_a}{d_p}\right) + \frac{3}{4} \right]} \quad (44)$$

Combining equations 34 and 44 give

$$C_D = \frac{\mu l \sigma^2}{\left[\ln\left(\frac{\sigma d_a}{4\alpha}\right) + \frac{3}{4} \right] \alpha^2 \rho v_{rp}} \quad (45)$$

Then equations 41 and 45 show

$$v_{rp} = \frac{2r\omega^2 (\rho_f - \rho) \alpha \left[\ln\left(\frac{d_a \sigma}{4\alpha}\right) + \frac{3}{4} \right]}{\rho_f \mu \sigma^2} \quad (46)$$

Therefore once again we see that the particle's radial velocity gets smaller as specific surface increases. This observation is independent of fibre orientation inside of the hydrocyclone. However, it should be noted that recent work on the measurement of drag coefficients of

fibres in a centrifugal field showed that fibres are usually oriented such that its length axis is perpendicular to the radius from the centre of rotation [80].

Our analysis on cylindrical model also provides some support for the findings in our literature review. Wood and Karnis have shown that low specific surface material is found in the rejects or underflow. Equations 37, 39, and 46 all show that particles with low specific surface have high radial velocities, this translates to these particles reporting to the flow closer to the hydrocyclone wall where they will exit through the underflow or rejects stream. Therefore our cylindrical model does provide some theoretical explanation to the experimental findings in the literature reviewed.

Interestingly, in our cylindrical model, fibre length does not appear as in our derived radial velocity relations. In some of the literature reviewed, long fibres tended to concentrate in the underflow or rejects [45,46]. Some others say short fibres go to the rejects [30,63,28,51]. The fact that length does not appear in our calculations may be due to our simple approach. Others have speculated that length differences result as secondary effects, this possibility has not been explored in our theoretical analysis. Others are currently working on a theoretical approach that incorporates the effect of length on pulp fractionation [32].

It is also worth mentioning the relation between pulp freeness and specific surface. We have shown above that particle radial velocity is inversely proportional to specific surface. El-Hosseiny et al. [20] have presented a theory which states specific surface is inversely proportional to freeness. Relating this to our theory then leads to the conclusion that low freeness material exiting via the overflow or accepts and high freeness material should exit via the rejects stream of a hydrocyclone. This has been observed by various researchers [41,45,84] in the literature reviewed. We can thus use the theory of El-Hosseiny to infer fibre specific surface trends from freeness values.

The literature reviewed also provides observations which show that hydrocyclones can fractionate based on coarseness. Now let us determine if we can provide some theoretical

explanation as to how hydrocyclones are capable of fractionating based on this fibre property.

Fibre coarseness is defined as the dry weight of fibre per unit length [73]. If we choose a cylinder as a representative geometry for a fibre, then coarseness can be defined as

$$C = \frac{\frac{\pi}{4} d_f^2 l \rho_f}{l} = \frac{\pi}{4} d_f^2 \rho_f \quad (47)$$

Where

C = fibre coarseness

d_f = fibre diameter

ρ_f = fibre density

Combining equations 35, 36, and 39 with 47 gives

$$C = \frac{4\pi\alpha}{\sigma^2} \quad (48)$$

Equation 48 relates coarseness specific volume and specific surface. We see that an inverse relationship exists for fibre coarseness and specific surface. Figure 14 plots fibre coarseness measured by the TAPPI T234 [76] method vs. specific surface as measured by the Robertson and Mason [68] technique, which also generated values for specific volume, for two types of pulp [14]. One was a pulp made from wheat straw which was cooked for 1 hour in a 5% NaOH solution, washed with water and then refined to various levels of intensity in a 12 inch, Sprout Waldron lab refiner. The other pulp was made from Aspen chips using a lab model Asplund Defibrator. This pulp was also refined to various degrees in a lab refiner. The curves of Figure 14 support qualitatively the form of equation 44 in that coarseness varies inversely in a non-linear way with specific surface. But equation 44 does not fit the data quantitatively, which may be due to our representing a refiner treated fibre as a simple cylinder.

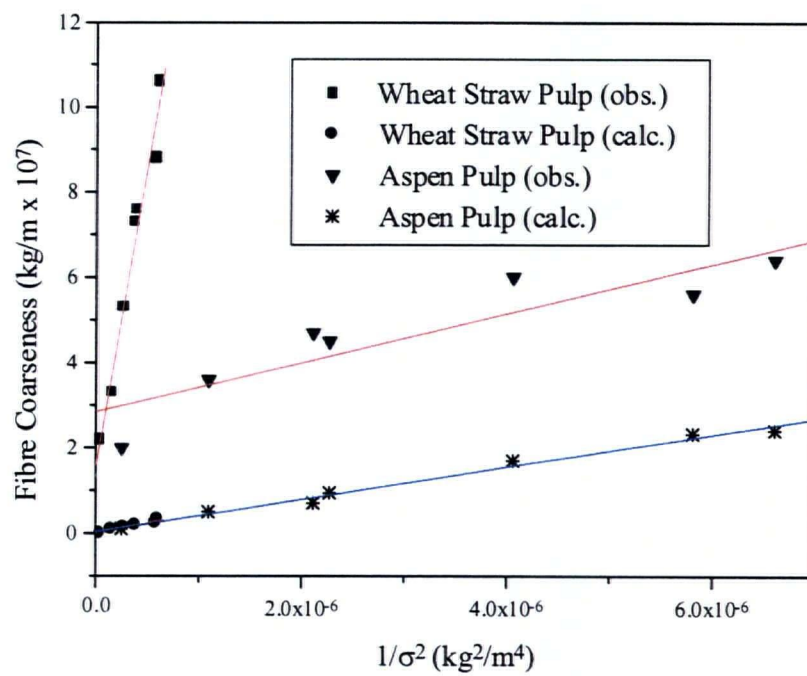


Figure 14 Fibre Coarseness vs. Specific Surface for Wheat Straw and Aspen Pulps

CHAPTER 5

Results and Discussion

5.1 Overview

Section 5.2 describes our initial experiments performed testing Hydrocyclones A and B. Section 5.3 explores the fractionating capabilities of Hydrocyclone A. Experiments testing various pulps are summarized.

Section 5.4 investigates the effects reject ratio has on fractionation. This variable is tested on two different pulps, Hydrocyclone A was used in this set of experiments.

Section 5.5 reports findings on how consistency can effect length fractionation.

Section 5.6 details experiments where fractionation was performed in multiple stages to investigate how much separation can be achieved in Hydrocyclone A.

Section 5.7 summarizes experiments performed using Hydrocyclone C. This section also details a refining study performed on fractionated streams.

5.2 Fractionation of TMP

5.2.1 Fractionating TMP_A in Hydrocyclone A

The experimental program of this thesis began with a summer student project to investigate fibre length distributions in the feed, accepts and rejects streams to and from a hydrocyclone (Hydrocyclone A) using a Kajaani FS200 fibre length analyzer to measure length distributions. This project showed that there were differences in these distributions and that the mean rejects fibre length tended to be shorter than the mean accepts fibre length [62]. Later, a review of the literature showed that when several commercial hydrocyclones were tested, all showed separation under particular operating conditions [45,28,58]. Clearly then the initial experiments for this thesis involved determining what operating conditions of the commercial hydrocyclones, available to us, produced fractionation.

We began with Hydrocyclone A. For the first experiment, market grade thermomechanical pulp obtained from an Eastern Canadian mill was tested, this pulp will be referred to as TMP_A (See Table 5, Chapter 3). This TMP_A having a consistency of 0.65% was pumped through Hydrocyclone A. The feed flowrate vs. pressure drop relationship is shown in Figure 15. The pressure drop is the difference between the feed pressure and accepts pressure; the rejects nozzle was open to the atmosphere so the pressure there was atmospheric. Figure 15 shows that pressure drop increased with increasing feed flowrate. Note that consistency, within the range of consistencies studied, was not important in relating flowrate to pressure drop [27].

Figure 16 shows the reject ratio (volumetric) vs. pressure drop relationship. The reject ratio (volumetric) is the ratio of the rejects flowrate to the feed flowrate. For the consistency used in this particular experiment, 0.65%, the reject ratio was found to decrease and then level off as the pressure drop across the cleaner increased. For Hydrocyclone A the rejects ratio was always rather low (3.5 – 4.5%), in this experiment and in ones done later.

Figure 17 plots thickening ratio vs. pressure drop. Thickening ratio is indicative of cleaner performance. It is the ratio of the rejects consistency to the feed consistency. Figure 17 shows that increasing the feed flowrate increased the thickening ratio. Increasing the pressure drop in a hydrocyclone results in a greater inlet velocity and hence greater centrifugal forces acting on the fibres in the cleaner. These cause fibres in the cleaner to be more concentrated at the wall resulting in a greater rejects consistency [27]. A thickening ratio equal to 1.0 indicates that the hydrocyclone is simply acting as a flow splitting device with no separating power. A thickening ratio less than 1 implies that the accepts are more concentrated than the feed. This condition was observed when Hydrocyclone A was operated at flowrates less than 70 kg/min. (see Figure 17).

Figure 18 is a plot of the mass of fibre rejected per unit time divided by the mass of fibre fed into the hydrocyclone per unit time vs. feed flowrate. This ratio is also referred to as the mass reject ratio. It is also the product of the volumetric reject ratio and the thickening ratio.

The mass fraction fibre rejected for Hydrocyclone A, as operated in these experiments ranged from 3 – 6%, a rather low range. This implies that the bulk of the feed which entered the hydrocyclone exited via the accepts stream

Fibre length measurements are summarized in Figure 19. The arithmetic average fibre lengths of the accepts and rejects streams are shown as functions of feed flowrate. At the various flowrates studied, the arithmetic average lengths of the rejects fibres were shorter than those of the accepts. The arithmetic average lengths of the accepts measured at flowrates less than 72 kg/min. did not differ by much from those of the feed (0.78 - 0.80 mm). However at flowrates greater than 61 kg/min., fibre lengths of the accepts were in the range 0.85 – 0.90 mm, this was slightly greater than the feed. Since the bulk of the feed which entered the hydrocyclone exited through the accepts, significant changes were only detected in the rejects stream. In some of the literature reviewed earlier, fractionation led to the preferential rejection of long fibres and therefore our results for fibre lengths are not consistent with those findings. In some of the work reviewed in Chapter 2 similar results to those found here were reported, i.e. preferential rejection of short fibres. This can be attributed to different types of hydrocyclone design.

Fibre coarseness results are shown in Figure 20 At feed flowrates less than 72 kg/min., the coarseness of the rejects fibres was found to be around 0.56 mg/m whereas the accepts fibre coarseness was 0.29 mg/m. Coarseness values of the accepts fibres and feed

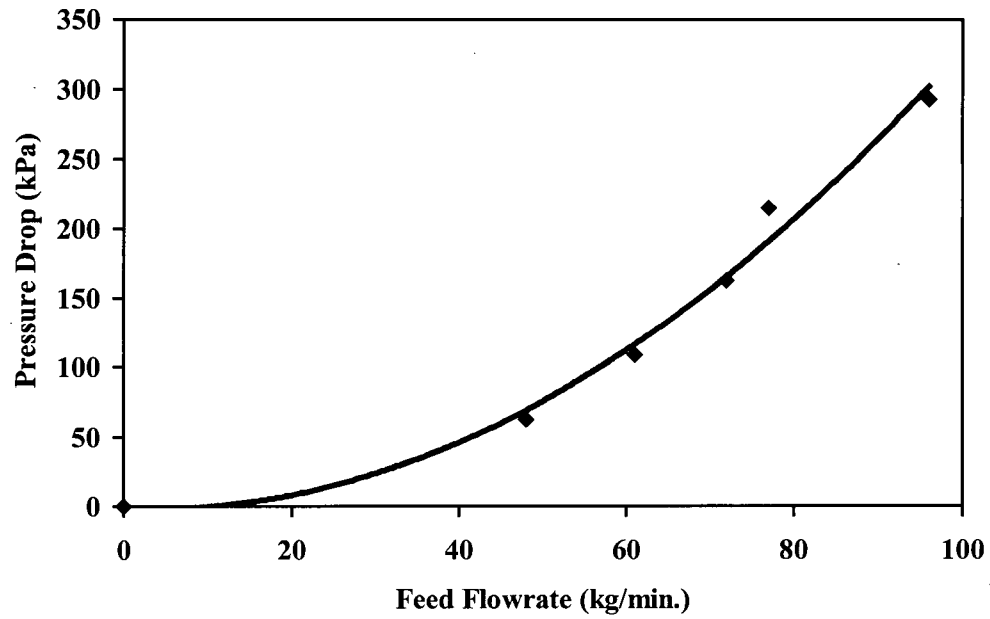


Figure 15 Pressure Drop versus Feed Flowrate for TMP_A Fractionated in Hydrocyclone A
(Pulp Consistency Tested: 0.65%)

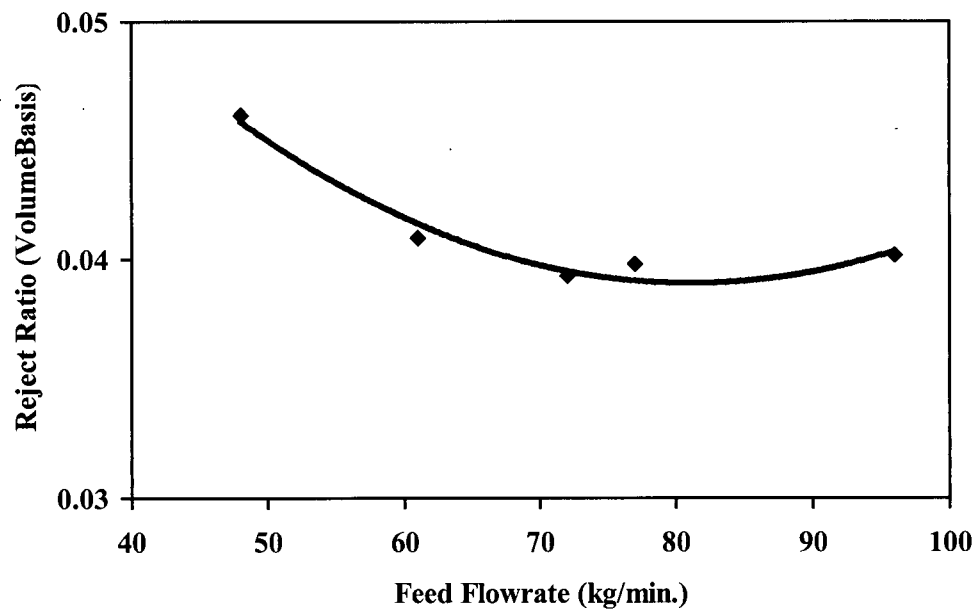


Figure 16 Reject Ratio versus Feed Flowrate Relationship for Fractionation of TMP_A in
Hydrocyclone A

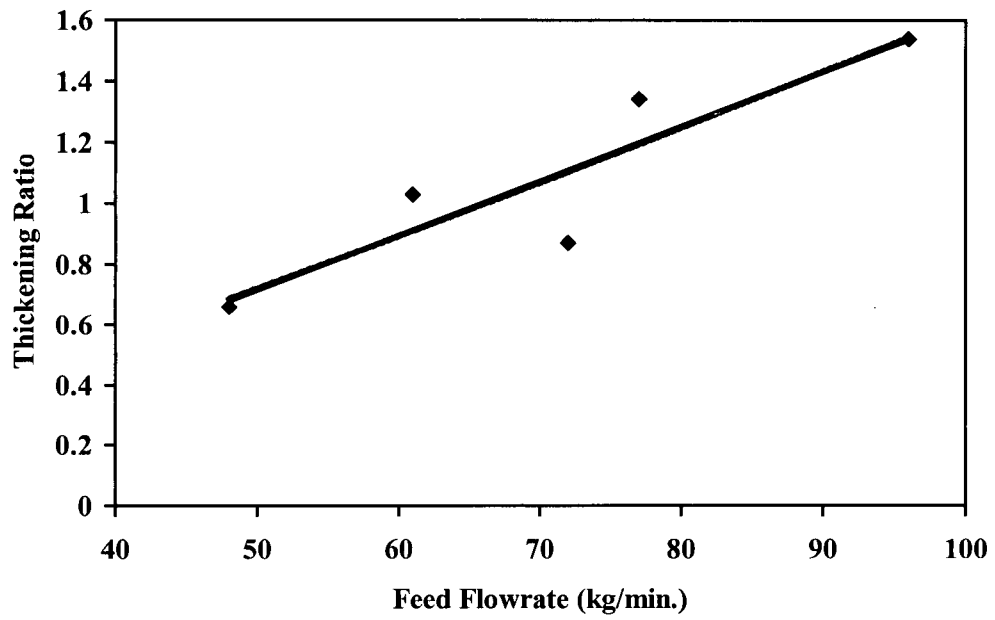


Figure 17 Thickening Ratio versus Feed Flowrate (TMP_A Fractionated in Hydrocyclone A at Consistency of 0.65%)

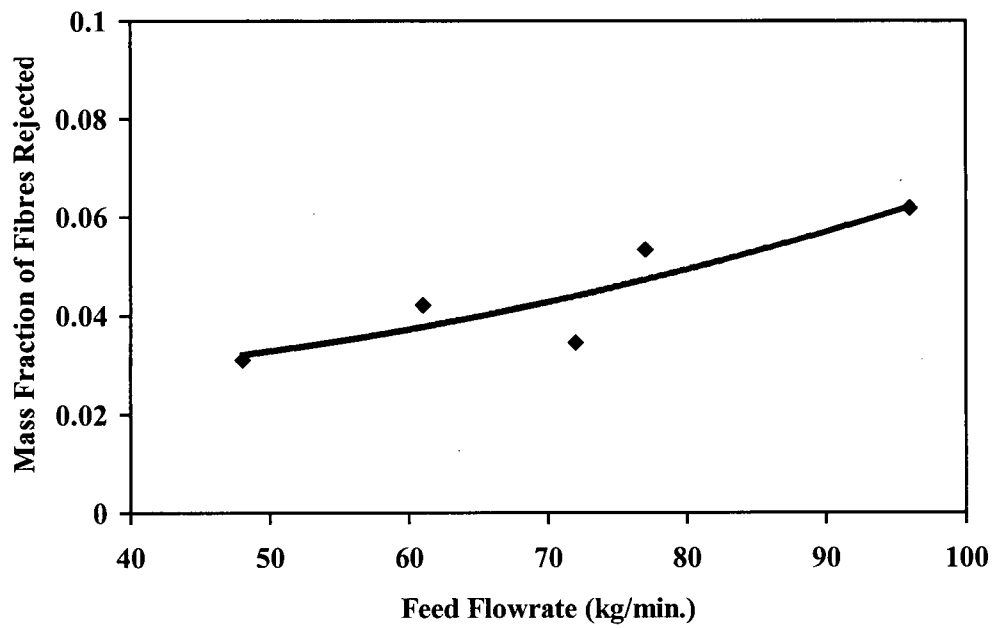


Figure 18 Mass Fraction Fibres Rejected Fractionating TMP_A in Hydrocyclone A

fibres were found to be more or less the same. Since the mass reject rate was low, changes in fibre properties were mainly detected only in the rejects stream. These fibre length and fibre coarseness results indicated that at low feed flowrates (< 75 kg/min.) Hydrocyclone A rejected short, coarse (stiff) fibres. At higher flowrates (> 75 kg/min.) there wasn't much difference between accepts and rejects coarseness values, but fibre lengths in the rejects were shorter.

Handsheets were formed from pulp samples obtained from the accepts and rejects streams at various flowrates. The results are presented in Figures 21 and 22. Burst index values and tear index values were found to be smaller for handsheets made from reject stream samples than for accepts samples. As feed flowrate increased, burst and tear indices for the rejects stream were found to increase up to a flowrate of 61 kg/min. and then decreased as the flow increased. Tear index values for the rejects sheets were constant with increasing flowrate up to 72 kg/min. At that point they sharply increased and remained constant with flowrate. Figure 21 shows that the accepts stream burst index values decreased at feed flowrates greater than 72 kg/min. This may have occurred because more short or coarse fibres, with poor sheet making characteristics, were being accepted at the higher flowrates. The burst and tear test results are consistent with our measurements of fibre length and coarseness. Short, stiff fibres are expected to yield poor sheet properties.

5.2.2 Fractionating TMP_A in Hydrocyclone B

Pulp TMP_A was also fractionated in another commercial cleaner, Hydrocyclone B. For this experiment a pulp consistency of 0.6% was tested. Figure 23 illustrates the relationship between feed flowrate and pressure drop. The maximum operating pressure drop of this hydrocyclone was 200 kPa, which was significantly lower than that of Hydrocyclone A (290 kPa, see Figure 15).

Figure 24 shows the reject ratio and feed flowrate relationship for Hydrocyclone B. This hydrocyclone produced a greater reject ratio at the various flowrates tested than

Hydrocyclone A (compare to Figure 16). For example, at a feed flowrate of 95 kg/min. Hydrocyclone A produced a reject ratio of 0.042 whereas Hydrocyclone B produced a ratio of 0.14. These differences are due to differences in their geometries. Note also that as flowrate increased, the reject ratio for Hydrocyclone A decreased slightly whereas for Hydrocyclone B it increased more significantly.

Figure 25 plots the thickening ratio as a function of flowrate. The thickening ratio was found to increase more or less linearly with increasing flow as did the thickening ratio for Hydrocyclone A. Over a flowrate range of 70 – 145 kg/min. the thickening ratio of Hydrocyclone B went from 0.9 – 2.1. For Hydrocyclone A a change in flowrate from 48 – 97 kg/min. brought about an increase in thickening ratio of 0.65 to 1.5. The slopes of Figures 17 and 25 indicate that Hydrocyclone A was slightly more effective in thickening the rejects than Hydrocyclone B but since the feed consistency for Hydrocyclone A (0.65%) was some what higher than for Hydrocyclone B (0.60%), this difference is probably negligible.

The higher reject rates observed with Hydrocyclone B resulted in a higher fraction of fibres being rejected (see Figure 26). At a flowrate of 95 kg/min., Hydrocyclone A rejected a fibre mass fraction of 0.058. At the same flowrate, Hydrocyclone B rejected a mass fraction of 0.15. Again these observations are attributable to the differences in the geometries of both hydrocyclones.

Figure 27 plots the fibre lengths of feed, accepts, and rejects for the various flowrates tested. At flowrates less than 100 kg/min., fibre lengths of the rejects were slightly smaller than for the accepts. Increases in flowrate resulted in no differences in length. The differences in fibre length are not appreciable in this test and therefore fractionation based on length did not occur.

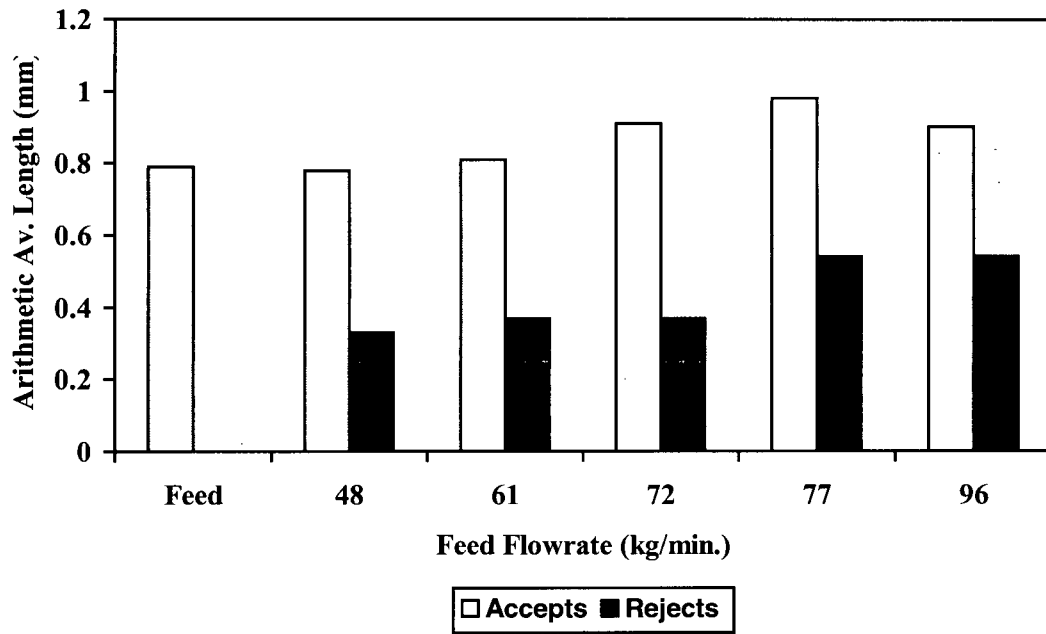


Figure 19 Fibre Length Results for TMP_A Fractionation in Hydrocyclone A

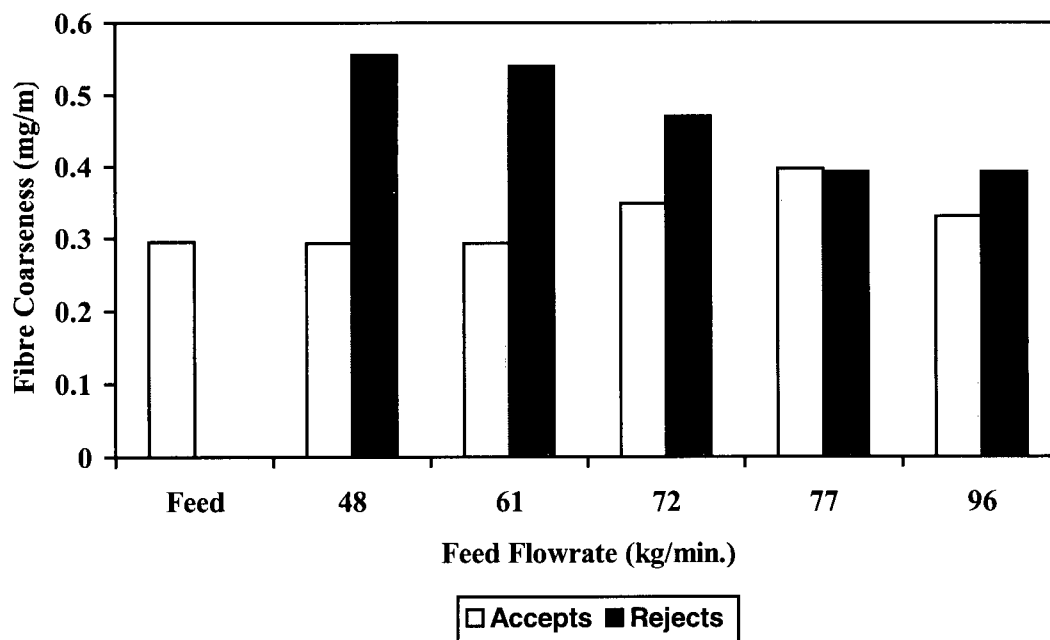


Figure 20 Fibre Coarseness Measurements for Fractionation of TMP_A in Hydrocyclone A

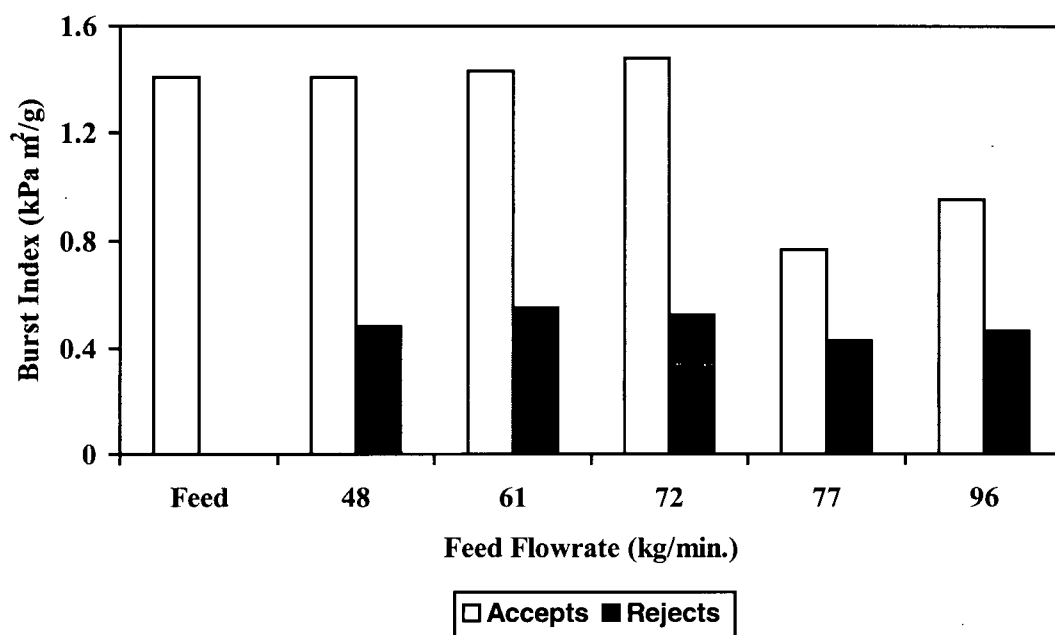


Figure 21 Burst Index Values for Accepts and Rejects for Fractionation of TMP_A in Hydrocyclone A

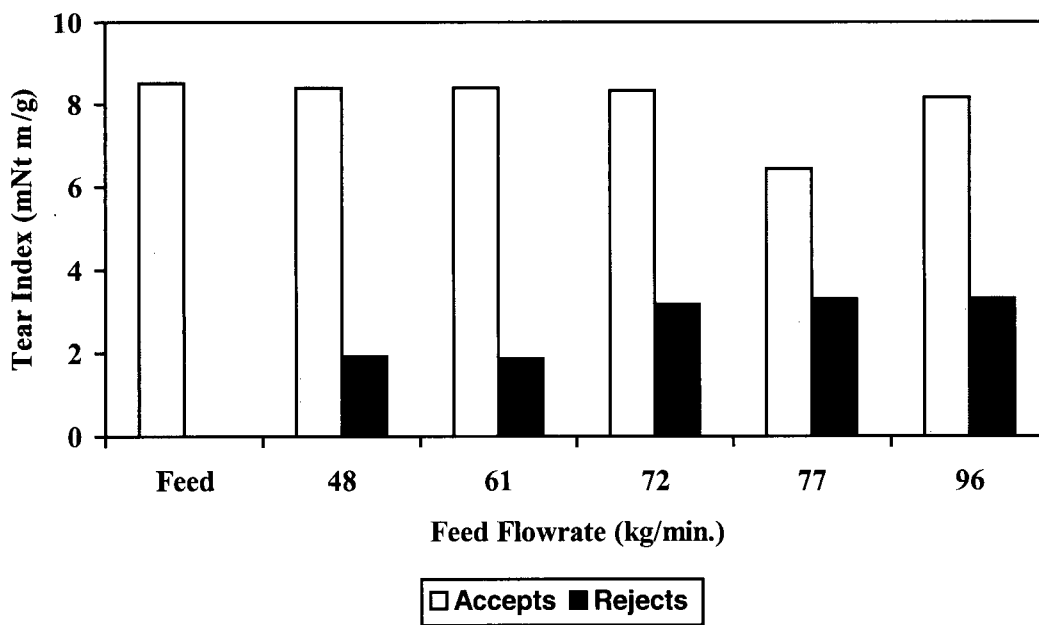


Figure 22 Tear Index Values for Accepts and Rejects for Fractionation of TMP_A in Hydrocyclone A

Figure 28 plots the coarseness values for feed, accepts, and rejects. The rejects fibres had greater coarseness values than both accepts and feed. The difference between accepts and rejects decreased as the feed flowrate increased.

Figures 29 and 30 illustrate the differences in sheet properties of fibres from the accepts and rejects. Accepts burst indices were greater for the accepts than for the feed and the rejects were the lowest. The coarse fibres of the rejects stream were incapable of producing a well bonded sheet and hence produce lower sheet strength. Burst index values of the accepts decreased with increasing flowrate. Tear index values showed that sheets made from fibres from the rejects stream produced lower tear indices than the feed stream. For flowrates of 90 and 120 kg/min. the accepts fibres produced greater tear indices than the feed.

5.3 Fractionation of Other Pulp Types with Hydrocyclone A

The literature review of Chapter 2 indicates that there is universal agreement that hydrocyclones can fractionate based on differences in fibre coarseness. Thus hydrocyclones tend to reject coarse fibres. There is not universal agreement about whether hydrocyclones tend to reject short fibres or long fibres. Our tests showed Hydrocyclone A tends to reject short fibres. Work done in our research group [32] using known two component mixtures of nylon fibres having known fibre lengths and coarseness, has shown that Hydrocyclone A tends to reject short, coarse fibres. Separating coarse fibres from fine fibres, all with same fibre length, is easier than separating short fibres from long fibres all with the same coarseness. From an economic standpoint, the higher reject rates of Hydrocyclone B make it more favourable than Hydrocyclone A in that it produces more of the rejects stream that would go on to further processing. However, our initial findings with Hydrocyclone A indicated that it was superior in being able to fractionate on the basis of fibre length differences. So further

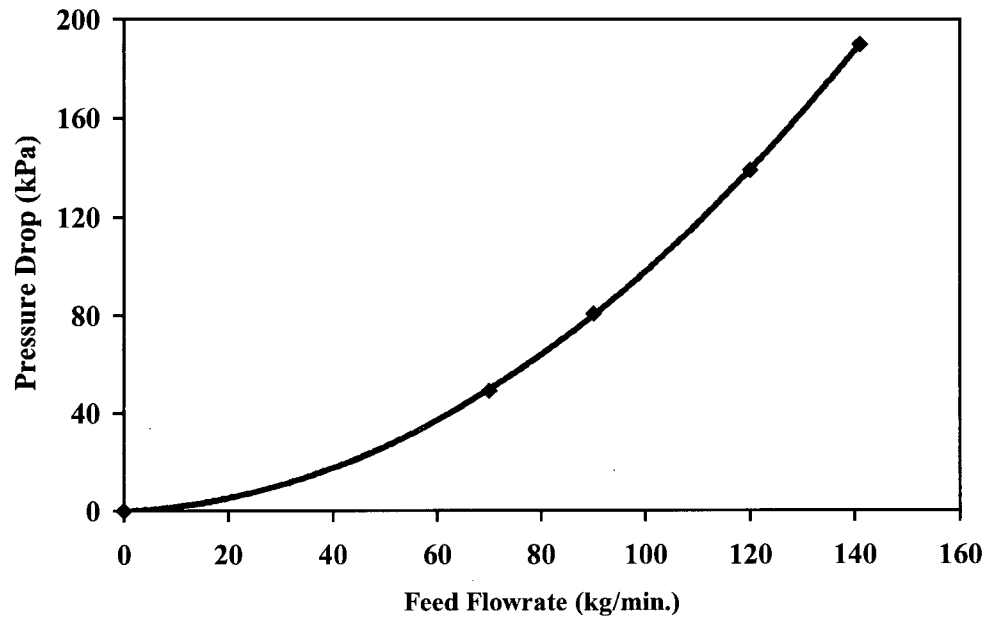


Figure 23 Pressure Drop versus Feed Flowrate for TMP_A Fractionated in Hydrocyclone B
(Pulp Consistency Tested: 0.60%)

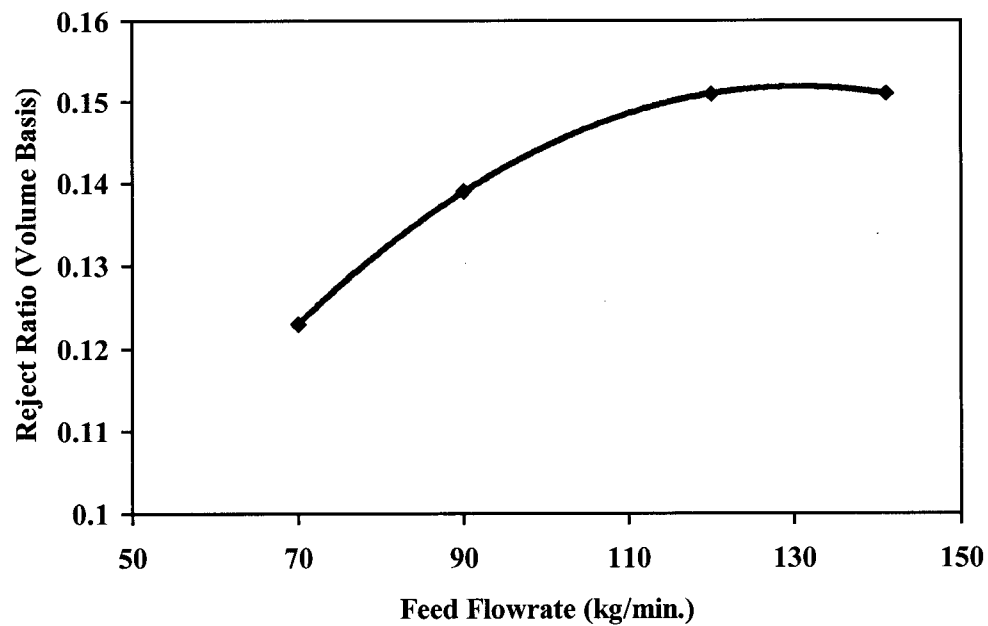


Figure 24 Reject Ratio versus Feed Flowrate Relationship for Fractionation of TMP_A in
Hydrocyclone B

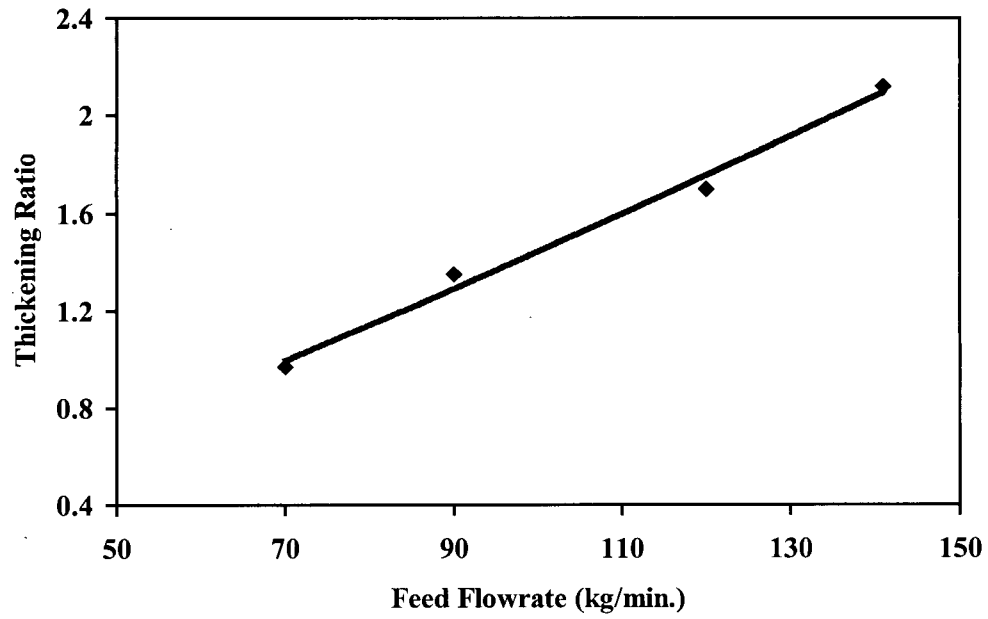


Figure 25 Thickening Ratio versus Feed Flowrate (TMP_A Fractionated in Hydrocyclone B at Consistency of 0.60%)

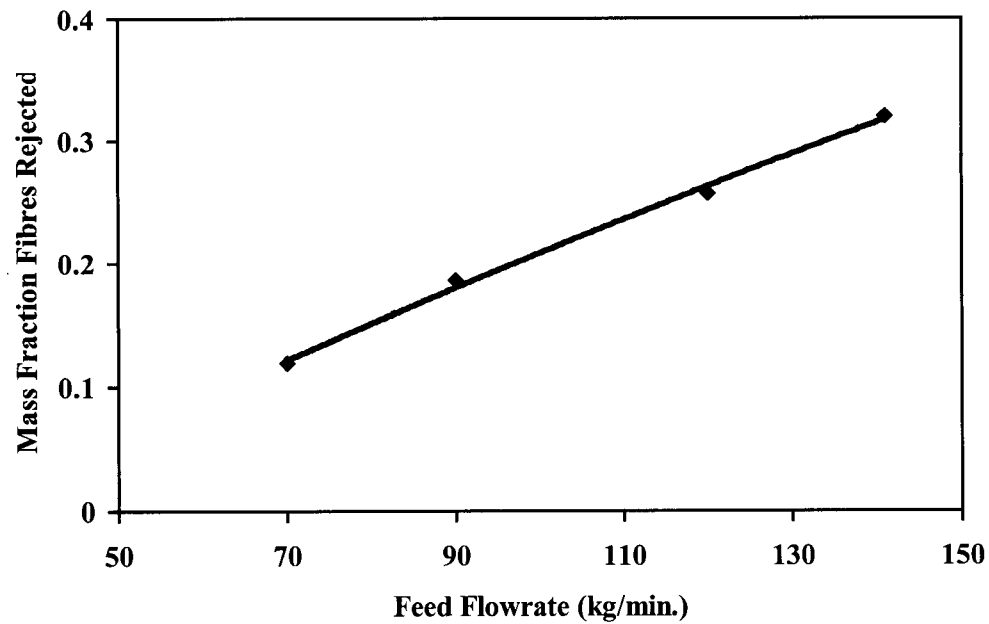


Figure 26 Mass Fraction Fibres Rejected Fractionating TMP_A in Hydrocyclone B

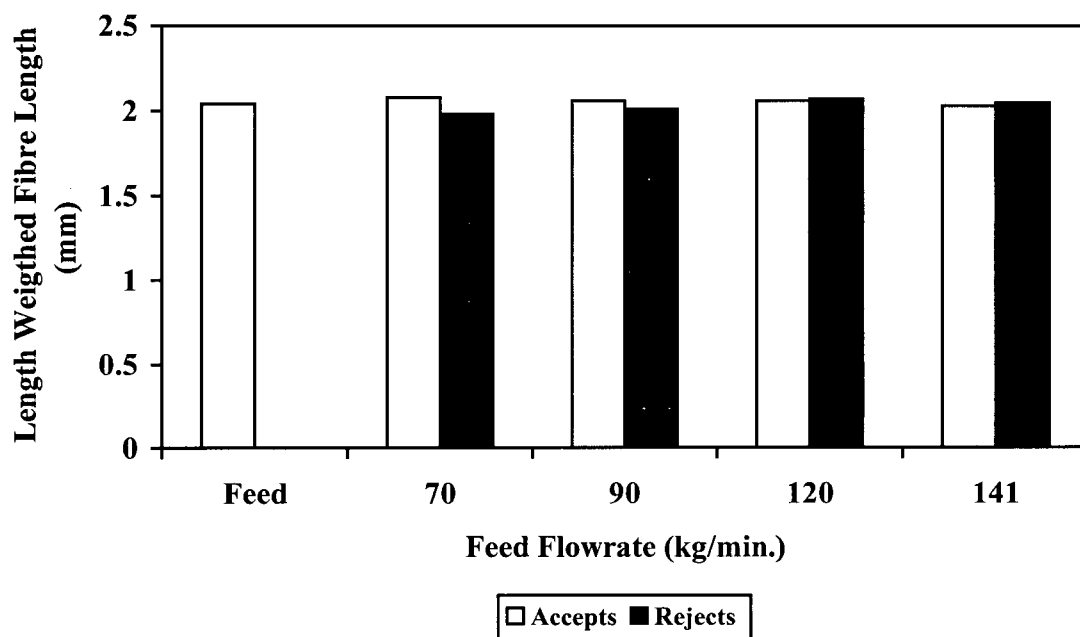


Figure 27 Fibre Length Results for TMP_A Fractionation in Hydrocyclone B

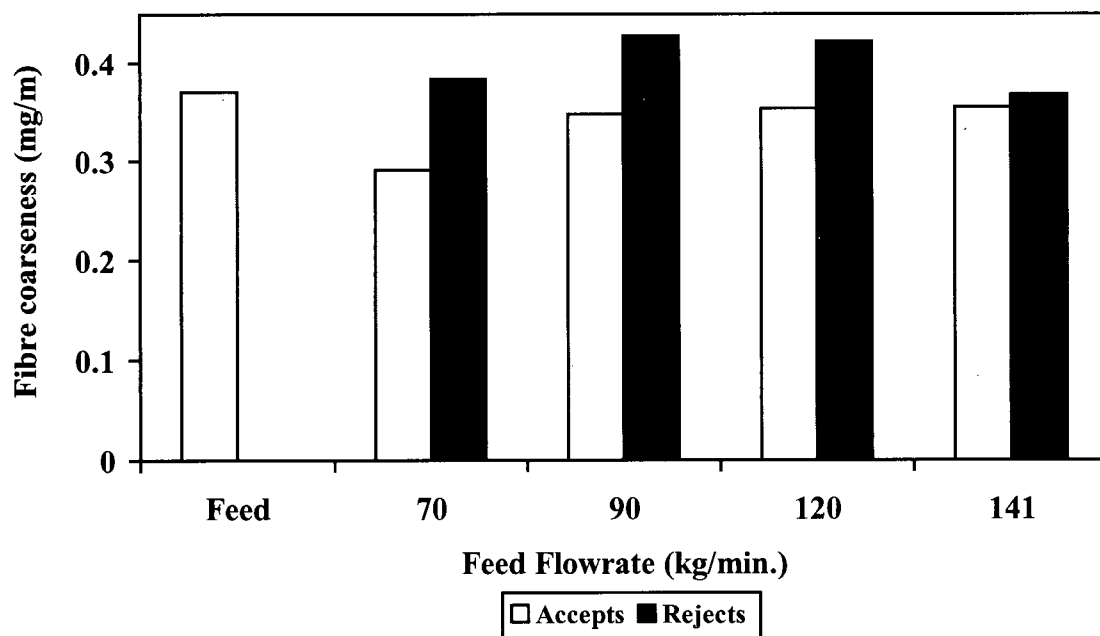


Figure 28 Fibre Coarseness Measurements for Fractionation of TMP_A in Hydrocyclone B

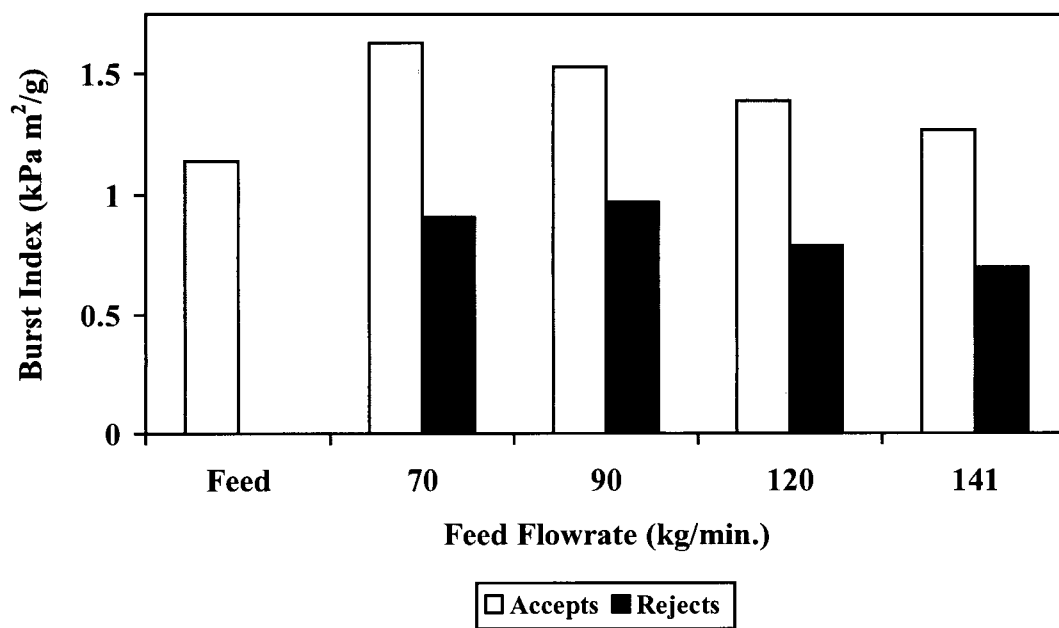


Figure 29 Burst Index Values for Fractionation of TMP_A in Hydrocyclone B

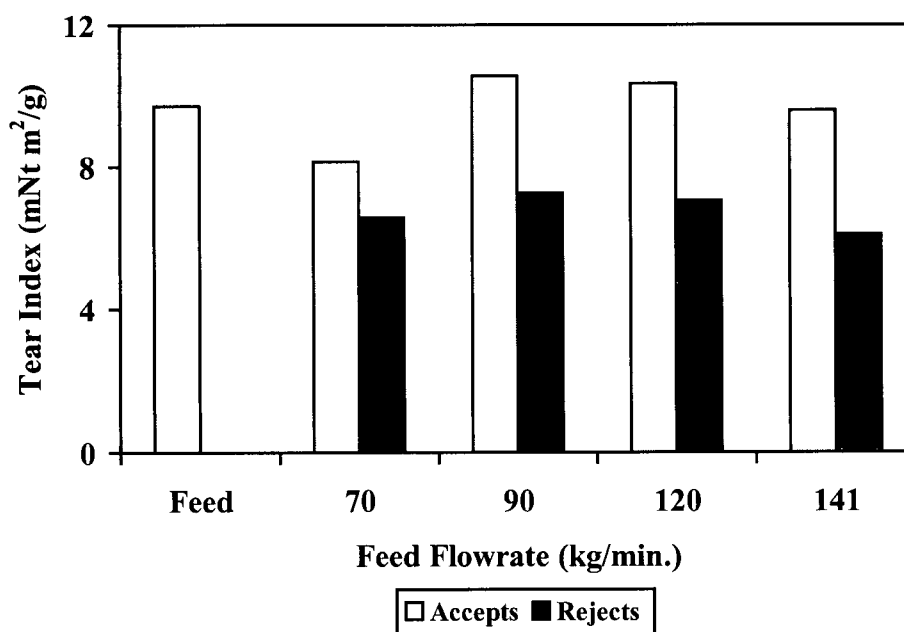


Figure 30 Tear Index Results for TMP_A Fractionation in Hydrocyclone B

studies following the initial experiments summarized in Section 5.2.1 were performed at the UBC Test Facility focussing on exploring the fractionating capabilities of Hydrocyclone A. The following sections will summarize our experiences of operating Hydrocyclone A. We began by testing this hydrocyclone with different pulp types.

5.3.1 Fractionation of CTMP_A and CTMP_B

Fractionation in Hydrocyclone A was also performed with chemithermomechanical pulp (CTMP) having a consistency of 0.65%. The fibre fractionation results are summarized in Figure 31. The arithmetic average fibre length of the accepts and rejects are shown as functions of feed flowrate. The arithmetic average lengths of the rejects were always shorter than those of the accepts. Once again, arithmetic average lengths of the accepts did not significantly differ from those of the feed (0.55 – 0.60 mm). As the feed flowrate increased the differences between the accepts and rejects fibre lengths decreased.

Fibre coarseness results are shown in Figure 32. At feed flowrates less than 58 kg/min., the coarseness of the rejects were found to be greater than the accepts fibre coarseness. Coarseness values of the accepts fibres and feed fibres were found to be similar. Both TMP and CTMP fractionation experiments indicated that at low feed flowrates Hydrocyclone A rejected short, coarse fibres. At the higher feed flowrates there was little difference in coarseness between accepts and rejects.

Handsheets were formed from the pulp samples obtained from the accepts and rejects streams at various feed flowrates and tested for bursting strength (see Figure 33). Burst index values were smaller for handsheets made from the rejects stream than those made from the accepts stream. Figure 32 shows that for flowrates greater than 58 kg/min. the rejects and accepts coarseness values were similar however the burst index values illustrated in Figure 33 showed differences between accepts and rejects for the range of flowrates studied. Perhaps the burst strength differences for the rejects and accepts mean

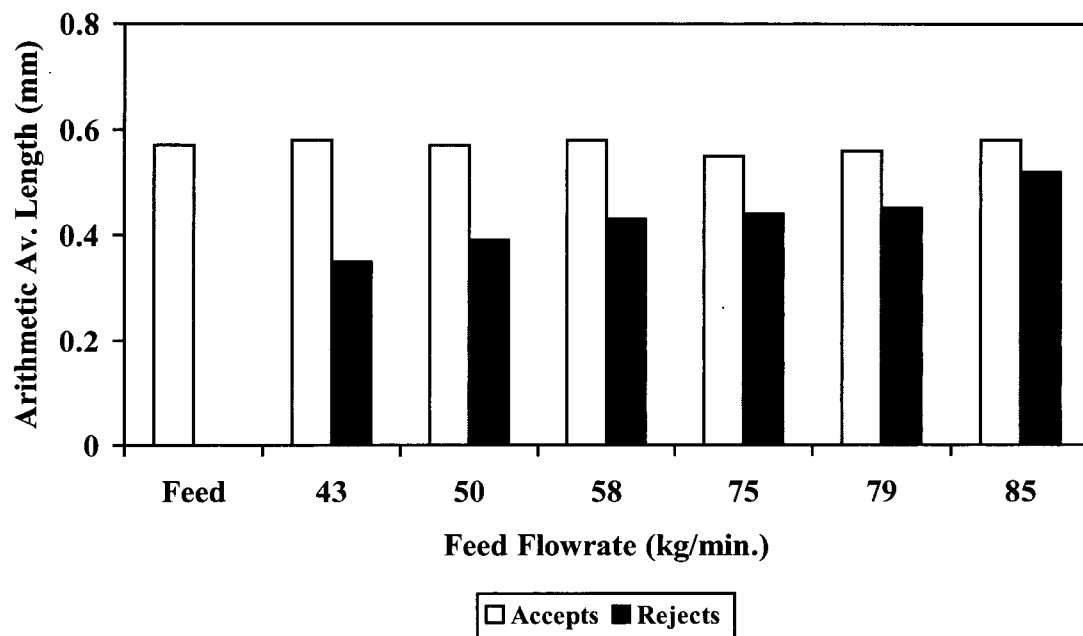


Figure 31 Arithmetic Average Length Values for Accepts and Rejects Stream for CTMP_A
(Pulp Consistency: 0.65%)

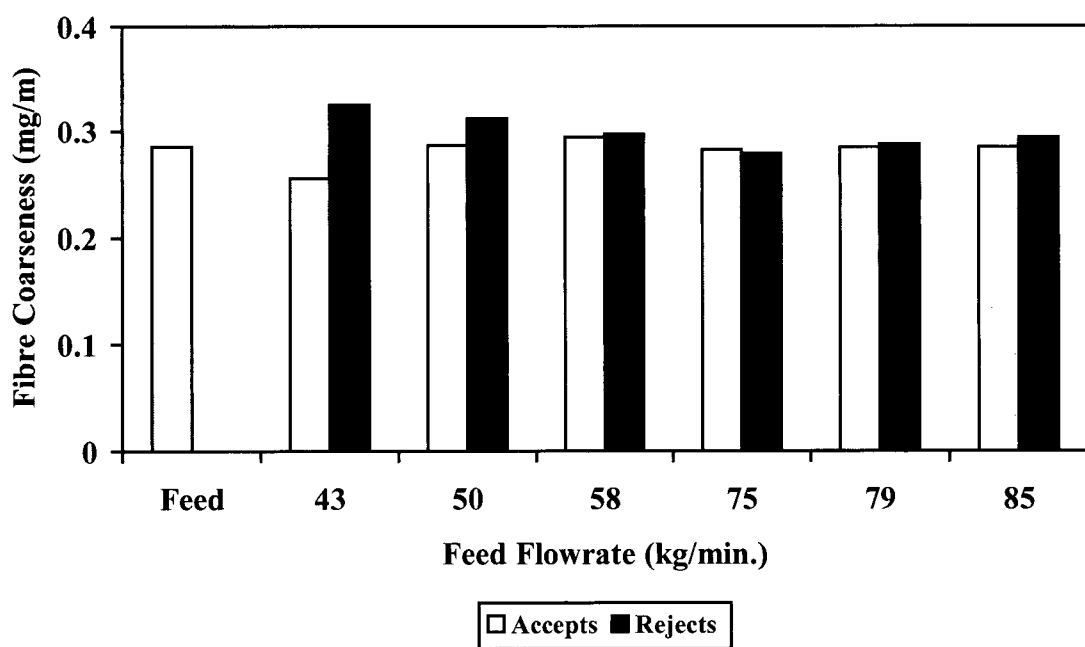


Figure 32 Fibre Coarseness Measurements for CTMP_A Fractionation

that handsheet strength is a more sensitive measure of fibre property differences than is the measurement of coarseness.

The literature review and theoretical analysis presented earlier indicated that hydrocyclones could separate fibres into fractions having different specific surfaces. As indicated by El-Hosseiny [20], specific surface influences Canadian Standard Freeness (CSF) values. A hydrocyclone then should be able to separate fibres into fractions having different freeness values. Low specific surface is associated with high freeness and vice versa. Experimental work of others and our theory show that a conventional forward hydrocyclone tends to reject low specific surface fibres and to accept high specific surface fibres. Thus the rejects freeness should be higher than the feed and accepts freeness and the accepts freeness lower than the feed freeness. The role of fibre fines in this fractionation may complicate matters.

We performed a freeness tests on the feed, accepts and rejects streams of Hydrocyclone A. CTMP_A having a consistency of 0.68% consistency was fractionated at various feed flowrates. The fibre length and freeness data are summarized in Figures 34 and 35. The length results presented show the fibre lengths of the rejects to be consistently shorter than the accepts for the range of flowrates studied. As feed flowrate was increased the rejects arithmetic average length tended to increase. Figure 35 illustrates the freeness data for this test. The rejects stream freeness was lower than the feed stream freeness and the accepts stream freeness up to a flowrate of 90 kg/min. The feed and accepts freeness values were similar for all flowrates. Observations reported in the literature review and also our derived theory suggest that a hydrocyclone should reject low specific surface (i.e. high freeness) material. Freeness values measured at feed flowrates less than 80 kg/min. were contrary to these observations. However at the highest flow rate tested, 90 kg/min., more typical of the usual operating conditions for this particular hydrocyclone, the rejects stream freeness was higher than that of the feed stream which was higher than that of the accepts stream. Thus at the higher flow rates the expected pattern was noted. These observations suggest that operation of Hydrocyclone A at lower than nominal flowrates

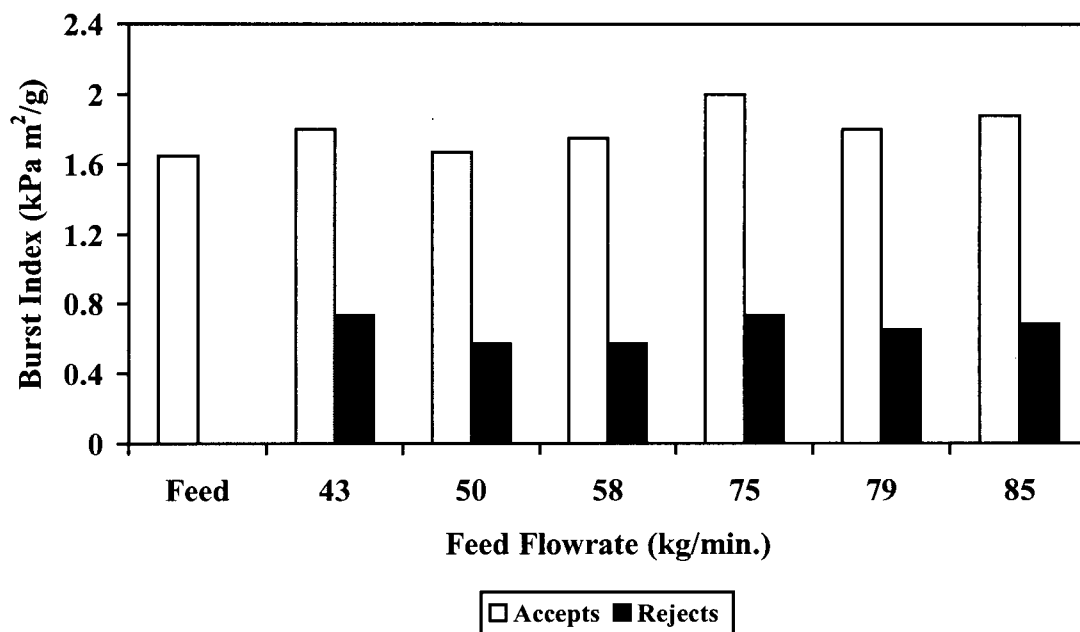


Figure 33 Burst Index Values for CTMP_A Fractionation Having a Consistency of 0.65%

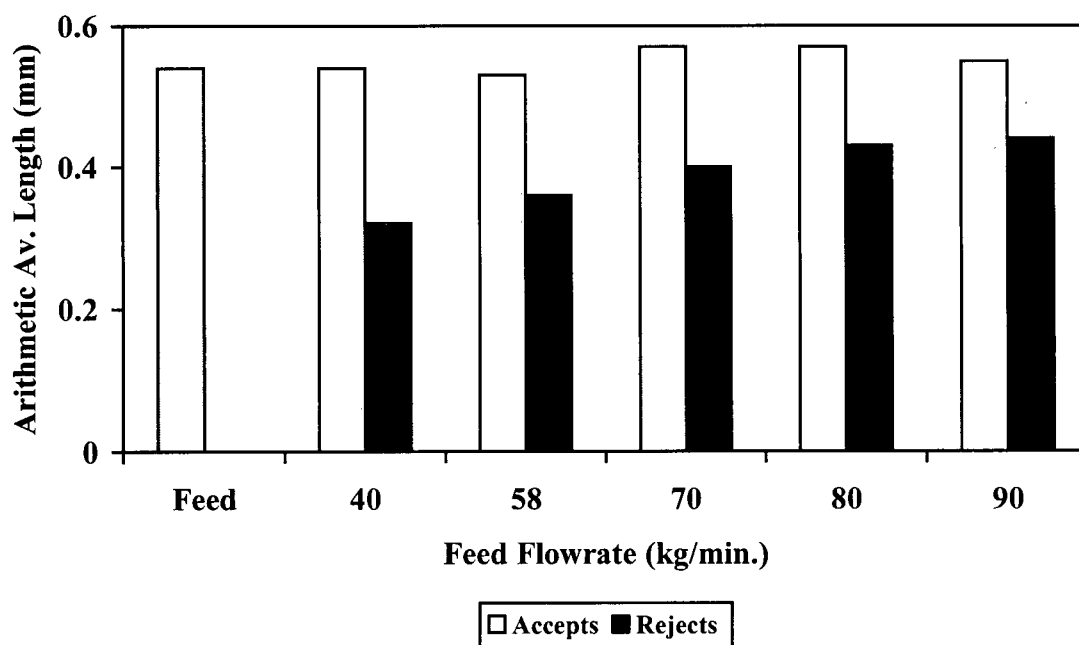


Figure 34 Arithmetic Average Fibre Length Measurements for CTMP_A Fractionation (Pulp Consistency: 0.68%)

tended to result in rejecting fibre fines. The presence of fines in the rejects at certain flowrates (< 70 kg/min.) could be the cause of discrepancies in observations made by others, who study fractionation, and by us. However, accepts and feed freeness values were similar for the range of flowrates studied and therefore it is difficult to conclude if fines concentrated in the accepts stream at the higher flowrates.

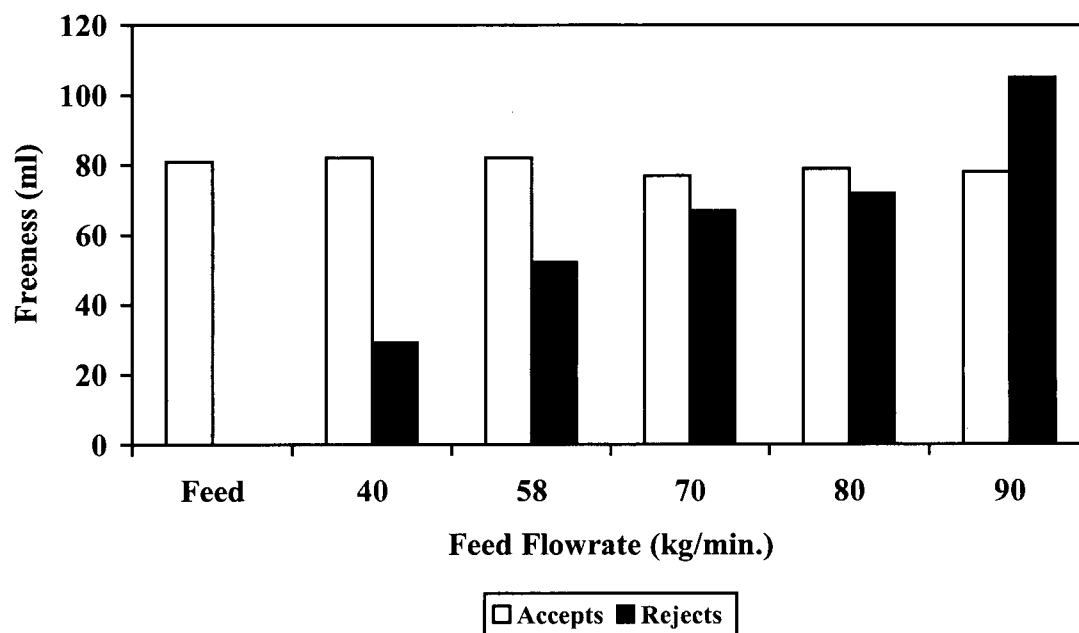


Figure 35 Accepts and Rejects Freeness Values for CTMP_B Fractionation (Pulp Consistency: 0.68%)

A second source of chemithermomechanical pulp (CTMP_B) was also tested in hydrocyclone A. The objective was to obtain length and coarseness distributions at a flowrate where the greatest differences in fibre properties of the accepts and rejects were observed.

In this experiment CTMP_B was fractionated at a consistency of 1%. Figure 36 plots the feed flowrate versus pressure drop relationship. Fibre length results showing that shorter fibres tended to be in the rejects are illustrated in Figure 37. Freeness values are shown in

Figure 38. The rejects samples had lower freeness and therefore would drain slower than the feed and accepts streams samples.

Feed, accepts, and rejects sampled at a feed flowrate of 47 kg/min. were then fractionated in a Bauer McNett fibre classifier to obtain length and coarseness distributions. Another reason for choosing this flowrate was that our previous tests with mechanical pulp had shown the greatest coarseness differences at low flowrates with Hydrocyclone A (see Figures 19 and 31). Fractionating pulp through the Bauer McNett classifier should confirm our length fractionation results and also show the preferential rejection of fines at this flowrate.

Table 8 summarizes the whole pulp length, freeness, and coarseness measurements for feed, rejects and accepts sampled at 47 kg/min. Figure 39 shows the weight percent fibre retained on the various chosen Bauer-McNett screen openings. The obvious observation is that the accepts had the greatest long fibre fraction (R14 and R16) content and the rejects contained the greatest pulp fines (P200) content. Large differences in the middle fractions (R28, R48, and R100) were not detected.

Table 8 Whole Pulp Characterization of Feed, Accepts and Rejects for CTMP_B
Fractionation Experiment (Hydrocyclone A Tested with Pulp Consistency of 1%)

Sample	Length Weighted Fibre Length (mm)	Fibre Coarseness (mg/m)	CSF Freeness (ml)
Feed	1.40	0.250	112
Accepts	1.47	0.248	123
Rejects	1.16	0.277	52

The length weighted average fibre length of the feed, accepts, and rejects of each screen opening is reported in Figure 40. The rejects fibre lengths were consistently shorter than the feed and accepts for each of the Bauer McNett fractions. Lengths of the feed and accepts were similar to each other.

The coarseness of the feed, accepts, and rejects for each of the Bauer McNett fractions was measured to obtain a distribution (See Figure 41). Coarseness measurements for Bauer McNett fractions of R14, R16, and R28 were greater for the accepts than the rejects, which seems contrary to our findings that mean rejects coarseness was higher than the mean accepts coarseness (see Table 8).

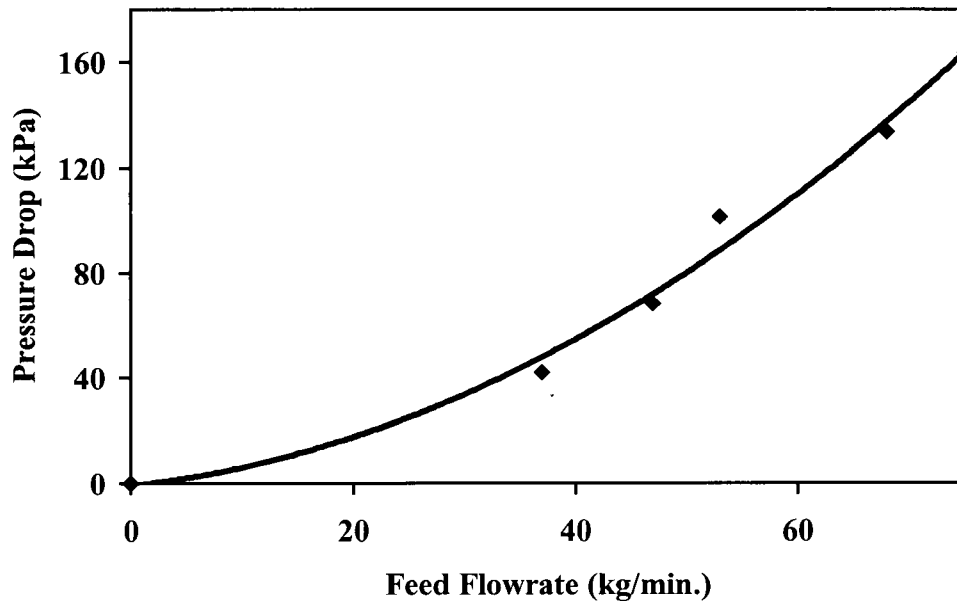


Figure 36 Feed Flowrate versus Pressure Drop for CTMP_B Fractionation
(Pulp Consistency 1%)

However, the average fibre lengths of the rejects stream fall in the range retained on the Bauer McNett R48 and R100 fractions. In this range rejects coarseness values were greater than the feed and accepts. This observation confirms that Hydrocyclone A is capable of rejecting short, coarse fibres when operated below nominal flowrate.

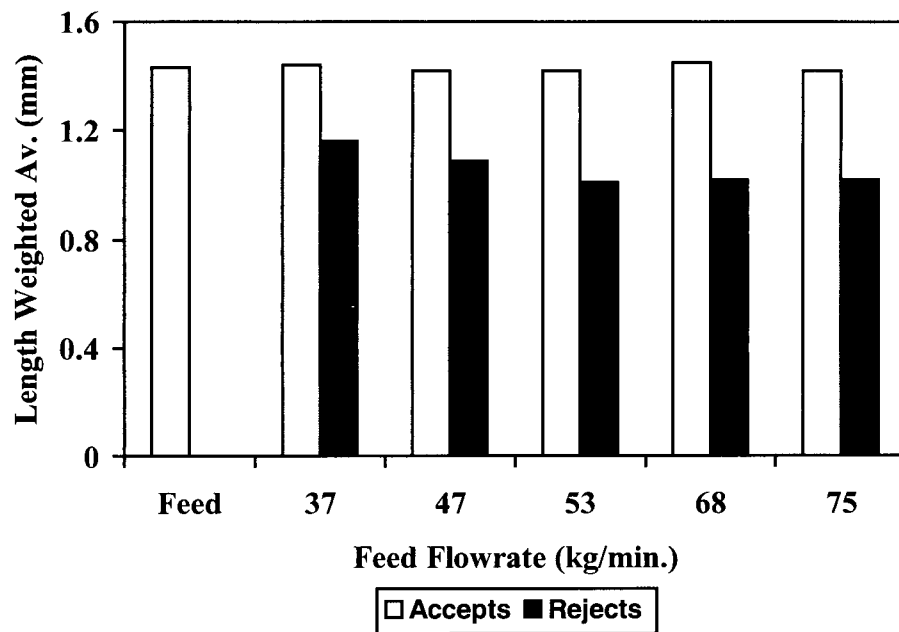


Figure 37 Feed, Accepts, and Rejects Fibre Length Measurements for Various Flowrates
(CTMP_B Fractionation at Consistency of 1%)

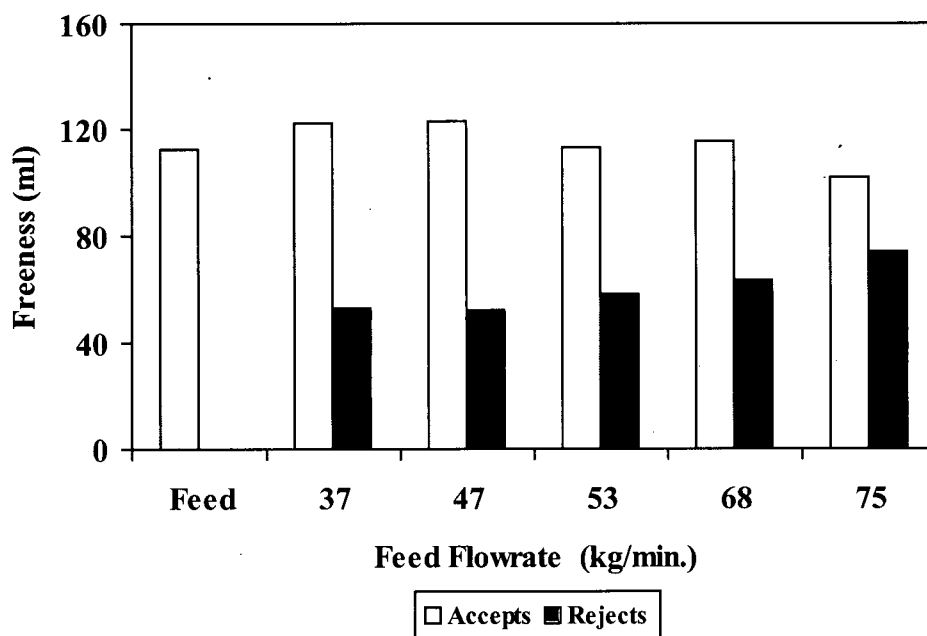


Figure 38 Feed, Accepts, and Rejects Freeness Measurements for Various Flowrates
(CTMP_B Fractionation at Consistency of 1%)

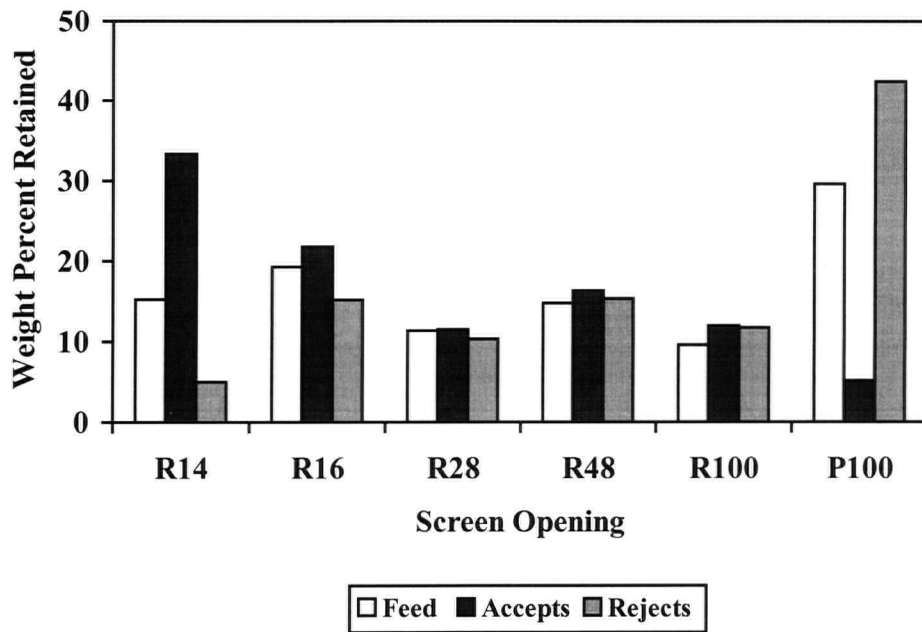


Figure 39 Weighted Percent Fibre Retained in Bauer McNett Classifier (CTMP_B Fractionated at Flowrate of 47 kg/min. and Consistency of 1%)

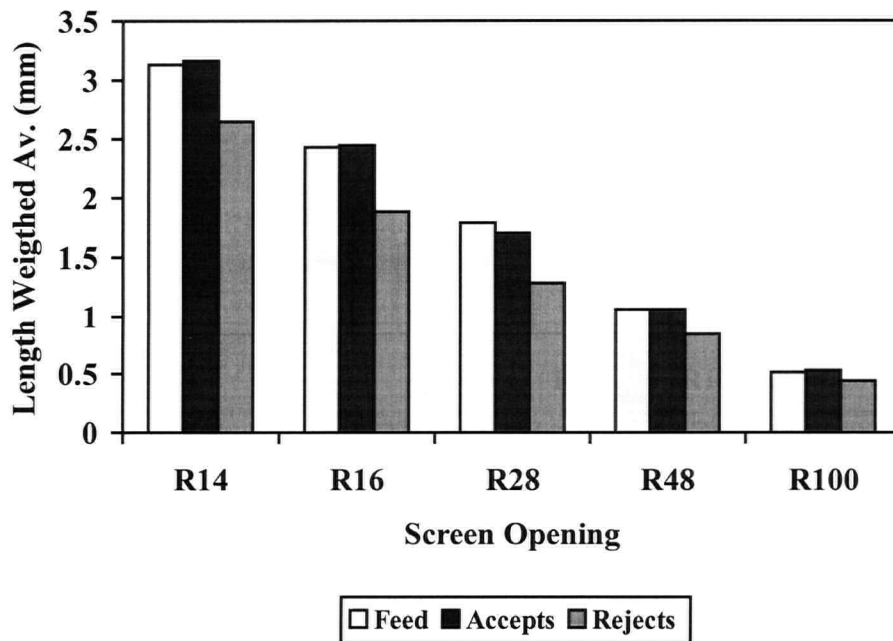


Figure 40 Length Weighted Average Fibre Distribution Feed, Accepts, and Rejects or CTMP_B Fractionated at 1% Consistency and Flowrate of 47 kg/min.

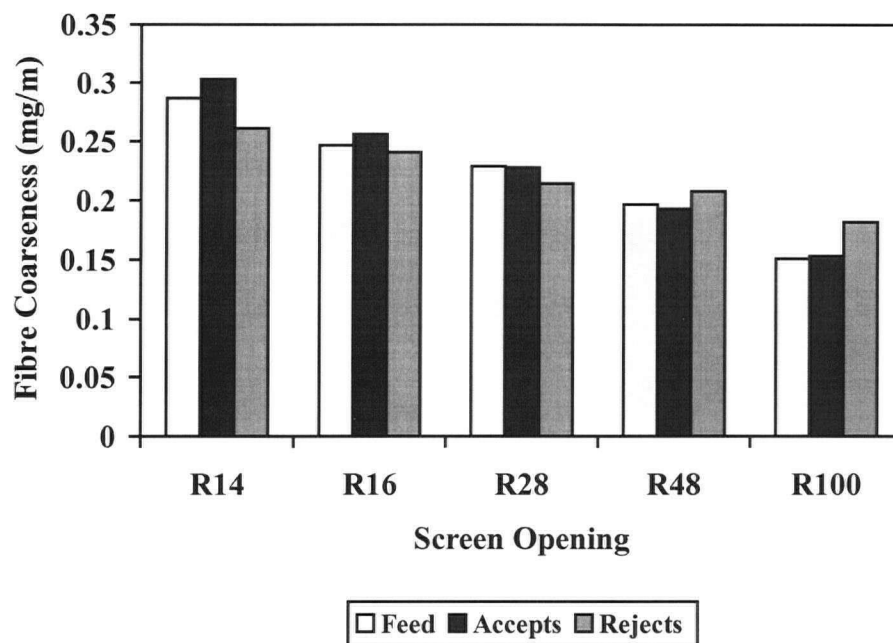


Figure 41 Coarseness Distribution Obtained from Bauer McNett Fractions (CTMP_B Fractionated at Flowrate of 47 kg/min. and Consistency of 1%)

5.3.2 Fractionation of Recycled Fibre

Bliss has summarized several reasons for fractionation (see Chapter 2). One of the objectives of his thesis (and this thesis too) was to show that fractionation of secondary fibre furnishes (recycled paper grades) prior to re-processing would allow for appropriate fibre development of the fractionated streams. Since secondary fibres are composed of both mechanically and chemically pulped fibres, they have a diverse pulping history and require different fibre treatments to upgrade their development potential [4].

Recycled fibre was fractionated in Hydrocyclone A at a pulp consistency of 1%. This pulp was typical of a newsprint furnish containing mainly mechanical and chemical pulp including some sulphite pulp. The chemical pulp component of the furnish was a mixture of hardwood and softwood. The mechanical component was predominantly softwood with some trace of hardwood; this was confirmed by testing the fibre specimens as suggested in CPPA Standard Method B.2P. This standard suggests using a Maule stain to distinguish between chemical,

mechanical and sulphite fibres. The objective of this experiment was to determine if different types of fibres could be separated from one another (i.e. to fractionate chemical fibres from mechanical fibres).

The feed flowrate versus pressure drop relationship for this experiment is illustrated in Figure 42. Fibre length results are presented in Figure 43, this figure indicates again that the rejects fibre lengths tended to be shorter than those of the accepts.

Paper strength for this experiment was evaluated by performing burst and tear tests (See Figures 44 and 45). Both strength tests showed that the accepts had greater burst and tear indices than the rejects, this was observed for the full range of flowrates studied.

Samples of feed, accepts, and rejects were collected at a flowrate of 49 kg/min. and photomicrographs were taken of the pulp samples at this flow. These photomicrographs are presented in Figure 46. The samples were stained and characterized by a professional fibre microscopist. The accepts appeared to have a slightly higher proportion of chemical pulp than the feed. Accordingly, the rejects appeared to have a slightly lower proportion of chemical pulp than the feed. The average fibres in the rejects were shorter than in the accepts. There were more short chemical fibres in the rejects than in the accepts. The reject sample had more small mechanical fibre fragments relative to the longer mechanical fibres. It appeared that there were more ray cells in the rejects than in the accepts.

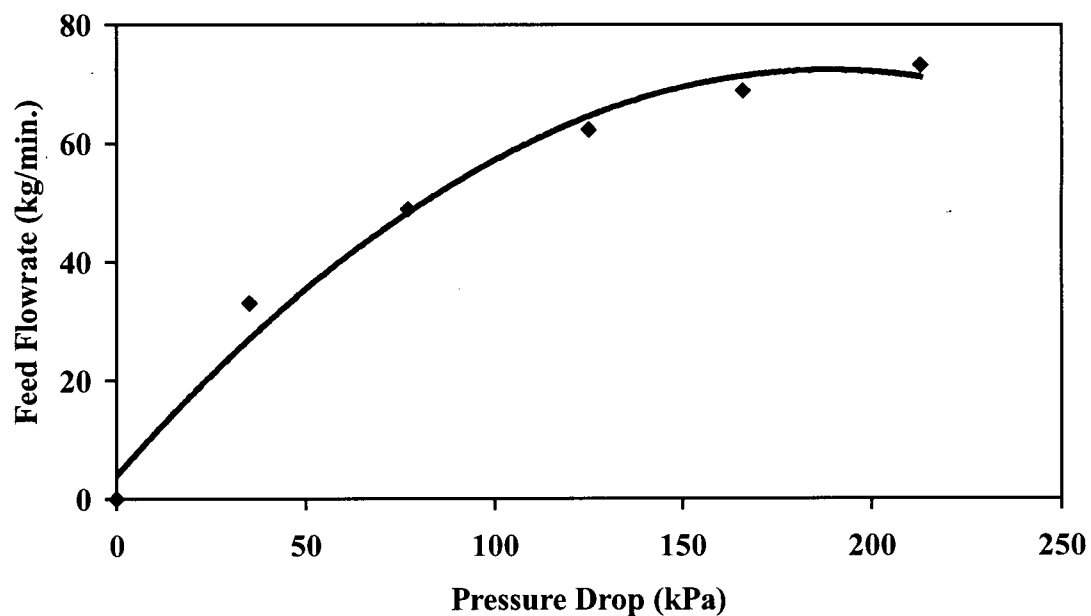


Figure 42 Pressure Drop versus Feed Flowrate Relationship for Hydrocyclone A
Fractionating Recycled Pulp Having a Consistency of 1%

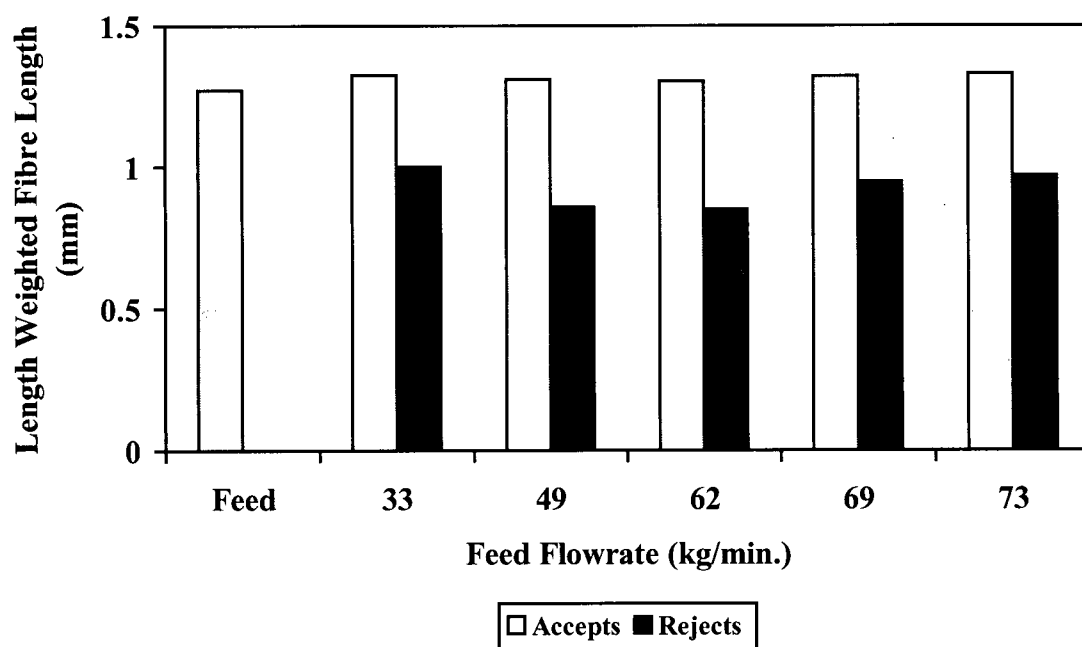


Figure 43 Fibre Length Measurements for Recycled Pulp Fractionation

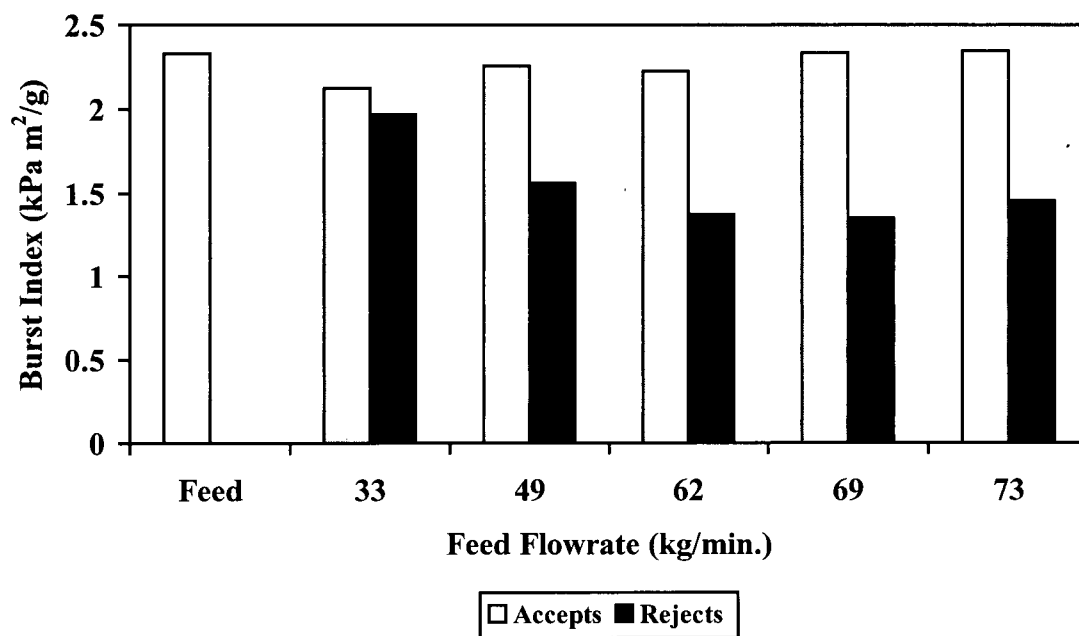


Figure 44 Burst Index Values for Feed, Accepts, and Rejects for Recycled Fibre Fractionation Study

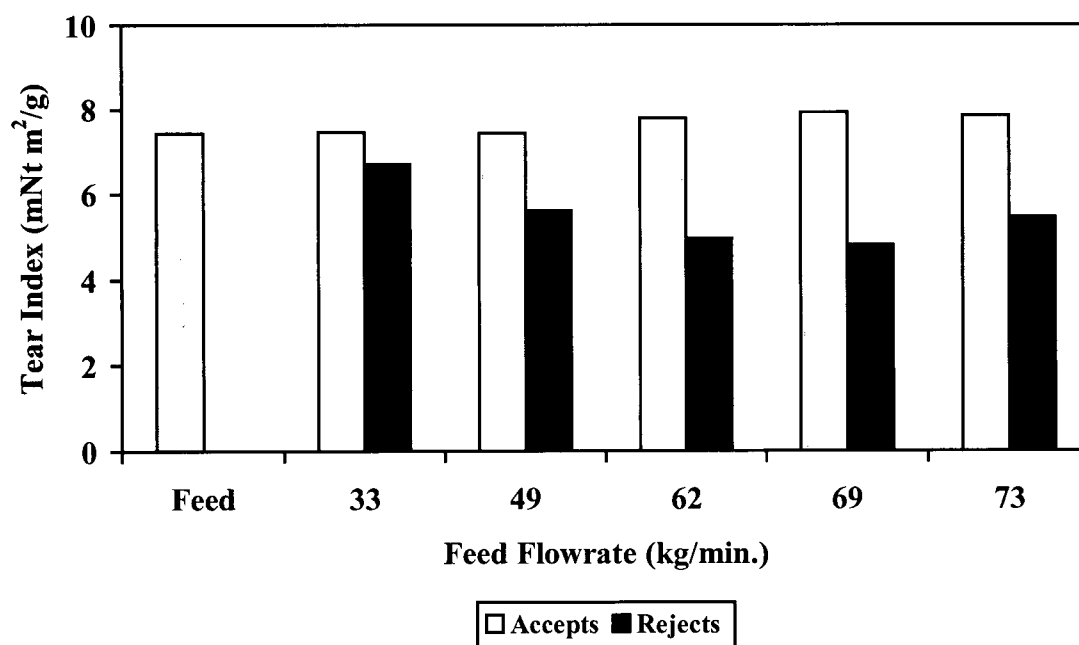
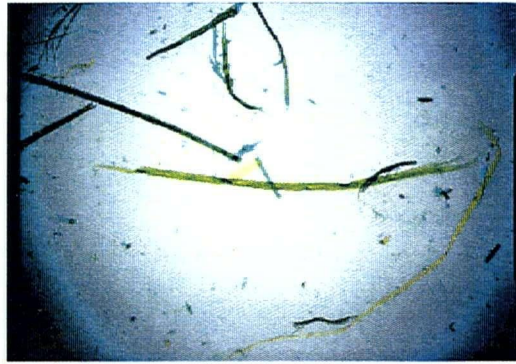
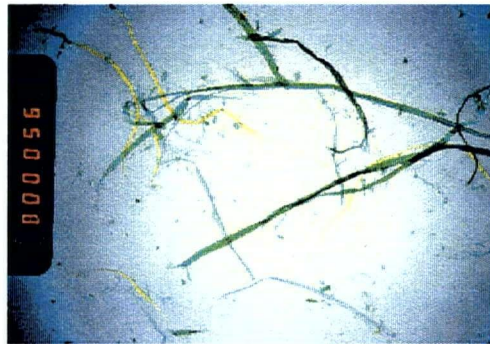


Figure 45 Tear Index Values for Feed, Accepts, and Rejects for Recycled Fibre Fractionation



Feed



Accepts



Rejects

Figure 46 Photomicrographs of Feed, Accepts, and Rejects for Recycled Fibre Fractionation Study. Samples Collected at a Feed Flowrate of 49 kg/min. In the photomicrographs above chemical fibres are stained yellow, mechanical fibres are stained dark green to blue green, and sulphite pulps are stained a yellowish green.

5.3.3 Fractionation of CTMP from a Latency Chest

All the tests summarized above tested market grade pulp which had been obtained in an initially dry state and re-slurried prior to use. To eliminate the possibility that our findings might have been due to such re-processing of the pulp, we tested never dried CTMP obtained from the latency chest of a western pulp mill. In a pulp mill, the latency chest functions to remove the "latent" properties of fibres. Latency is a term given to describe fibre aggregates which are held together by a hemicellulose-lignin bond. These aggregates exhibit high freeness and low physical strength properties. The latency chest softens the hemicellulose-lignin network; this is accomplished by heating the fibre to above 60 °C. The resultant pulp has lower freeness and higher strength due to this process. In our experiment this pulp was tested at a consistency of 0.6%, which was the concentration as received.

Figure 47 once again shows that similar fractionation by fibre length resulted as was the case for market grade pulp used earlier. Reject fibre lengths were shorter than the feed and accepts fibre lengths. Rejects fibre coarsenesses were greater than the accepts and feed (see Figure 48). Handsheet results, illustrated in Figures 49 and 50, indicated that the short coarse fibres rejected at the various feed flowrates produced sheets with lower burst and tear strength indices than the feed and accepts. These tests confirm our earlier findings that Hydrocyclone A is capable of rejecting short coarse fibres.

In addition to the above fibre and paper testing measurements, we also measured the drainage time of our samples to indicate the freeness behaviour of this pulp. This was accomplished by measuring the time the pulp stock drained in a handsheet tester. This time was then divided by the sheet basis weight to account for any concentration differences between the samples and the result was defined as the drainage index. Figure 51 plots the drainage index for the feed, accepts, and rejects samples at the various flowrates we tested. For a feed flowrate of 39 kg/min. we saw that the drainage time of the rejects samples was considerably greater for the rejects than that of the feed and accepts. When flowrates were increased above 50 kg/min., the rejects drainage time decreased. This behaviour was due to the behaviour of

pulp fines reporting to the accepts at the higher flowrates and to the rejects at lower flowrates. Fines would tend to block the channels in developing fibre mat through which water flows as a sheet is being formed thus making for a higher resistance to the flow of water through the mat and a longer drainage time. Drainage time differences between accepts and feed did not differ considerably.

5.4 Varying Reject Ratio of Hydrocyclone A

5.4.2 Reject Ratio Variations when Fractionating CTMP_B

Fibre length differences between accepts and rejects noted with Hydrocyclone A were observed at reject ratios of the order 0.04 – 0.05. From an economic standpoint, it would be more desirable if fractionation could be achieved at higher reject ratios since fewer hydrocyclones would need to be installed. Again it should be pointed out that if greater mass reject ratios were accompanied by adequate fractionation, there would be a sufficiently large rejects stream to warrant some sort of downstream processing.

In the work reported in this section we increased the reject ratio of Hydrocyclone A to investigate its effect on fractionation by length and freeness. Reject ratios were varied by increasing the underflow tip size of the hydrocyclone. CTMP_B having a consistency of 0.7% was tested at underflow reject tip opening diameters of 3, 5, and 6 mm.

Figure 52 plots the reject ratio for the three underflow tips. Over the range of feed flowrates tested, for the 3 mm tip reject ratios in the range of 0.04 – 0.05 were achieved, for the 5 mm tip ratios of 0.07 – 0.11 were noted. The 6 mm tip achieved reject ratios in the range of 0.13 – 0.16. For all reject tip openings the reject ratio decreased as the flowrate increased.

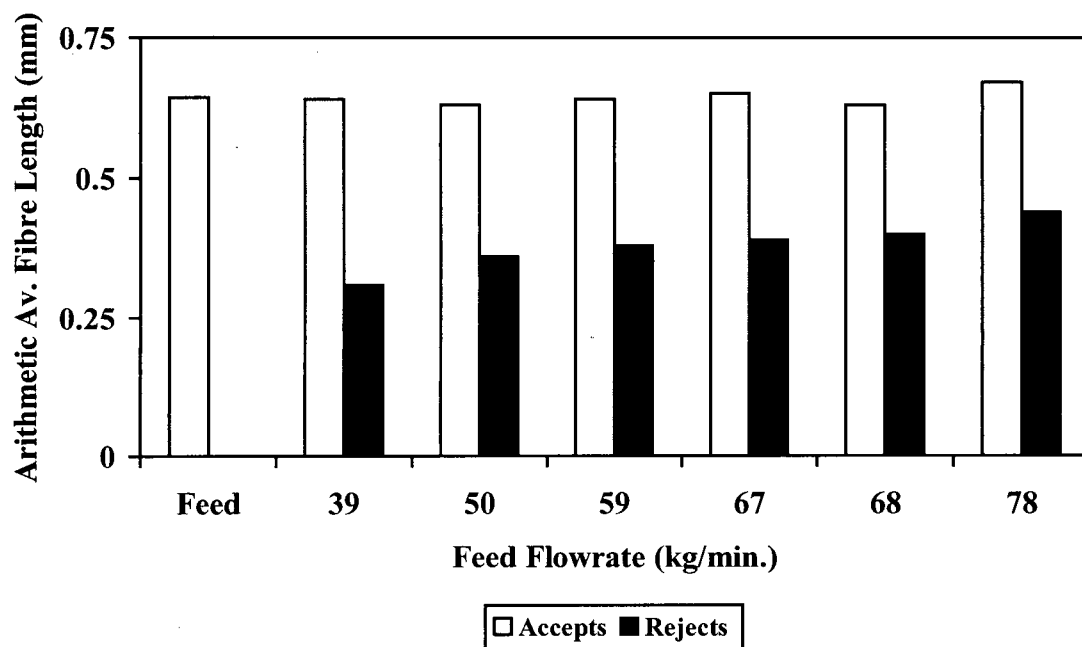


Figure 47 Arithmetic Average Fibre Lengths for CTMP_C Fractionation (Pulp Obtained from Latency Chest having Consistency of 0.6%)

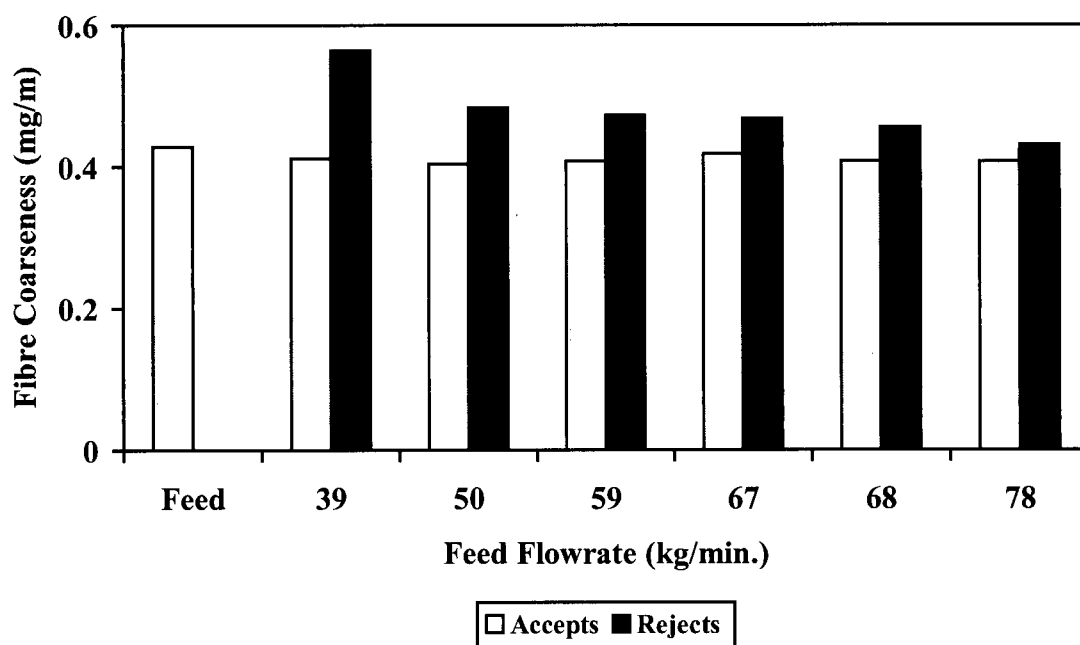


Figure 48 Fibre Coarseness Measurements for Latency Chest CTMP_C Fractionation

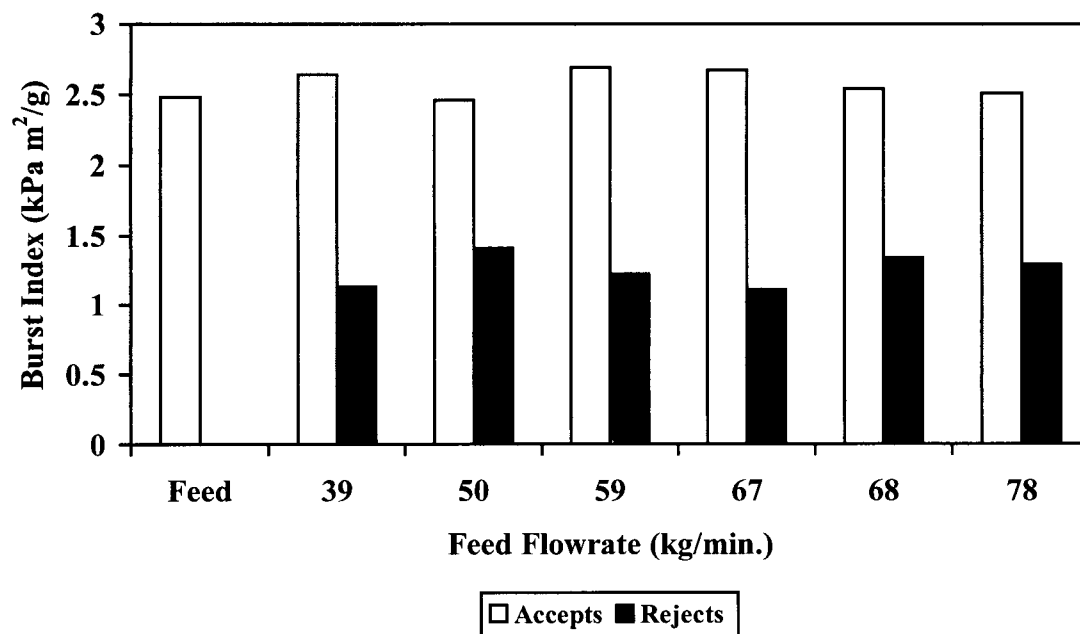


Figure 49 Burst Index Values for Feed, Accepts, and Rejects from Latency Chest
CTMP_C Fractionation

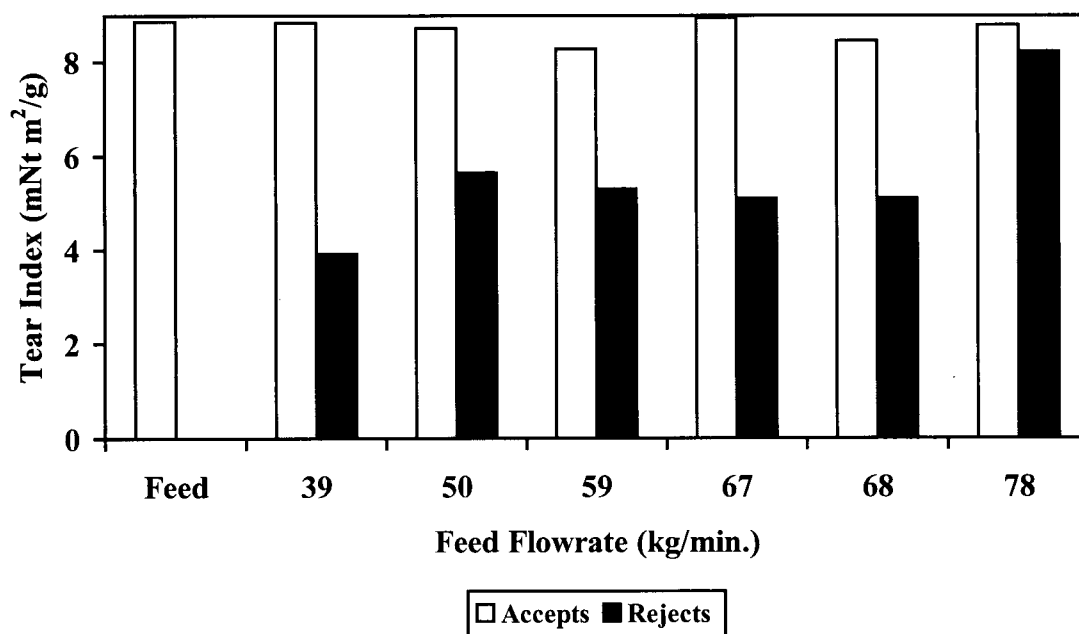


Figure 50 Tear Index Values for Samples Collected at Various Flowrates from Fractionating
CTMP_C at 0.6%

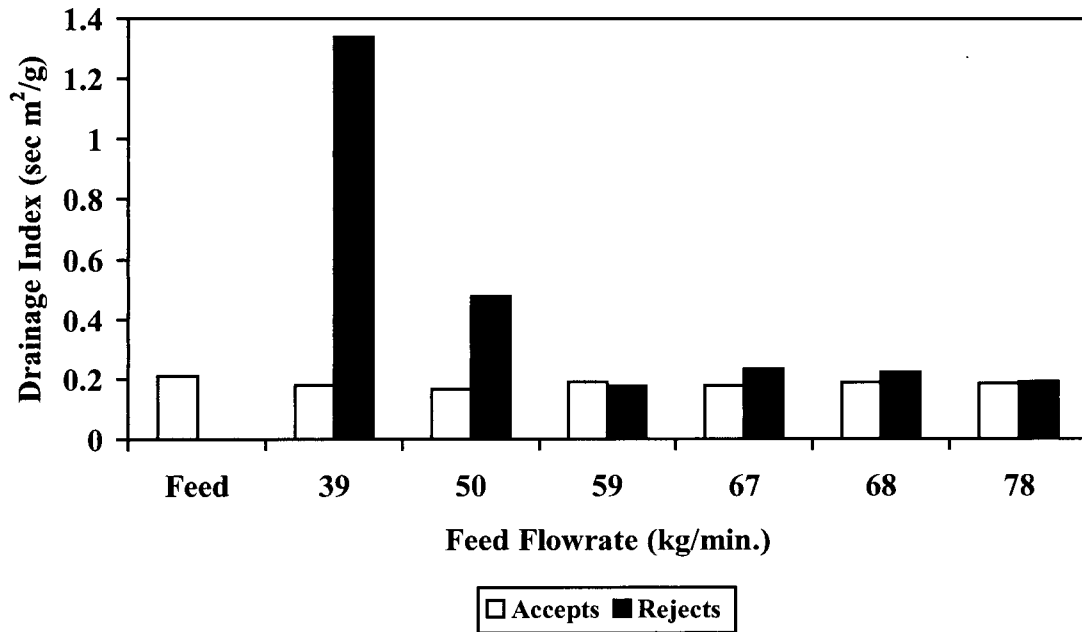


Figure 51 Drainage Index of Feed, Accepts, and Rejects from CTMP_C
Fractionation Study

Figure 53 plots the mass fraction fibres rejected as a function of feed flowrate for the three underflow tips. Over the range of feed flowrates tested, for the 3 mm tip the fraction of fibres rejected was in the range of 0.04 – 0.06 , for the 5 mm tip ratios of 0.08 – 0.12 were noted. The 6 mm tip resulted in fibre rejection ratios in the range of 0.15 - 0.22. For all reject tip openings the mass fraction of fibres rejected increased as the flowrate increased.

Length weighted average fibre length measurements for accepts and rejects are shown in Figures 54 and 55 respectively. For feed flowrates greater than 49 kg/min., accepts lengths were slightly greater than the feed for each of the underflow tip sizes tested. However these differences were small. Rejects fibre lengths showed clearer trends as a result of varying the hydrocyclone reject ratio. As the reject ratio increased, the length weighted average fibre length increased. Figure 55 shows that for all cases of reject ratios and range of feed flowrates tested, the fibre lengths continued to be smaller for the rejects than the feed. It can also be seen that as flowrate increased the difference between the accepts and rejects fibre

lengths decreased. We can conclude then that fibre length differences between accepts and rejects are pronounced when Hydrocyclone A was operated at low reject ratios.

Figures 56 and 57 show freeness values for the feed, accepts, and rejects streams from this experiment. Figure 56 for the accepts CSF indicates that as feed flowrate increased the accepts CSF for all three tip openings tended to decrease. At the highest flowrate, tip opening didn't affect the accepts CSF as all were more or less the same. At lower flowrates there may have been differences due to tip size but no consistent pattern could be seen. Figure 57 plots rejects CSF values. Here it's clear that as flowrate increased CSF increased for all tip openings. The 3 mm opening always produced the lowest CSF. The CSF values for the 5 and 6 mm tips were about the same. As feed flowrate increased accepts freeness tended to be lower than rejects freeness. This indicated that as flowrate increased, fines were preferentially accepted.

5.4.2 Reject Ratio Variations for Fractionation of BCTMP

Reject ratio effects of Hydrocyclone A were further studied testing BCTMP (Bleached chemithermomechanical pulp). In this set of experiments underflow tip diameters of 5 mm and 6 mm were used. Here we wanted to test if length differences occurred at larger underflow diameters using a different type of pulp. This BCTMP tested was a high freeness pulp (500 ml), i.e. it drains faster than the other pulps previously tested (CSF = 80 – 120 ml). Because this pulp was quite different from the others previously tested, the hydrocyclone performance curves showing reject ratio, thickening ratio, and mass reject ratio are illustrated for the two rejects tip opening diameters tested (5 and 6 mm). See Figures 58 – 60. For the 5 mm underflow tip, the reject ratio was found to decrease and then level off. The reject ratio measured was in the range of 0.08 – 0.1, which was the same as the range encountered for the fractionation trial with CTMP (refer to Section 5.3). The 6 mm tip also showed a similar trend. Thickening ratios and mass fraction of fibres rejected were found to increase with increasing feed flowrates for both underflow tips tested.

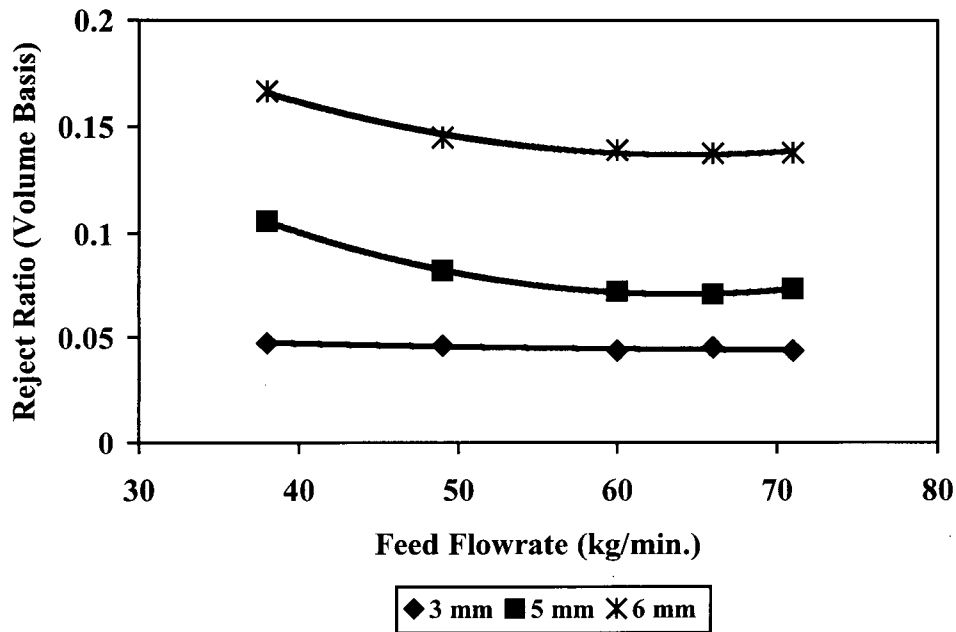


Figure 52 Reject Ratio Values for Operation of Hydrocyclone A with Underflow Sizes of 3, 5, and 6 mm (Experiment Testing CTMP_B with 0.7% Consistency)

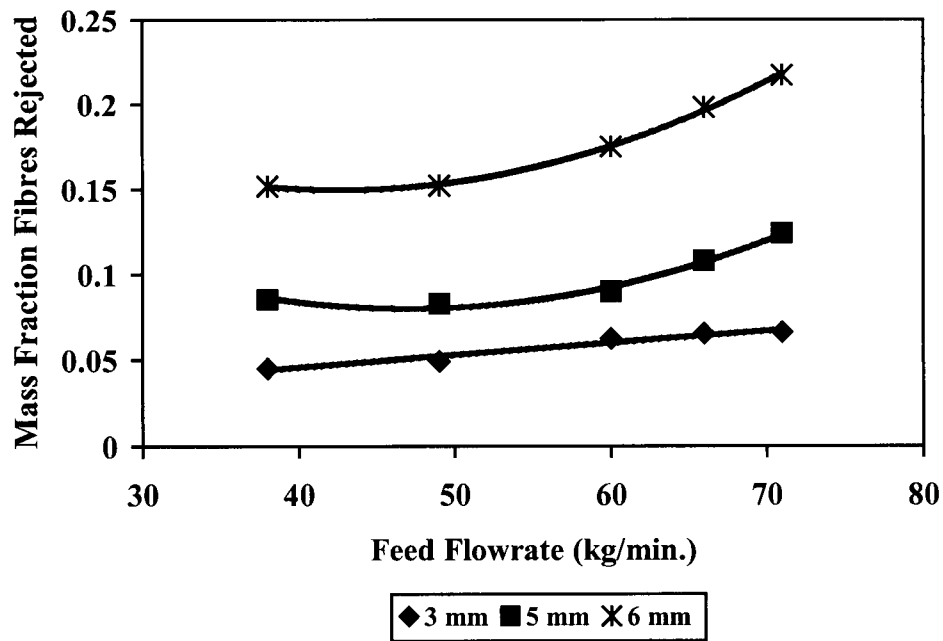


Figure 53 Mass Fraction Fibres Rejected for Operation of Hydrocyclone A with Underflow Sizes of 3, 5, and 6 mm (Experiment Testing CTMP_B with 0.7% Consistency)

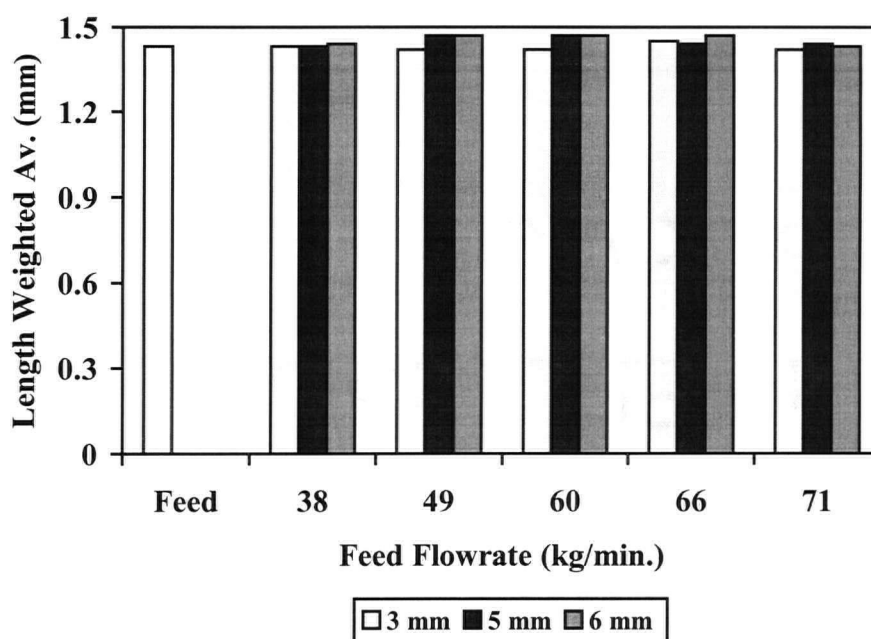


Figure 54 Length Weighted Av. Fibre Length of Accepts Stream for Experiment Varying Hydrocyclone Underflow Opening

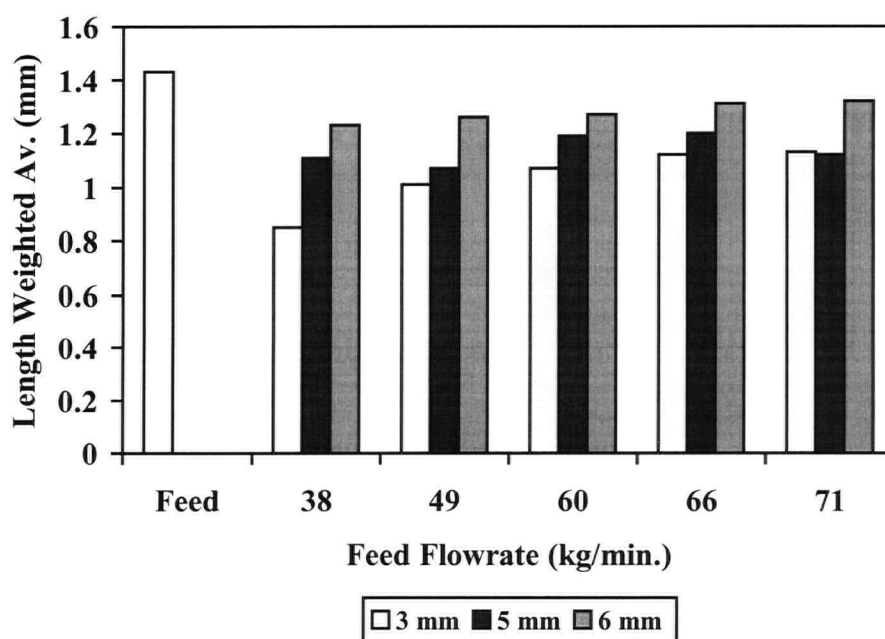


Figure 55 Length Weighted Av. Fibre Length of Rejects Stream for Experiment Varying Hydrocyclone Underflow Opening

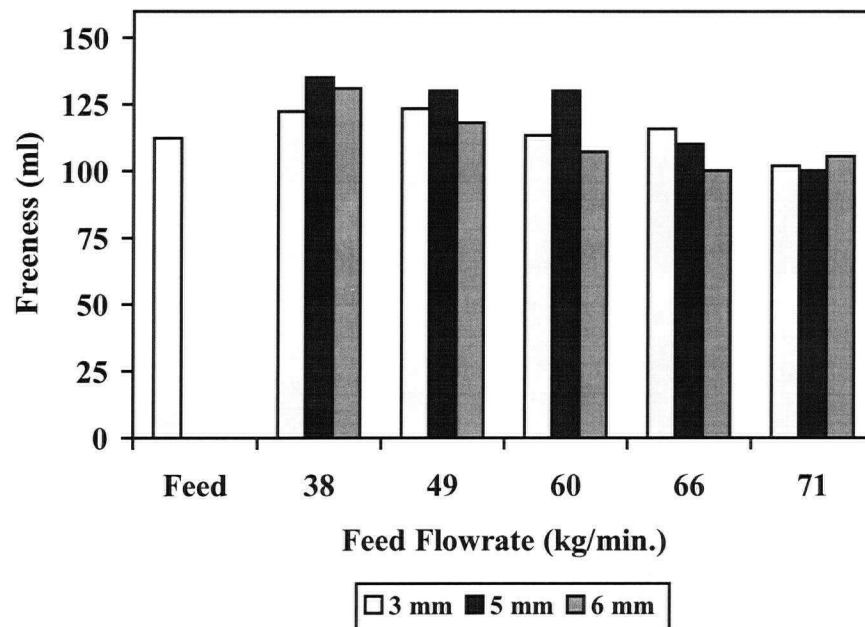


Figure 56 Freeness of Accepts Stream for Experiment Varying Hydrocyclone Underflow Opening

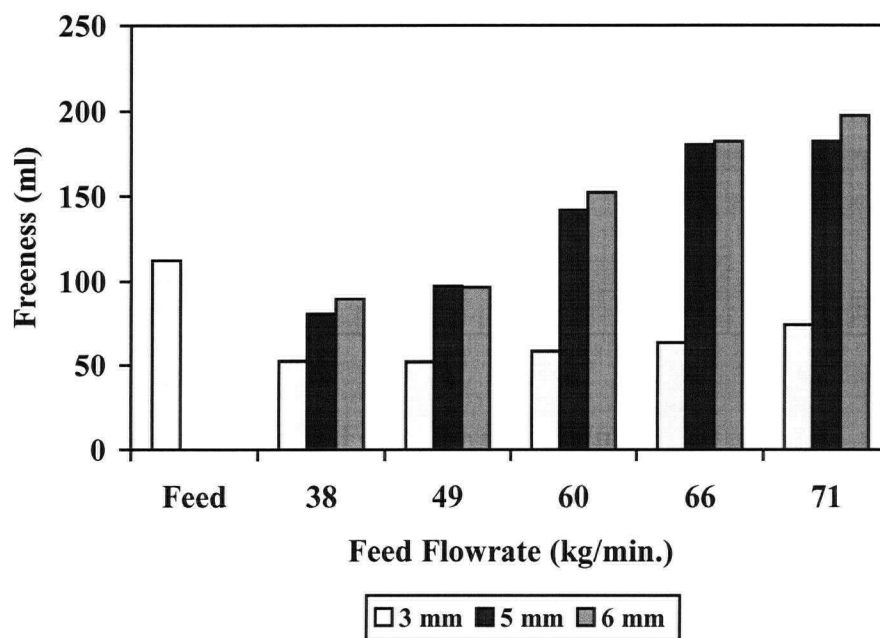


Figure 57 Rejects Freeness Measurements for Experiment Varying Underflow Opening of Hydrocyclone A

The fibre length data are illustrated in Figures 61 and 62. Freeness data are presented in Figures 63 and 64. For both underflow tips, the average fibre lengths of the rejects were smaller than those of the accepts. Differences between accepts and rejects mean fibre lengths were greater with the 5 mm opening. Increasing the feed flowrate resulted in an increase in the length weighted average fibre length of the rejects samples for both underflow tips.

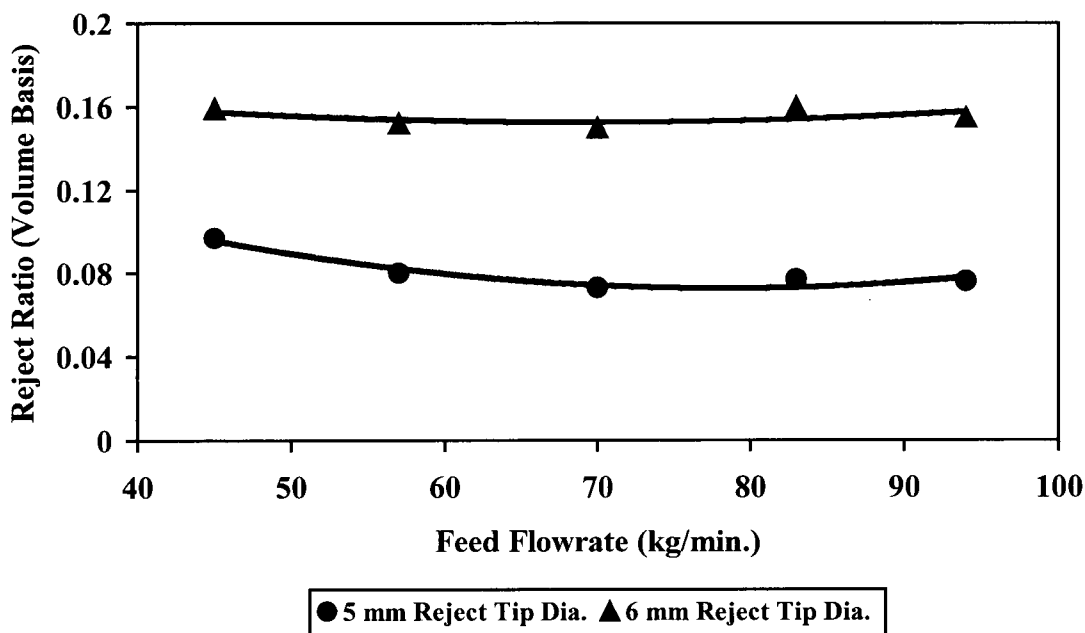


Figure 58 Reject Ratio Relationship for Fractionation of BCTMP in Hydrocyclone A Using Underflow Tip Sizes of 5 and 6 mm

Freeness results for experiments performed with the 5 mm underflow tip show that at low feed flowrates, the rejects samples had lower freeness than the accepts. This indicated that a greater amount of fines were being rejected at low feed flowrates. But at higher flowrates the rejects freeness values were greater than those of the accepts. This suggests that at low flowrates fines were rejected but at high flowrates they were accepted.

For experiments performed with the 6 mm underflow tip, the reject freeness values were equal or greater than the accepts for all feed flowrates studied. Accepts freeness values were observed to decrease with increasing feed flowrates. The CSF results for the 6 mm

underflow tip can be interpreted to mean that the accepts had greater specific surface areas than the rejects, this observation is in agreement with our theory and work discussed in the literature review.

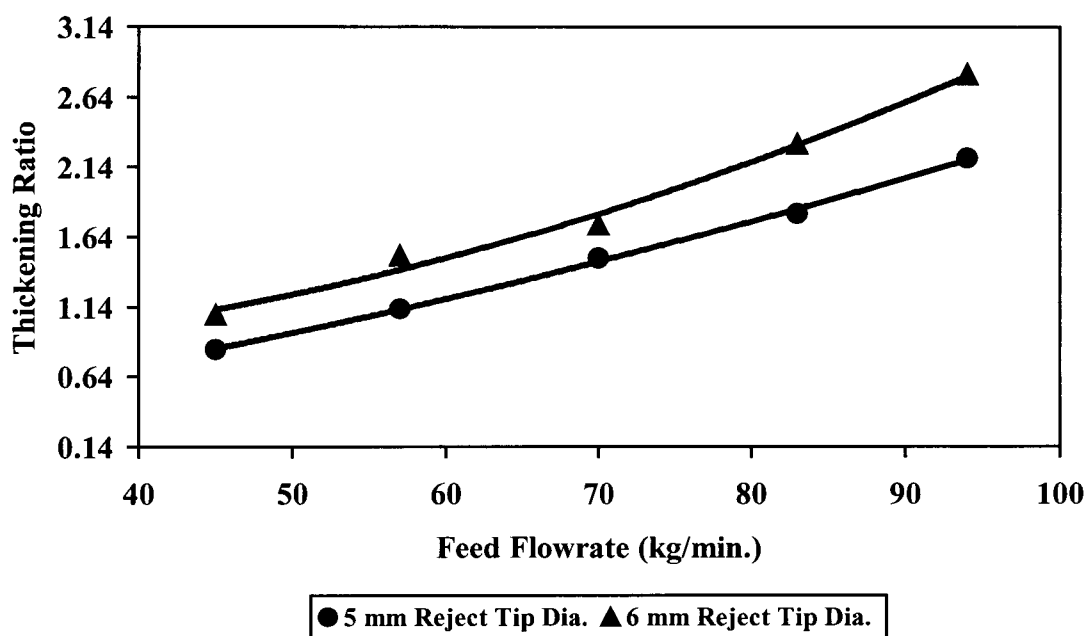


Figure 59 Thickening Ratio for BCTMP Fractionation in Hydrocyclone A Having Underflow Tip Sizes of 5 and 6 mm

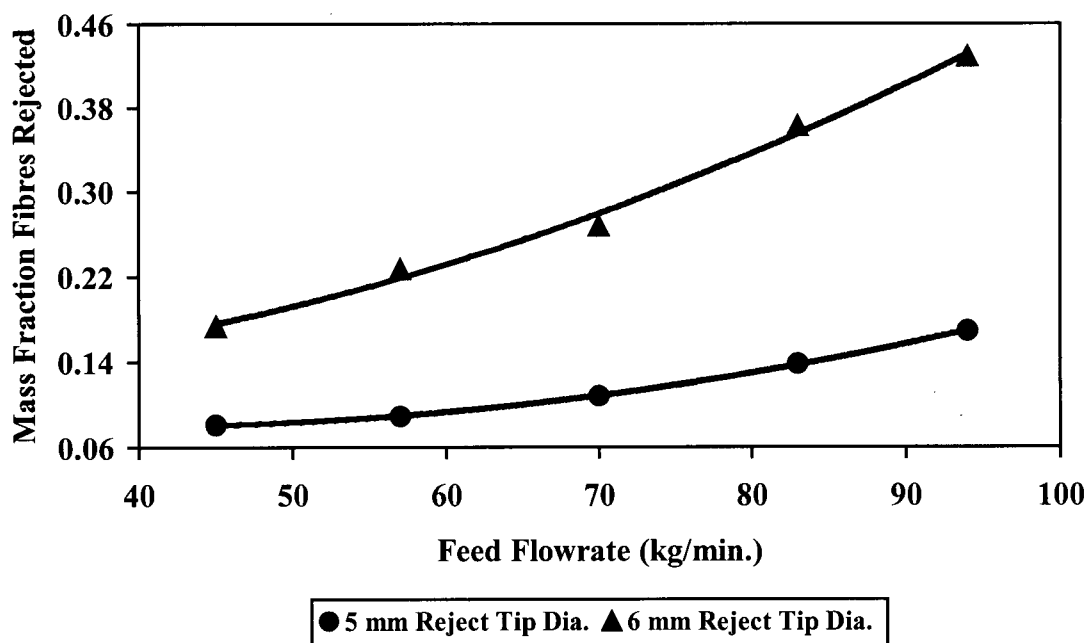


Figure 60 Mass Fraction Fibres Rejected for BCTMP Fractionation in Hydrocyclone A Having Underflow Tip Sizes of 5 and 6 mm

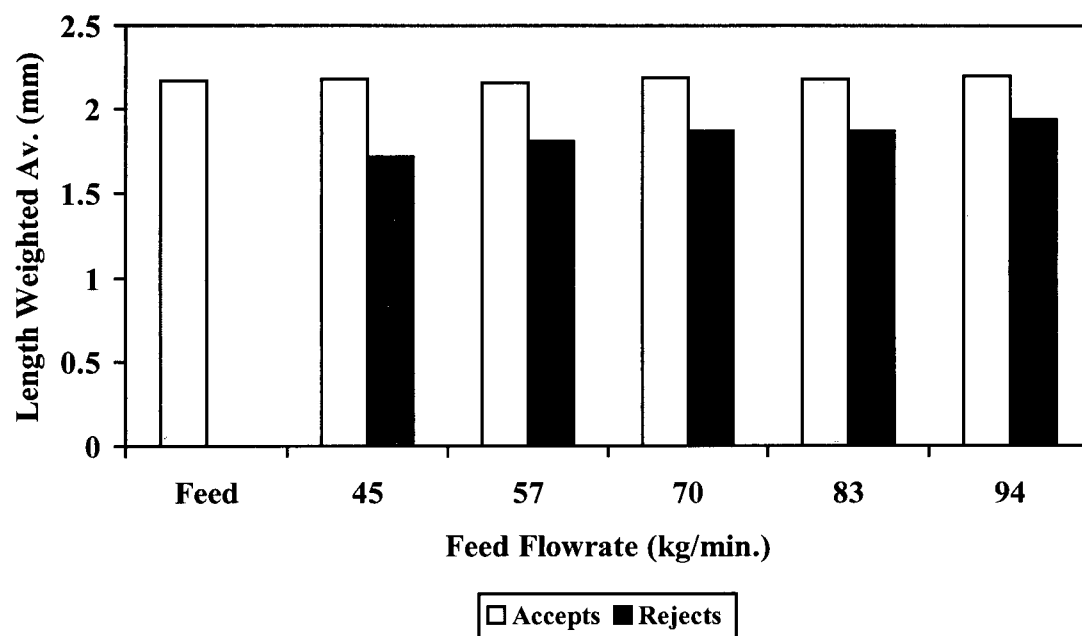


Figure 61 Length Weighted Fibre Measurements for Feed, Accepts, and Rejects for BCTMP Fractionation (Underflow Tip Size: 5 mm)

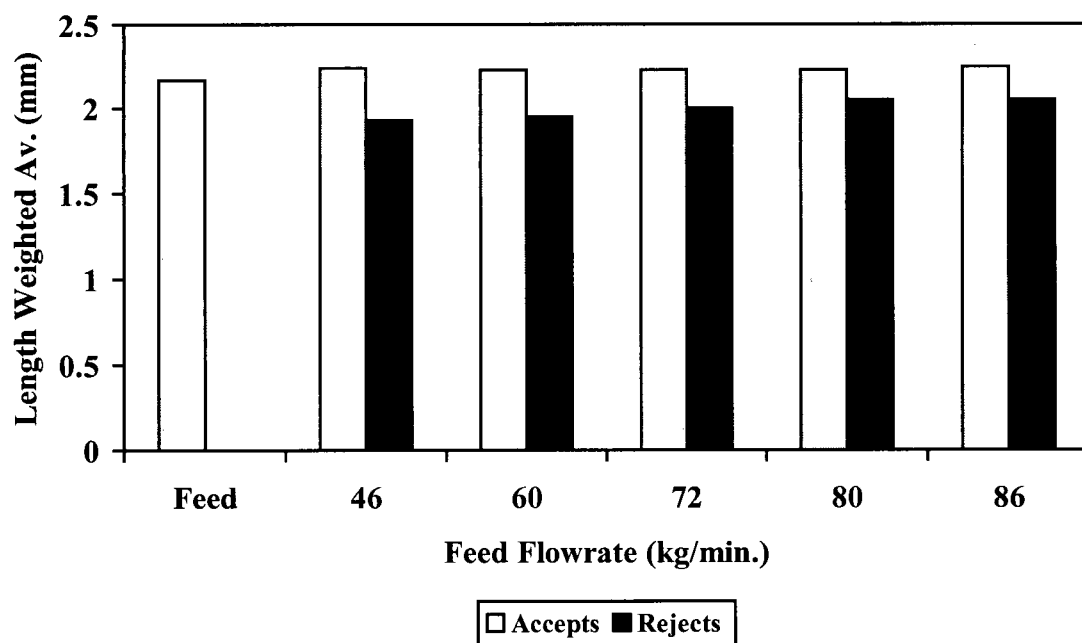


Figure 62 Length Weighted Fibre Measurements for Feed, Accepts, and Rejects for BCTMP Fractionation (Underflow Tip Size: 6 mm)

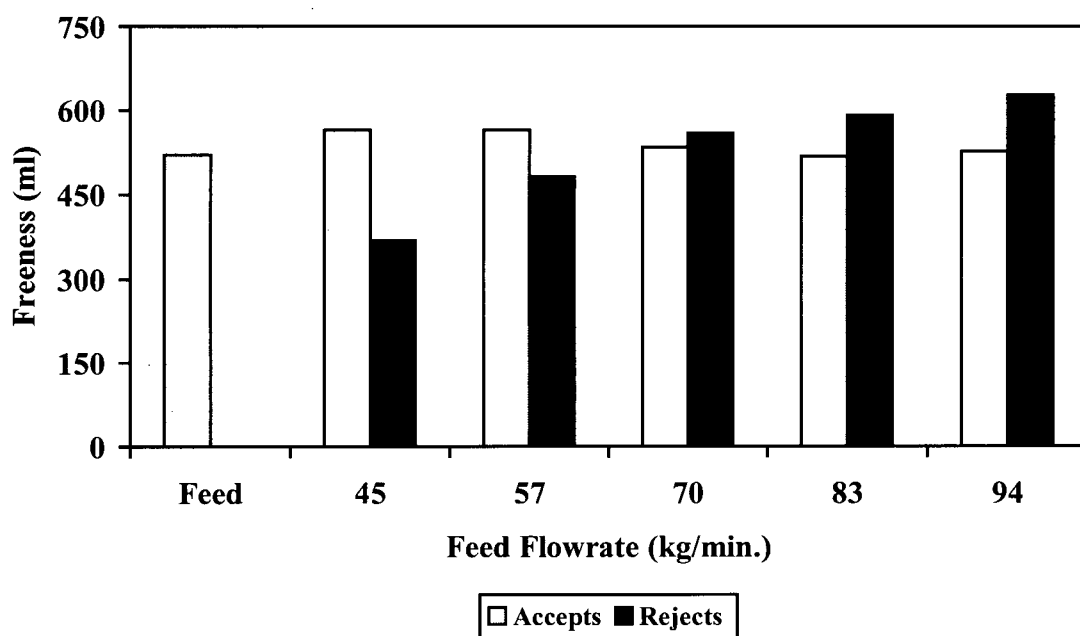


Figure 63 Freeness Measurements for Feed, Accepts, and Rejects for BCTMP Fractionation
(Underflow Tip Size: 5 mm)

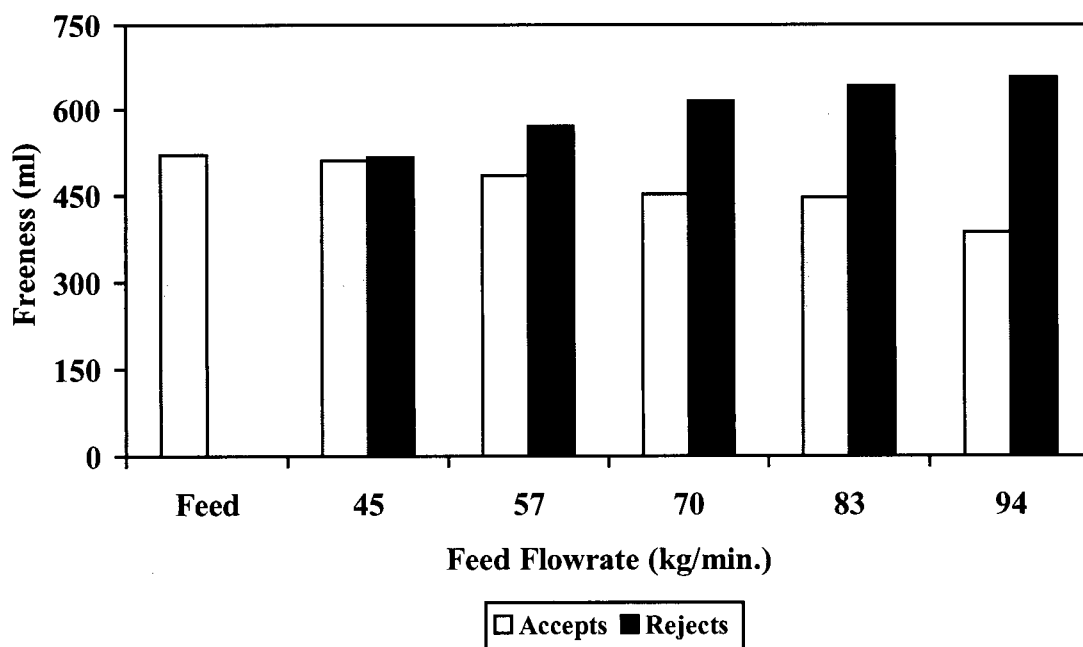


Figure 64 Freeness Measurements for Feed, Accepts, and Rejects for BCTMP Fractionation
(Underflow Tip Size: 6 mm)

5.5 Consistency Effects on Fractionation

Some hydrocyclone researchers in the pulp and paper industry have expressed the opinion that fibre fractionation would be economically inefficient due to consistency constraints. They believe that to effectively process a large amount of pulp, consistencies would have to be comparable, at least, to what could be used in fractionating screens. Using low consistency slurries in hydrocyclones results in high pumping costs and the need for downstream dewatering devices to bring up the consistencies to levels required for papermaking. Above a pulp consistency of 0.5% fibre-fibre interaction may result in decreased fractionation capability when the objective is to separate fibres based on fibre wall thickness, fibre coarseness or fibre length.

Tests performed on Hydrocyclone A and reported in this thesis have shown that separation of short and coarse fibres can be achieved at consistencies greater than 0.6% when the hydrocyclone is operated at low reject rates (refer to Sections 5.2 – 5.3). The objective of this section was to vary pulp consistency and monitor fractionation by length and then to determine how consistency would affect the observations.

CTMP_A was fractionated in Hydrocyclone A at consistencies of 0.25, 0.50, and 0.75%. Figure 65 plots the length weighted fibre lengths for the feed, accepts and rejects. Accepts fibre lengths did not differ appreciably from the feed for each of the consistencies tested. These tended to be constant over the range of flowrates tested. For rejects stream fibre lengths, a first observation was that for each of the consistencies tested, the lengths were always smaller for the rejects than the feed or accepts. As flowrate increased the rejects fibre lengths increased. Thus as flowrate increased the difference between accepts and rejects fibre length decreased. It appears that the difference was least at the lowest consistency (0.25%). The differences at 0.5 and 0.75% consistency were about the same. The conclusion is that low consistency is not necessarily better for fractionation on the basis of fibre length.

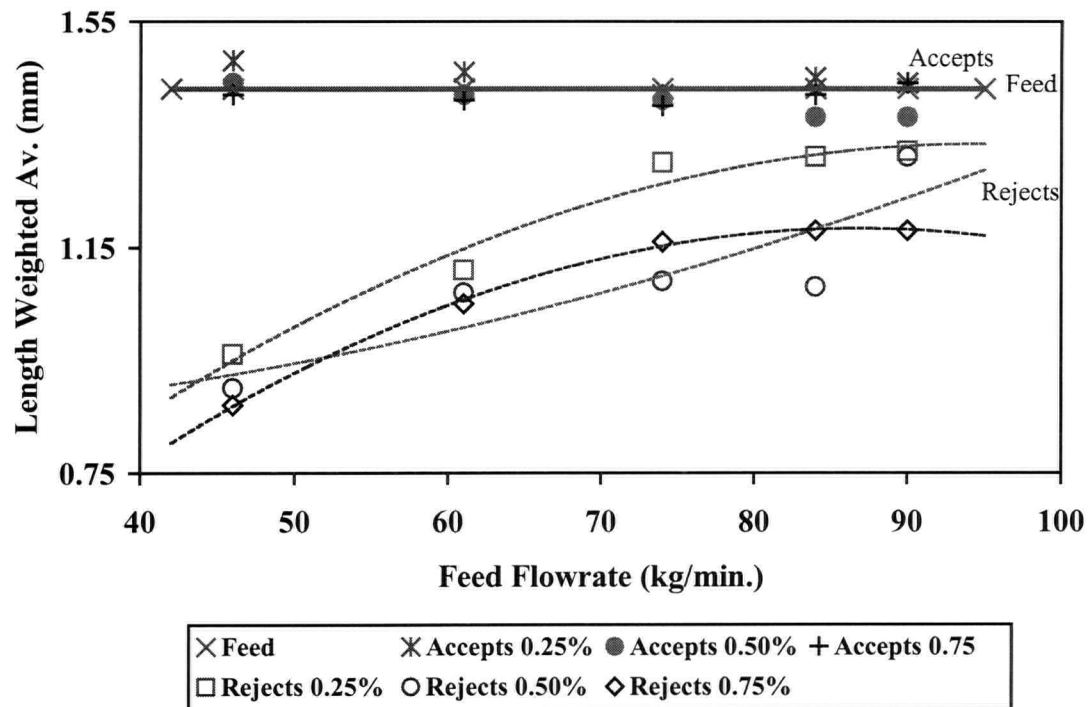


Figure 65 Length Weighted Fibre Lengths of Accepts for Fractionation at Varying Consistencies

5.6 Multistage Fractionation

5.6.1 Multistage Fractionation of CTMP_A With Hydrocyclone A

Since Hydrocyclone A operates at low reject rates, differences between feed and accepts are not easily detected since the bulk of the flow exits the accepts stream. So to try to enhance these differences, a multistage fractionation experiment was performed by discarding the rejects from the first stage and re-fractionating only the accepts. After the second pass the rejects were again discarded and the accepts sent for a third pass. Proceeding in this fashion six passes were made through the hydrocyclone for the accepts. Six stages were chosen since after this stage we found appreciable differences between the accepts and feed properties.

This six stage fractionation was performed with CTMP_A (eastern Canada source) having a consistency of 0.8%; the pulp was fractionated in Hydrocyclone A; the feed flow was maintained at 50 kg/min. The accepts and rejects streams were diverted to two separate tanks and only the accepts stream was re-fractionated.

Fibre length and fibre coarseness results are shown in Figures 66 and 67. An increase in the arithmetic fibre length of the accepts stream and of the rejects stream resulted with an increase in the number of fractionation stages. This was because the discarded rejects had a high proportion of short fibres. Fibre coarseness results showed a tendency to decrease in the coarseness of the fibres in the accepts stream as the number of stages increased. The rejects coarseness values also decreased a little as the number of stages increased. Again these results for both accepts and rejects resulted from discarding the rejects after each pass. With an increasing number of fractionation stages, Hydrocyclone A consistently rejected fibres which were shorter and coarser than the fibres in the accepts stream.

Burst strengths of handsheets made from samples taken from both the accepts stream and rejects stream were found to improve with an increased number of fractionation stages. See Figure 68. This occurred because more and more of the poorly bonding coarse material was removed in the discarded rejects. Figure 69 plots the tear index values. There was an

increase in tear as the number of stages increased for the accepts. For the rejects there was no change after two stages, but an increase occurred after the third stage. After that the tear index was more or less constant. Tear is more sensitive to long fibre content than burst. As more and more short, coarse rejects were discarded from the pulp the mean fibre length of the accepts and rejects would be expected to increase and it did (See Figure 66). Thus one would expect tear to increase as well, and it did.

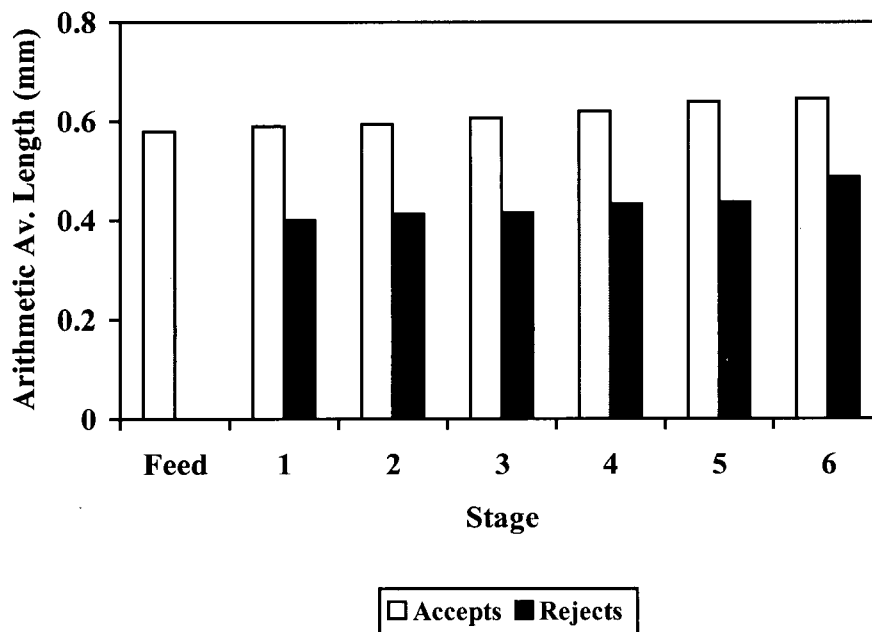


Figure 66 Length Measurements of Feed, Accepts, and Rejects for 6 Stage Fractionation of CTMP_A (Pulp Consistency Tested: 0.8%)

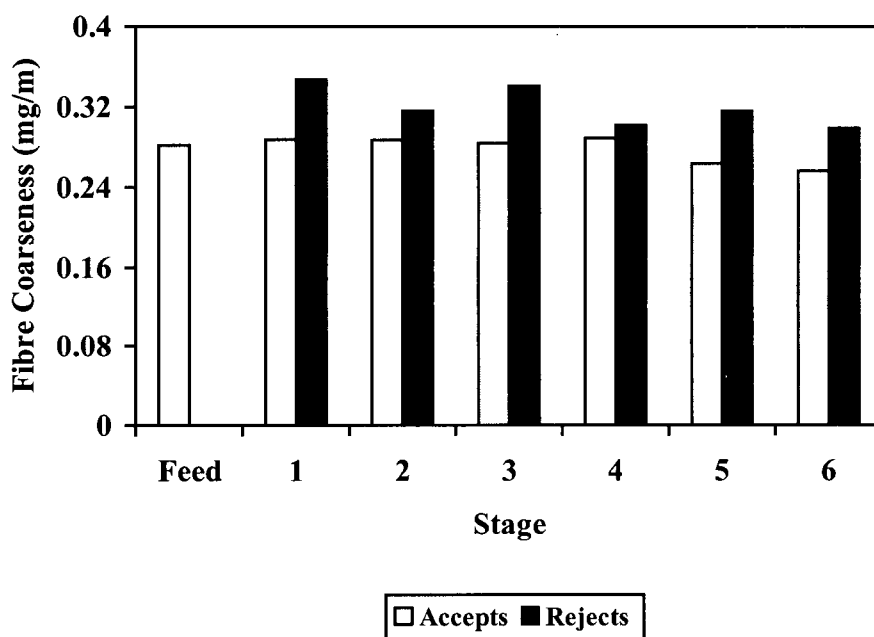


Figure 67 Coarseness Measurements of Feed, Accepts, and Rejects for 6 Stage Fractionation of CTMP_A (Pulp Consistency Tested: 0.8%)

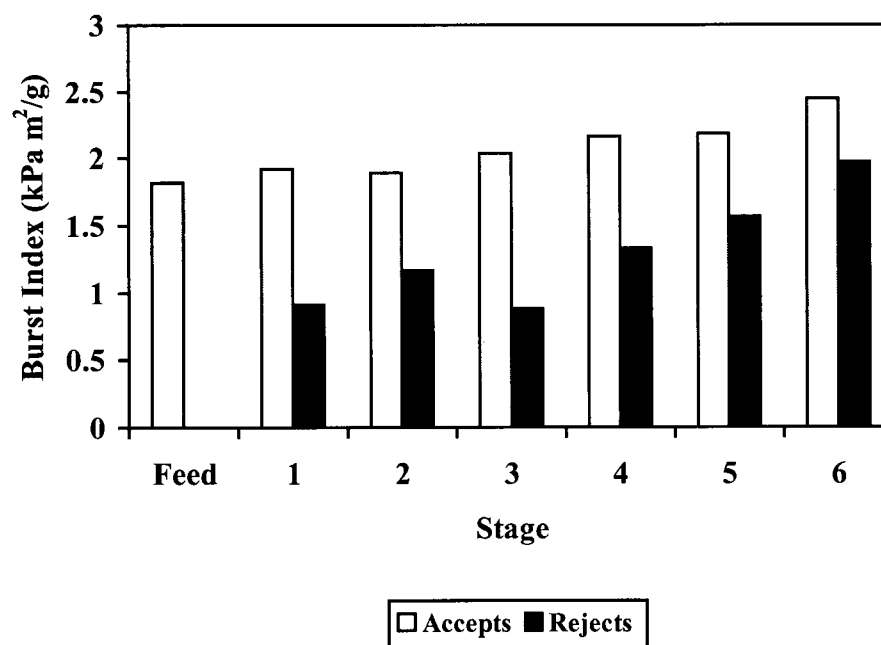


Figure 68 Burst Index Values of Feed, Accepts, and Rejects for 6 Stage Fractionation of CTMP_A (Pulp Consistency Tested: 0.8%)

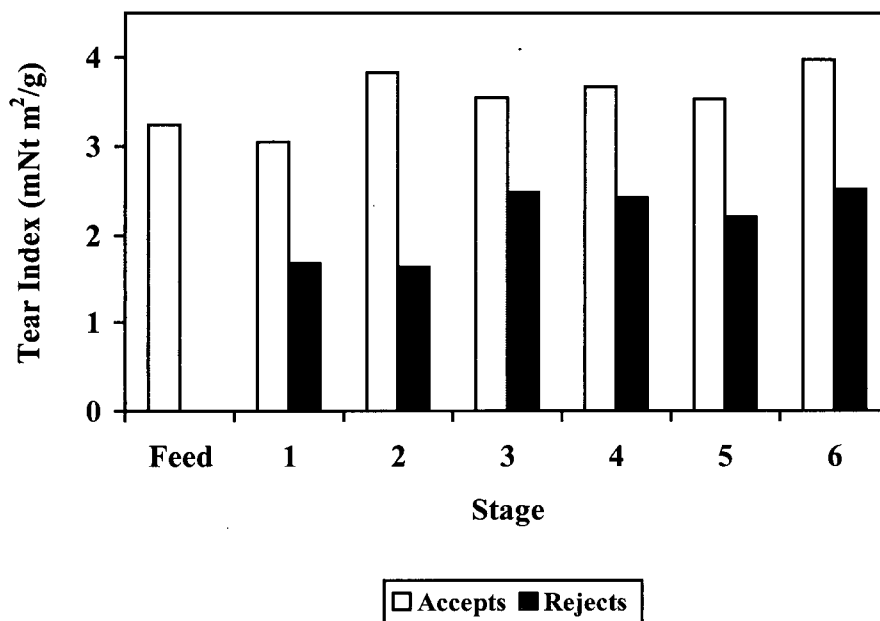


Figure 69 Tear Index Values of Feed, Accepts, and Rejects for 6 Stage Fractionation of CTMP_A (Pulp Consistency Tested: 0.8%)

5.6.2 Multistage Fractionation of TMP_B With Hydrocyclone A with Varying Reject Ratios

The six stage fractionation experiment was repeated with TMP_B. The pulp was tested at a feed flow of 52 kg/min. and had a consistency of 0.9%. The experiment was performed in the same manner as above where only the accepts were re-fractionated and the rejects were discarded.

In this experiment we re-investigated varying reject ratios by testing different diameters for the rejects tip opening. Hydrocyclone A was tested with two reject tip diameters, 3 mm and 5 mm. The reject ratios for the 3 and 5 mm tip diameters were 4 and 7.5% respectively. The objective was to test if varying the reject opening diameter made any difference to the degree of separation achievable when fractionation was performed in multiple stages. The difference between the pulp and paper properties observed for the two different diameters then should be indicative of the success of the fractionation.

Figures 70 and 71 present some photomicrographs of the accepts and rejects taken at the first and sixth stages respectively using Hydrocyclone A with a 3 mm underflow opening. These demonstrate that the accepts from stage 1 contained more long fibres than the rejects from stage 1. The rejects from stage 1 tended to contain a lot of fibre fragments, shives, ray cells and fines. The accepts from stage 6 contained both earlywood and latewood fibres which showed evidence of fibrillation. The rejects from stage 6 were similar to the rejects from stage 1 in that they contained a lot of fibre fragments and short, latewood fibres that showed little evidence of fibrillation.

Table 9 contains values measured for mean length weighted fibre length, freeness (CSF), burst and tear indices. From this Table it can be concluded that the accepts fibres had a mean fibre length that was greater than the mean fibre length of the fibres in the rejects in all cases. The accepts mean fibre lengths were also greater than the feed mean fibre lengths, which were also always greater than the rejects fibre lengths.

In all cases in Table 9 the accepts freeness values were greater than the rejects freeness values. Also for each case, burst and tear indices were in the order accepts \geq feed \geq rejects.

As far as mean fibre length was concerned the difference between accepts and rejects was always greater with the 3 mm opening than the 5 mm opening, which was indicative of a better degree of fractionation if our objective was to fractionate by length.

The difference in accepts and rejects CSF between the 3 mm and 5 mm opening was greater with the 3 mm opening for both the single and 6 stage fractionation again indicating the 3 mm opening gave rise to a greater degree of fractionation. The same was true for the burst index results. For both the 1 and 6 stage fractionation the 3 mm opening showed a bigger difference between accepts and rejects tear factor than was observed with the 5 mm opening.

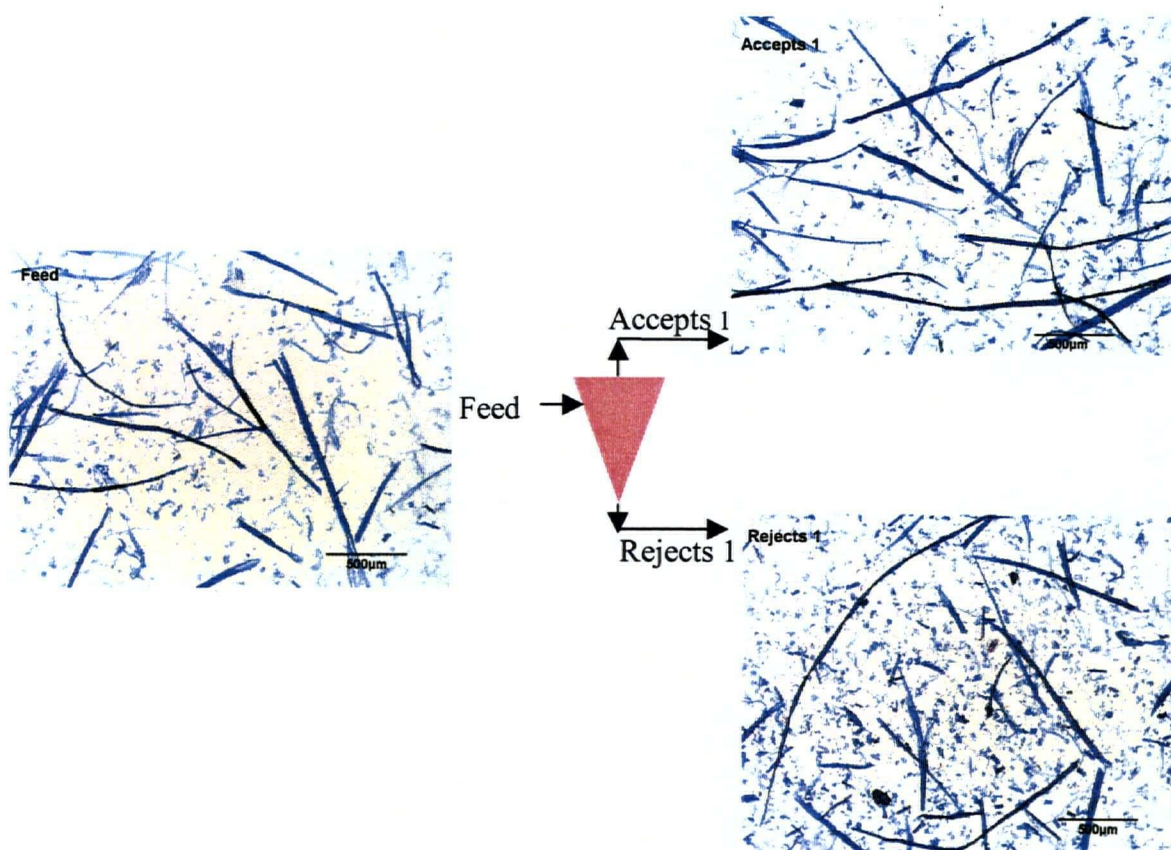


Figure 70 Photomicrographs of Accepts and Rejects from Stage 1 and TMP_B Fractionation Experiment

In comparing Table 9 's single stage fractionation with its 6 stage fractionation there wasn't much difference for accepts fibre length minus rejects fibre length. For CSF there was a bigger difference with the 6 stages between accepts and rejects. The differences between burst and tear factor were not significant.

Figures 72 and 73 are the Bauer McNett distributions for the feed, accepts (stage 1 and stage 6) and rejects (stage 1) for the 3 mm and 5 mm reject tip openings. The most important finding here was that there were significantly more P200 (fines) in the rejects from the 3 mm opening than there were in the feed. With the 5 mm opening, the rejects P200 fraction was the same as in the feed and accepts (both stage 1 and 6). With the 5 mm opening hydrocyclone it was noted that there was significantly more of the R14 (long fibre) material

in the accepts than in the feed. The 6 stage process increased the R14 fraction in the accepts compared to the 1 stage fractionation. This indicated that our multistage fractionation scheme was successful in concentrating long fibres in the accepts stream.

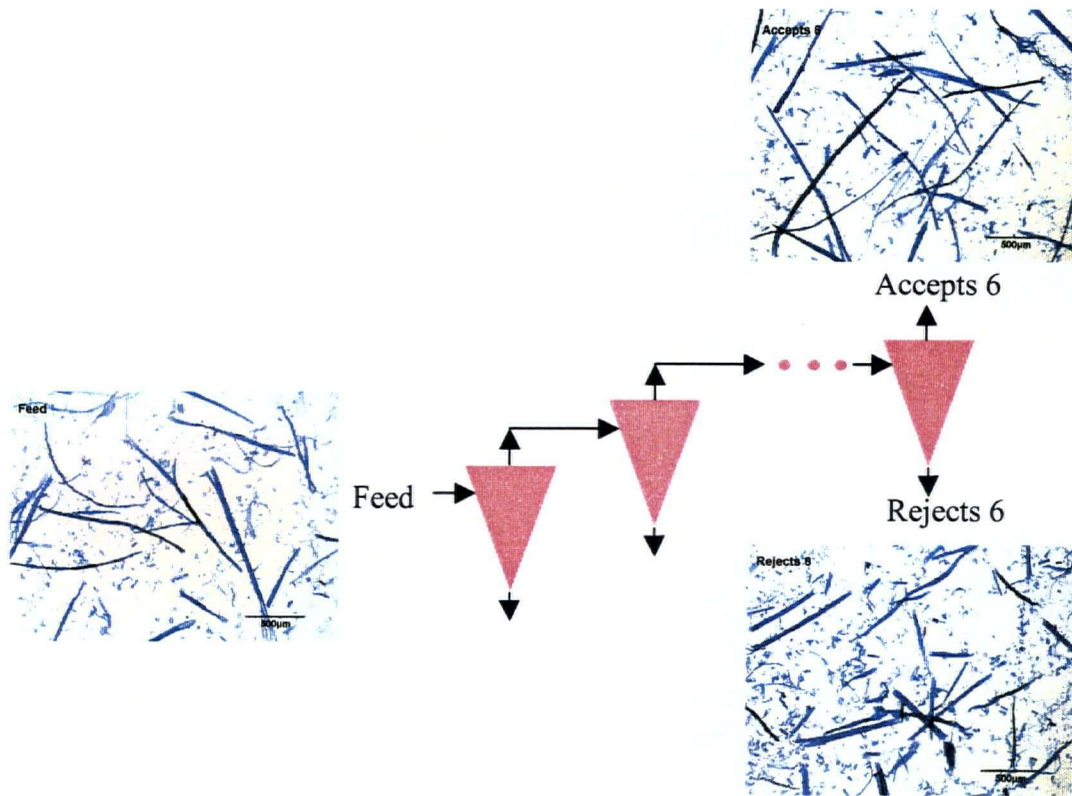


Figure 71 Photomicrographs of Accepts and Rejects from Stage 6 and TMP_B Fractionation Experiment

Table 9 Pulp and Paper Properties for TMP_B 6 Stage Fractionation (Hydrocyclone A Tested With Underflow Diameters of 3 and 5 mm)

		3 mm Underflow				5 mm Underflow			
		Stage 1		Stage 6		Stage 1		Stage 6	
	Initial Feed	Accepts	Rejects	Accepts	Rejects	Accepts	Rejects	Accepts	Rejects
Length Weighted Average (mm)	1.33	1.4	0.86	1.38	0.91	1.36	1.11	1.43	1.18
Freeness (ml)	105	95	36	107	40	88	86	94	66
Burst Index (kPa m ² /g)	1.90	1.90	1.18	2.20	1.42	2.10	1.48	2.23	1.77
Tear Index (mNt m ² /g)	6.20	6.80	4.40	7.20	4.50	6.91	5.67	7.72	6.13

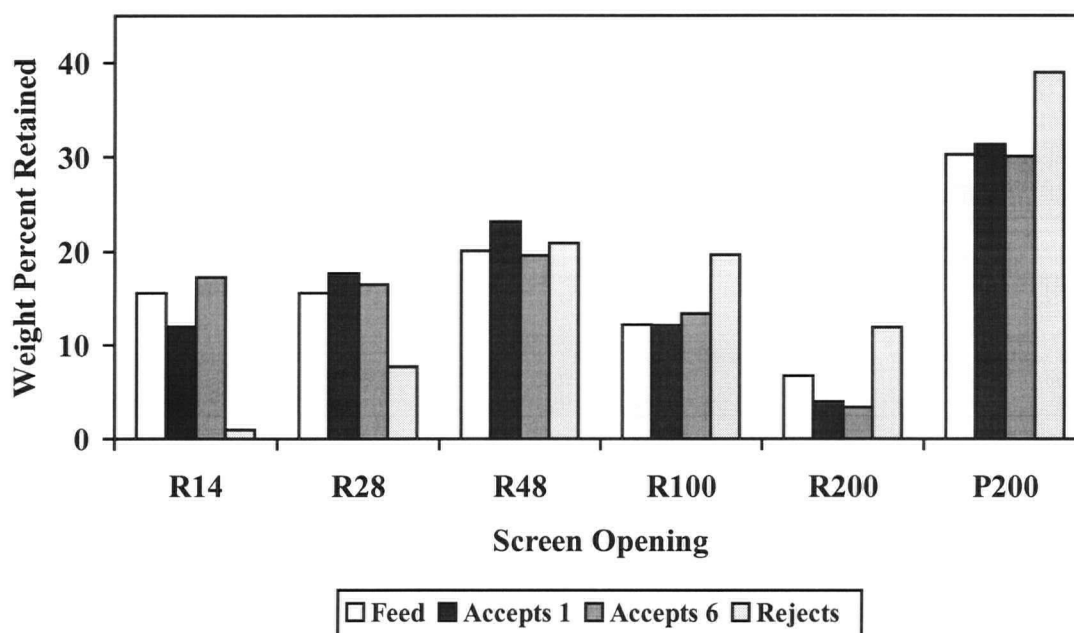


Figure 72 Bauer McNett Fibre Weight Distribution of Feed, Accepts 1 and 6, and Rejects for Underflow Opening of 3 mm

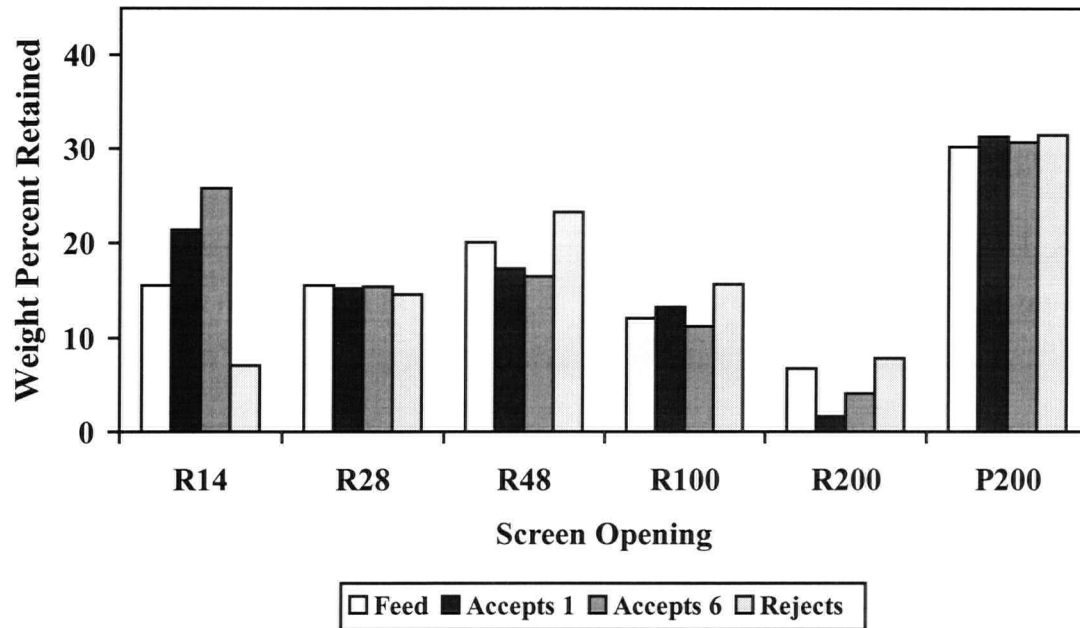


Figure 73 Bauer McNett Fibre Weight Distribution of Feed, Accepts 1 and 6, and Rejects for Underflow Opening of 5 mm

5.6.3 Multistage Fractionation of Chemical Softwood and Refining of Accepts and Rejects

5.6.3.1 Preliminary Experiments Testing Operation of Hydrocyclone C

A fractionation study was performed at the Swedish Pulp and Paper Institute (STFI). A Scandinavian chemical softwood was tested in a commercial cleaner, Hydrocyclone C. The goal was to separate earlywood and latewood fibres in a multistage fractionation scheme. The separated accepts and rejects containing these fibres were then refined to study fibre strength development of the separated fibres.

The first step of this study was to investigate the fractionating capabilities of Hydrocyclone C. The hydrocyclone was tested at four flowrates. A pulp consistency of 0.25% was used since earlier experiments with this pulp involving separation of earlywood from latewood had shown that little separation occurred at higher consistencies [60]. Separation was evaluated by measuring properties on the STFI FibreMaster Fibre Analyzer and by measuring freeness. The FibreMaster has the capability of measuring fibre length, fibre width, and fibre shape. We could assess separation of earlywood and latewood fibres by studying those fibre properties since streams rich in latewood fibres or earlywood fibres should produce different distributions for each fibre property measured. Freeness data could further help characterize fractionation, since latewood fibres should have greater freeness than earlywood due to their reduced collapsibility. In addition microscopy was used to distinguish earlywood fibres from latewood fibres.

Figures 74 – 77 illustrate performance curves for Hydrocyclone C. Pressure Drop, thickening ratio and mass fraction of fibres rejected all increased as feed flowrate increased. The volumetric reject ratio slightly increased and then became constant as feed flowrate increased. When comparing the performance of Hydrocyclone C to our previously tested hydrocyclones (Hydrocyclone A and B) summarized in Section 5.2 we found that Hydrocyclone C had reject ratios (volume and mass basis) closer to those of Hydrocyclone B. Reject ratios of 0.09 – 0.10 were noted for Hydrocyclone C. Hydrocyclone B had reject ratios in the range of 0.12 – 0.15 for the flowrates we tested. These higher reject ratios for

Hydrocyclones B and C resulted from their geometries. Recall that Hydrocyclone A operated at reject ratios of the order of 0.03 –0.05.

Figures 78 –89 plot the fibre property distributions (length, width, and shape factor) for the four flowrates tested. Arithmetic and length weighted average fibre properties (length, width, and shape factor) for the distributions are recorded in the legends of each of the distributions. Fibre length distributions for a flowrate of 150 kg/min. (see Figure 78) showed that for lengths less than 0.5 mm, rejects fibre lengths were smaller than feed and accepts fibre lengths. No clear differences between feed, accepts, and rejects were found for lengths greater than 0.5 mm.

Figure 79 illustrates the width distributions for our test at 150 kg/min. This graph shows differences in fibre widths existed in the range of 25 –35 μm . In this range fibre widths showed the trend rejects>feed>accepts.

Figure 80 shows the fibre shape factor distribution resulting from operation of Hydrocyclone C at 150 kg/min. The STFI FiberMaster calculates the shape factor as the diameter of the smallest circle than can contain the fibre divided by the fibre length [40]. The shape factor for fibres is usually in the range 50 – 100%. The greater the shape factor value the straighter the fibre. For example a shape factor of 100% indicates a perfectly straight fibre. For our test performed at 150 kg/min., a smaller fraction of accepts fibres as compared to the feed and rejects had shape factors in the range of 75 –90%. For shape factors > 90%, accepts fibres had slightly greater values than the feed and rejects. This implies that the accepts have straighter fibres than the feed and rejects fibres.

When the flowrate was increased to 200 kg/min., fibre length differences (Figure 81) among the feed, accepts and rejects fibres could be seen. The accepts stream had the greatest fraction of fibres in the range of 0 – 0.5 mm. There was a lower fraction of rejects fibres in this range as compared to the feed and accepts. Over the rest of the fibre length range there appeared to be little difference among the three streams.

Figure 82 plots the width distribution for the test performed at 200 kg/min. Reject fibres tended to have a lower fraction of fibres in the width range of 0 – 20 μm . Above 20 μm all three distributions were similar.

Shape factors are presented in Figure 83. A lower fraction of accepts fibres than rejects and feed fibres fell into the shape factor range 70 – 85%. No obvious differences in the width and shape factor distributions between the rejects and feed were detected at this flowrate.

Hydrocyclone C was designed to operate at 270 kg/min. At this flowrate we found the fibre length distributions showed larger differences than at 200 kg/min. between the feed, accepts, and rejects (Figure 84). The most obvious observation was that the fraction of fibres in the range 0 – 0.5 mm in the accepts sample increased as compared to the lower flowrates tested. This implies that there were more fines in the accepts at higher flowrates

Figure 85 shows the width distributions for this flowrate. There was a lower fraction of fibres with widths in the range 20 – 30 μm in the accepts than in the feed and rejects. Once again a lower fraction of accepts fibres, as compared to the feed and rejects, were found to have shape factors in the range of 75 – 85% (Figure 86). A greater fraction of accepts fibres had shape factors greater than 90%.

Figure 87 shows that as the feed was increased to 400 kg/min., there was a greater percentage of fibres in the length range 0 – 1 mm for the accepts than for the rejects and feed. The fibre width distributions illustrated in Figure 88 showed that there was a greater fraction of accepts fibres having fibre widths in the range 0 – 20 μm than the feed. There was a greater fraction of feed fibres in this range than there was in the rejects. A lower fraction of accepts fibres was detected in the width range 20 – 40 μm than in the feed. A greater fraction of rejects fibres were in this range than in the feed. No differences resulted for widths greater than 40 μm . With this flowrate, larger differences in the shape factor distribution were detected. There were less fibres in the accepts stream which possessed shape factors in the range of 60 – 90 % as compared to the feed and rejects. There were more accepts fibres than rejects and

feed fibres which had shape factors greater than 90%. This indicates that Hydrocyclone C is accepting fibres which are straighter than those found in the rejects stream.

Figure 90 plots the freeness data for this experiment. As the flowrate increased the accepts freeness decreased and rejects freeness increased. This signified that a larger quantity of fines and flexible fibres had reported to the accepts stream.

Figures 91 – 93 plot the length weighted length, width and shape factor averages from the distributions illustrated above. The length weighted average properties are shown since they are less sensitive to the fines content of the samples. Figure 91 shows that as feed flowrate was increased, the accepts fibre length decreased and the rejects fibre lengths increased. Also as flowrate increased the difference between rejects and accepts fibre length increased. Note that Hydrocyclone C tended to reject longer fibres in contrast to Hydrocyclone A. Figure 92 demonstrates that as flowrate increased, the average widths of fibres in the accepts decreased and the widths of the rejects fibres increased. Again as flowrate increased the difference between rejects and accepts fibre width increased. Hydrocyclone C tended to reject thick fibres. No measurements of fibre width were made for Hydrocyclone A. Differences in average shape factors were small, (Figure 93) however the graph shows that the shape factors of the accepts increased slightly as flowrate increased. Shape factors of the rejects tended to slightly decreased as the flowrate increased.

In Figures 91 – 93 only average values for length weighted fibre length, fibre width, and fibre shape factor are reported. Prior to this part of the work described in this thesis we only reported average values for fibre length and coarseness. We could have presented distributions for the fibre lengths but we didn't. It is better to report both the mean values and the distribution. The mean value is simply an attempt to characterize a distribution of values by a single number which in many cases is an oversimplification. For example in Figure 91 at a flowrate of 150 kg/min. there is hardly any difference in average fibre length between rejects and accepts. Yet considering Figure 78 it can be seen that there are regions (e.g. 0 – 0.2 mm) where the rejects fibres were shorter than the accepts and feed fibres and other regions (e.g. 1 – 2 mm) where the accepts fibres tended to be shorter.

From the above preliminary study of Hydrocyclone C it was concluded that increases in the feed flowrate to this hydrocyclone resulted in large differences between the feed, accepts, and rejects fibre length distributions. In this commercial cleaner we found that fines reported to the accepts stream. Differences in the shape factor distributions indicated that fibres in the accepts were straighter than those in the feed and rejects fibres. Some differences were noted in the width distributions, particularly in the width range of 25 – 35 μm . The freeness data imply that at flowrates of 150 - 400 kg/min. the accepts fibres had a greater specific surface than the feed and rejects fibres.

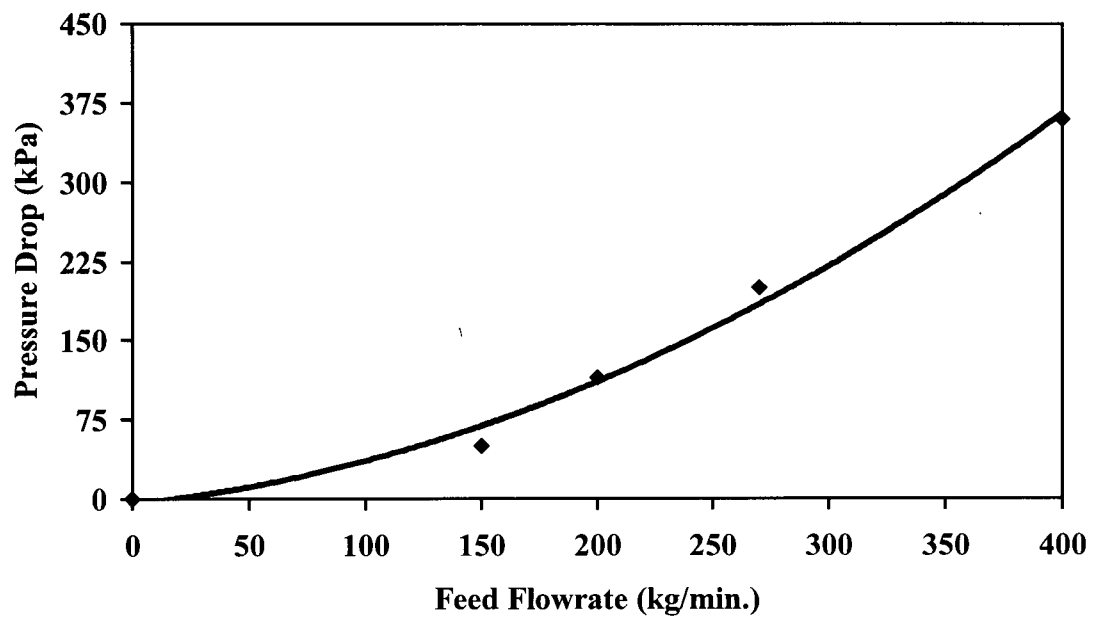


Figure 74 Feed Flowrate versus Pressure Drop for Hydrocyclone C

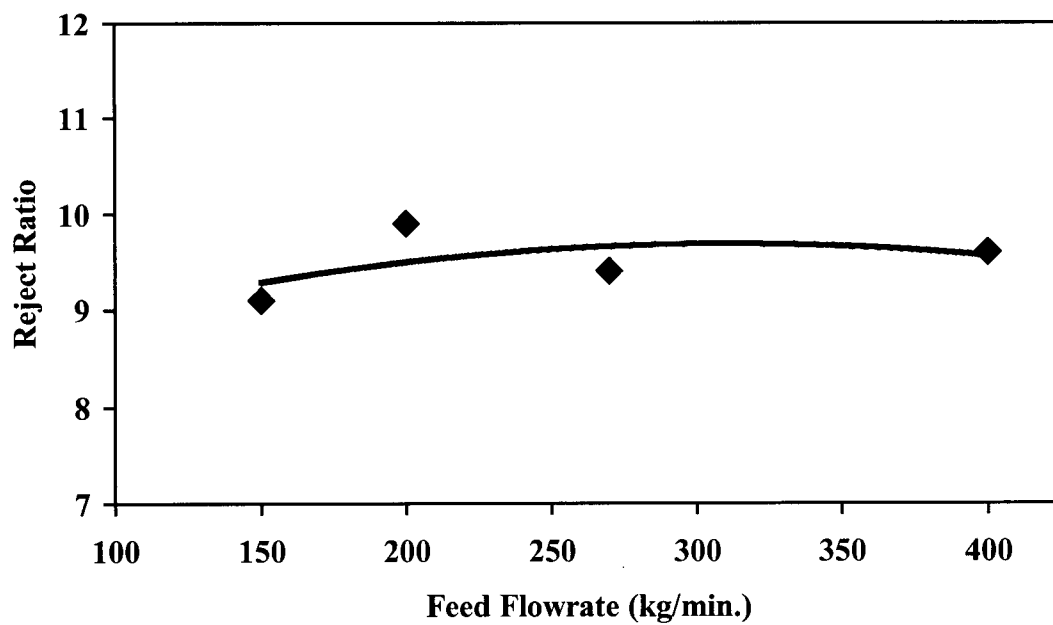


Figure 75 Volumetric Reject Ratio Relationship for Hydrocyclone C

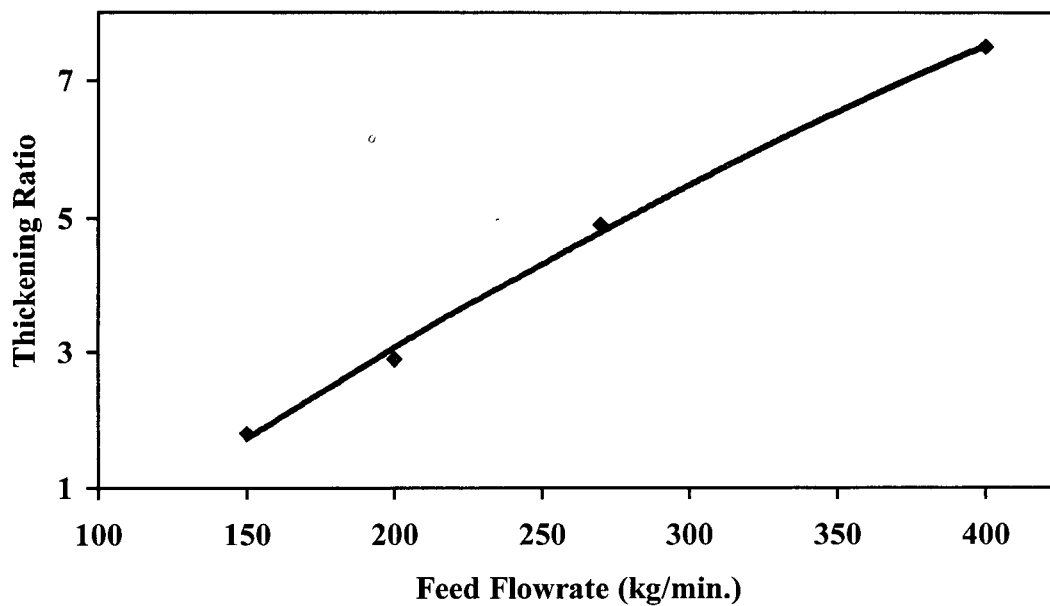


Figure 76 Thickening Ratio versus Feed Flowrate for Hydrocyclone C

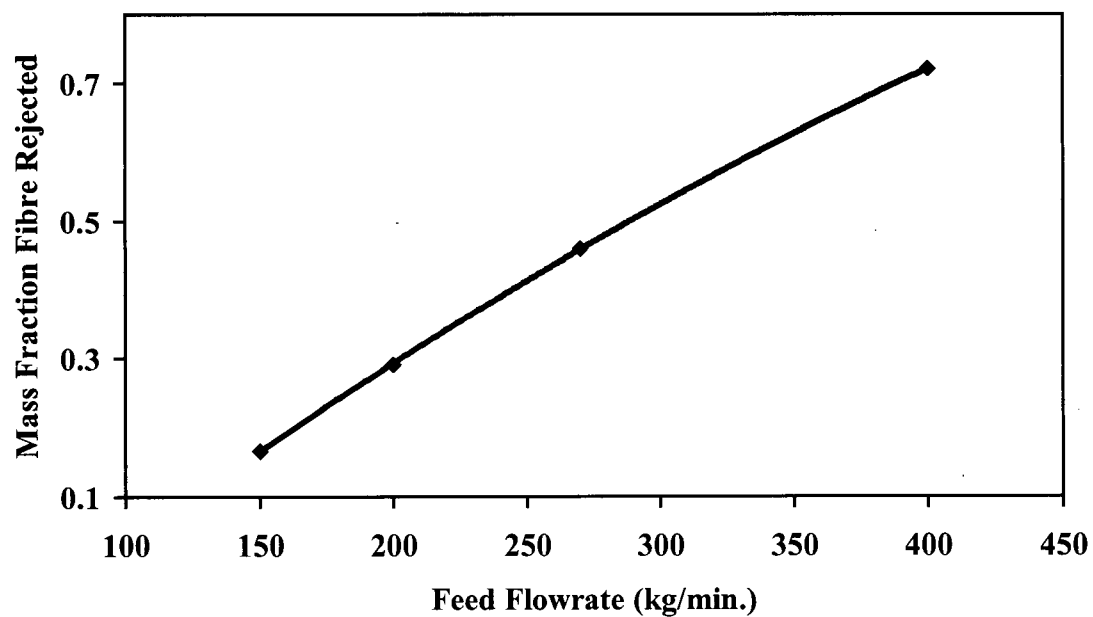


Figure 77 Mass Fraction of Fibre Rejected with Hydrocyclone C Operated at Various Flowrates

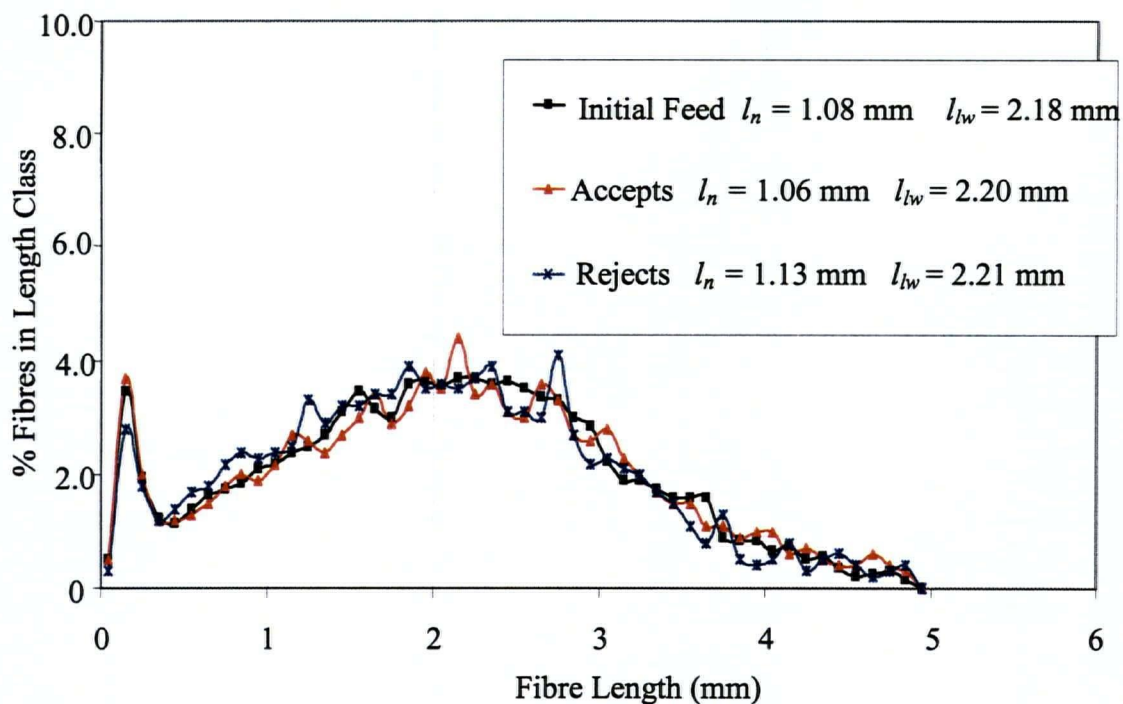


Figure 78 Length Distribution for Hydrocyclone C Operating at a Feed Flowrate of 150 kg/min. and Pressure Drop of 42 kPa

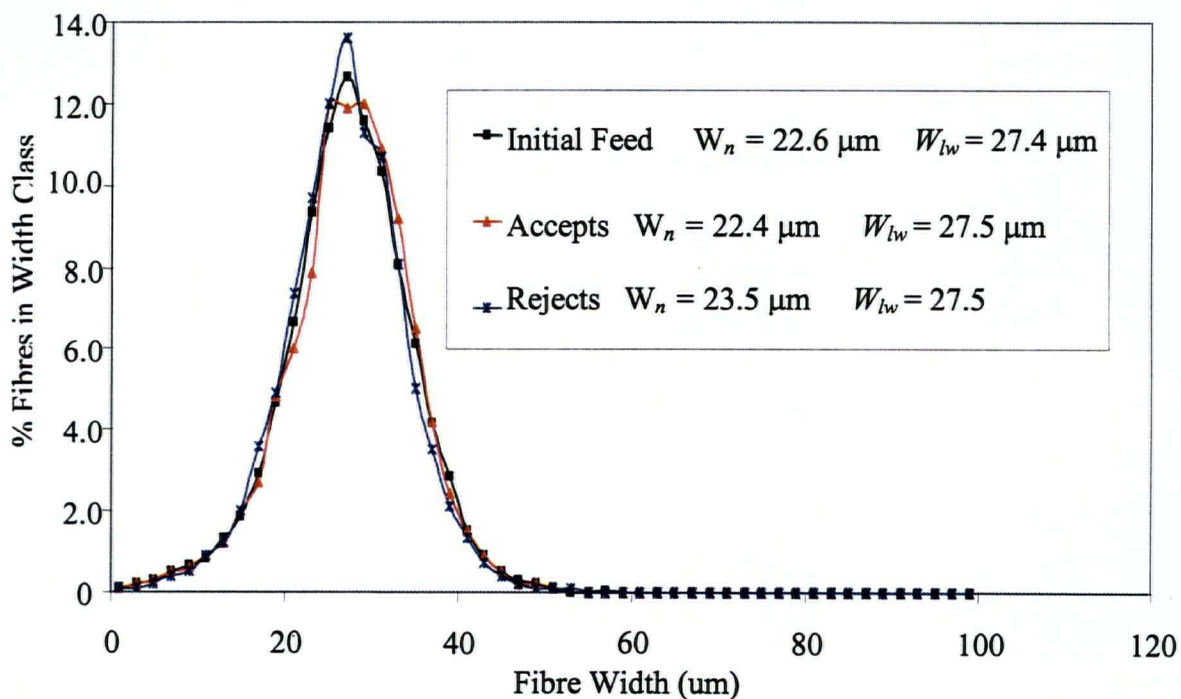


Figure 79 Fibre Width Distribution for Hydrocyclone C Operating at a Feed Flowrate of 150 kg/min. and Pressure Drop of 42 kPa

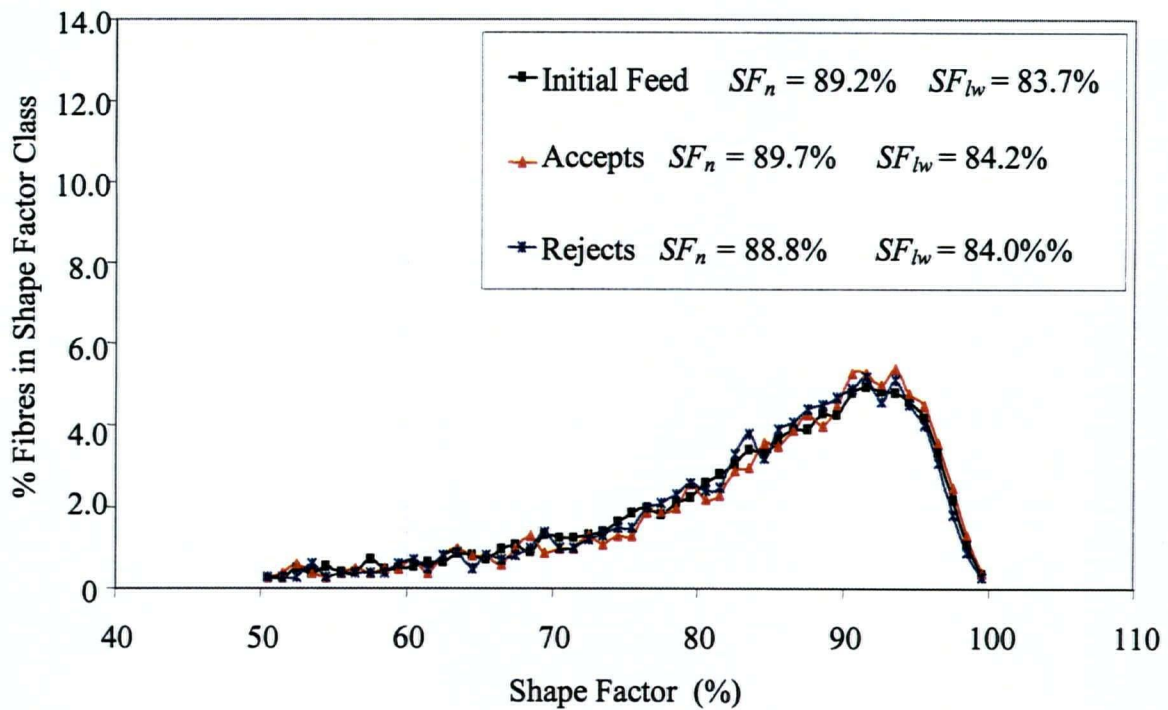


Figure 80 Shape Factor Distribution for Hydrocyclone C Operating at a Feed Flowrate of 150 kg/min. and Pressure Drop of 42 kPa

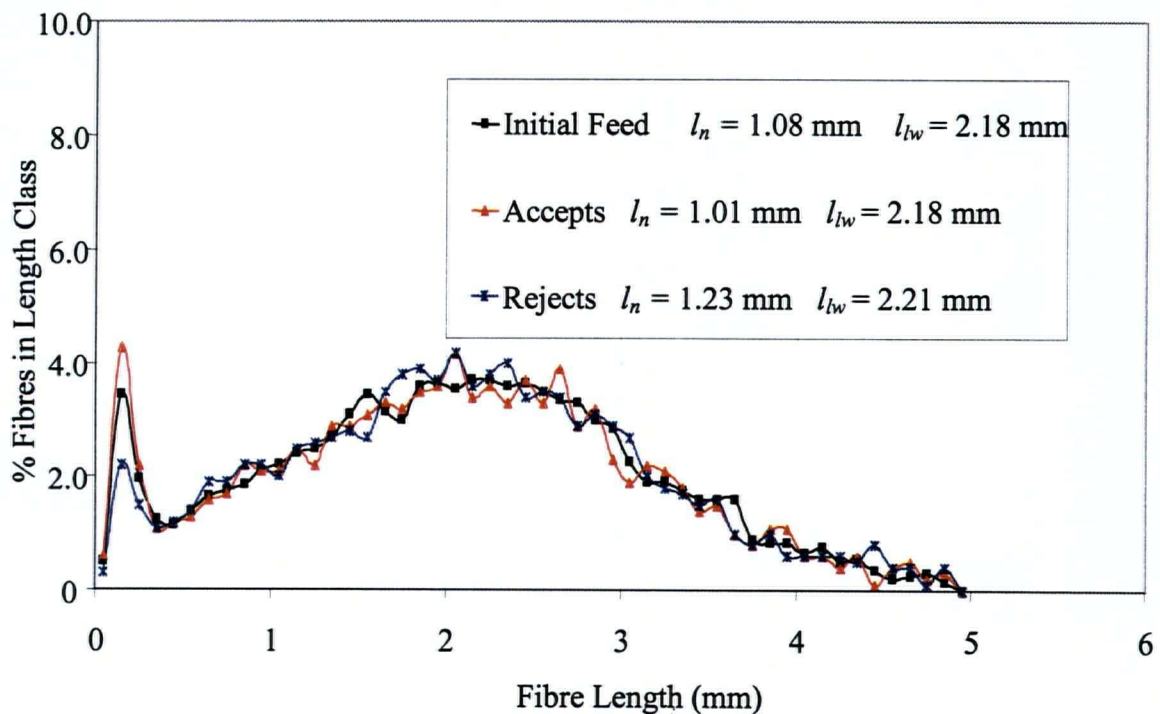


Figure 81 Length Distribution for Hydrocyclone C Operating at a Feed Flowrate of 200 kg/min. and Pressure Drop of 75 kPa

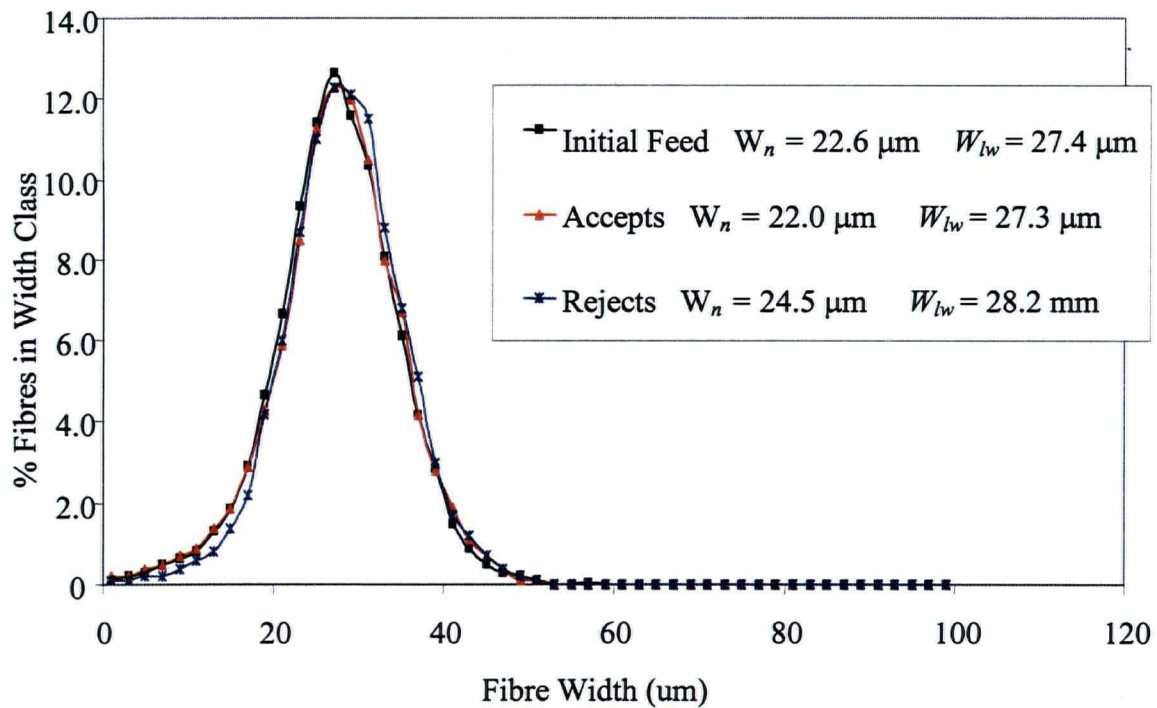


Figure 82 Fibre Width Distribution for Hydrocyclone C Operating at a Feed Flowrate of 200 kg/min. and Pressure Drop of 75 kPa

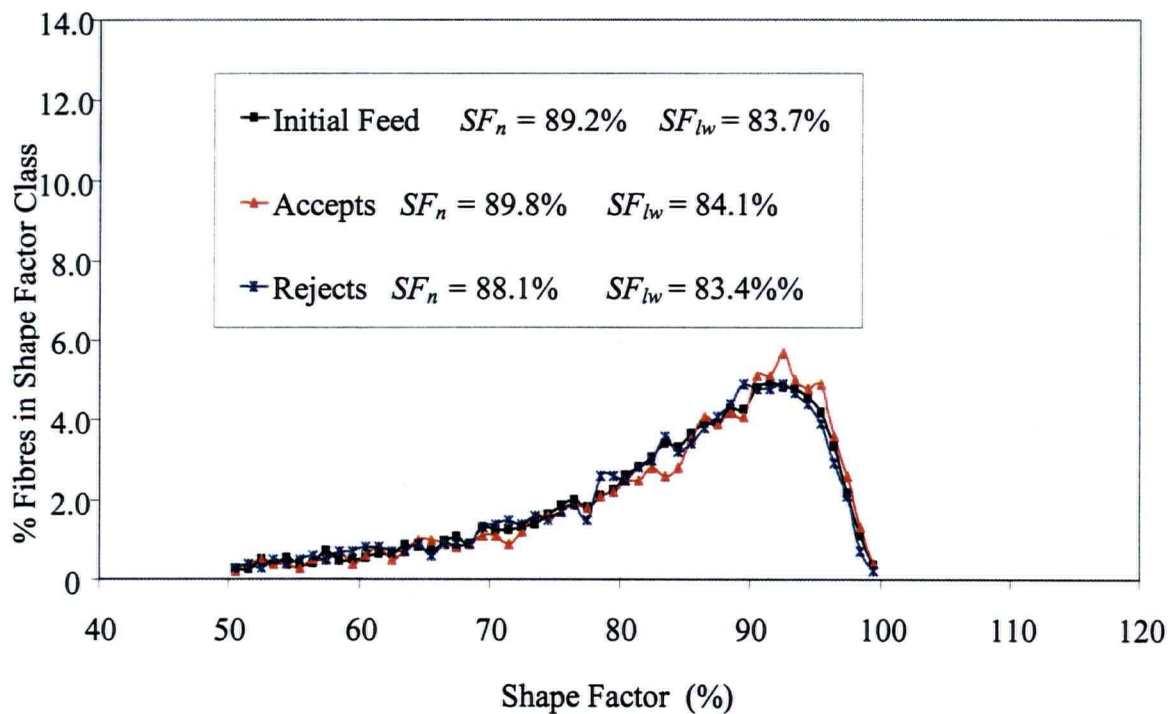


Figure 83 Shape Factor Distribution for Hydrocyclone C Operating at a Feed Flowrate of 200 kg/min. and Pressure Drop of 75 kPa

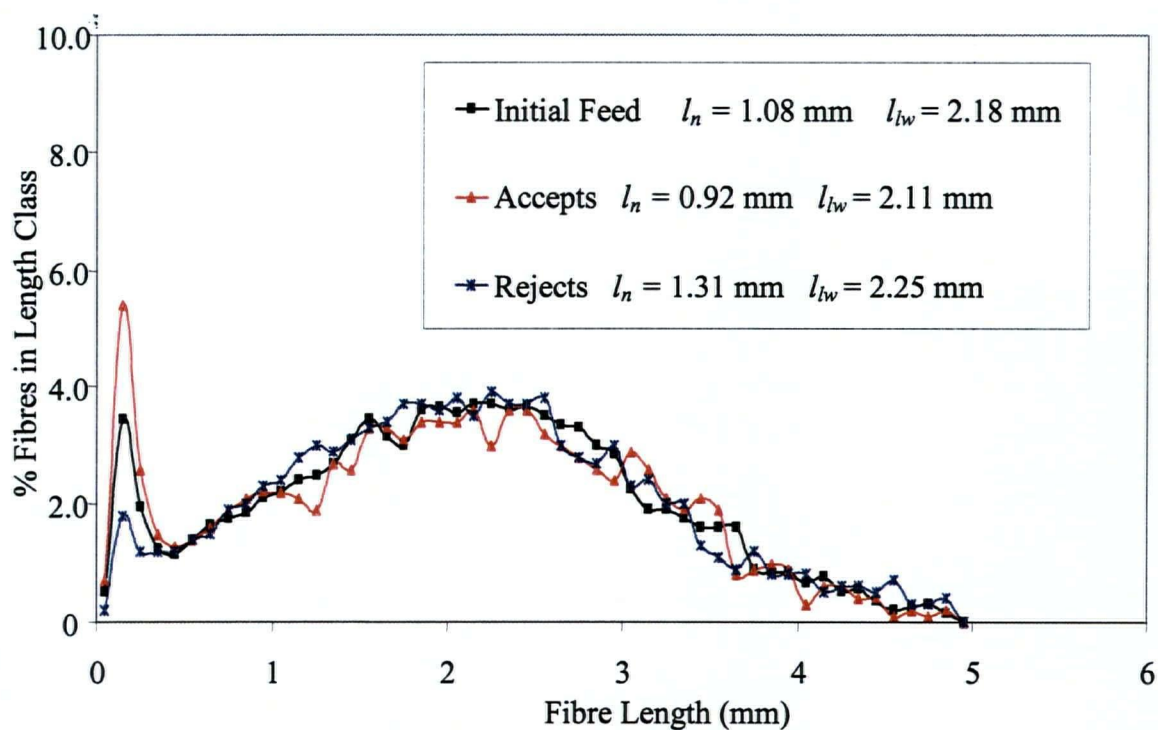


Figure 84 Length Distribution for Hydrocyclone C Operating at a Feed Flowrate of 270 kg/min. and Pressure Drop of 130.5 kPa

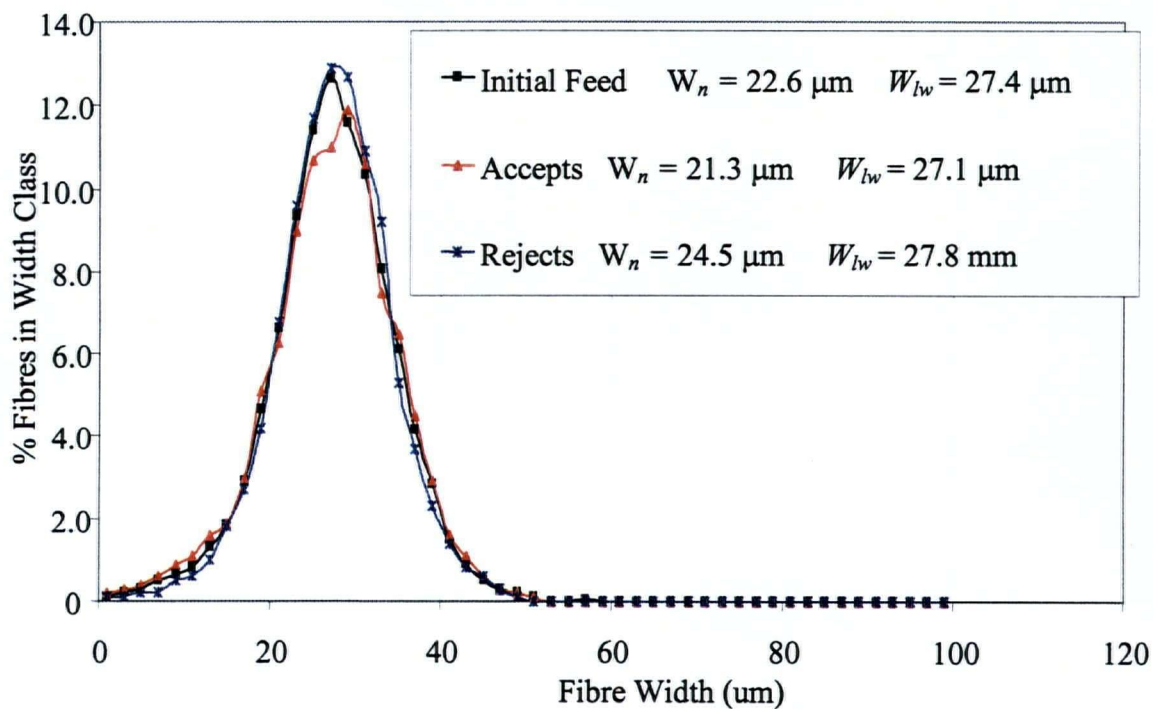


Figure 85 Fibre Width Distribution for Hydrocyclone C Operating at a Feed Flowrate of 270 kg/min. and Pressure Drop of 130.5 kPa

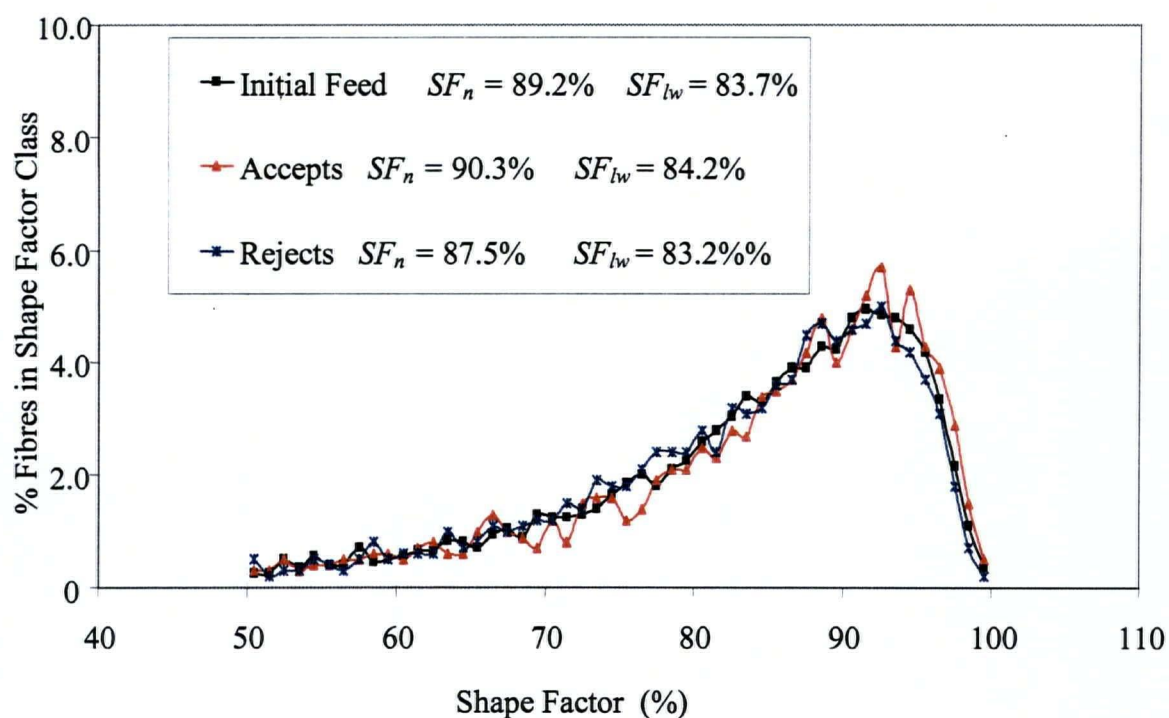


Figure 86 Shape Factor Distribution for Hydrocyclone C Operating at a Feed Flowrate of 270 kg/min. and Pressure Drop of 130.5 kPa

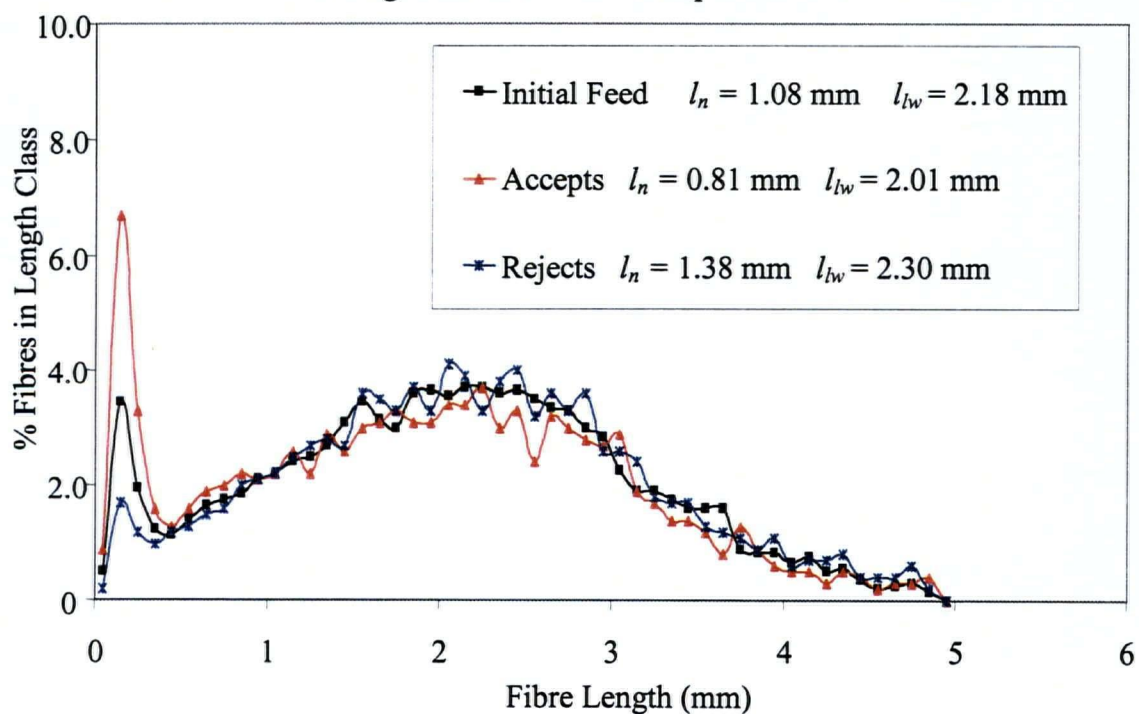


Figure 87 Length Distribution for Hydrocyclone C Operating at a Feed Flowrate of 400 kg/min. and Pressure Drop of 230 kPa

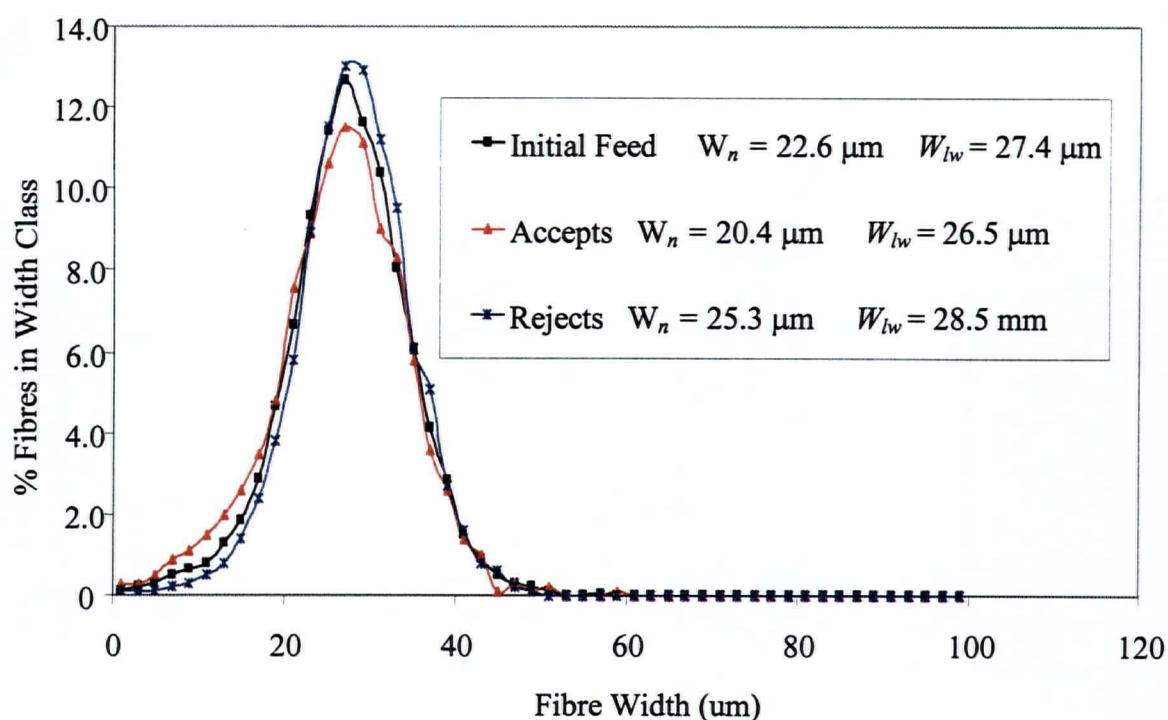


Figure 88 Fibre Width Distribution for Hydrocyclone C Operating at a Feed Flowrate of 400 kg/min. and Pressure Drop of 230 kPa

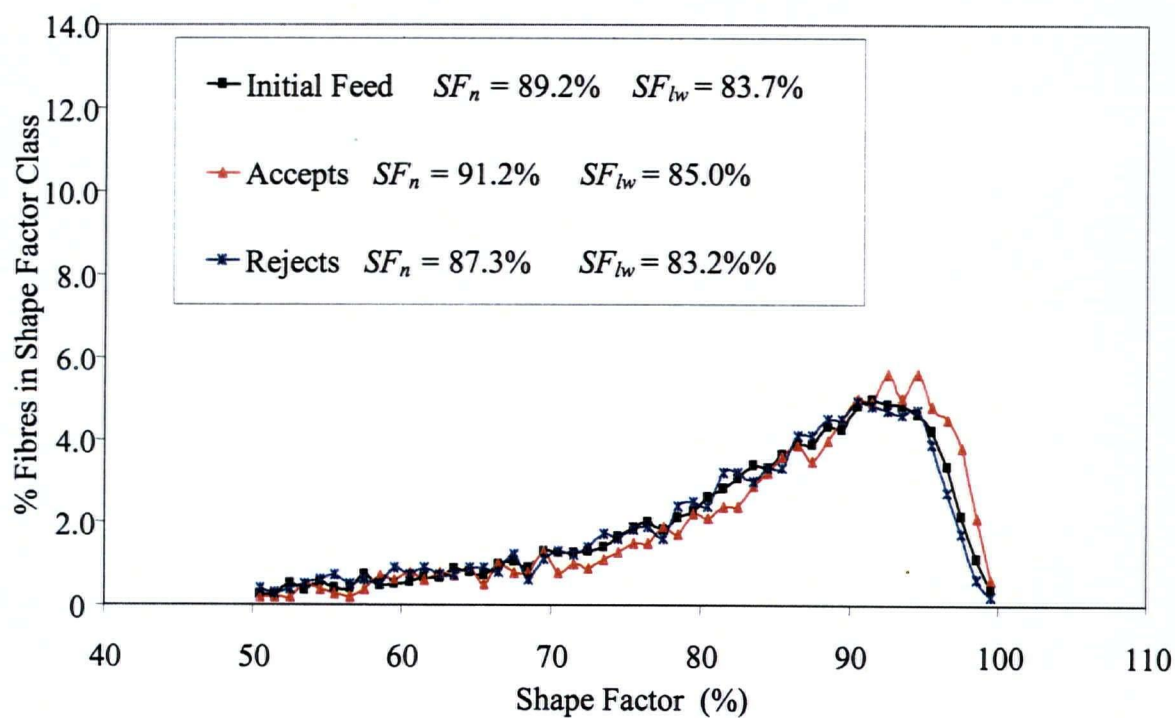


Figure 89 Shape Factor Distribution for Hydrocyclone C Operating at a Feed Flowrate of 400 kg/min. and Pressure Drop of 230 kPa

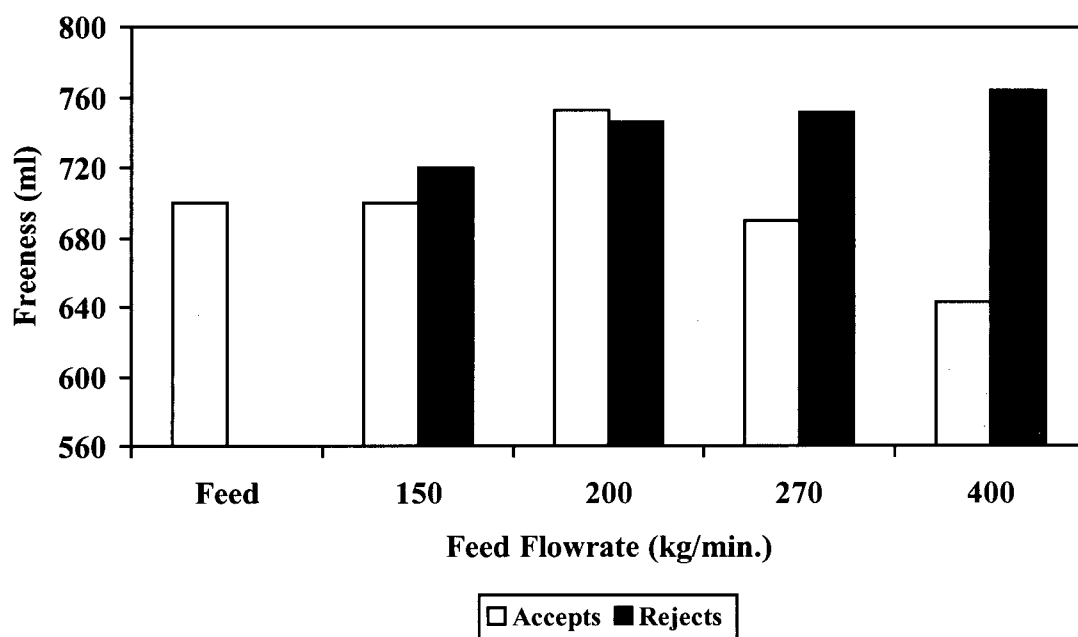


Figure 90 Freeness Measurements for Feed, Accepts and Rejects From Scandinavian Softwood Fractionation Using Hydrocyclone C

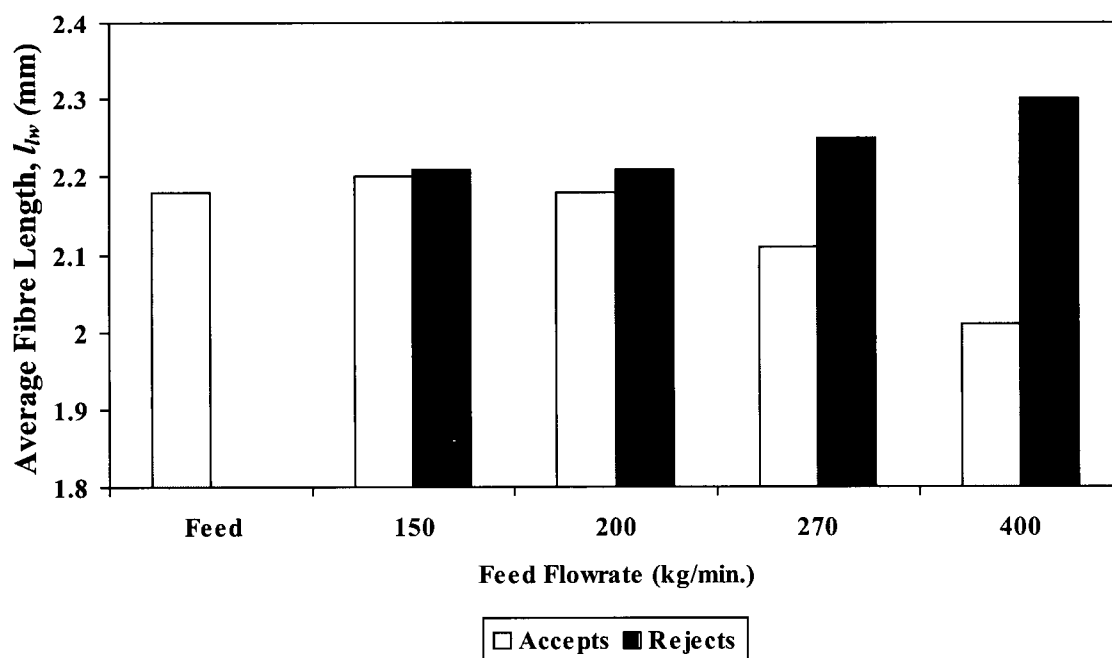


Figure 91 Length Weighted Average Fibre Length Measurements for Feed, Accepts and Rejects From Scandinavian Softwood Fractionation Using Hydrocyclone C

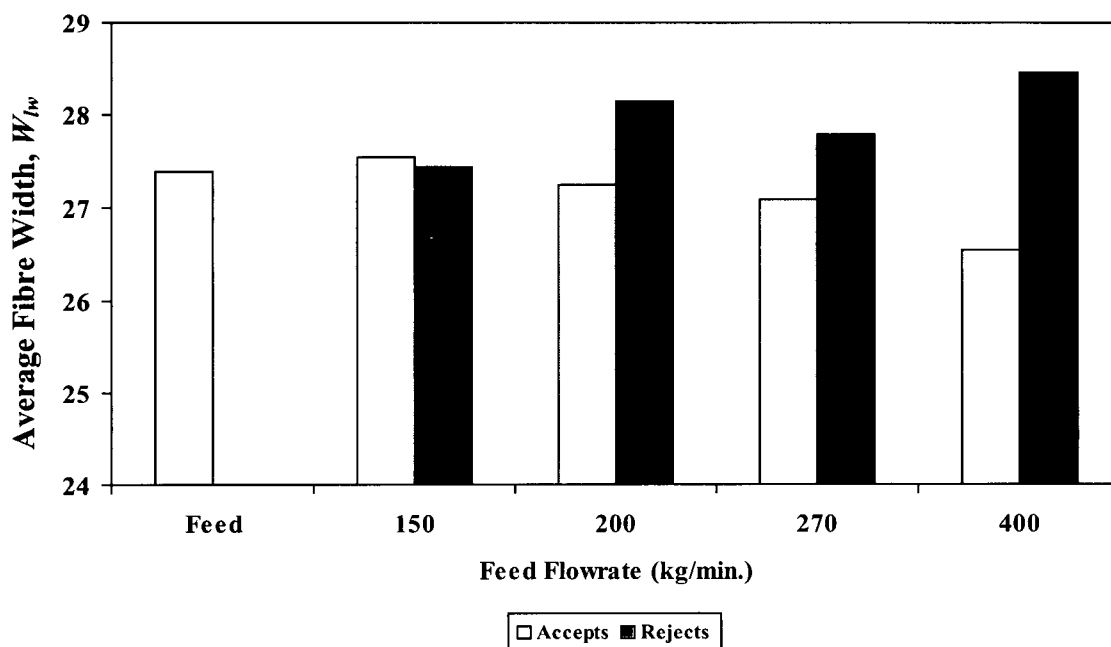


Figure 92 Average Fibre Width Measurements for Feed, Accepts and Rejects From Scandinavian Softwood Fractionation Using Hydrocyclone C

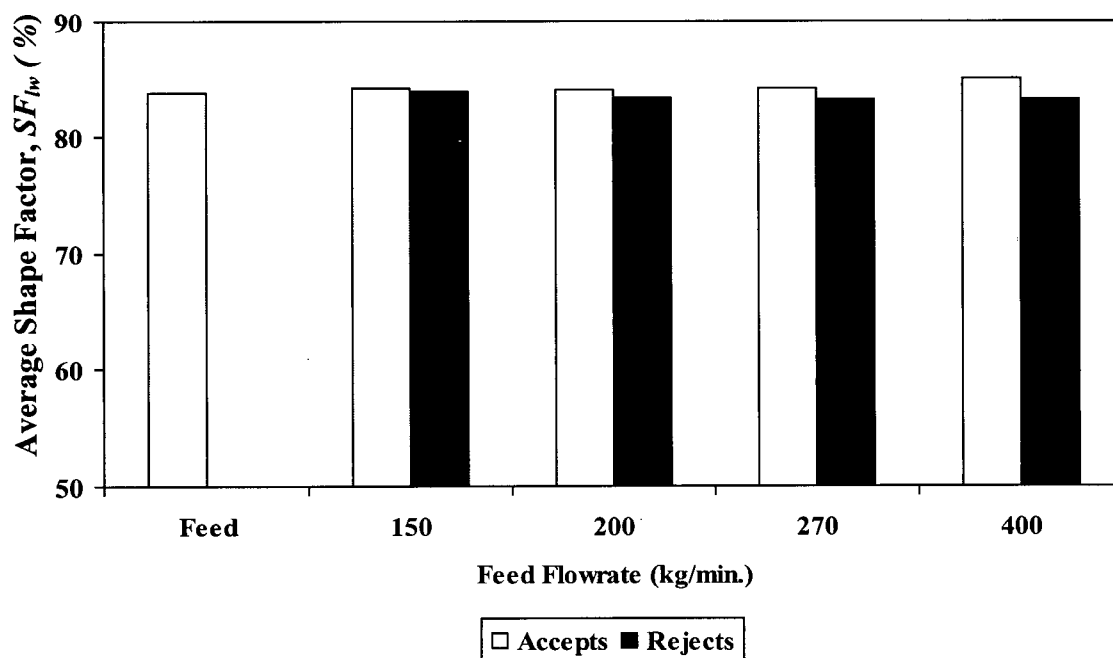


Figure 93 Average Fibre Shape Factor Measurements for Feed, Accepts and Rejects From Scandinavian Softwood Fractionation Using Hydrocyclone C

5.6.3.2 Three Stage Fractionation of Hydrocyclone Accepts and Rejects

After performing the initial tests on Hydrocyclone C, a multistage fractionation test of hydrocyclone accepts and rejects was performed. The experimental schemes chosen for the three stage accepts and rejects fractionation are illustrated in Figures 94 and 95 respectively. Some adjustments were made to Hydrocyclone C by the manufacturer prior to performing this experiment so identical conditions to those for the preliminary conditions could not be matched [59]. Nonetheless we set up the multistage fractionation based on the findings summarized in Section 5.6.3.1. Pulp having an initial consistency of 0.25% was pumped to the system. The fractionation experiment was set up so that both the accepts and the rejects could be fractionated in three stages (see Figures 94 and 95). These figures show a naming scheme given to identify the various fractionated streams.

In these three stage fractionations our goal was to try to get earlywood fibres into the accepts and latewood fibres into the rejects. Let's first consider the three stage accepts fractionation illustrated in Figure 94. The initial feed to Hydrocyclone C was supplied at a flowrate of 428 kg/min. corresponding to a pressure drop of 318 kPa. The accepts from the first stage were collected and then passed through the same hydrocyclone again at a flowrate of 412 kg/min. (pressure drop = 253 kPa). These flowrates were chosen because the preliminary experiments described in section 5.6.3.1 indicated that at these flowrates fractionation occurred. The initial feed was characterized as having an earlywood content of 66% and a latewood content of 34%. Figure 77 shows that at flowrates of 400 kg/min. about 72% of the fibres were rejected, thus much earlywood was being rejected. To try to accept as much as possible of the remaining earlywood the feed flowrate was reduced to 270 kg/min.

The rejects from the first and second stage of the process outlined in Figure 94 were saved in a storage tank for the subsequent three stage rejects fractionation scheme of Figure 95. The first stages were common to the three stage accepts and rejects fractionation schemes. The rejects AR3 from the accepts fractionation scheme were discarded.

Table 10 summarizes the operating conditions for the three stage accepts fractionation. Note that in these experiments the volumetric reject ratios at flowrates of the order of 400 kg/min. were 4 – 5 % whereas in the preliminary experiments at similar flowrates they were around 9.5 – 10%. This difference probably occurred because of underflow tip modifications made to Hydrocyclone C by its manufacturer between the two sets of tests. The 3rd stage fractionation was done at an inlet consistency of 0.13% since this was the consistency of the AA2 stream.

Figures 96 – 101 illustrate the length and width distributions for each of the streams identified for the three stage accepts fractionation (Figure 94). Table 11 summarizes the length weighted average length, width and shape factor for each of the streams (l_{lw} , W_{lw} , and SF_{lw}). Both arithmetic and length weighted property averages are included in the legends of the property distribution graphs.

The length distribution of Figure 96 for the 1st stage shows that in the fibre length range 0 – 0.2 mm (fibre fines) there was a higher percentage of such fibres in the accepts than in the feed and there was a higher percentage in the feed than in the rejects. In the 2nd stage since fines were concentrated in the accepts of stage 1 which was the feed to stage 2 the pattern observed in stage 1 was again observed but the difference between accepts and feed was increased. The difference between feed and rejects decreased. In the 3rd stage there was an even greater difference between accepts and feed. For stage 3 the difference between feed and accepts was again increased compared to stage 2.

In the 1st stage (Figure 96) for the length range 0.5 – 2 mm there was a higher proportion of such fibres in the rejects than in the feed and a lower proportion usually, but not always, in the accepts. Above 2.5 mm the three distributions were more or less the same implying no fractionation was occurring in this range.

In the second stage (Figure 97) there were more fibres in the rejects having lengths between 0.3 – 1.4 mm than either the feed or accepts. In the range 2.5 – 3.2 mm there were fewer such fibre in the rejects compared to the feed and accepts. From 3.3 – 3.6 mm the percentage

of fibres in this range was higher in the rejects. Above 3.6 mm all three distributions were similar again.

In stage 3 (Figure 98) in the length range of 0.8 – 2.5 mm there were more fibres in the rejects than in the feed which contained more than the rejects. Above 2.8 mm no differences amongst the streams were observed.

The average fibre lengths noted in Table 11 indicate that Hydrocyclone C tends to reject longer fibre than it accepts. But this simple picture is not really representative of what was seen in the distributions of Figures 96 – 98. The average fibre length of the accepts is shorter than that of the rejects because the fines go to the accepts.

Analyzing the first stage width distribution illustrated in Figure 99 showed that there were fewer fibres having widths in the range 0 – 18 μm in the rejects than in the feed and more in the accepts than in the feed. For the width range 25 – 30 μm , there were more fibres in the rejects followed by the feed and then the accepts. Above 35 μm there were no significant differences among the three distributions implying that thick fibres didn't fractionate as well as thin ones. The second stage showed a pattern similar to first stage however, the differences were more pronounced. Again no fractionation of thick fibres was seen. The third stage fractionation showed width differences in a broader range than the first two stages. This time there were more fibres in the accepts range in the range 0 – 25 μm than the feed (AA2) and fewer in the rejects. The trend in this range followed $\text{AA3} > \text{AA2} > \text{AR3}$. Analysis of the width range 25 – 40 μm showed that more fibres concentrated in the rejects in this width range. Average property data of Table 12 led to the conclusion that this accepts fractionation resulted in a final accepts stream (AA3) containing a large content of fines and average fibre lengths which were smaller than the rejects. Fibre widths were smaller for the accepts for each stage tested. Shape factors indicated that accepts fibres were always straighter than rejects and feed fibres.

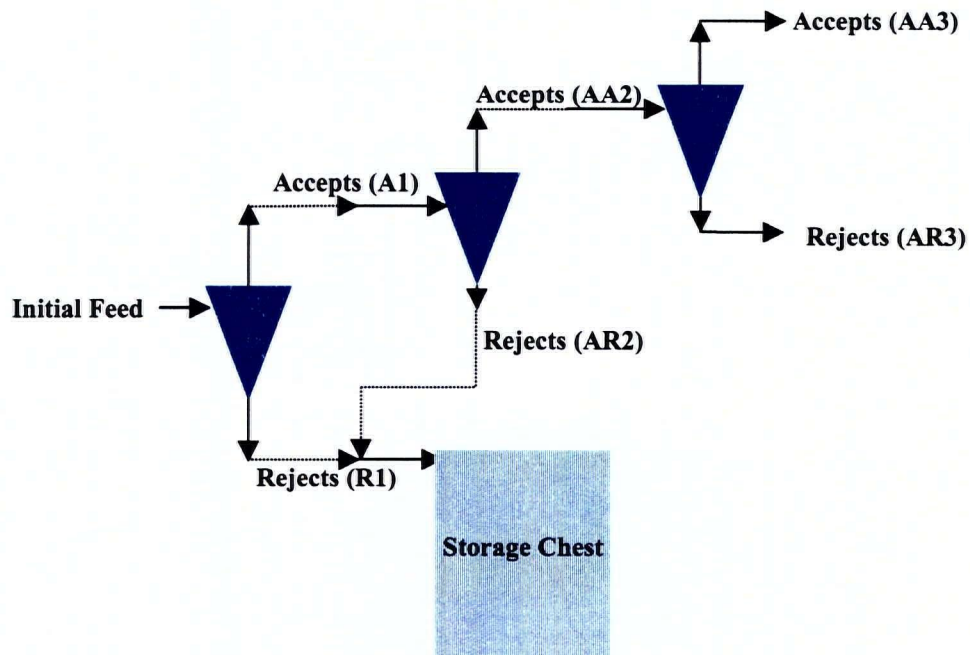


Figure 94 Three Stage Scheme for Fractionation of Accepts

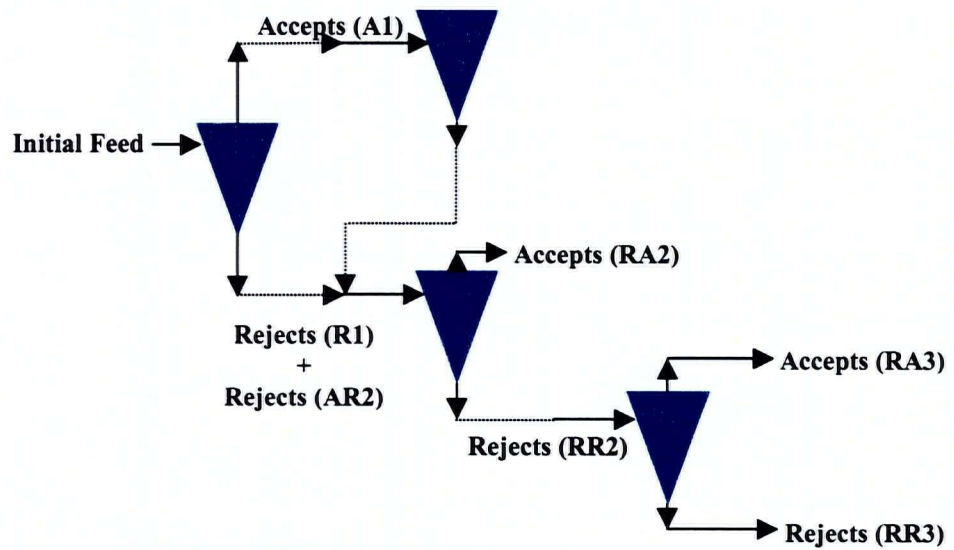


Figure 95 Three Stage Scheme for Fractionation of Rejects

Table 10 Operating Conditions and Performance Parameters for Three Stage Accepts Fractionation

	1 st Stage	2 nd Stage	3 rd Stage
Feed Flowrate (kg/min.)	428	412	270
Pressure Drop (kPa)	244	253	115
Inlet Consistency (%)	0.25	0.24	0.13
Reject Ratio (Volume Basis)	0.04	0.05	0.10
Thickening Ratio	9.3	4.7	3.7
Mass Fraction Fibres Rejected	0.34	0.23	0.37

Table 11 Average Length Weighted Length, Width, and Shape Factor Measurements for Streams Resulting from Three Stage Accepts Fractionation

Length Weighted Av. Property	1 st Stage			2 nd Stage			3 rd Stage		
	Initial Feed	A1	R1	A1	AA2	AR2	AA2	AA3	AR3
Length, l_{lw} (mm)	2.37	2.31	2.41	2.31	2.21	2.35	2.21	2.15	2.39
Width, W_{lw} (μ m)	27	26.6	27.1	26.6	26.5	26.8	26.5	25.4	27.6
Shape Factor, SF_{lw} (%)	85	85.2	84.3	85.2	85.7	86.5	85.7	86	84.8

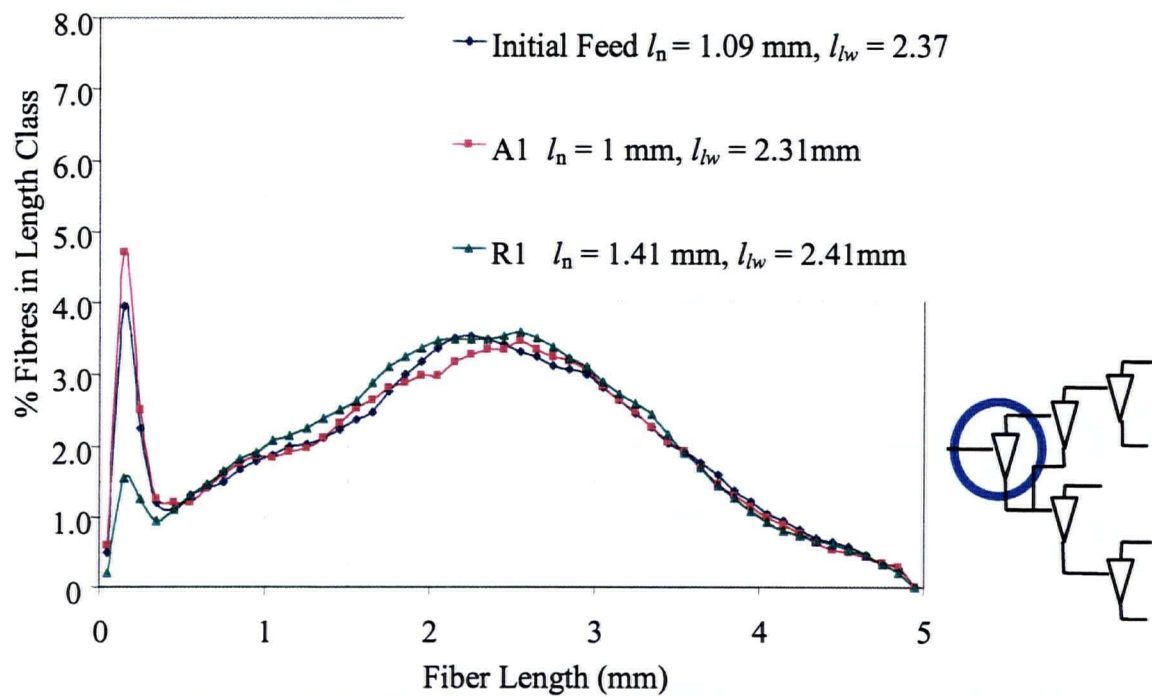


Figure 96 Length Distribution for Feed, Accepts and Rejects for 1st Stage of Multistage Fractionation of Accepts

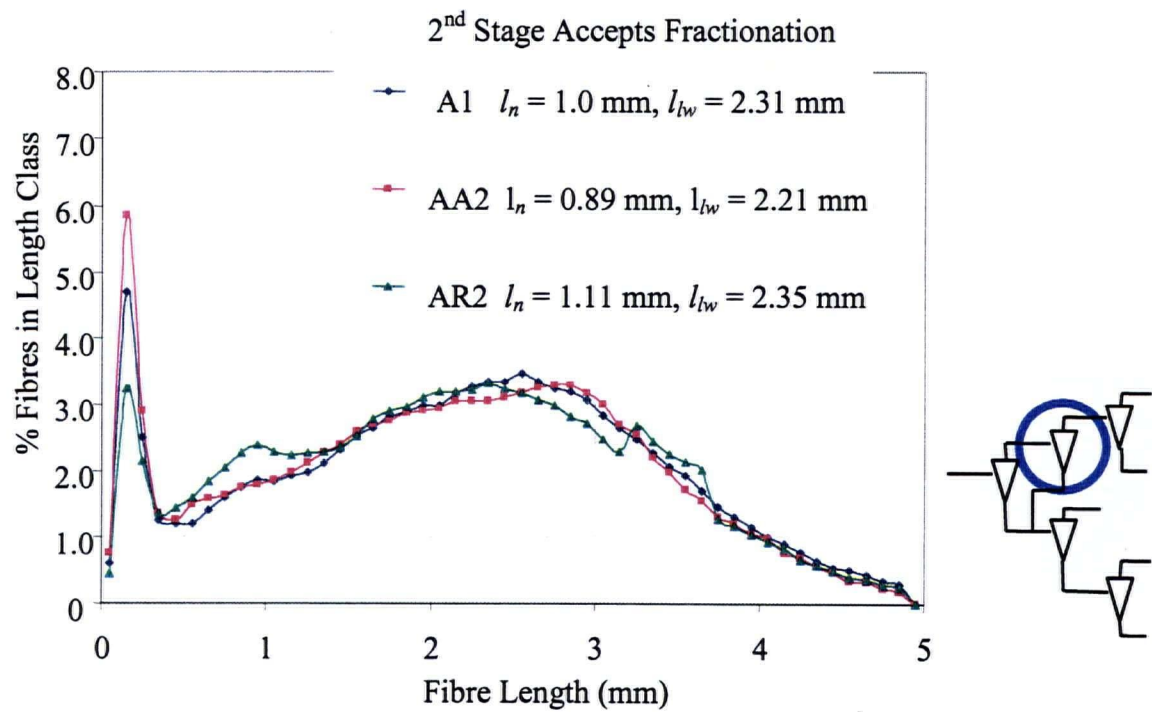


Figure 97 Length Distribution for Feed, Accepts and Rejects for 2nd Stage of Multistage Fractionation of Accepts

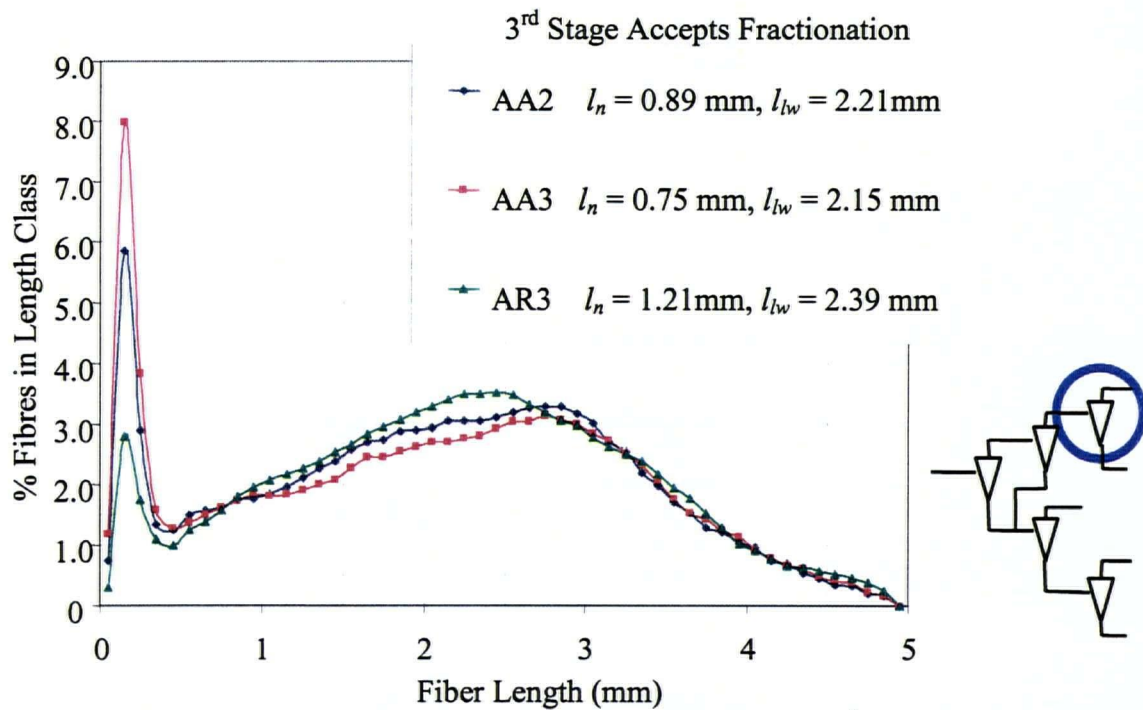


Figure 98 Length Distribution for Feed, Accepts and Rejects for 3rd Stage of Multistage Fractionation of Accepts

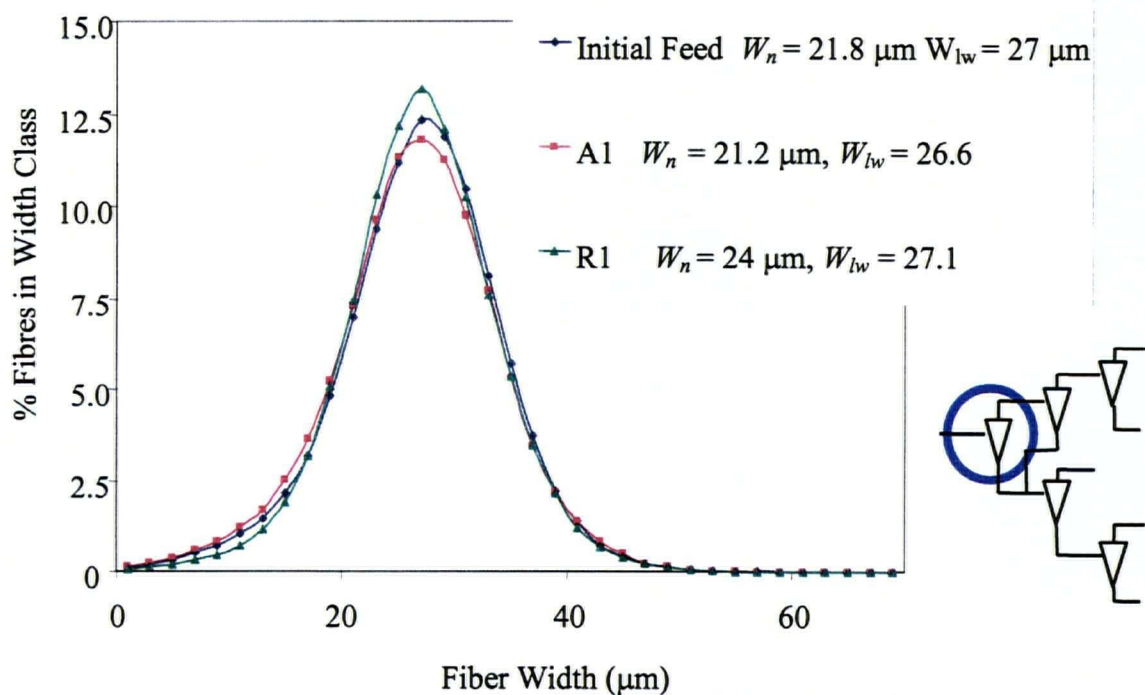


Figure 99 Width Distribution for Feed, Accepts and Rejects for 1st Stage of Multistage Fractionation of Accepts

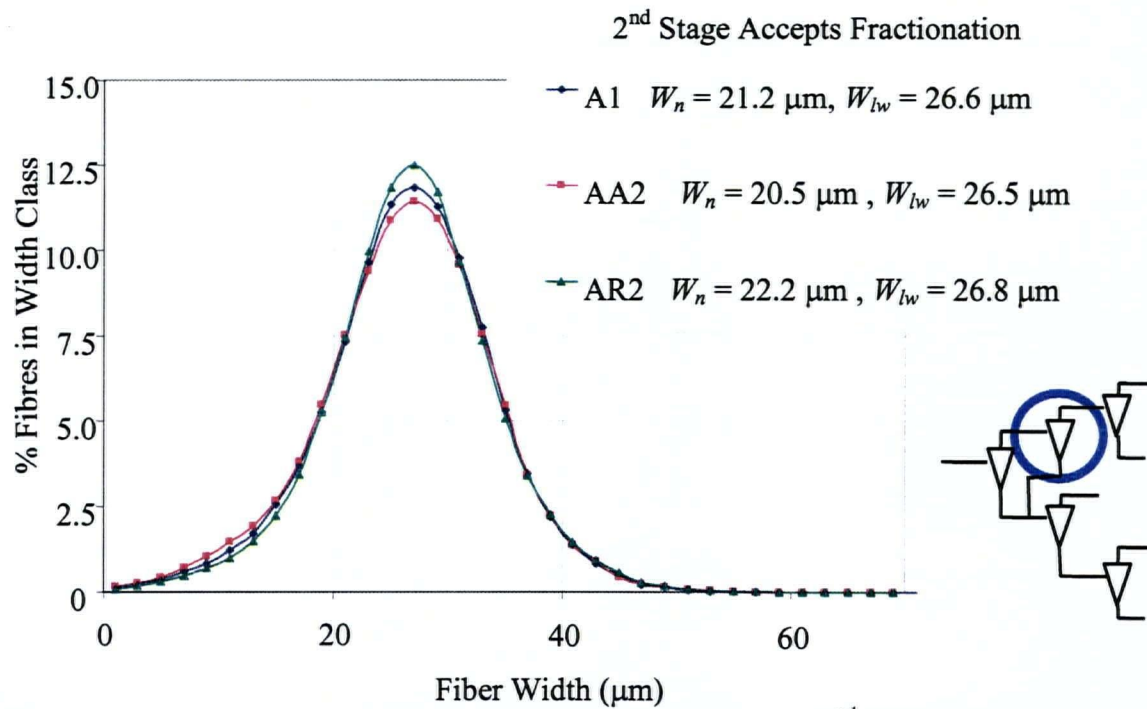


Figure 100 Width Distribution for Feed, Accepts and Rejects for 2nd Stage of Multistage Fractionation of Accepts

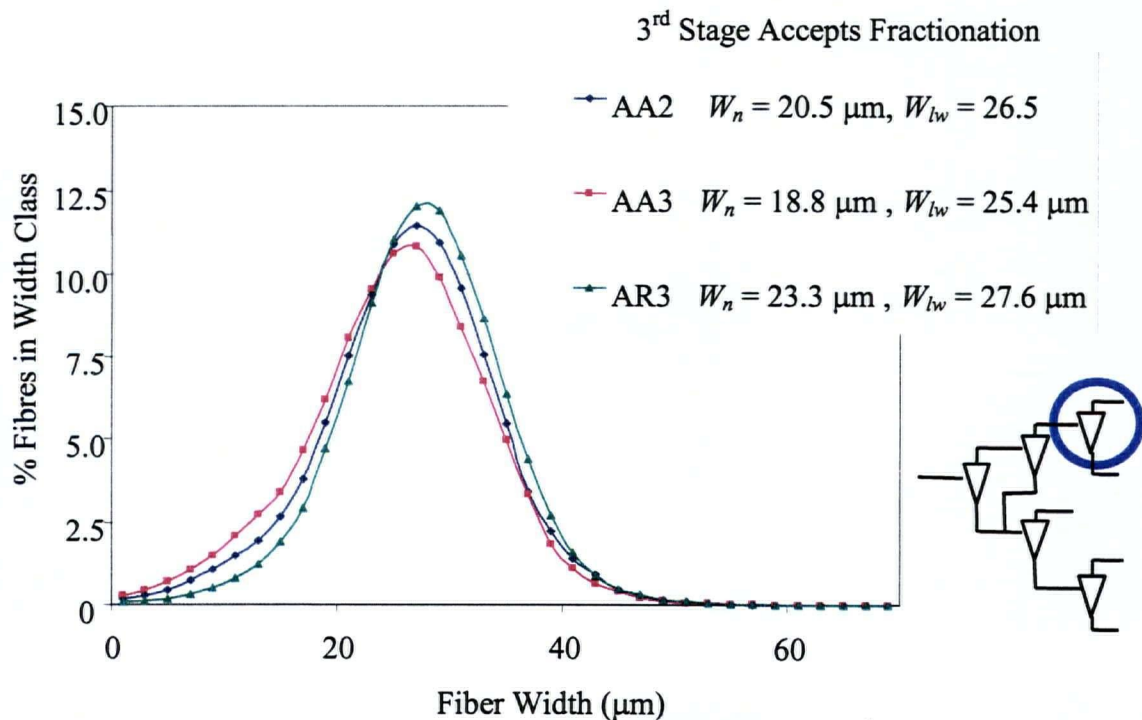


Figure 101 Width Distribution for Feed, Accepts and Rejects for 3rd Stage of Multistage Fractionation of Accepts

The three stage rejects fractionation was performed in a similar fashion as the accepts fractionation. The first stage was performed at a higher flowrate than the second and third stages. This was to remove the well fibrillated fibres and any remaining fibre fines. The first stage was the same first stage of the accepts fractionation experiment summarized above. The first stage and second stage rejects from the accepts fractionation were diluted to a consistency of 0.18% and served as the feed for the second stage. The second stage fractionation was performed at a flowrate of 270 kg/min. and pressure drop of 125 kPa. The resulting rejects from the second stage were diluted to a consistency of 0.17% and fed to the third stage at a flowrate of 270 kg/min. and pressure drop of 120 kPa. See Figure 95. The last two stages of this test were performed at 270 kg/min. to further fractionate earlywood to the accepts. These conditions were determined using information from our preliminary study of Hydrocyclone C summarized in Section 5.6.3.1. Table 12 is a summary of the operating conditions from the three stage rejects fractionation.

The length and width distributions for streams resulting from the second and third stage of our rejects fractionation experiment are illustrated in Figures 102 –105, average property values are summarized in the legends of each of the figures. Length and width distributions of the first stage are the same as those for the accepts fractionation illustrated earlier in Figures 96 and 99. Table 13 contains the average length weighted length, width and shape factor measurements for each of the streams.

Now we will examine the length distributions for the three stage rejects fractionation. The second stage fractionation, illustrated in Figure 102, once again indicated the greater presence of fibres in the range 0 – 0.3 mm for the accepts (RA2). This distribution also showed the rejects (RR2) to have the greatest fibre content in the length range 1.5 – 3 mm; this was then followed by the feed (R1 + AR2) having the next greatest content and then the accepts (RA2). There also appeared to be some fractionation occurring in the 4 – 5 mm range. Figure 103 shows that the feed (RR2) and resulting rejects (RR3) from the third stage had fibre contents less than 1% in the range 0 – 0.3 mm, thus indicating that these samples had very little fines content. Accepts (RA3) from the third stage had a considerably lower fibre content in the range 1.25 - 2.6 mm.

The width distribution of the second stage rejects fractionation showed again the greater content of accepts fibres in the range 0 – 20 μm . In the width range 0 – 18 μm we found a greater content of feed (R1 + AR2) fibres than rejects (RR2). In the width range 25 – 35 μm the fibre content resulted in the trend rejects (RR2) > feed (R1 + AR2) > accepts (RA2). The third stage showed a more pronounced increase in fibre content for the accepts (RA3) in the width range 0 – 20 μm and a decrease in the range 25 – 30 μm . Figure 105 shows that the feed (RR2) and rejects (RR3) had similar distributions. Figures 99, 104 and 105 indicate that no fractionation occurred for the widest fibres as the distributions of feed accepts and rejects were the same. Length weighted average properties summarized in Table 13 conclude that the three stage fractionation resulted in longer fibres reporting to the rejects. These rejects fibres had average widths which were greater than the feed and accepts and shape factors which were smaller. Again we can conclude that shorter fibres and fines reported to the accepts, and that these accepts fibres were straighter than the rejects as indicated by the larger average shape factor value.

Recall that our objective for performing the three stage fractionation of accepts was to produce a stream that contained a greater content of earlywood fibres than the original feed and the objective of the three stage rejects fractionation was to produce a stream rich in latewood fibres. The analysis summarized so far has shown that the accepts fractionation produced a stream, AA3, which had a shorter average fibre length than the original feed and our reject fractionation produced a stream, RR3, which had a greater fibre length than the feed streams. Latewood fibres are reported to have larger fibre lengths than earlywood fibres [58]. This then is the first indication that we have met our objective. We have further characterized streams AA3 and RR3 in terms of paper properties and microscopic analysis to determine how well we conducted our multistage fractionation. The final accepts stream (AA3) accounted for 31% of the initial feed and the final rejects stream (RR3) accounted for 20%. The remaining fractions described earlier were not further characterized.

Table 12 Operating Conditions and Performance Parameters for Three Stage Rejects Fractionation

	1 st Stage	2 nd Stage	3 rd Stage
Feed Flowrate (kg/min.)	428	270	270
Pressure Drop (kPa)	244	125	120
Inlet Consistency (%)	0.25	0.18	0.17
Reject Ratio (Volume Basis)	0.04	0.15	0.11
Thickening Ratio	9.3	3.9	5.1
Mass Fraction Fibres Rejected	0.34	0.57	0.61

Table 13 Average Length Weighted Length, Width, and Shape Factor Measurements for Streams Resulting from Three Stage Rejects Fractionation

Length Weighted Av. Property	1 st Stage			2 nd Stage			3 rd Stage		
	Initial Feed	A1	R1	R1 + AR2	RA2	RR2	RA2	RA3	RR3
Length, l_{lw} (mm)	2.37	2.31	2.41	2.47	2.35	2.60	2.60	2.51	2.59
Width, W_{lw} (μm)	27	26.6	27.1	27.7	26.8	27.8	27.8	27.4	28.0
Shape Factor, SF_{lw} (%)	85	85.2	84.3	84.2	85.3	83.7	83.7	84.4	83.3

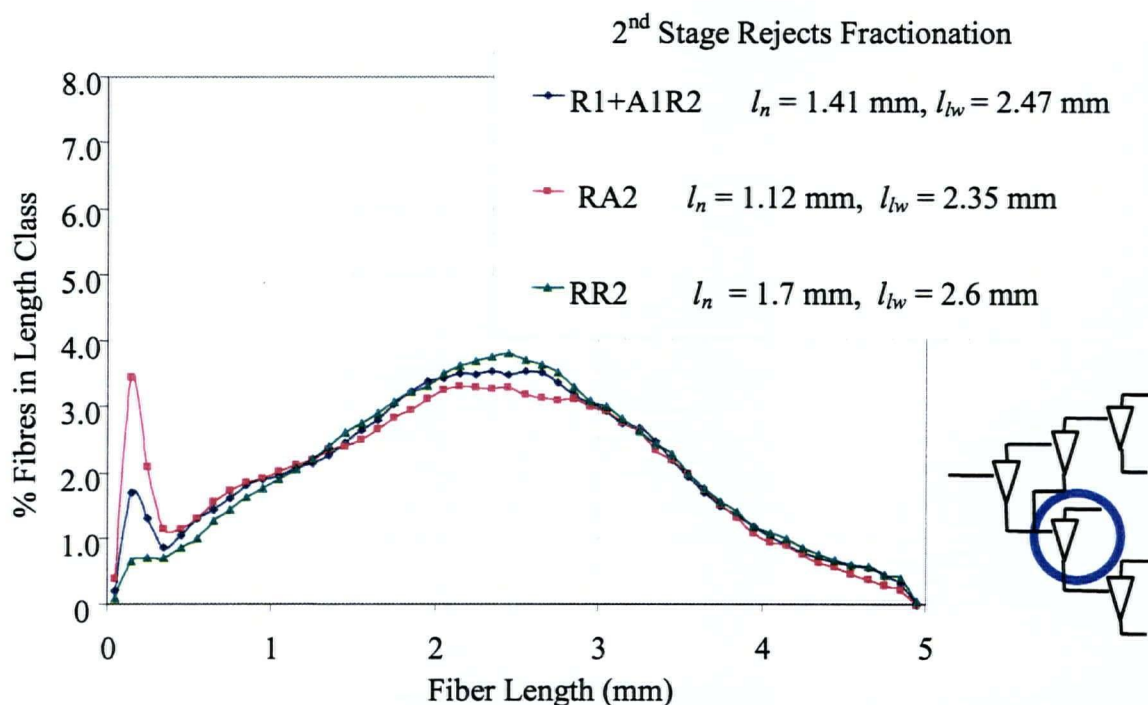


Figure 102 Length Distribution for Feed, Accepts and Rejects for 2nd Stage of Multistage Fractionation of Rejects

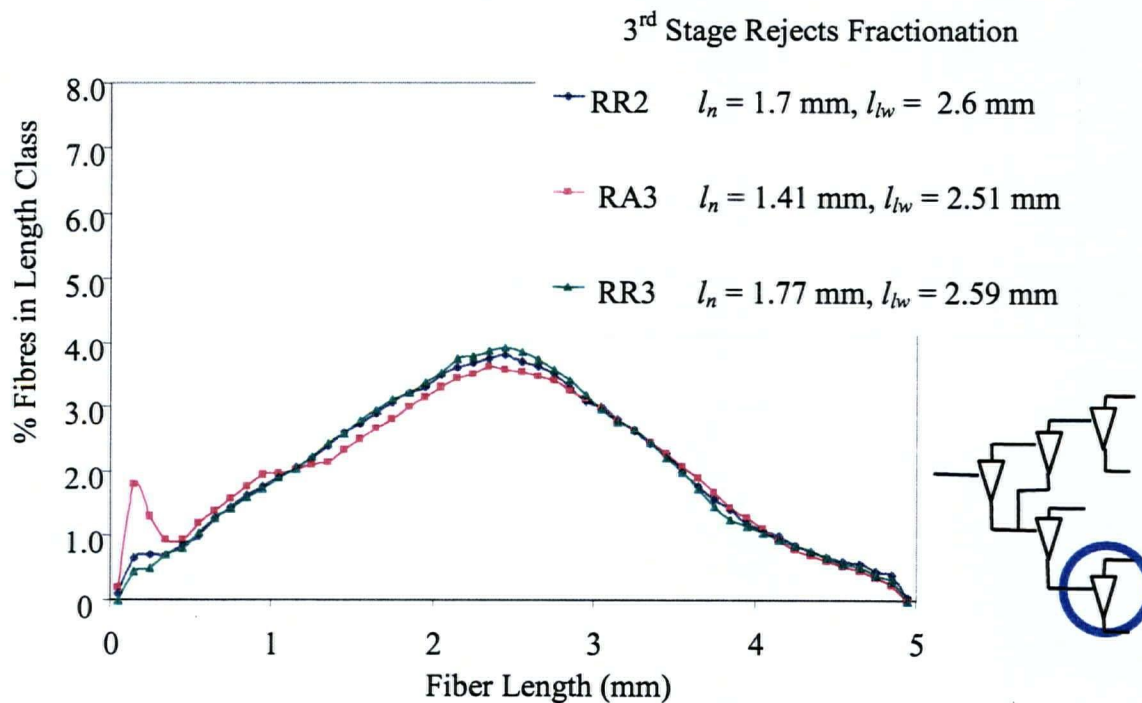


Figure 103 Length Distribution for Feed, Accepts and Rejects for 3rd Stage of Multistage Fractionation of Rejects

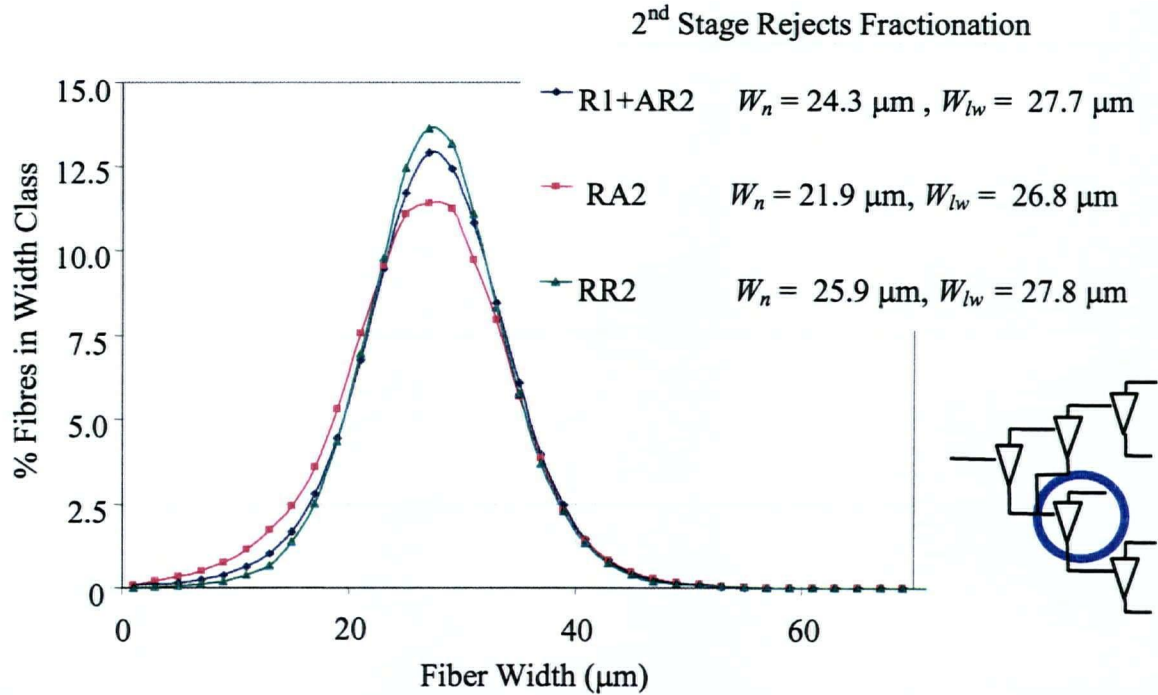


Figure 104 Width Distribution for Feed, Accepts and Rejects for 2nd Stage of Multistage Fractionation of Rejects

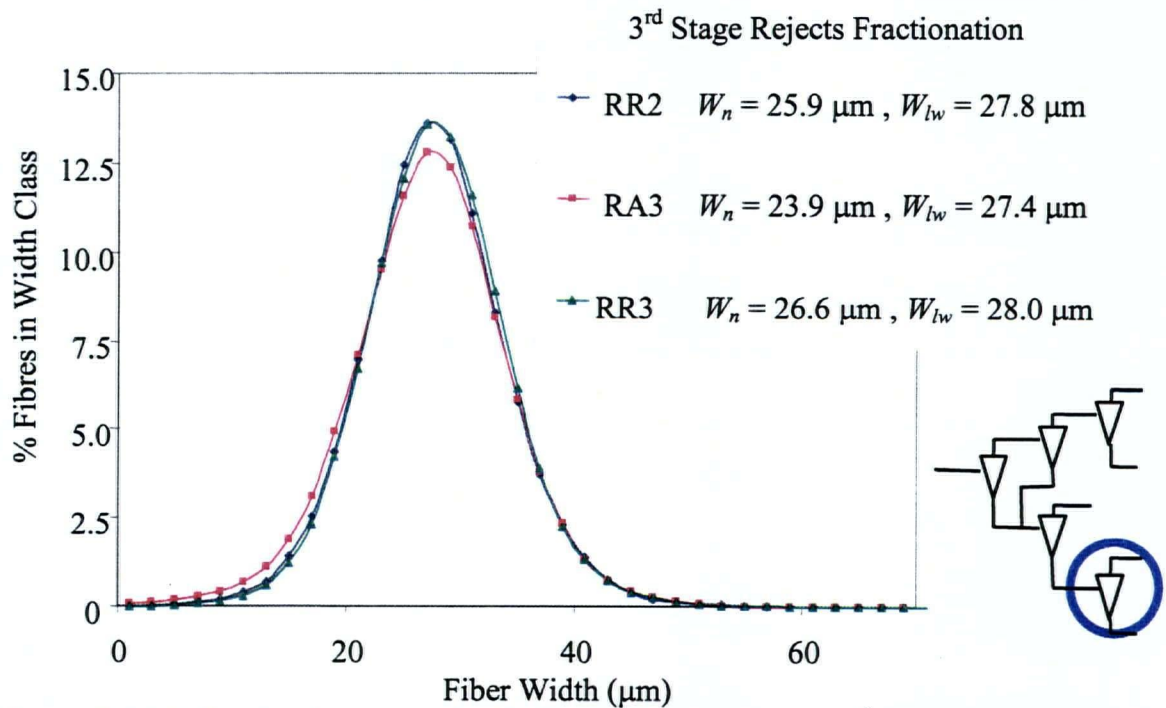


Figure 105 Width Distribution for Feed, Accepts and Rejects for 3rd Stage of Multistage Fractionation of Rejects

Figure 106 includes photomicrographs of the initial feed, accepts (AA3), and rejects (RR3). Analysis of the photomicrographs revealed that the fibres in AA3 were mostly earlywood. The fibres in AA3 were flexible and some fibrillation of the fibres was detected. Latewood fibres were prevalent in the rejects stream (RR3), none of these fibres showed signs of fibrillation. A greater presence of fines was detected in AA3, RR3 seemed to contain almost no fines.

Feed, accepts (AA3) and rejects (RR3) fibres from the 3 stage fractionation studies were characterized for length, coarseness, freeness, and fines content (see Table 14). The mean fibre length of the RR3 fibres was greater than the mean fibre length of the feed which was approximately the same as that of the accepts (AA3), however the differences were rather small. This observation is contrary to what we have observed in our work summarized earlier using Hydrocyclone A, but is in agreement with the observations of other investigators in the field (see Chapter 2). The rejects (RR3) coarseness was greater than the accepts (AA3) coarseness confirming our results with Hydrocyclones A and B. RR3 freeness was higher than AA3 freeness in accord with some of our Hydrocyclone A data and with others as noted in Chapter 2. The measurements of fines content confirm our conclusions drawn from analysis of the distributions that fines report to the accepts and there are few fines in the rejects.

Figures 107 –109 plot the length, width and shape factor distributions for the multistage experiment considering only the initial feed and streams AA3 and RR3. The average property data are included in the legends of these graphs. Analysis of the fibre length distributions (Figure 107) showed that almost all of the fines were in the accepts stream. There was a greater percentage of fibres having lengths in the 1.5 – 2.75 mm range in the accepts (AA3) than there was in the feed and there were more fibres in this length range in the feed than in the rejects (RR3). At greater fibre lengths the three distributions were more or less the same.

Width distributions (Figure 108) showed that in the range of 0 – 20 μm fibre width there was a higher fraction of such fibres in AA3 than in the feed and a higher fraction in the feed than

in RR3. In the 20 – 40 μm range there were more fibres having these widths in RR3 than in the feed, and more in the feed than in AA3. Above 40 μm the distributions were the same but there were very few fibres in this range.

The shape factor distribution (Figure 109) showed the rejects to have a greater fibre content for the shape factor range 70 – 90%. This indicated that these fibres were not very straight. There were more AA3 fibres having shape factors greater than 90%, thus we can once again conclude that accepts fibres are straighter than rejects fibres.

The average property data shown in the legends of Figures 107 – 109, led to the conclusion that the fibres of the AA3 sample were shorter and had a greater fines content than our RR3 sample. Average fibre widths were the greatest for RR3. Accepts fibres were straighter than rejects fibres.

Table 15 summarizes the paper strength properties of the feed, AA3 and RR3 streams. Handsheets made with the accepts fibres resulted in a greater sheet density than handsheets prepared with the initial feed and rejects fibres. Accepts handsheets also had higher tensile strength and light scattering. The opposite was found with the rejects fibres; these handsheets had a lower tensile strength and lower sheet density when compared to the original feed and the accepts sheets. The lower strength of the sheets made from the rejects can be attributed to the greater content of latewood fibres since these fibres have reduced bonding ability.

The surface smoothness of handsheets from the feed, accepts, and rejects was measured, Table 15 summarizes this property in terms of Bendsten Roughness. The handsheets prepared from the accepts pulp had considerably higher surface smoothness than the feed and rejects.

The earlywood and latewood fibre content in the fractionated streams was quantified by microscopy. These results are presented in Table 16. Figure 110 illustrates what typical earlywood and latewood fibres look like. Earlywood fibres have greater fibre diameters and

thinner walls than latewood fibres. Because of their thicker walls, latewood fibres are stained darker, See Figure 110. When quantifying earlywood and latewood content, we characterized the fibres based on identifying them in this manner. For our three stage accepts fractionation trial, we were able to produce an accepts stream which contained 75% earlywood and 25% latewood, the initial feed contained 66% earlywood and 34% latewood. In the case of fractionating the rejects stream in three stages, the final rejects contained 50% earlywood and 50% latewood.

Comparison of pulp, fibre and sheet properties of AA3 and RR3 to the initial feed showed that we did fractionate earlywood fibres to the accepts and latewood fibres to the rejects. We would need to analyze the other streams identified in Figures 94 and 95 before we can accurately quantify how well the fractionation was performed. However, the analysis presented above does show that differences in AA3 and RR3 were appreciable.

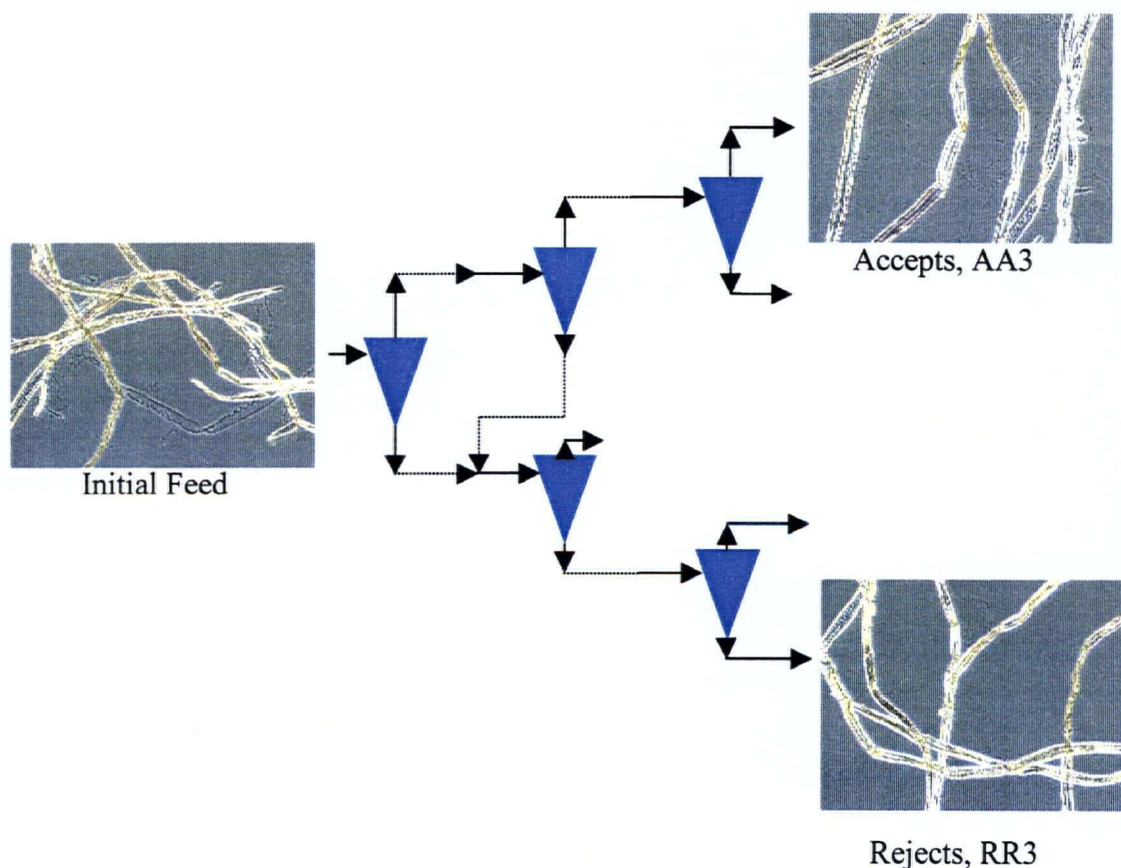


Figure 106 Multistage Fractionation Schemes and Photomicrographs of Initial Feed, AA3 and RR3

Table 14 Pulp and Fibre Characteristics for Feed, Accepts, and Rejects

	Initial Feed	Accepts (AA3) Fractionated in 3 Stages	Rejects (RR3) Fractionated in 3 Stages
Kajaani Length Weighted Av. (mm)	2.2	2.18	2.30
Kajaani Coarseness (mg/m)	0.247	0.222	0.263
CSF Freeness (ml)	696	481	727
Fines Content (%)	3.6	5.8	0.1

Table 15 Paper Properties for Feed, Accepts, and Rejects for Three
Stage Fractionation Experiment

	Initial Feed	Accepts (AA3) Fractionated in 3 Stages	Rejects (RR3) Fractionated in 3 Stages
Sheet Density (kg/m ³)	563	650	487
Sheet Roughness (ml/min.) Bendtsen 0.1 MpaS1	853	285	1748
Tensile Index (Nm/g)	26.4	42.72	12.73
Tensile Stiffness Index (kNm/g)	3.62	4.48	2.25
Tear Index (Mn m ² /g)	19.2	18.1	9.11
Burst Index (kPa m ² /g)	1.43	3.36	Outside the limits for test method since sample too weak
Light Scattering Coefficient (m ² /kg)	30.6	33	27.8

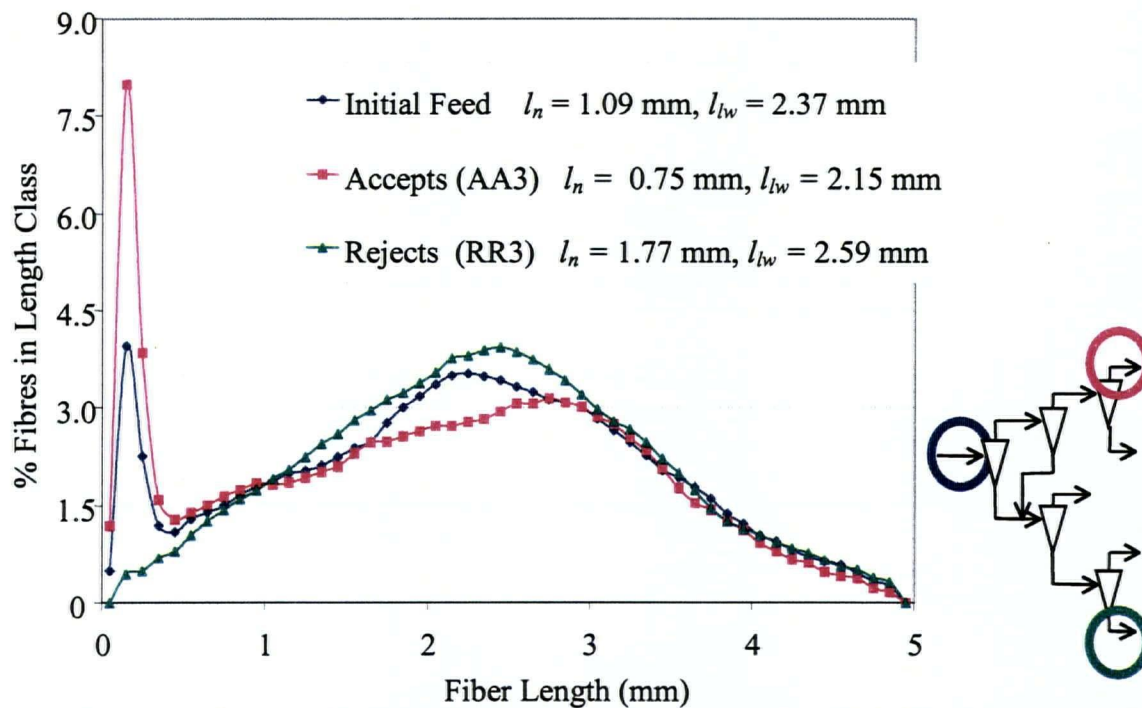


Figure 107 Length Distribution for Initial Feed, AA3 and RR3 from Three Stage Fractionation Study Using Hydrocyclone C

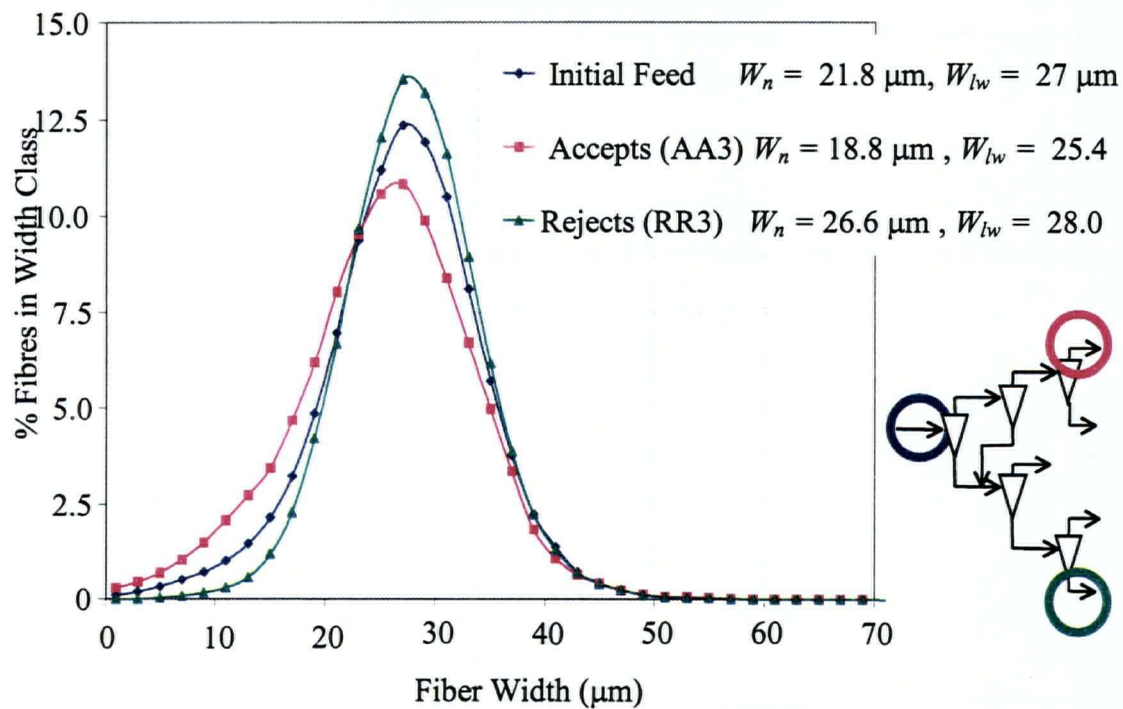


Figure 108 Width Distribution for Initial Feed, AA3 and RR3 from Three Stage Fractionation Study Using Hydrocyclone C

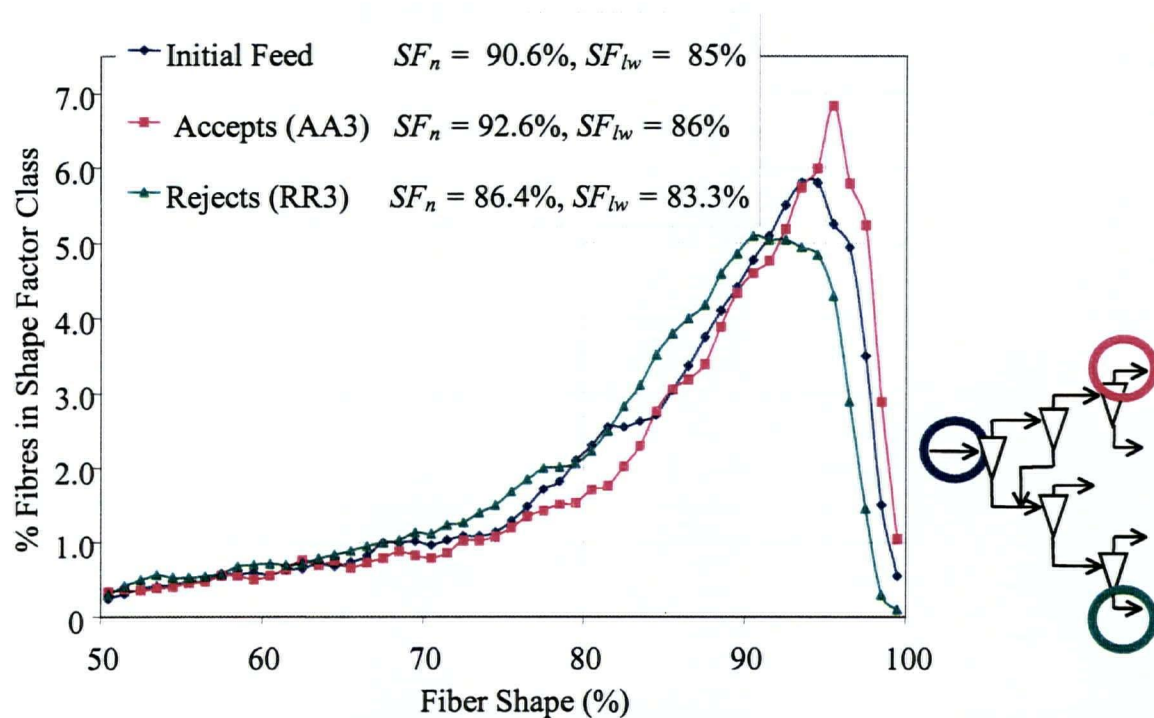


Figure 109 Shape Factor Distribution for Initial Feed, AA3 and RR3 from Three Stage Fractionation Study Using Hydrocyclone C

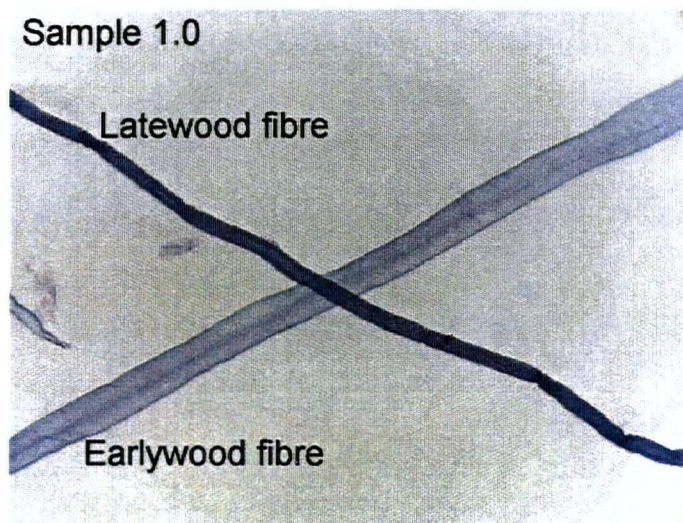


Figure 110 Earlywood and Latewood Fibre Characterization

Table 16 Earlywood and Latewood Fibre Content for Initial Feed, AA3, and RR3

Sample	% Earlywood	% Latewood
Initial Feed	66	34
AA3	75	25
RR3	50	50

5.6.3.3 Refining of Initial Feed and Fractionated Accepts (AA3) and Rejects (RR3)

The initial feed fractionated accepts (AA3) and rejects (RR3) were then refined in an Escher Wyss laboratory conical refiner. The refiner was tested at two specific edge loads (SEL), 2.0 and 3.5 Wsm⁻¹, and two levels of energy consumption (50 and 100 kWh⁻¹) were applied at each SEL. Pulp properties and paper properties were characterized to determine the differences in fibre development of the accepts and rejects streams which were relatively rich in earlywood and latewood fibres respectively. We also wanted to determine if the rejects could be refined to levels which would make them into usable fibre.

Figures 111 – 113 illustrate the fibre length distributions for the unrefined and refined feed, accepts (AA3) and rejects (RR3) for a refiner SEL 2.0 Ws/m and energy consumption of 0, 50, and 100 kWh/ton. Figures 114 – 116 are similar plots for SEL = 3.5 Ws/m.

Figures 111 and 112 demonstrates that refining the feed and accepts (AA3) at SEL = 2.0 Ws/m and energy levels of 50 and 100 kWh/ton did not much affect the fines fraction (i.e. length range 0 – 0.5 mm). In Figure 112 however, refining the rejects resulted in producing more fines. The higher the energy level, the more fines generated. Figure 114 shows that at SEL = 3.5 Ws/m as energy consumption went to 50 kWh/ton in refining the feed, the amount of fines decreased, which doesn't make sense, but at 100 kWh/ton the amount of fines increased. Figure 115 (refining AA3 at SEL = 3.5 Ws/m) shows some decrease in the amount of fines as energy consumption rose. Figure 116 clearly indicates an increase in fines content as RR3 stream was refined.

For all of the fibre length distributions illustrated in Figures 111 –116 there was a decrease in average and length weighted average fibre length and a shift in the fibre distributions to the left indicating shortening caused by the cutting action of the refiner. The higher the energy consumption the greater the fibre shortening. The higher the SEL the greater the fibre shortening.

Fibre width distributions for the unrefined and refined feed, accepts (AA3) and rejects (RR3) are presented in Figures 117 – 119 for energy consumption levels of 0, 50, and 100 kWh/ton at an SEL of 2.0 Ws/m and in Figures 120 – 122 for SEL of 3.5 Ws/m.

In Figure 117 it can be seen that refining the feed at SEL = 2.0 Ws/m and an energy consumption of 50 kWh/ton resulted in little change. Increasing the energy to 100 kWh/ton caused the width distribution to shift to the right implying that fibre widths had increased as a result of refining. The only explanation we can think of for this trend, which also occurred in the rest of the width distributions, is that refining collapses the fibres causing them to appear wider in the FiberMaster image analysis system.

Figure 118 for refining AA3 shows evidence of a shift to the right of SEL = 2 Ws/m and energy level of 50 kWh/ton and a further rightward shift as the energy rose to 100 kWh/ton. This pattern was again found when refining RR3.

Figure 120 for refining the feed at SEL = 3.5 Ws/m also exhibits the shifting to the right, i.e. towards wider fibres with refining as do Figure 121 (SEL = 3.5 Ws/m) for refining AA3 and Figure 122 (SEL = 3.5 Ws/m) for refining RR3.

Average length, width and shape factors for our refining trials are summarized in Tables 17 - 19. Average lengths for the samples were found to decrease with increased refining. The lengths for trials performed at SEL 3.5 Ws/m were lower than for SEL 2.0 Ws/m. A higher SEL indicates a low number of high intensity impacts per fibre, this represents “a cutting or chopping action [78].” This behaviour is illustrated in our length measurements.

Table 17 Average Length Weighted Fibre Lengths of Initial Feed, Accepts and Rejects from Refining Trials

	l_{lw} (mm)				
	Unrefined	SEL = 2.0 Ws/m		SEL = 3.5 Ws/m	
		50 kWh/ton	100 kWh/ton	50 kWh/ton	100 kWh/ton
Initial Feed	2.37	2.26	2.08	2.21	1.91
Accepts (AA3)	2.15	2.03	1.86	1.94	1.69
Rejects (RR3)	2.59	2.48	2.29	2.34	2.15

Average fibre widths were found to increase with increased refining. The differences in this property for the two SEL's tested was small, but it seemed that the higher SEL resulted in a higher average width. Increasing energy consumption increased the average fibre width.

Table 18 Average Length Weighted Fibre Widths of Initial Feed, Accepts and Rejects from Refining Trials

	W_{lw} (mm)				
	Unrefined	SEL = 2.0 Ws/m		SEL = 3.5 Ws/m	
		50 kWh/ton	100 kWh/ton	50 kWh/ton	100 kWh/ton
Initial Feed	27.0	27.0	27.9	28.2	28.5
Accepts (AA3)	25.4	26.2	26.6	26.6	26.3
Rejects (RR3)	28.0	29.0	29.3	30.1	29.8

Average shape factors are summarized in Table 19. They show that this property increased as the energy consumption and SEL parameters increased. This means that the fibres became straighter as they were refined.

Table 19 Average Length Weighted Fibre Shape Factors of Initial Feed, Accepts and Rejects from Refining Trials

	SF_{lw} (%)				
	Unrefined	SEL = 2.0 Ws/m		SEL = 3.5 Ws/m	
		50 kWh/ton	100 kWh/ton	50 kWh/ton	100 kWh/ton
Initial Feed	85.0	86.8	87.9	87.1	88.8
Accepts (AA3)	86.0	87.1	88.5	87.8	89.1
Rejects (RR3)	83.3	86.0	87.9	86.9	87.6

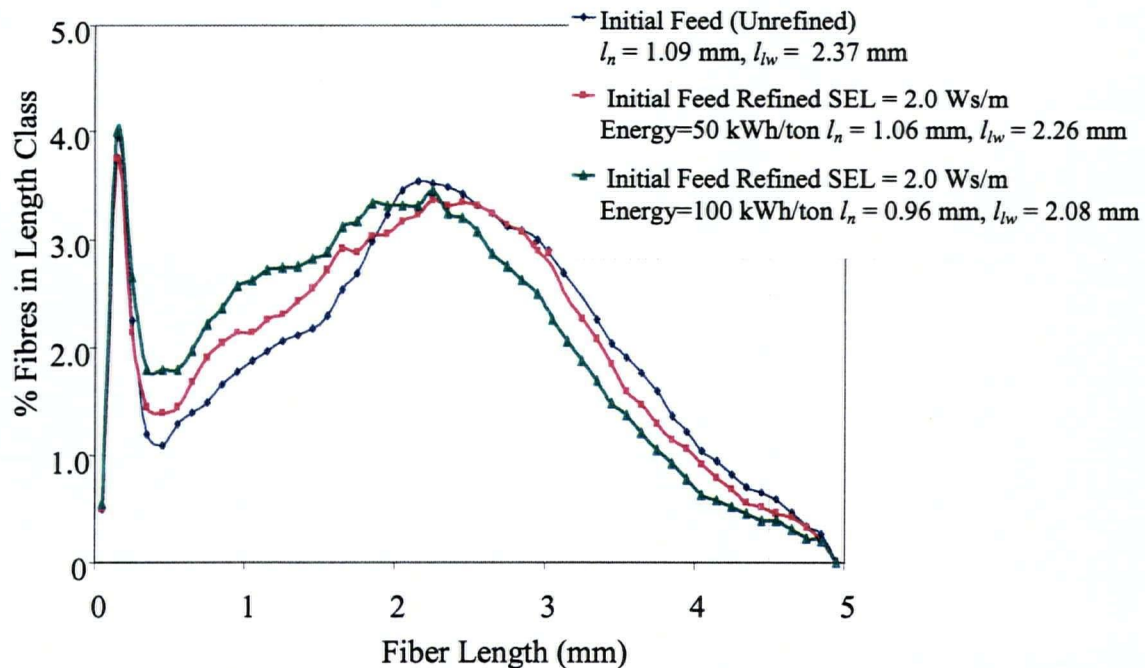


Figure 111 Length Distribution of Initial Feed. Pulps Refined at SEL = 2.0 Ws/m and Energy Consumption of 50 and 100 kWh/ton

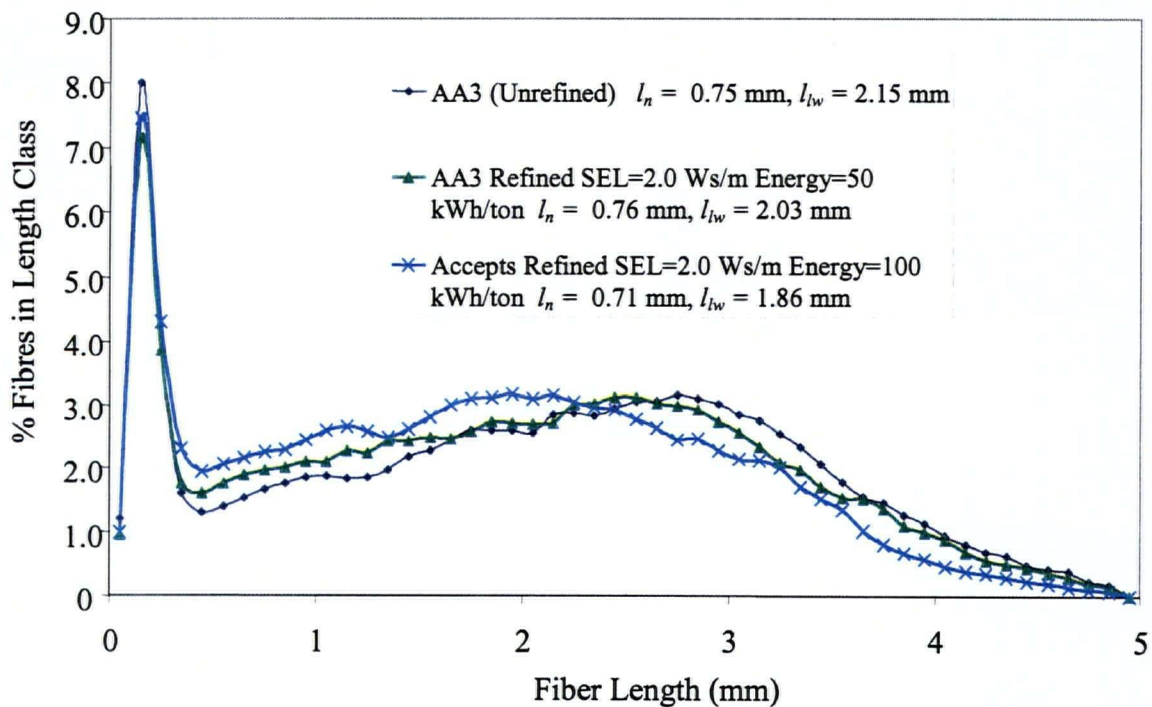


Figure 112 Length Distribution of AA3. Pulps Refined at SEL = 2.0 Ws/m and Energy Consumption of 50 and 100 kWh/ton

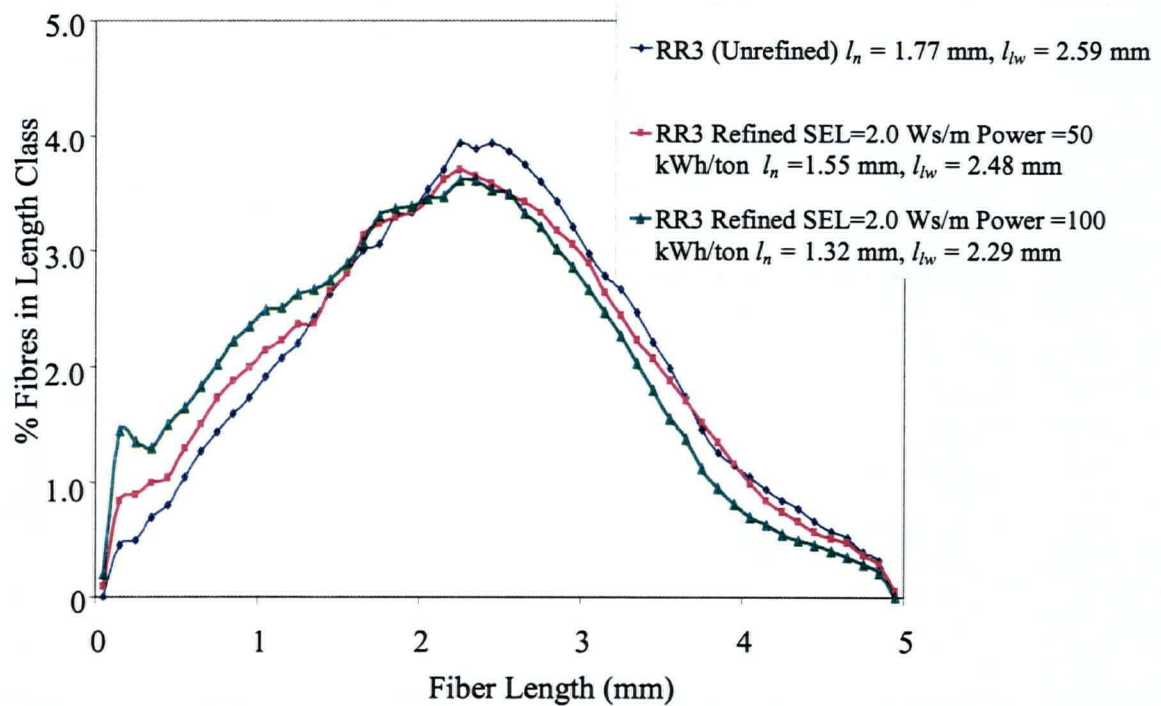


Figure 113 Length Distribution of RR3. Pulps Refined at SEL = 2.0 Ws/m and Energy Consumption of 50 and 100 kWh/ton

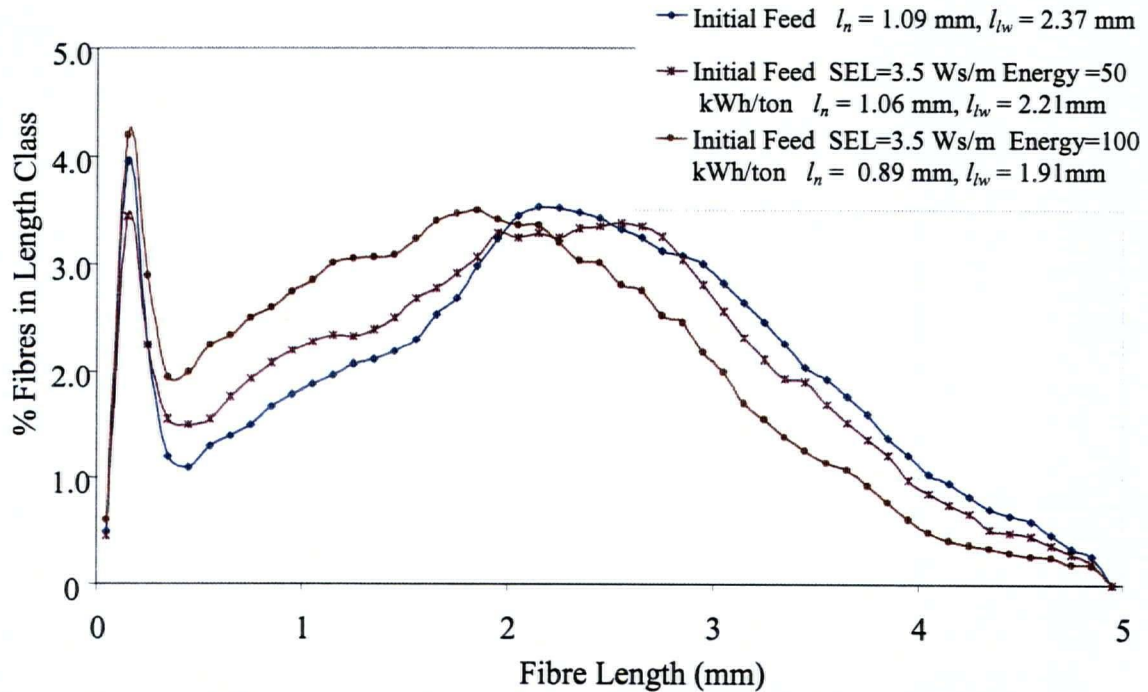


Figure 114 Length Distribution of Initial Feed. Pulps Refined at SEL = 3.5 Ws/m and Energy Consumption of 50 and 100 kWh/ton

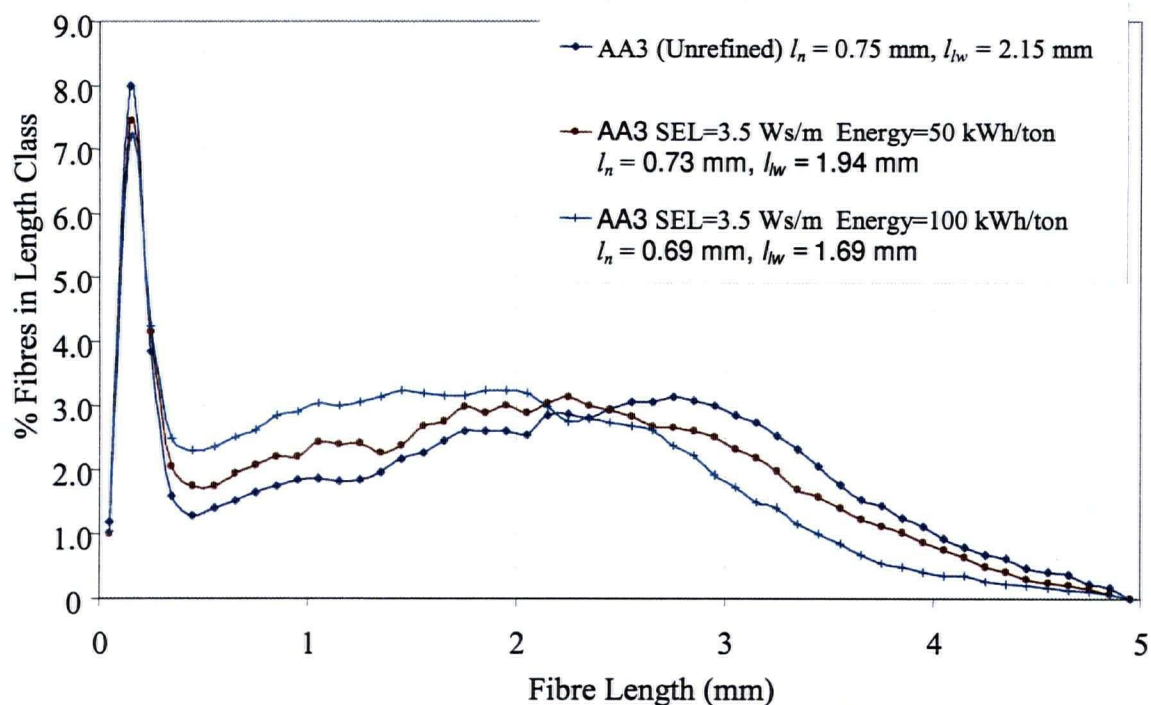


Figure 115 Length Distribution of AA3. Pulps Refined at SEL = 3.5 Ws/m and Energy Consumption of 50 and 100 kWh/ton

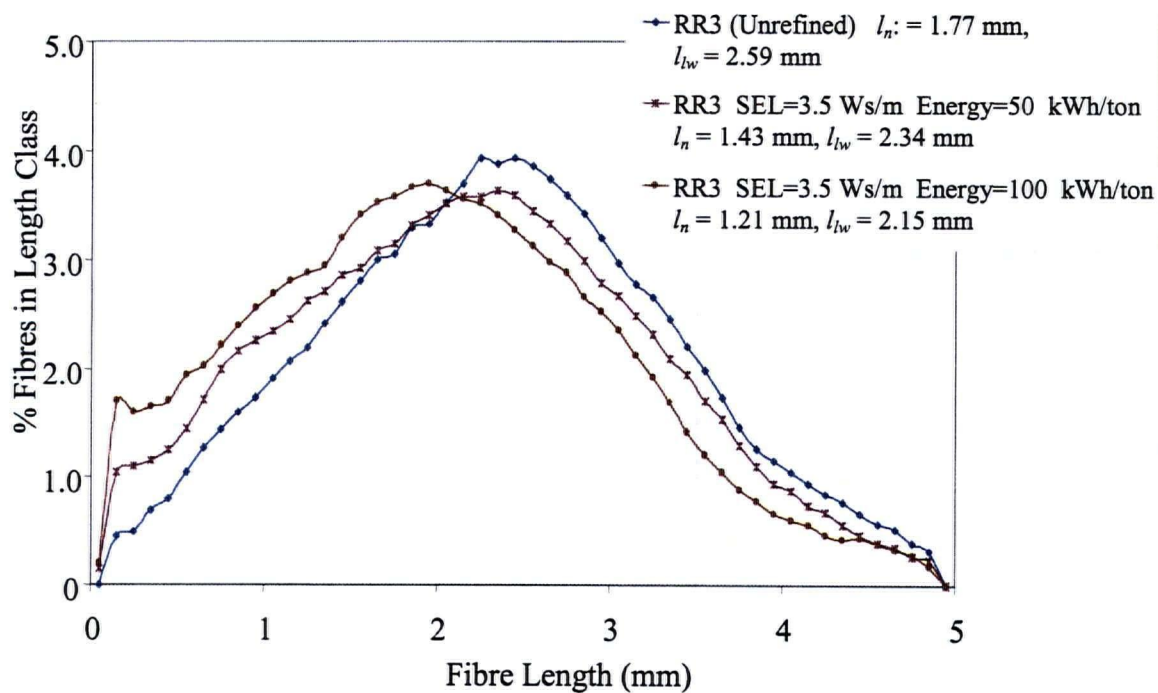


Figure 116 Length Distribution of RR3. Pulps Refined at SEL = 3.5 Ws/m and Energy Consumption of 50 and 100 kWh/ton

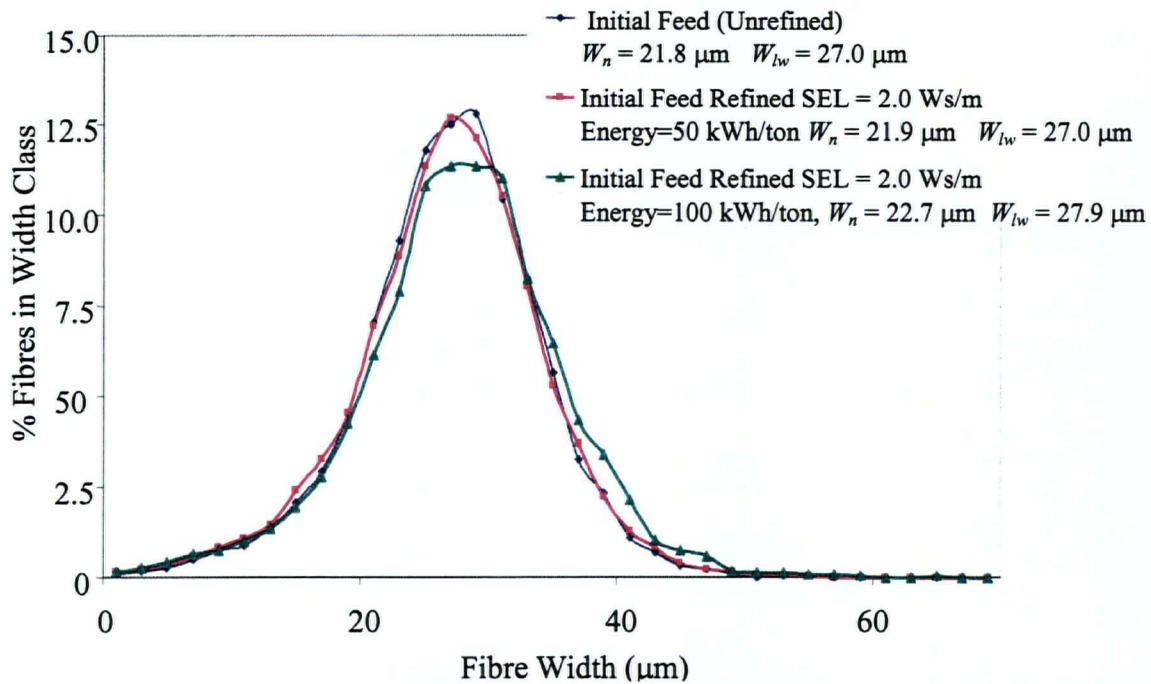


Figure 117 Width Distribution of Initial Feed. Pulps Refined at SEL = 2.0 Ws/m and Energy Consumption of 50 and 100 kWh/ton

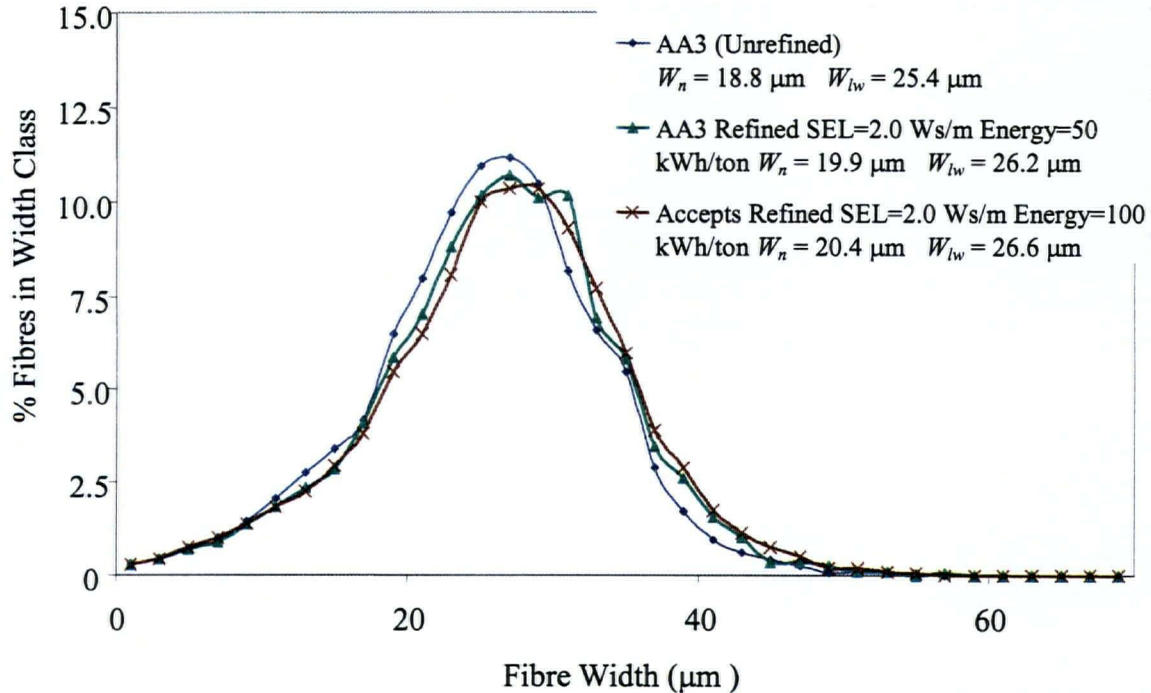


Figure 118 Width Distribution of AA3. Pulps Refined at SEL = 2.0 Ws/m and Energy Consumption of 50 and 100 kWh/ton

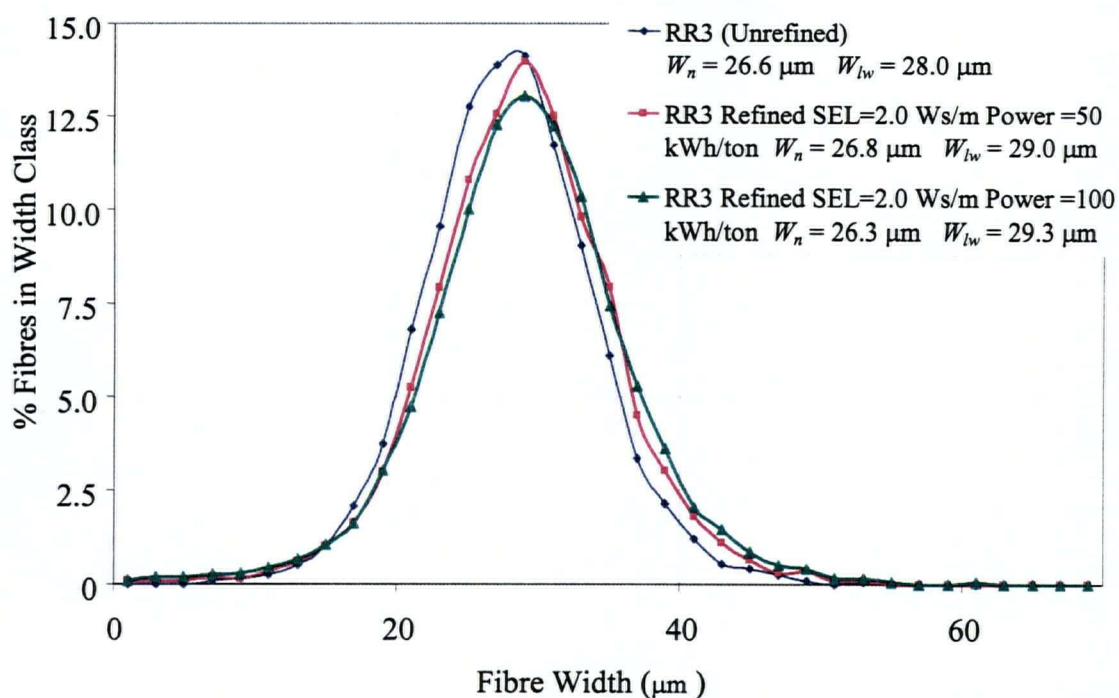


Figure 119 Width Distribution of RR3. Pulp Refined at SEL = 2.0 Ws/m and Energy Consumption of 50 and 100 kWh/ton

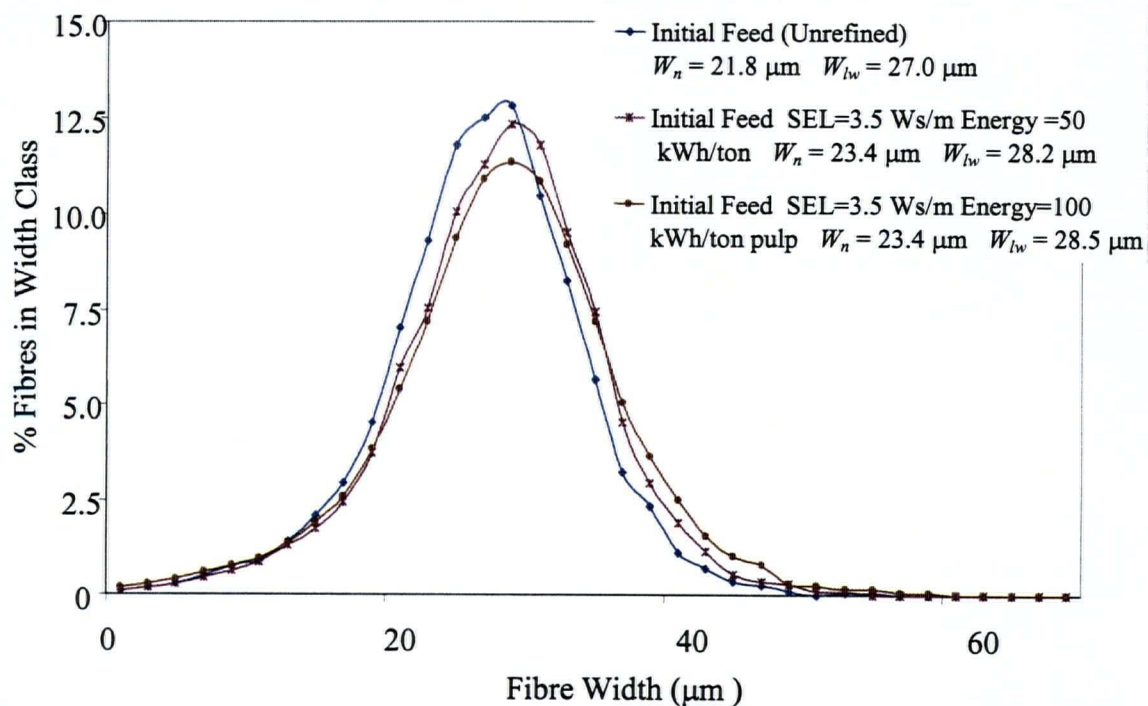


Figure 120 Width Distribution of Initial Feed. Pulp Refined at SEL = 3.5 Ws/m and Energy Consumption of 50 and 100 kWh/ton

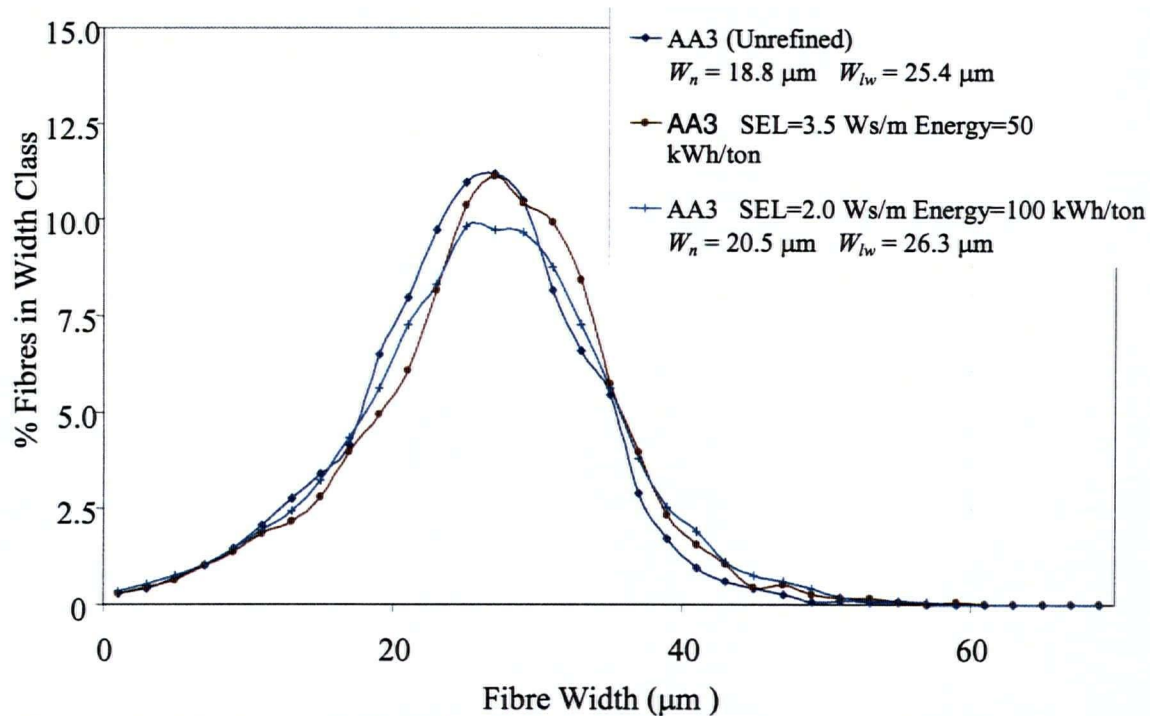


Figure 121 Width Distribution of AA3. Pulps Refined at SEL = 3.5 Ws/m and Energy Consumption of 50 and 100 kWh/ton

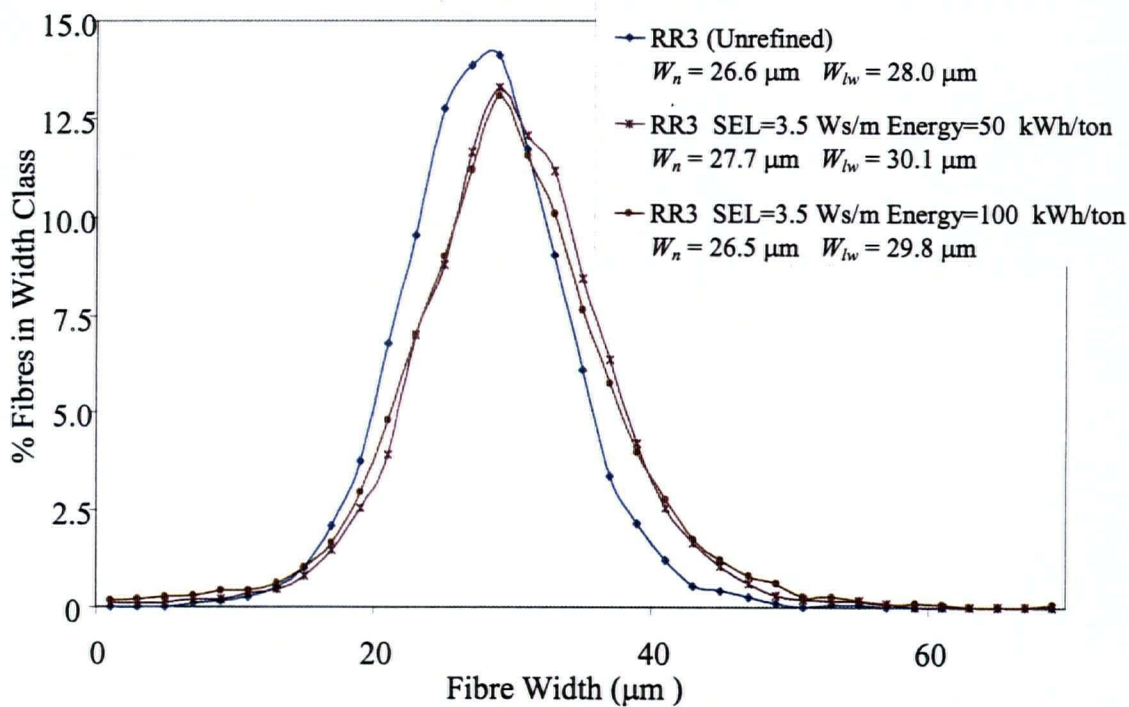


Figure 122 Width Distribution of RR3. Pulps Refined at SEL = 3.5 Ws/m and Energy Consumption of 50 and 100 kWh/ton

The pulp and paper properties measured before and after refining are shown in Figures 123 – 131. Figure 123 summarizes the findings of measuring pulp freeness at the refining conditions tested. Freeness is a measure of pulp drainability. Refining causes external and internal fibrillation of fibres, this results in increased fibre flexibility and fines generation. Also, refining cuts and shortens fibres as demonstrated in the length distributions presented earlier in this section. Figure 123 shows that feed, accepts and rejects all decreased in freeness when refining energy was increased. Since the accepts stream initially contained more earlywood fibres, the freeness was already lower than for the feed and rejects, increasing the refining energy further reduced the freeness of this stream. The rejects stream maintained higher freeness values than the feed and accepts since the rejects stream contained more of the coarse latewood fibres and less fines than the other streams. The freeness measurements coincide with the theory presented in Chapter 4 where we showed that coarseness and freeness are inversely proportional to specific surface and concluded that a hydrocyclone would tend to reject low specific surface, high freeness pulp. Differences in freeness measurements between the two SEL's tested were not appreciable.

Figures 124, 127 and 128 plot the paper strength indices for tensile, tear and burst respectively. Refining improves interfibre bonding and therefore increased refining resulted in increases in the tensile and burst indices, this is shown in Figures 124 and 128.

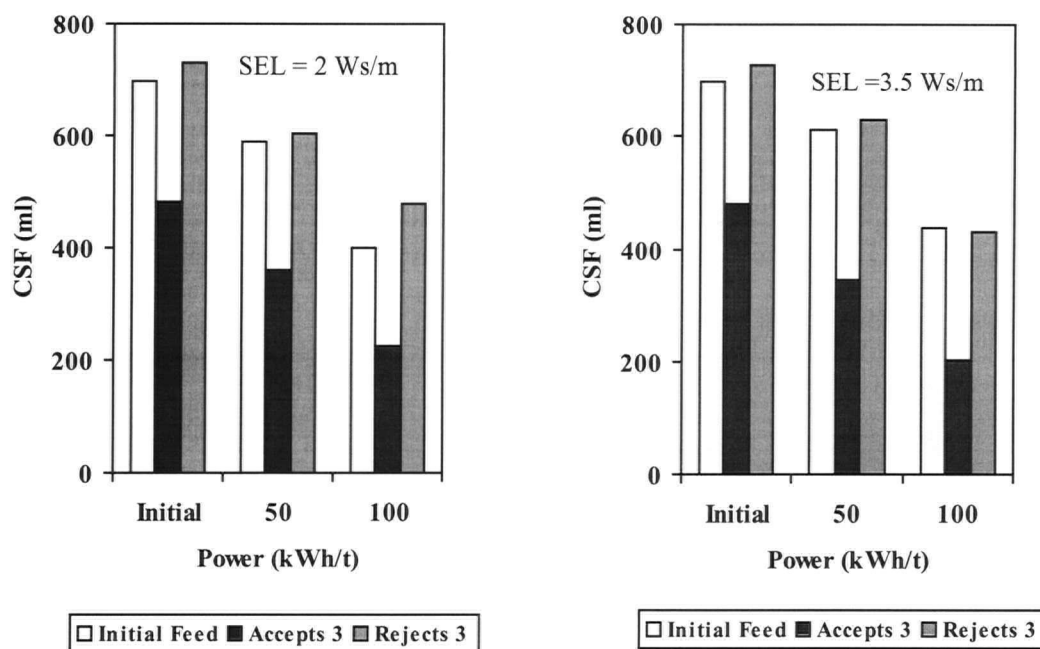
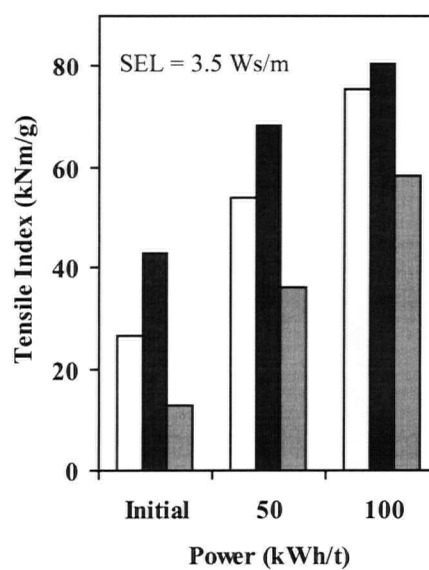
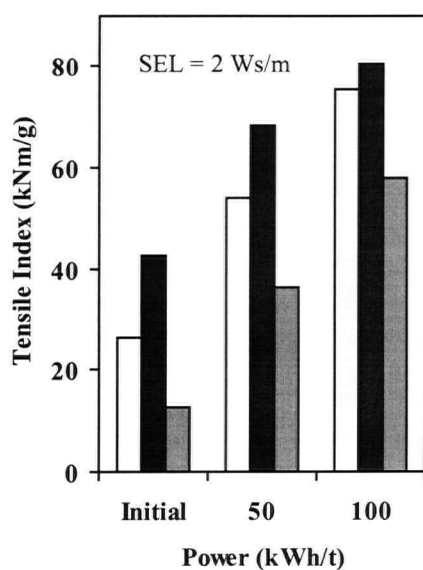


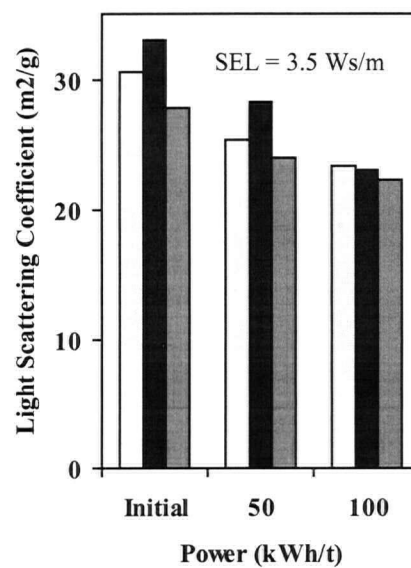
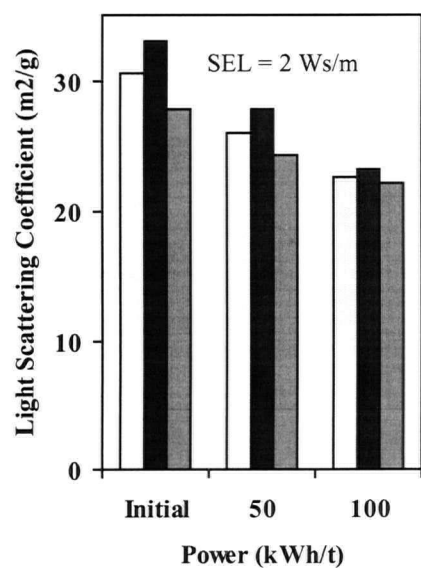
Figure 123 Freeness Values for Feed, and Fractionated Accepts and Rejects versus Refining Energy for SEL of 2 and 3.5 Ws/m



□ Initial Feed ■ Accepts 3 ▒ Rejects 3

□ Initial Feed ■ Accepts 3 ▒ Rejects 3

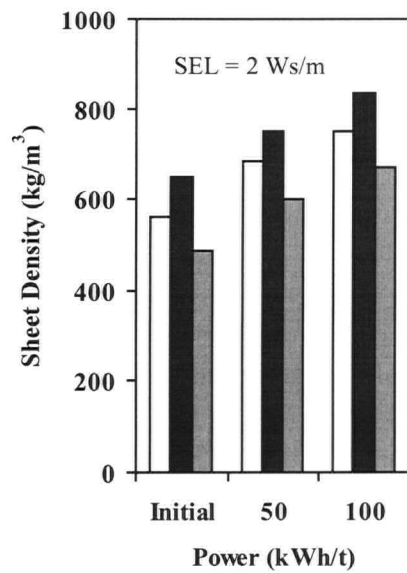
Figure 124 Tensile Index of Feed, and Fractionated Accepts and Rejects versus Refining Energy Measured for SEL's of 2 and 3.5 Ws/m



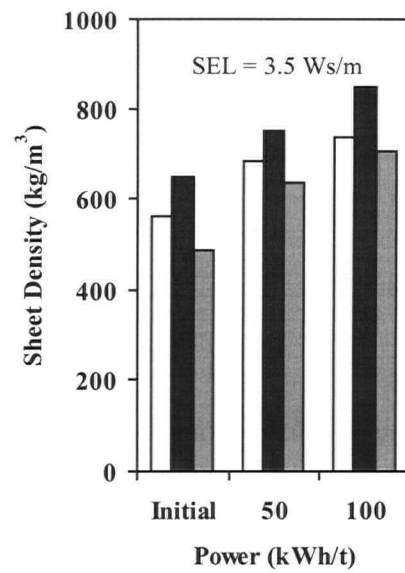
□ Initial Feed ■ Accepts 3 ▒ Rejects 3

□ Initial Feed ■ Accepts 3 ▒ Rejects 3

Figure 125 Light Scattering Coefficient Measurements of Feed, and Fractionated Accepts and Rejects versus Refining Energy for SEL's of 2 and 3.5 Ws/m

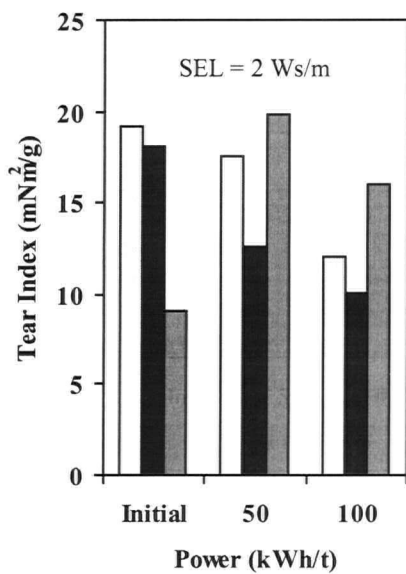


□ Initial Feed ■ Accepts 3 ▒ Rejects 3

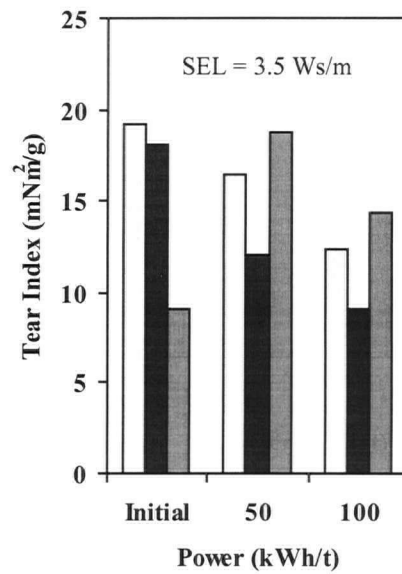


□ Initial Feed ■ Accepts 3 ▒ Rejects 3

Figure 126 Sheet Density Structure Measurements of Feed, and Fractionated Accepts and Rejects versus Refining Energy for SEL's of 2 and 3.5 Ws/m



□ Initial Feed ■ Accepts 3 ▒ Rejects 3



□ Initial Feed ■ Accepts 3 ▒ Rejects 3

Figure 127 Tear Index Measurements of Feed, and Fractionated Accepts and Rejects versus Refining Energy for SEL's of 2 and 3.5 Ws/m

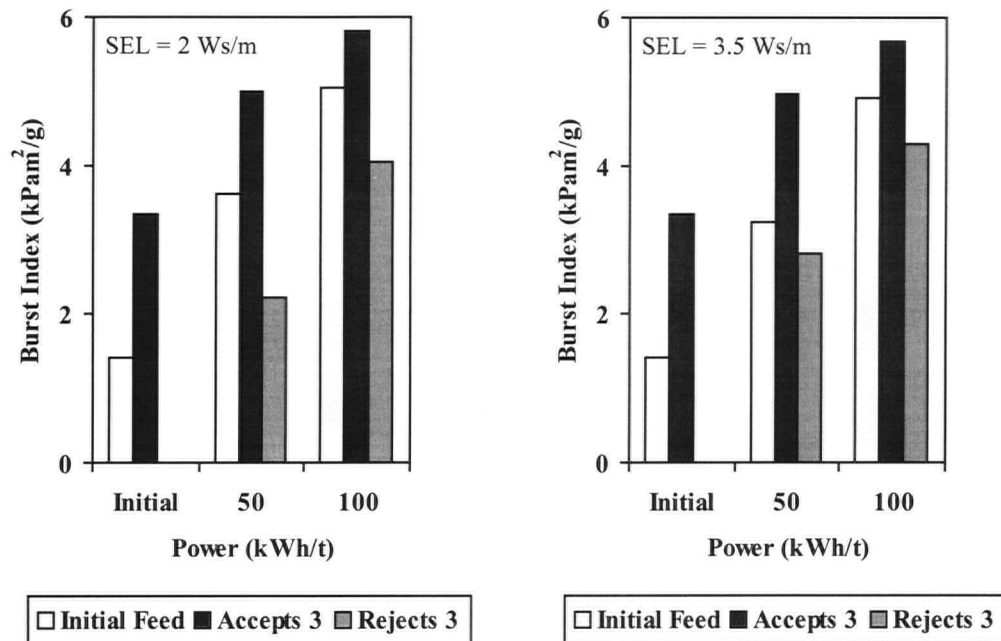


Figure 128 Burst Index Measurements of Feed, and Fractionated Accepts and Rejects versus Refining Energy for SEL's of 2 and 3.5 Ws/m

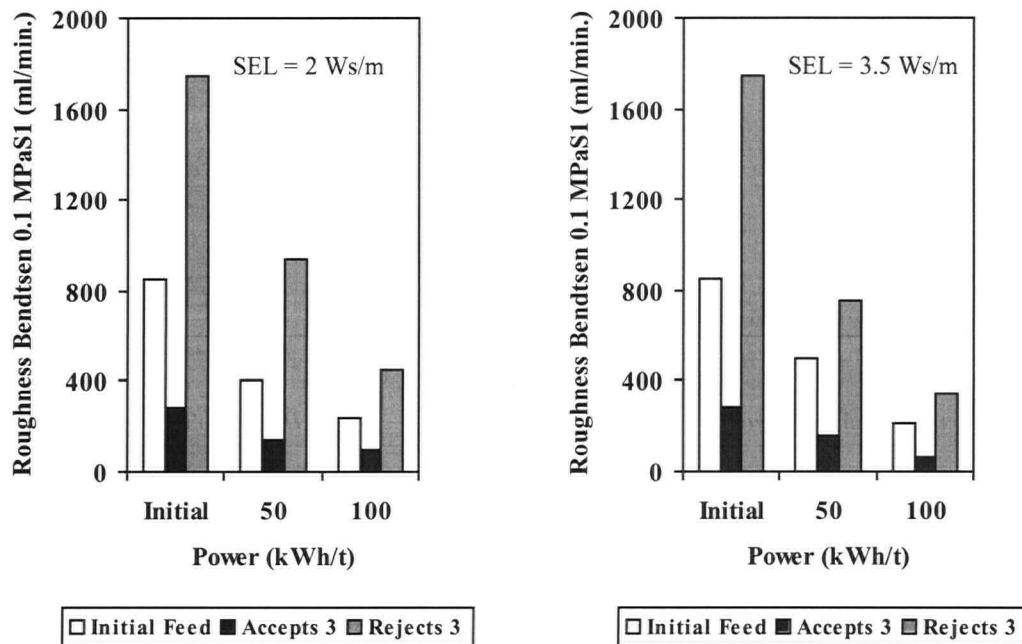


Figure 129 Sheet Roughness Measurements of Feed, and Fractionated Accepts and Rejects versus Refining Energy for SEL's of 2 and 3.5 Ws/m

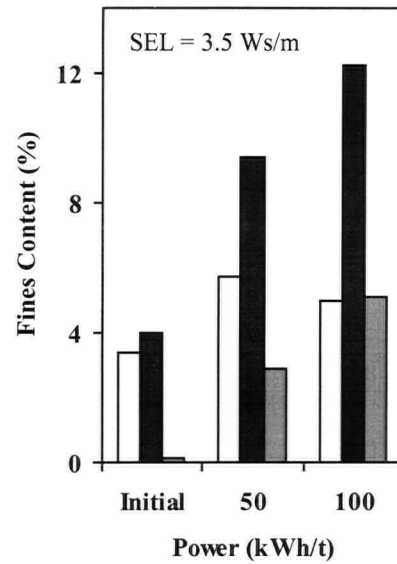
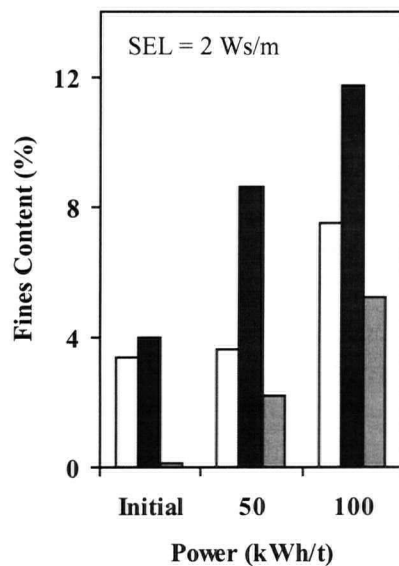


Figure 130 Fines Content of Feed, and Fractionated Accepts and Rejects versus Refining Energy for SEL's of 2 and 3.5 Ws/m

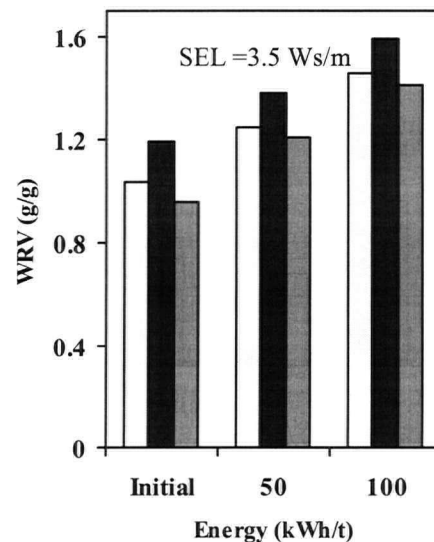
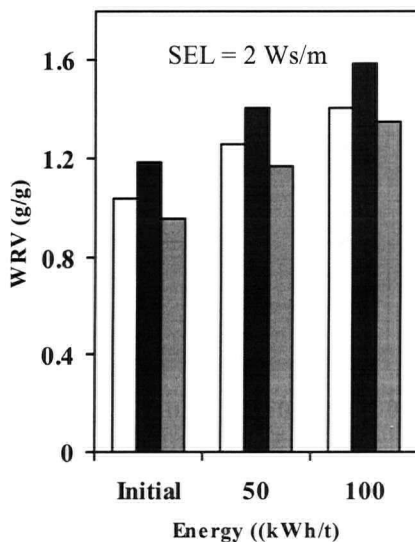


Figure 131 Water Retention Value (WRV) of Feed, and Fractionated Accepts and Rejects versus Refining Energy for SEL's of 2 and 3.5 Ws/m

These figures show that refining resulted in sheets made from the accepts fibres having the greatest tensile and burst. The initial burst index value for sheets made from the rejects fibres could not be measured since those fibres were too weak. However refining the rejects sample did show that fibre development and sheet strength resulted for this sample. Refining the rejects at 50 kWh/ton made these fibres better than the unrefined initial feed; strength of the rejects further improved when refined at 100 kWh/ton (See Figures 124 and 128).

Tear index values summarized in Figure 127 show that increasing refining energy reduced the tear index value for the accepts and feed. The rejects tear index values were found to increase when a refining energy of 50 kWh/t was supplied at SEL values of 2.0 and 3.5 Ws/m. These increases in tear resulted in a sheet having a tear index greater than that of the initial unrefined feed. Therefore, we have illustrated that it is possible to upgrade the rejects stream to levels better than the initial feed stream. Increasing the power level to 100 kWh/t resulted in lowering the tear index. This is in accord with what one would expect, i.e. refining initially increases tear, further refining reduces this property.

Figures 125 and 126 plot the light scattering coefficient and sheet density. Initial values showed that this measurement was greatest for sheets prepared from the accepts fibres. Refining results in a reduction in the light scattering coefficient. Applying a refining energy of 100 kWh/t at both the SEL values tested showed the coefficient to be more or less equal for all three samples. Sheet density measurements for the initial and refined cases resulted in the accepts fibres producing a sheet with the greatest density. The light scattering coefficient and sheet density for the initial and refined sheets made from the accepts fibres showed high strength and good interfibre bonding. Refining of the feed and rejects also showed strength development, however the accepts showed the greatest improvement over the refined rejects and feed.

Figure 129 summarizes the surface roughness of our samples. Initially the rejects showed the greatest surface roughness. Paper surface irregularities were likely to arise with these

rejects sheets since their predominantly latewood fibre content does not bond well. However surface roughness of the rejects seemed to greatly improve when these fibres were refined. Initial feed samples also showed appreciable improvements in surface roughness as a result of refining. Decreases in surface roughness measurements of the accepts handsheets were small since these sheets initially exhibited quite smooth surfaces. Refining at an SEL of 3.5 Ws/m reduced surface roughness of the rejects to a greater extent than refining at 2.0 Ws/m. No such effect was noted for the initial feed or the accepts.

Fines generation during the refining tests are shown in Figure 130. The fines content increase upon refining was greatest for the accepts stream fibres. The earlywood content of this stream initially had thin cell walls. Refining probably induced external fibrillation and for these thin walled fibres, fibre fibrils tended detach from the fibre wall thus generating fines. Note that the initial fines content of the rejects was non-measurable. Fines generated in this stream resulted only from the refining process. A greater degree of fines generation resulted for the feed stream when refined at a SEL of 2.0 Ws/m than 3.5 Ws/m when the energy was 100 kWh/ton. These differences resulted from operation of the refiner, the pulp experienced more passes through the refining zone for the case of operation at SEL of 2.0 Ws/m.

Figure 131 reports measurements of the fibre water retention value (WRV) for our samples. The results show that increased refining results in increased water retention. These results are because refining induces fibre swelling and in turn increases fibre volume. The amount of water held within the fibre increases, this is demonstrated by measuring the WRV. WRV measurements were greater for tests performed at SEL of 3.5 Ws/m than those for 2.0 Ws/m.

The presence of fines in the accepts makes it difficult to quantify the refining effects on the earlywood content of this stream. We screened a sample of the unrefined fractionated accepts to remove the fines and then refined this sample at a SEL of 2 W s/m and energy consumption levels of 50 and 100 kWh/t. We also combined our fractionated accepts

(AA3) and rejects (RR3) in a mixture having 70% accepts fibres and 30% rejects fibres. These proportions were arbitrarily chosen. This mixture was refined under the same conditions as the fines removed accepts stream. The mixed stream was tested to see how these fibres developed when refined together.

Figures 132 and 133 present the length distribution curves for our 70:30 accepts and rejects mixture and our fines removed AA3 after these stream were refined. Length and width data for the unrefined 70:30 mixture were not measured and therefore these data are lacking. However, we can study the changes in length and width distribution of the refined mixture. The corresponding width distributions for our samples are illustrated in Figures 134 and 135. The length distributions indicated that fibre cutting and shortening took place. Fibre contents in the fibre length range 0.4 – 2.0 mm increased with increased refining, contents in the range greater than 2.2 mm decreased. Width distributions showed that increased refining resulted in slight decreases in fibre content in the width range of 22 – 35 μm .

Average length, width and shape factors for the refined fines removed and mixture sample are summarized in Table 20. Refining resulted in a lowering of the average fibre length. The average width and shape factor were found to increase with increased refining

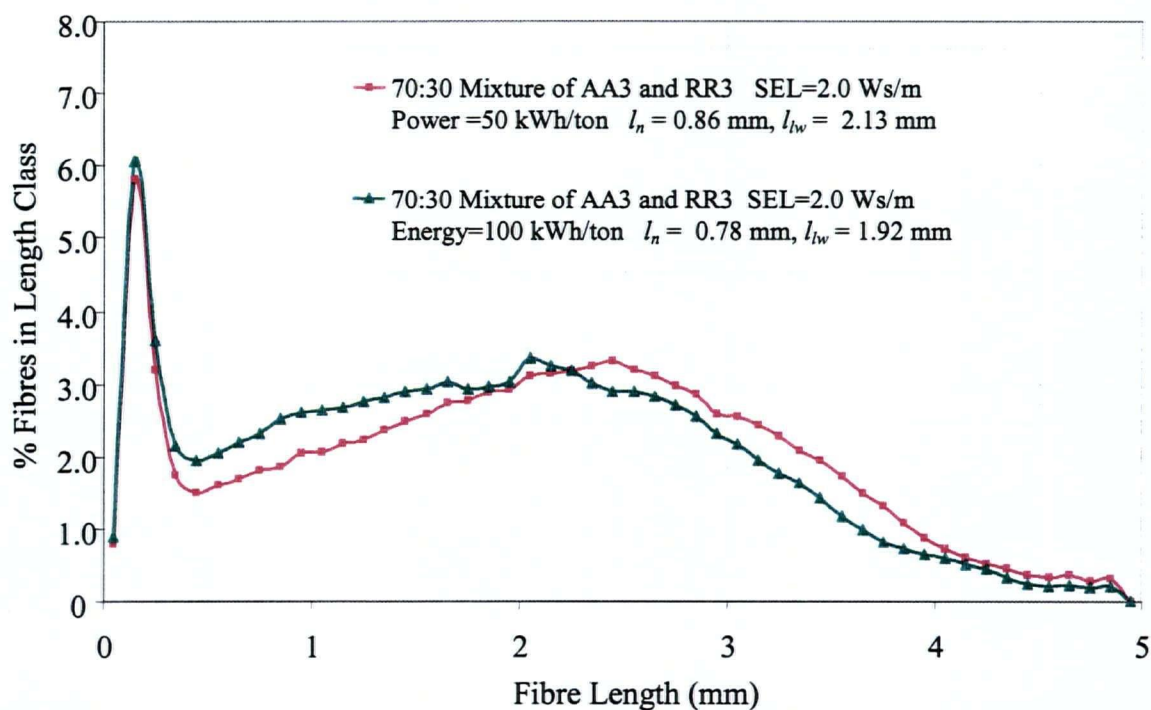


Figure 132 Length Distribution of Accepts and 70:30 Mixture of Accepts and Rejects. Samples Refined at SEL of 2 Ws/m

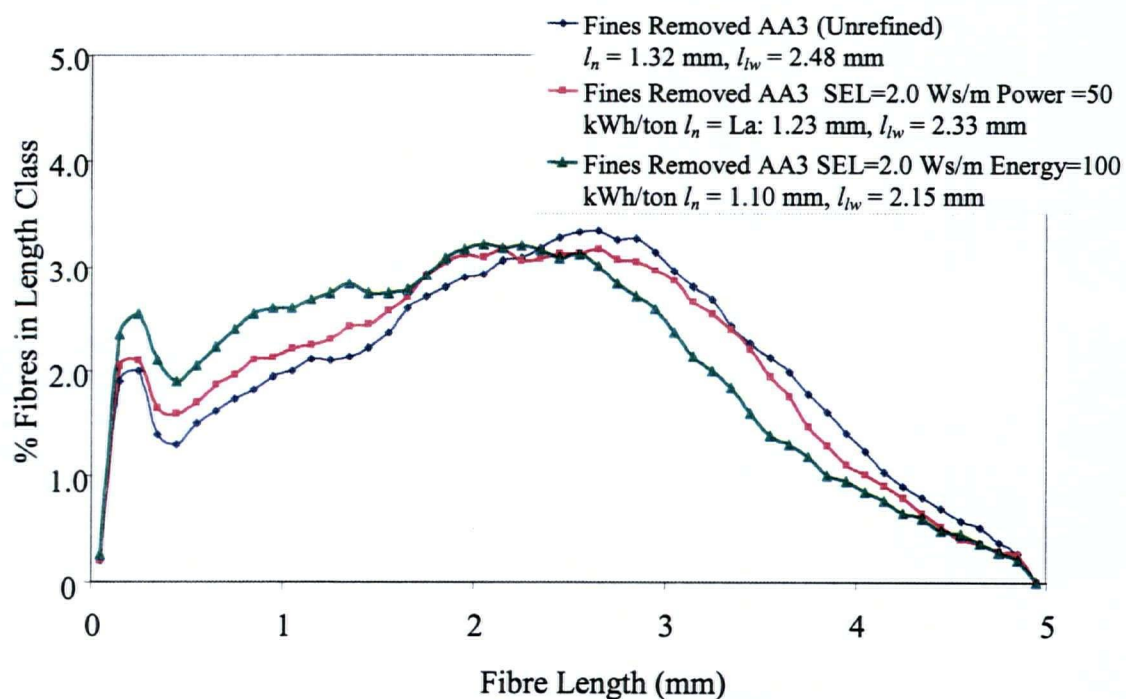


Figure 133 Length Distribution of Fines Removed Accepts. Samples Refined at SEL of 2 Ws/m

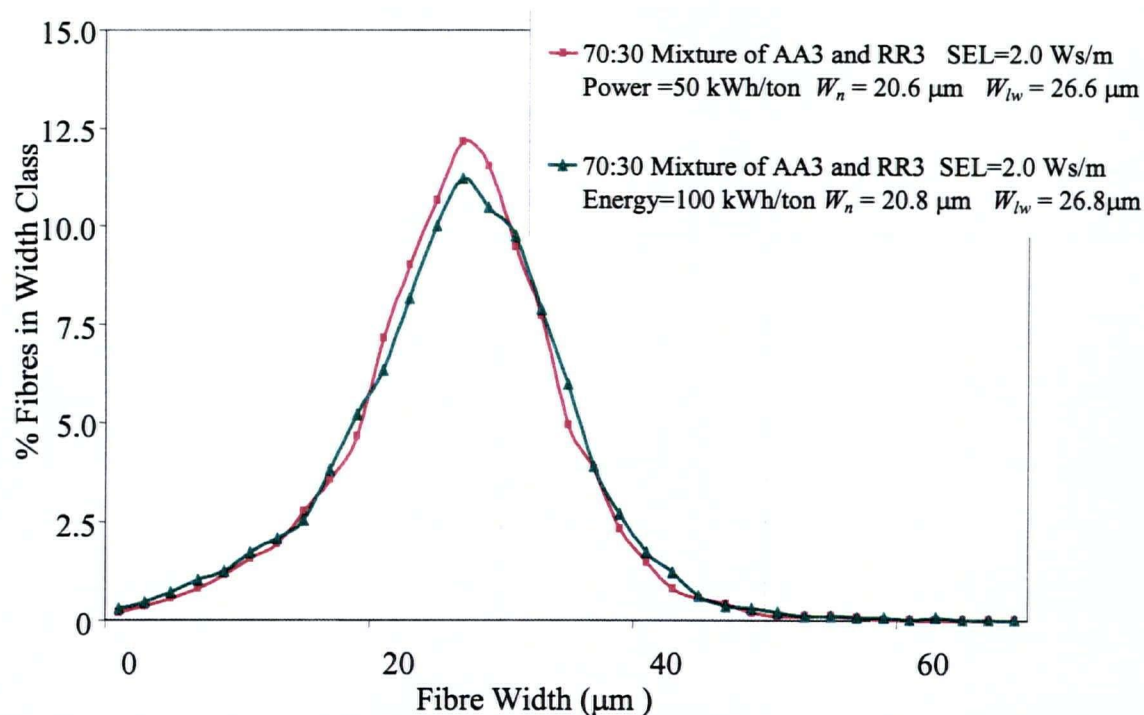


Figure 134 Width Distribution of Accepts and 70:30 Mixture of Accepts and Rejects.
Samples Refined at SEL of 2 Ws/m

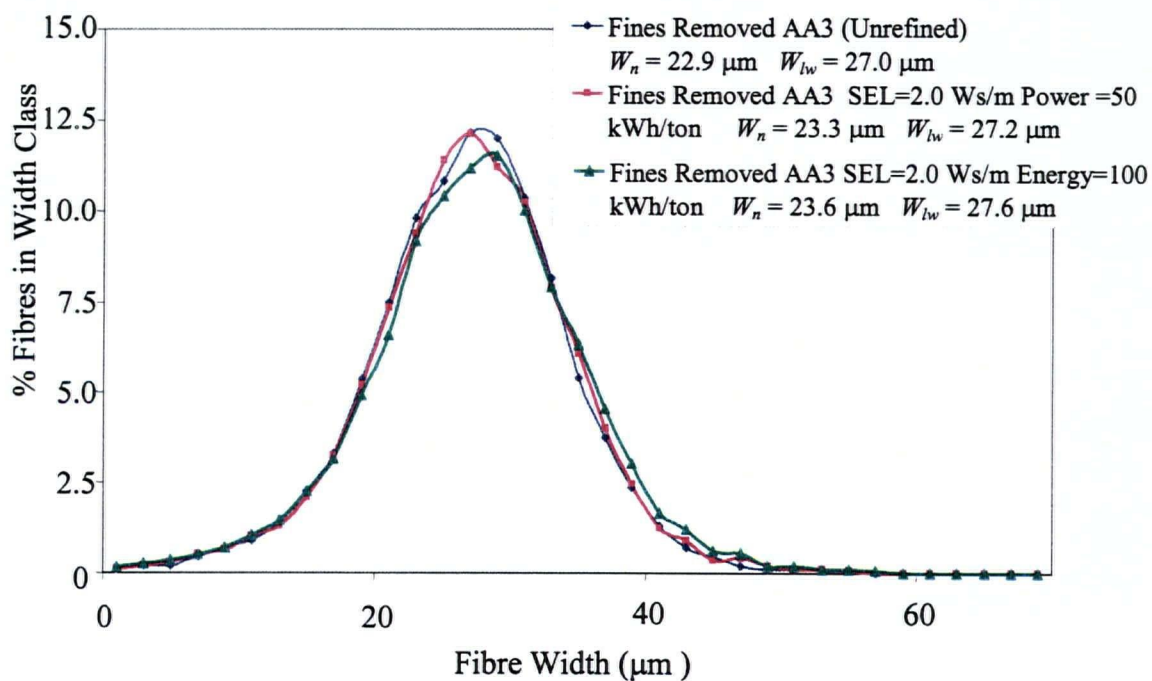


Figure 135 Width Distribution of Fines Removed Accepts. Samples Refined at
SEL of 2 Ws/m

Table 20 Average Length, Width and Shape Factor Measurements of Feed, Accepts, Fines Removed Accepts and 70:30 Mixture of Accepts and Rejects. Samples Refined at SEL of 2 Ws/m

Sample	Unrefined			50 kWh/ton			100 kWh/ton		
	l_{lw} (mm)	W_{lw} (μ m)	SF_{lw} (%)	l_{lw} (mm)	W_{lw} (μ m)	SF_{lw} (%)	L_{lw} (mm)	W_{lw} (μ m)	SF_{lw} (%)
Initial Feed	2.37	27.0	85.0	2.26	27.0	86.8	2.08	27.9	87.9
AA3	2.15	25.4	86.0	2.03	26.2	87.1	1.86	26.6	88.5
AA3 (Fines Removed)	2.48	27.0	83.7	2.33	27.2	85.8	2.15	27.6	86.6
70 :30 Mixture of AA3 and RR3	-	-	-	2.13	26.6	86.8	1.92	26.8	88.8

Figures 136 – 144 illustrate the pulp and paper property changes resulting from refining the fines removed accepts and the 70:30 accepts and rejects mixture. Our original fractionated accepts and initial feed are also shown once again for comparative purposes.

Freeness values (Figure 136) of the fines removed accepts stream had similar values to the initial feed when refined at the two power levels (See Figure 98). The mixed stream resulted in lower freeness values than the fines removed accepts and initial feed streams after being refined, this was due to the larger quantity of fines present in the mixed stream.

Tensile index values are plotted in Figure 137. The fines removed accepts and the mixed stream produced lower tensile indices than the feed and original accepts stream when refined. But refining at energy levels of 100 kWh/ton resulted in tensile strengths that were almost double those of the initial feed. Under these conditions the feed, accepts, fines removed accepts, and mixture produced sheets of almost equal tensile strength (Figure 137). Burst index values shown in Figure 141 produced similar trends to the tensile index values. These results indicated that the greater presence of fines in the original accepts and feed contribute positively to burst and tensile strength, these observations were noted even after the samples were refined.

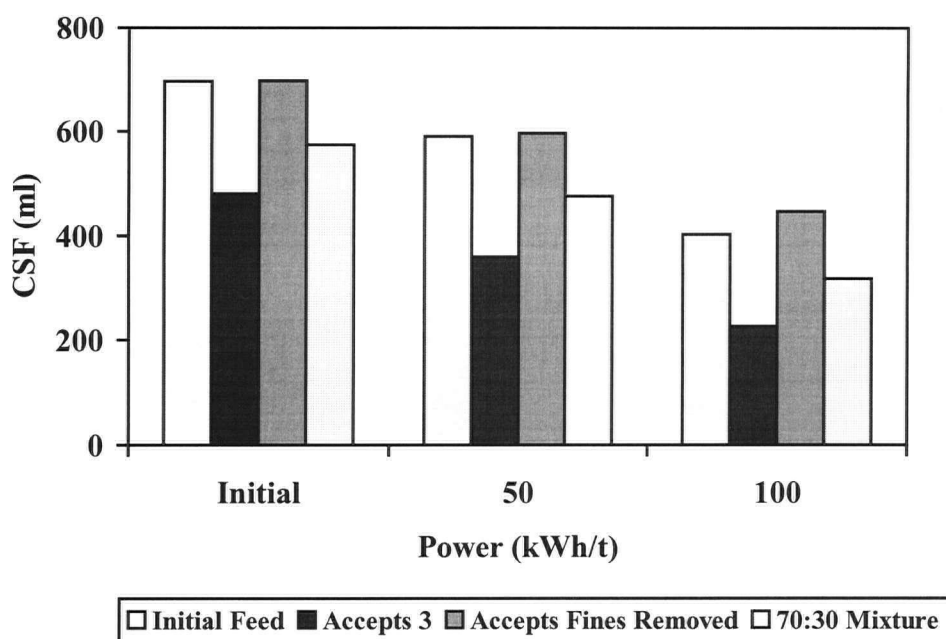


Figure 136 Freeness Measurements of Feed, Accepts, Fines Removed

Accepts and 70:30 Mixture of Accepts and Rejects. Samples Refined at SEL of 2 Ws/m

Tear index measurements are presented in Figure 140. The initial tear index value of the fines removed accepts stream was greater than the initial feed, initial accepts and mixed stream. Refining the fines removed accepts stream brought the tear index value lower than the initial feed stream. This can be attributed to the increase in the fines content in this accepts sample. The mixed stream had tear values lower than the initial feed stream, refining this sample led to further reduction in tear strength.

Initial light scattering coefficients (See Figure 138) of both accepts samples and the mixture were similar to the initial feed. Upon refining, the fines removed accepts sample did not decrease in this measurement to the same extent as the original accepts. The mixed sample produced light scattering coefficients which fell between the initial feed and both accepts samples.

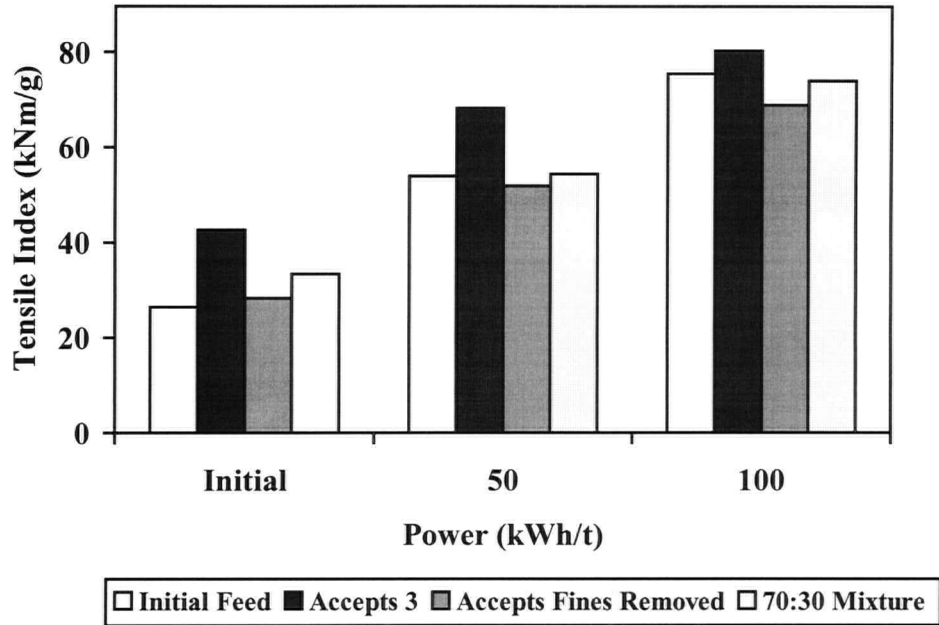


Figure 137 Tensile Strength of Feed, Accepts, Fines Removed Accepts and 70:30 Mixture of Accepts and Rejects. Samples Refined at SEL of 2 Ws/m

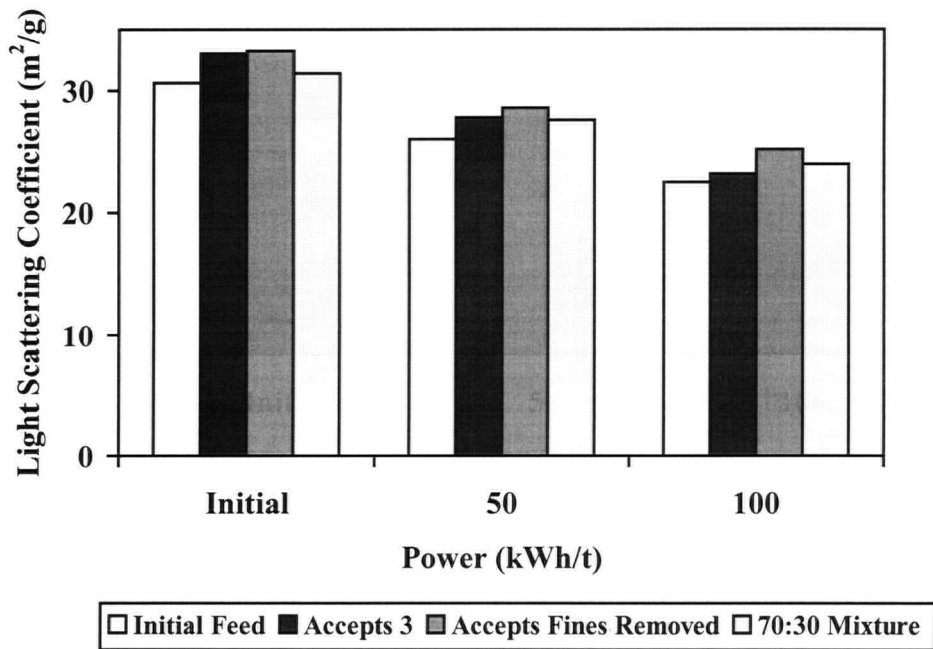


Figure 138 Light Scattering Measurements of Feed, Accepts, Fines Removed Accepts and 70:30 Mixture of Accepts and Rejects. Samples Refined at SEL of 2 Ws/m

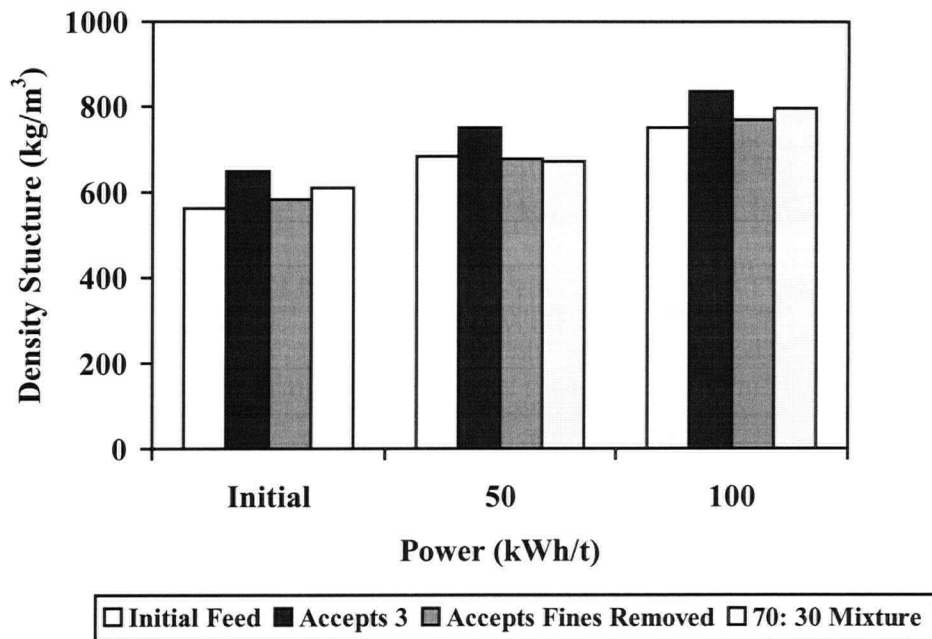


Figure 139 Sheet Density of Handsheets Prepared from Feed, Accepts, Fines Removed Accepts and 70:30 Mixture of Accepts and Rejects. Samples Refined at SEL of 2 Ws/m

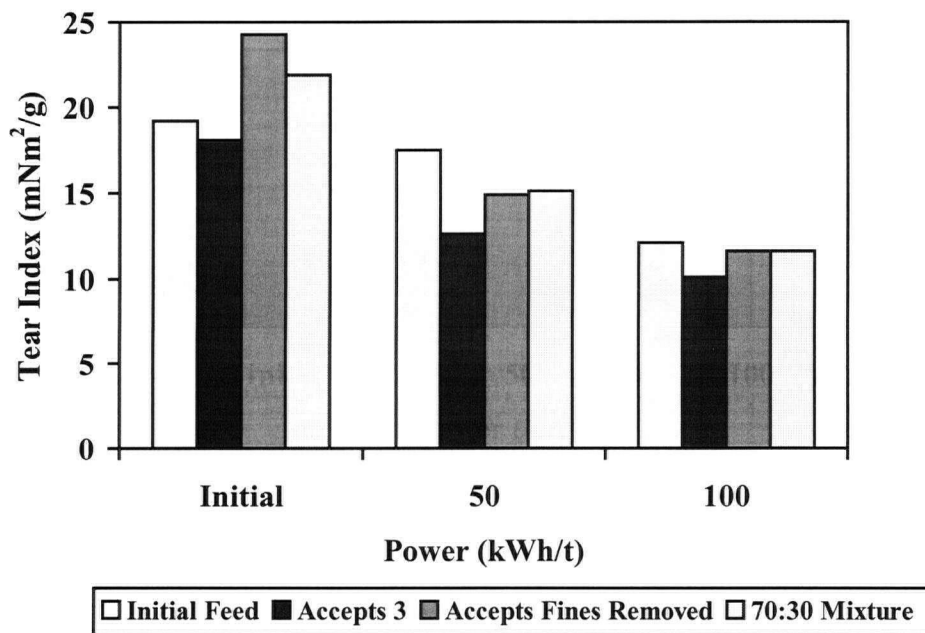


Figure 140 Tear Index Measurements of Feed, Accepts, Fines Removed Accepts and 70:30 Mixture of Accepts and Rejects. Samples Refined at SEL of 2 Ws/m

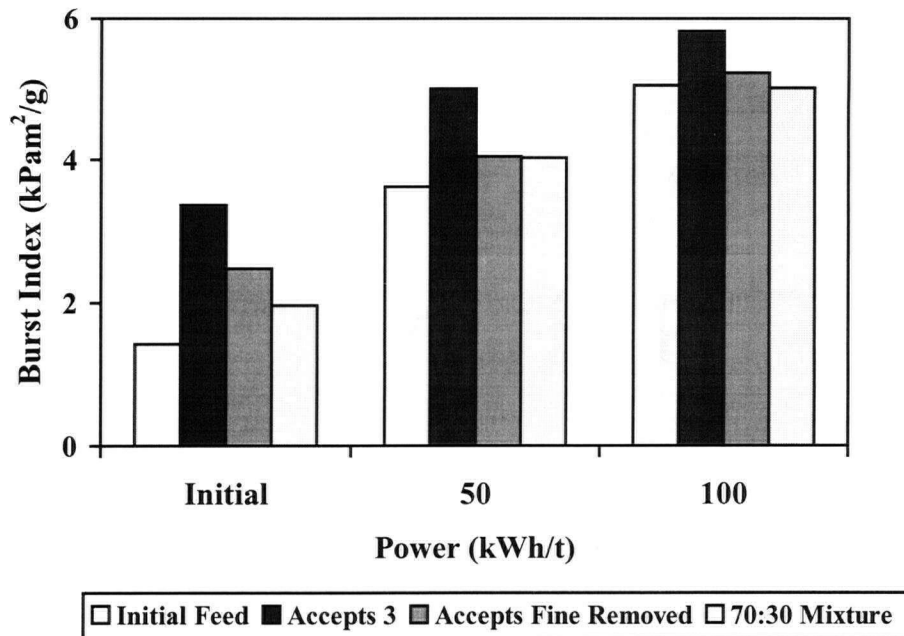


Figure 141 Burst Index Measurements of Feed, Accepts, Fines Removed Accepts and 70:30 Mixture of Accepts and Rejects. Samples Refined at SEL of 2 Ws/m

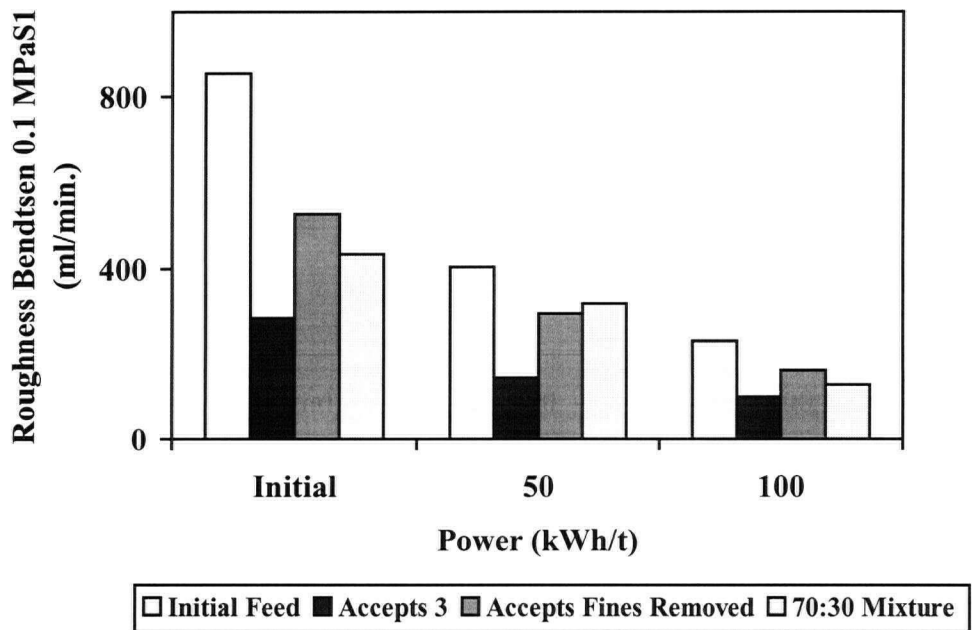


Figure 142 Sheet Roughness Measurements of Feed, Accepts, Fines Removed Accepts and 70:30 Mixture of Accepts and Rejects. Samples Refined at SEL of 2 Ws/m

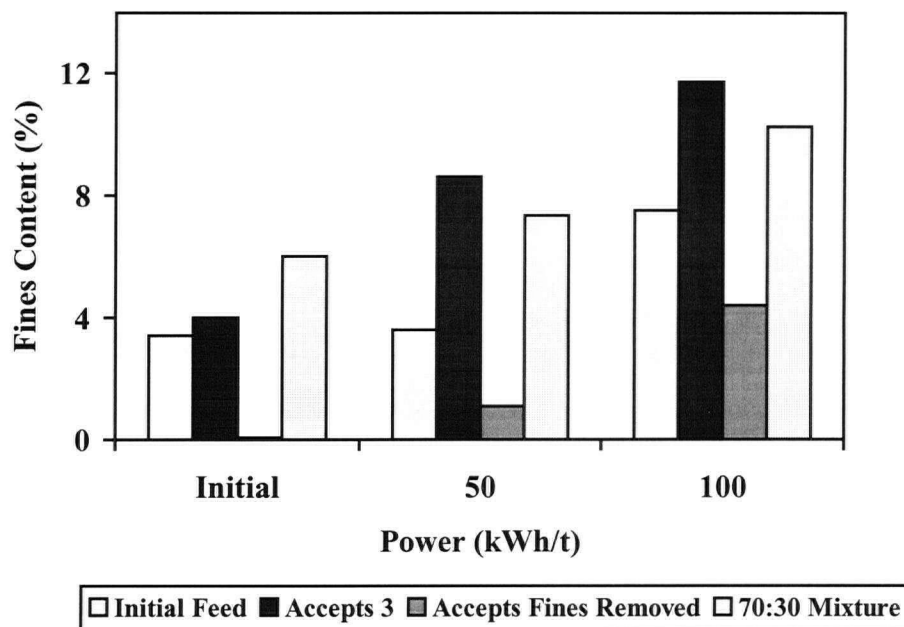


Figure 143 Fines Content of Feed, Accepts, Fines Removed Accepts and 70:30 Mixture of Accepts and Rejects. Samples Refined at SEL of 2 Ws/m

Sheet density measurements are shown in Figure 139. The fines removed and mixed samples did not achieve the same sheet density as the initial accepts. These streams showed some improvement over the initial feed when they were refined at an energy consumption of 100 kWh/t.

Removal of the fines content from the accepts led to an initial surface roughness which was greater than the original accepts sample (See Figure 142). The mixed stream prior to refining had greater surface smoothness as compared to the fines removed accepts stream. As the samples were refined, surface smoothness increased. However, the original accepts produced better surface smoothness than the other streams.

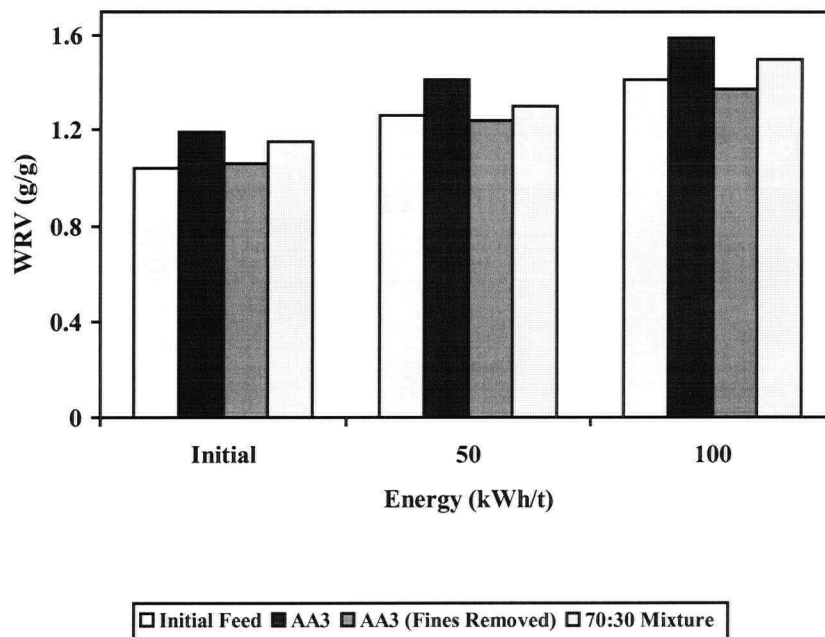


Figure 144 Water Retention Value (WRV) of Feed, Accepts, Fines Removed Accepts and 70:30 Mixture of Accepts and Rejects. Samples Refined at SEL of 2 Ws/m

Figure 143 presents the fines content of the samples. Quantifying the fines in our unrefined fines removed accepts sample showed an un-measurable quantity of fines, this indicated that we were effective in removing the fines from this sample. Refining of the fines removed accepts produced fines contents which were lower than refining the mixed fraction and the original feed and accepts samples.

Figure 144 summarizes the water retention content (WRV) for the samples. WRV increased with increasing energy levels for all the samples. The WRV for the refined fines removed accepts were lower than the refined original feed and accepts. The WRV for the refined mixture was lower than the refined accepts but greater than the refined feed. WRV is dependent on fibre swelling and fines content. There was a greater fines content in our original accepts and mixture samples, therefore these samples retain more water upon refining as compared to the original feed and fines removed accepts samples.

These results demonstrated the effect of fines on our refining results. The fines content in the original accepts streams positively affected properties such as sheet density, tensile index and burst index, and surface smoothness of the handsheets. This experiment also showed that fines content affected the tear strength of the handsheets prepared from the accepts samples. Fines generated during refining reduced the tear strength of handsheets. The fines removed accepts sample did not decrease in tear strength to the same extent as the original accepts due to the reduced fines content of this sample.

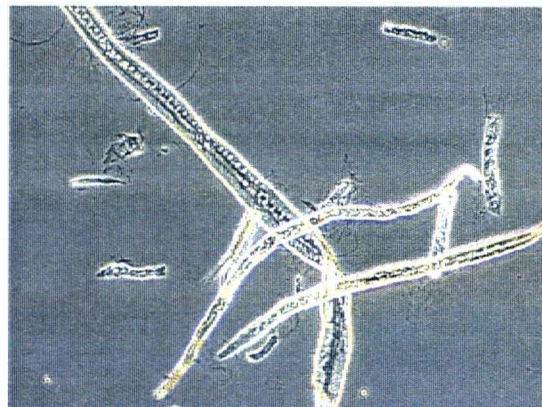
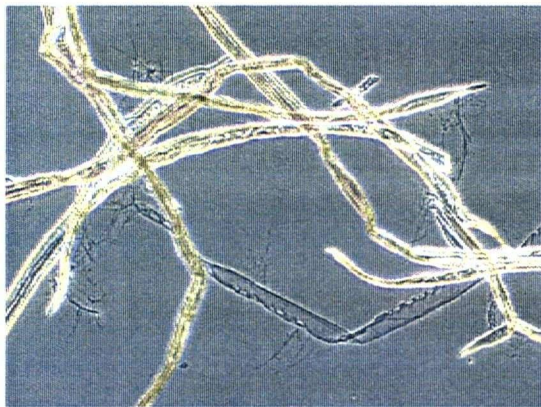
Photomicrographs of the refined and unrefined feed, AA3, RR3, 70:30 mixture, and fines removed AA3 are shown in Figures 145 – 149. These photomicrographs were prepared from samples refined at $SEL = 2.0$ Ws/m and energy consumption levels of 50 and 100 kWh/ton.

Figure 145 illustrates refined feed fibres. The unrefined fibres showed little fibrillation whereas external fibrillation was evident at both energy levels tested. Lengths of fibre fibrils were longer for tests performed at energy levels 100 kWh/ton. Refined accepts (AA3) fibres shown in Figure 146 indicated that internal as well as external fibrillation occurred for these fibres. Fibre peeling induced through the refining process is also evident in these photomicrographs. This sample had a greater proportion of earlywood; these fibres have thin walls and therefore fibrillate easily.

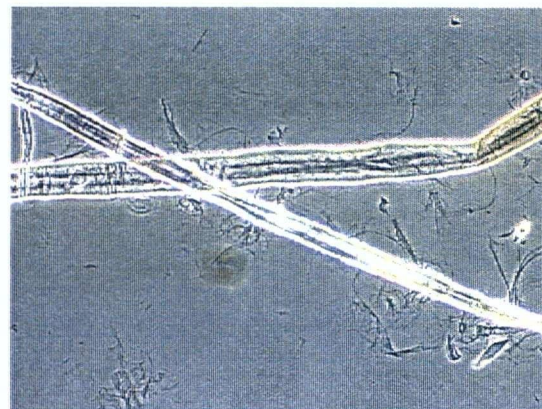
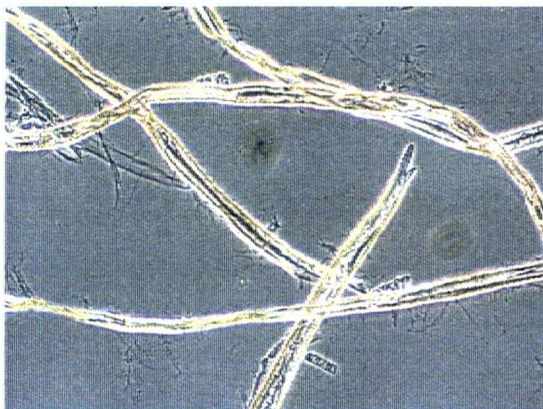
Figure 147 illustrates unrefined and refined rejects (RR3) fibres. This sample was prevalently latewood and therefore had more thick-walled fibres. For both energy levels tested, there still existed some fibres without fibrillation. Lengths of fibre fibrils were longer for tests performed at 100 kWh/ton. This indicated that these fibres required higher levels of refining than accepts fibres (AA3).

Figure 148 shows photomicrographs of the AA3 and RR3 mixture. Fibrillation of these fibres was detected at both energy levels however, fibril length was greater when the sample was refined at an energy consumption of 100 kWh/ton. Figure 149 illustrates refining effects on our fines removed accepts pulp. These photomicrographs showed the

greater presence of earlywood than latewood fibres. For fibres refined at 50 kWh/ton slight fibrillation was detected. When these fibres were refined at 100 kWh/ton external and internal fibrillation occurred. Fibril lengths were greater for fibres refined at 100 kWh/ton.



Unrefined Feed

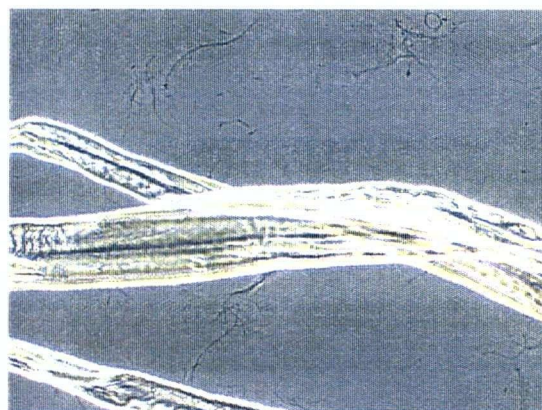
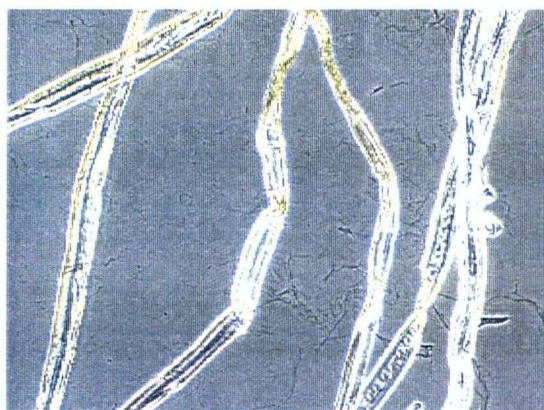


Feed Refined at Energy Consumption of 50 kWh/ton



Feed Refined at Energy Consumption of 100 kWh/ton

Figure 145 Photomicrographs of Unrefined and Refined Feeds. Escher Wyss Refiner
Operated at $SEL = 2.0 \text{ Ws/m}$ and Energy Consumption of 50 and 100 kWh/ton



Unrefined Accepts (AA3)

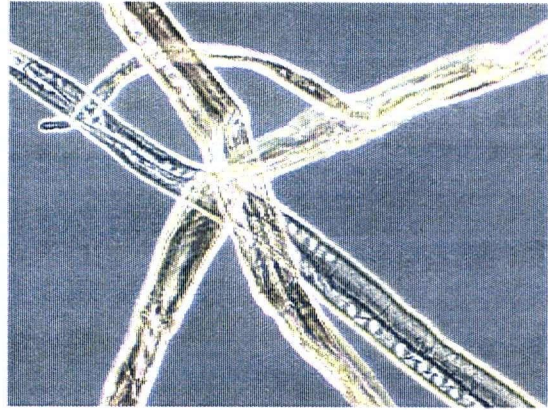
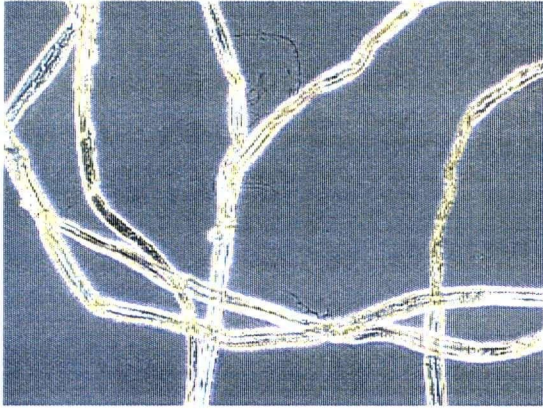


Accepts (AA3) Refined at Energy Consumption of 50 kWh/ton

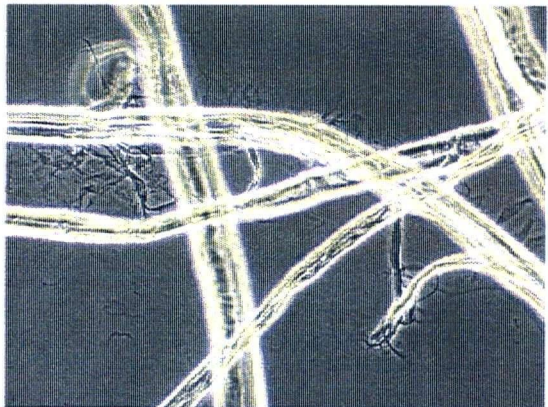
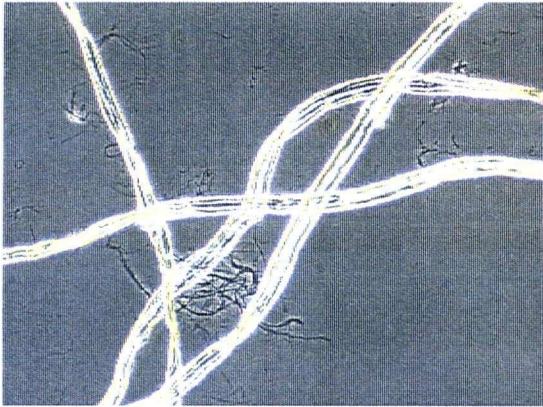


Accepts (AA3) Refined at Energy Consumption of 100 kWh/ton

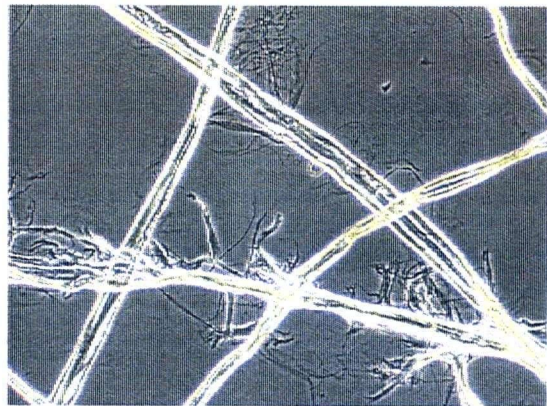
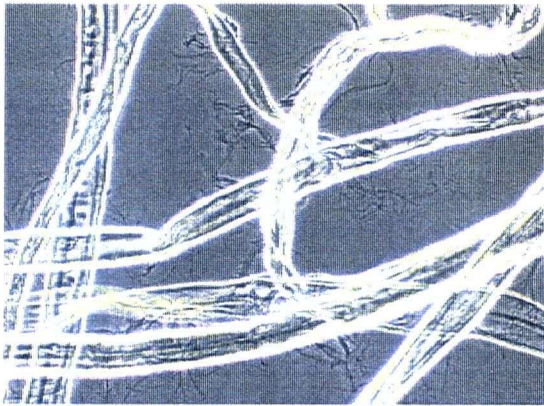
Figure 146 Photomicrographs of Unrefined and Refined Accepts (AA3). Escher Wyss Refiner Operated at SEL = 2.0 Ws/m and Energy Consumption of 50 and 100 kWh/ton



Unrefined Rejects (RR3)

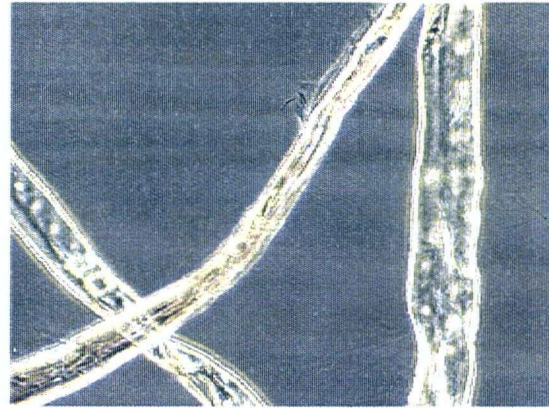
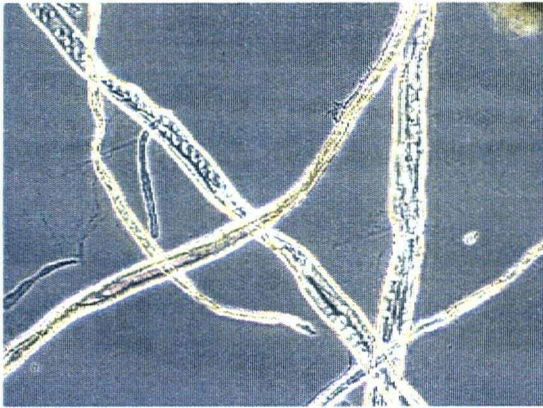


Rejects (RR3) Refined at Energy Consumption of 50 kWh/ton

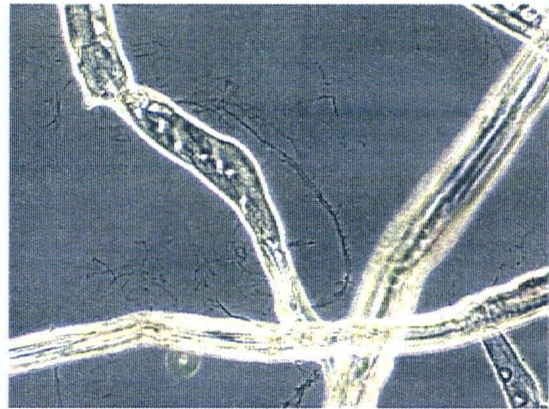
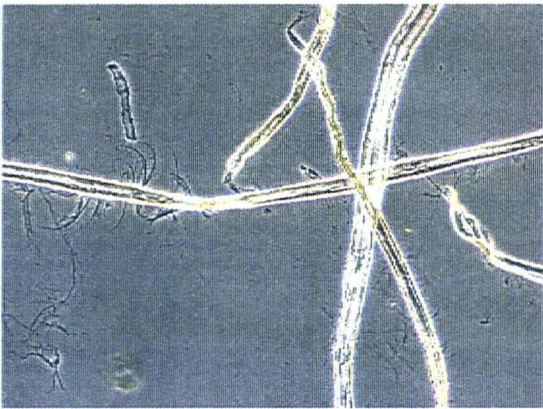


Rejects (RR3) Refined at Energy Consumption of 100 kWh/ton

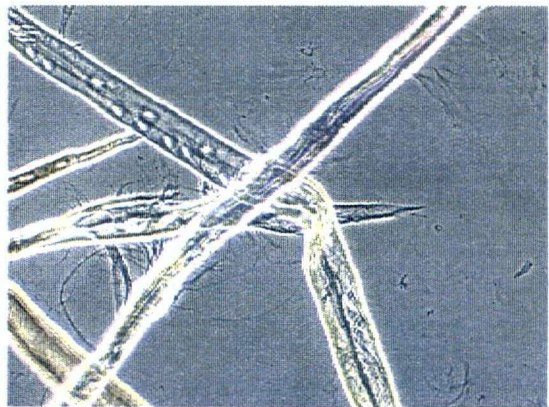
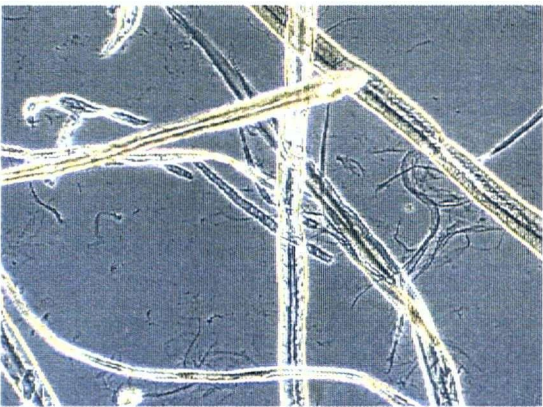
Figure 147 Photomicrographs of Unrefined and Refined Rejects (RR3). Escher Wyss Refiner Operated at $SEL = 2.0 \text{ Ws/m}$ and Energy Consumption of 50 and 100 kWh/ton



Unrefined 70:30 Mixture of AA3 and RR3

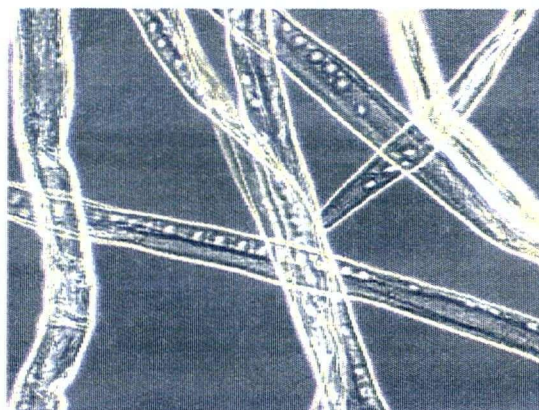
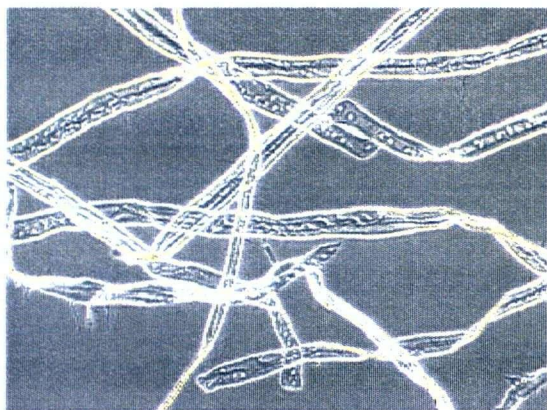


70:30 Mixture of AA3 and RR3 Refined at Energy Consumption of 50 kWh/ton

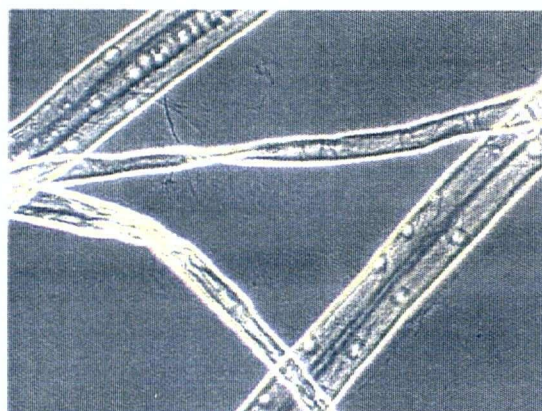
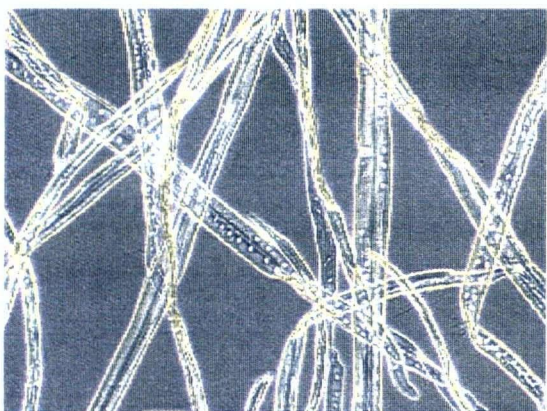


70:30 Mixture of AA3 and RR3 Refined at Energy Consumption of 100 kWh/ton

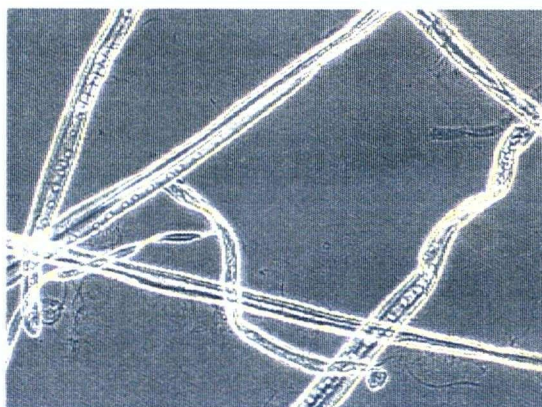
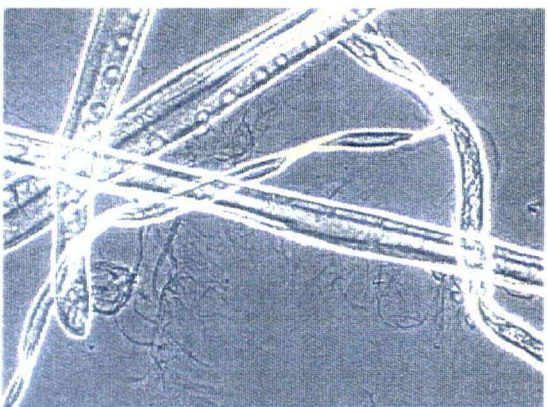
Figure 148 Photomicrographs of Unrefined and Refined 70:30 Mixture of AA3 and RR3. Escher Wyss Refiner Operated at SEL = 2.0 Ws/m and Energy Consumption of 50 and 100 kWh/ton



Unrefined Fines Removed AA3



Fines Removed AA3 Refined at Energy Consumption of 50 kWh/ton



Fines Removed AA3 Refined at Energy Consumption of 100 kWh/ton

Figure 149 Photomicrographs of Unrefined and Refined Fines Removed AA3. Escher Wyss Refiner Operated at $SEL = 2.0 \text{ Ws/m}$ and Energy Consumption of 50 and 100 kWh/ton

Chapter 6

Conclusions and Future Recommendations

6.1 Objectives

The objectives of this thesis were:

1. To review relevant literature on fractionation and provide some theoretical understanding regarding how fibres fractionate in hydrocyclones.
2. To experimentally determine how hydrocyclone operating variables can affect fibre separation. These variables include hydrocyclone operation (flowrate, reject rate) and pulp properties (consistency, pulp type, freeness).
3. To study multistage fractionation schemes and characterize the degree of fractionation based on the measurement of fibre properties (length, width, shape factor and coarseness), pulp freeness, and sheet properties.
4. To refine fractionated Kraft pulp to demonstrate the differences in fibre development of separated streams.

A summary of the findings of our investigation is presented in this chapter.

6.2 Literature Review and Theoretical Analysis

A review of the literature showed that there is universal acceptance that hydrocyclones fractionate on the basis of specific surface and coarseness. The various hydrocyclones tested in the literature showed that thick walled, coarse fibres with low specific surface area tended to be rejected whereas thin walled (i.e. low coarseness) fibres having high specific surface area tended to be accepted. There wasn't, however, universal agreement that hydrocyclones fractionate on the basis of fibre length. In some of the literature reviewed, hydrocyclones tended to reject long fibres, others found short fibre rejection.

The observations regarding length fractionation were dependent on the hydrocyclone tested and presumably on the fluid flow patterns in it.

By performing a force balance on an idealized pulp fibre flowing inside a hydrocyclone, it was shown that the fibre radial velocity was inversely related to fibre specific surface. The literature reviewed also provided evidence that freeness was inversely related to fibre specific surface. Also, it was demonstrated that fibre coarseness was inversely related to specific surface. These relations indicated that hydrocyclones are capable of rejecting fibres which have a higher coarseness, higher freeness, and lower specific surface than the fibres which are accepted.

Although the literature reviewed illustrated that fibre length differences occurred between the hydrocyclone accepts and rejects stream, we could not provide any theoretical reasoning for this observation. This is partly due to the fact that the theoretical analysis provided in this thesis was a simple first approach. Improvement of this analysis by applying a different representation for the geometry of a pulp fibre or applying drag coefficient relations measured from studying fibre motion might provide some understanding regarding fractionation based on length.

6.3 Experimental Studies on Fractionation

Several experiments were presented in this thesis which showed that fractionation on the basis of fibre coarseness was possible when testing Hydrocyclones A, B, and C. In each of these hydrocyclones fibre coarseness of the rejects stream was always greater than the accepts stream.

Fibre fractionation on the basis of length was most obvious when testing Hydrocyclones A and C. However the findings for these two hydrocyclones were opposite to each other. Fractionating mechanically pulped fibres in Hydrocyclone A tended to fractionate short coarse fibres and fibre fines to the rejects and long fibres with lower coarseness than the rejects reported to the accepts stream. Operation of Hydrocyclone A at low reject rates (4

– 5%) and flowrates of 40 – 50 kg/min. resulted in pulp fines reporting to the rejects stream. Earlier we mentioned that pulp freeness was proportional to coarseness (i.e. fibres that had higher coarseness also had high freeness since they tended to drain faster than fibres having lower coarseness). The tendency of Hydrocyclone A to reject pulp fines at flowrates of 40 – 50 kg/min. led to freeness and specific surface relationships which were opposite to some of the literature reviewed. This was because this hydrocyclone rejected fines which are characterized as high specific surface material. Operation of Hydrocyclone A at flowrates greater than 50 kg/min. or at reject ratios greater than 10% led to the accepts having lower freeness than the rejects, this observation was similar to findings reported in the literature reviewed. From these freeness differences we showed that, theoretically, accepts have higher specific surface and lower coarseness than the rejects stream.

Hydrocyclone C was used to study separation of earlywood and latewood fibres. A Scandinavian Kraft pulp was tested. For this experiment we found that latewood fibres reported to the rejects and earlywood fibres and pulp fines were accepted. Latewood fibres are coarser and thick-walled whereas earlywood fibres are thin-walled. For these experiments, the average fibre lengths of the rejects were greater than the accepts since latewood fibres tend to be longer than earlywood fibres. This may be the reason why fractionation based on fibre length appeared to occur. Sheets prepared from the accepts stream were always stronger than those prepared from the rejects stream. Freeness of the rejects stream was always greater than that of the accepts stream, thus it can be concluded that the specific surface of the rejects fibres was always less than that of the accepts fibres.

The experiments performed in this thesis also demonstrated that it was possible to fractionate various types of pulps. For the mechanical pulps tested (CTMP, TMP, and BCTMP) we assessed fractionation based on length, coarseness, freeness and sheet strength differences. Fractionation of mechanical pulp was performed on Hydrocyclones A and B, in these tests we found that rejects fibres possessed higher coarseness than the accepts fibres. Sheets prepared from the rejects were always weaker than those prepared

from the accepts. Length differences were appreciable only in Hydrocyclone A, average fibre lengths of the rejects were always smaller than the accepts.

The strength properties of paper sheets tended to be a more sensitive measure of fibre fractionation than the measurement of fibre properties.

For tests performed on recycled pulp, we looked at differences in length, sheet properties, and fibre characterization to identify fibres which were mechanically or chemically pulped. For these tests fibre lengths were always smaller for the rejects than the accepts. Sheets made of accepts fibres were stronger than for rejects sheets. Microscopic examination of the accepts and rejects fibres showed that chemically pulped fibres tended to concentrate in the accepts and mechanically pulped fibres tended to report to the rejects. Chemically pulped fibres have a lower coarseness and thinner cell wall than mechanically pulped fibres and therefore tend to be accepted in the fractionation process.

6.4 Multistage Fractionation Experiments

CTMP and TMP were fractionated in six stages using Hydrocyclone A. These tests demonstrated that fractionating out short coarse fibre material into the rejects stream led to an accepts stream which had greater burst and tear strength than the original un-fractionated pulp.

Chemical softwood was fractionated in Hydrocyclone C. The objective of this experiment was to concentrate earlywood fibres in the accepts stream and latewood fibres in the rejects stream. Accepts and rejects were both fractionated in three stages. The accepts fractionation experiment resulted in a stream which contained 75% earlywood and 25% latewood, the original un-fractionated feed stream contained 66% earlywood and 34% latewood. This stream had lower freeness and lower sheet strength than the un-fractionated pulp.

The rejects fractionation experiment produced a stream that had 50% latewood and 50% earlywood. This stream had higher freeness and lower sheet strength than the initial feed stream.

6.5 Refining of Accepts and Rejects Fibres

The resulting accepts and rejects from a multistage fractionation of chemical softwood were subjected to various levels of refining to study fibre strength development. When refined at similar conditions, the results showed that the earlywood rich accepts stream had higher sheet strength, lower freeness, and higher water retention than the latewood rich rejects stream. Earlywood fibres were less coarse and thin-walled than latewood fibres and hence fibre development (external and internal fibrillation) could be achieved at lower levels of refining.

6.6 Suggestions for Further Research

Our results have shown that fractionation can be achieved in hydrocyclones. There are currently mill scale fractionation processes employing hydrocyclones for this purpose. However there still exists areas which need further investigation. Some recommendations for further work include:

- Obtaining more information on fibre properties such as fibre wall thickness, fibre width, and fibre coarseness distributions. This type of data can be used to understand which fibre properties govern separation.
- Extension of our theoretical analysis. The theoretical analysis presented in Chapter 4 is a rather simple approach. The flow inside a hydrocyclone is complex, studying the flow using computational fluid dynamics may bring further understanding of how fibre separation occurs inside a hydrocyclone.
- Further investigating consistency effects on separation. In our work we showed that consistency does not affect length separation. However literature reports that consistency can affect separation by coarseness and fibre wall thickness. Since it is

desirable to fractionate pulp at consistencies of 0.7 – 1.0 %, it is worthwhile to investigate how this can be achieved. Some reports have stated that short fibred pulps can be fractionated at higher consistencies than long fibred pulps, tests to confirm this should be performed.

- In our work on Hydrocyclone C was designed specifically for fibre fractionation. Hydrocyclones A and B are typically used for dirt and contaminant removal. Future experiments should concentrate on those hydrocyclones specifically designed for fractionation purposes.

References

1. **Alho, T.**, "The Fractionation Of Springwood And Summerwood Fibres With Hydrocyclone", (in Finnish), M.Sc. Thesis, Helsinki University of Technology, Laboratory of Pulping Technology, Helsinki, 1966.
2. **Allen, T.A.**, "Particle Size Measurement 3rd Edition", page 341, Chapman Hall, London, 1983.
3. **Bliss, T.L.**, "A Study Of Fibre Fractionation Using Centrifugal Cleaners", M.Sc. Thesis, Department of Paper Science and Engineering, Miami University, Oxford, Ohio, 1983.
4. **Bliss, T.**, "Secondary Fibre Fractionation Using Centrifugal Cleaners", TAPPI Pulping Conference, Proceedings, page 217, 1984.
5. **Bliss, T.**, "Pulp Fractionation Can Benefit Multilayer Paperboard Operations", Pulp & Paper, 61(Feb.), 104, 1987a.
6. **Bliss, T.**, "Models Can Predict Centrifugal Cleaner Fractionation Trends", Pulp & Paper, 61(may), 131, 1987b.
7. **Bliss, T.**, "Centrifugal Cleaning", Chapter XIII in Pulp and Paper Manufacture, Third Edition, Volume 6, Stock Preparation ed. R.W., Hagemayer and D.W. Manson, Joint Textbook Committee of the Paper Industry, 1992.
8. **Bliss, T.**, "Stock Cleaning Technology, A Literature Review", Pira International, Leatherhead, U.K., 1997
9. **Boadway, J.D., Freeman, H.**, "Centrifugal Classifier For Cleaning Pulp And Paper Stocks", Tappi, 39(11), 797, 1956.
10. **Boadway, J.D.**, "Theoretical Considerations Of Vortex Separators", Tappi, 45(4), 265, 1962.
11. **Boadway, J.D.**, "A Centrifugal Fibre Classifier", personal communication, 1994, based on a report written for Consolidated Paper Corporation in 1963.
12. **Boadway, J.D.**, "A Centrifugal Fibre Classifier", personal communication, 1994.
13. **Bradley, D.**, "The Hydrocyclone", Pergamon Press, London 1965.
14. **Branion, R.M.R.**, "Some Factors Affecting The Strength Of Rigid Insulation Boards", Tappi, 46(4), 240, 1963.
15. **Corson, S.R.**, "Size Analysis Of Disc Refined Pulp Fibre Distributions", Svensk Papperstid. 75(8), 277, 1972.
16. **Corson, S.R., Tait, J.D.**, "Prediction Of The Performance Characteristics Of A Centrifugal Cleaner", Tappi, 60(8), 126, 1977.
17. **CPPA Standard Testing Methods**, Technical Section Canadian Pulp and Paper Association, Nov. 1998, Montreal, Quebec.
18. **Dabir, B.**, "Mean Velocity Measurements in a 3"-Hydrocyclone Using Laser Doppler Anemometry", Michigan State University Department of Chemical Engineering, Ph.D. Thesis, 1983.
19. **Demuner, B.J.**, "Opportunities for Market Pulp Differentiation via Fractionation", Paper 4, PIRA, 5th International Paper and Board Industry Conference Scientific and Technical Advances in Refining, Vienna, 1999.
20. **El-Hosseiny, F., Yan, J.F.**, "Analysis Of Canadian Standard Freeness, Part II, Practical Implications", Pulp & Paper Canada, 81(6), T116, 1980.

21. **Ellis, E.R., Jewett, K.B., Smith, K.A., Ceckler, W.H., Thompson, E.V.**, "Water Retention Ratio and its Use to Study the Mechanism of Water Retention in Paper", *Journal of Pulp and Paper Science* 9, TR12, 1983.
22. **Escher Wyss** Erection and Operating Instruction for Laboratory Refiner, Sulzer Escher Wyss, Ravensburg Stock Preparation Dept. 1988
23. **Forgacs, O.L.**, "The Characterization Of Mechanical Pulps" *Pulp & Paper Magazine of Canada*, 64, T89, 1963.
24. **Franko, A.**, "Centricleaning", Chapter XVI in *Pulp and Paper Manufacture*, Third Edition, Volume 2, Mechanical Pulping, ed. R.A Leask, Joint Textbook Committee of the Paper Industry, 1987.
25. **Freeman, H., Skelton, C.H.**, "The Removal Of Dirt From Paper Making Stock", *Pulp & Paper Magazine of Canada*, 38(2), 170, 1937.
26. **Fiber Quality Analyzer**, FQA Operation Manual, Code LDA96, OpTest Equipment Inc., 1996.
27. **Galloway, L.R., Branion, R.M.R.**, "Separation Of Light Weight Particles From Pulp Suspensions With Three Different Commercial Cleaners", preprints 1990 Spring Conference, Technical Section, Canadian Pulp and Paper Association, Jasper, 1990.
28. **Gavelin, G., Backman, J.**, "Fractionation With Hydrocyclones", *Proceedings TAPPI Pulping Conference*, pg. 753, 1991.
29. **Happel, J.**, Brenner, H., "Low Reynolds Number Hydrodynamics", Prentice Hall, Englewood Cliffs, 1965, page 341.
30. **Hill, J., Høglund, H., Johnsson, E.**, "Evaluations Of Screens By Optical Measurements", *Tappi*, 58(10), 120, 1975.
31. **Ho, S-L, Rehmat, T., Branion, R.**, "Fibre Fractionation in Hydrocyclones" paper 3A-3, preprints PACWEST 1999 Conference, Pulp and Paper Technical Association of Canada, Whistler, 1999.
32. **Ho, S-L, Rehmat, T., Branion, R.**, "Fibre Fractionation in Hydrocyclones" 86th Annual Meeting PAPTAC, Montreal, Quebec, 2000 Pages C193-C215.
33. **Ho, S-L., Branion, R.M.R., Rehmat, T.**, "Fibre Fractionation in Hydrocyclones II: A Theory to Explain Fibre Fractionation in Terms of Differences in Fibre Specific Surface and/or Coarseness", to be submitted for publication as a Paprican PGRL Report.
34. **Hoffman, J.D., Welch, L.V.**, "The Escher Wyss Refiner: A Tool for Pulp Evaluation", Canadian Pulp and Paper Association (Pacific Coast Branch), Parksville, B.C. April 1992.
35. **House, K.L.**, "Hydrocyclone Thickening Of Wood Pulp Suspensions", M.Sc. Thesis, Department of Chemical Engineering, University of Washington, Seattle, 1982.
36. **Hoydahl, H.E., Dahlqvist, G.**, "The Dual Demand on Fibres in SC Papers", *Proceedings International Mechanical Pulping Conference*, page 337, 1997.
37. **Jayme, G.** "Properties of Wood Celluloses: II Determination and Significance of Water Retention Value", *Tappi*, 41(11), 180A, 1958.
38. **Jones, E.D., Campbell, R.T., Nelson, G.G.**, "Springwood-Summerwood Separation of Southern Pine Pulp to Improve Paper Qualities", *Tappi*, 49(9), 410, 1966.
39. **Kajaani Electronics Ltd.**, Kajaani FS-200 User's Manual, December 1989.

40. **Karlsson, H., Fransson, P., Mohlin, U.**, "STFI FiberMaster", SPCI Conference on New Available Technologies, The World Pulp and Paper Week, Stockholm, Sweden, Proceedings pages 367-374, June 1999.
41. **Karnis, A.**, "Refining Of Mechanical Pulp Rejects", *Paperi ja Puu*, 64(4), 257, 1982.
42. **Karnis, A.**, "Pulp Fractionation by Fibre Characteristics", *Paperi ja Puu*, 79(7), 480, 1997.
43. **Kelsall, D.F., McAdam, J.C.H.**, "Design And Operating Characteristics Of A Hydraulic Cyclone Elutriator", *Transactions of the Institution of Chemical Engineers*, 41, 84, 1963.
44. **Kerekes, R.J.**, "Characterization of Pulp Refiners by a C-Factor", *Nordic Pulp & Paper Journal* 5, no. 1, Pages 3-8, 1990.
45. **Kure, K-A, Dahlqvist, G., Ekstrom, J., Helle, T.**, "Hydrocyclone Separation, and Reject Refining, of Thick-Walled Mechanical Pulp Fibres", *Nordic Pulp and Paper Research Journal*, 14(2), 100, 1999.
46. **Li, M., Johnston, R., Xu, L., Filonenko, Y., Parker, I.**, "Characterization of Hydrocyclone- Separated Eucalypt Fibre Fractions", *Journal of Pulp and paper Science*, 25(8), 299, 1999.
47. **Marton, R., Robie, J.D.**, "Characterization Of Mechanical Pulps By A Settling Technique", *Tappi*, 52 (12), 2400, 1969.
48. **McCulloch, C.D.**, "Cleaning Groundwood With Vorjects At Port Alfred", *Pulp & Paper Magazine of Canada*, 60(1), T22, 1959.
49. **Miles, K.B. and Karnis, A.**, "The Response of Mechanical and Chemical Pulps to Refining," *Tappi Journal* 74, no. 1, pages 157-164, 1991.
50. **Mohlin, U-B.**, "Fibre Bonding Ability - A Key Pulp Quality Parameter For Mechanical Pulps To Be Used In Printing Papers", *Proceedings of the International Mechanical Pulping Conference*, pg. 49, Helsinki, 1989.
51. **Mukoyoshi, S., Ohsawa, J.**, "Mechanism Of Vessel Separation With Hydrocyclone I. Vessel Separation with Centri-Cleaner" (in Japanese), *Japan TAPPI*, 40(11), 55, 1986.
52. **Mukoyoshi, S., Ohsawa, J.**, "Mechanism Of Vessel Separation With Hydrocyclone II. Settling Velocity Of Pulp And Model Particles" (in Japanese, translation available), *Japan TAPPI*, 40(12), 71, 1986.
53. **Muvundamina, M., Li, M.**, "Fractionation Of Recycled Pulp Obtained From Mixed Paper", *Tappi* 80(2), 149, 1997.
54. **Noss AB**, "Improved Mechanical Pulp For Wood Containing Printing Paper With Radiclone Fractionation Systems", brochure.
55. **Ohtake, T., Usuda, M., Kadoya, T.**, "A Fundamental Study Of Hydrocyclones Part 1. Flow Pattern In The Hydrocyclone", (in Japanese, translation available) *Japan TAPPI*, 41(2), 60, 1987.
56. **Olgard, G.**, "Fractionation Of Fibre Suspensions By Liquid Column Flow", *Tappi* 53(7), 1240, 1970.
57. **Olson, J.A., Robertson, A.G., Finnigan, T.D., Turner, R.R.H.**, "An Analyzer for Fibre Shape and Length," *Journal of Pulp and Paper Science* 21, no. 11, 1995, J367-373.
58. **Paavilainen, L.**, "The Possibility Of Fractionating Softwood Sulfate Pulp According To Cell Wall Thickness", *Appita*, 45(5), 319, 1992.

59. Personal Communication with Jan Backman, GL&V (Celleco-Hedemora AB)
60. Personal Communication with Karl-Johan Grundström (STFI)
61. **Pesch, A.W.**, US patent 3,083,927, April 16, 1963.
62. **Rehmat, T.**, "Pulp Fractionation In Hydrocyclones", student project report, Department of Chemical Engineering, University of British Columbia, 1991.
63. **Rehmat, T., Branion, R.M.R.**, "Fibre Fractionation in Hydrocyclones", preprints Western Meeting Canadian Pulp and Paper Association, Jasper 1994.
64. **Rehmat, T., Branion, R.M.R.**, "Fibre Fractionation in Hydrocyclones", preprints 81st Annual Meeting Technical Section Canadian Pulp and Paper Association, Montreal 1995.
65. **Rehmat, T., Ho, S-L, Branion, R.M.R.**, "Fibre Fractionation in Hydrocyclones III: Experimental Demonstration of Mechanical Wood Pulp and Synthetic Fibre Fractionation", to be submitted for publication as a Paprican PGRL Report.
66. **Rewatakar, V.B., Masliyah, J.H.**, "Woodpulp Fibre Fractionation", report available from Department of Chemical Engineering University of Alberta, Edmonton Alberta, 1998.
67. **Ricker, N.L., House, K.L.**, "Thickening Of Pulp Suspensions In A Hydrocyclone", AIChE Symposium Series Vol. 80, No.232, page 8, 1984.
68. **Robertson, A.A., Mason, S.G.**, "Specific Surface Of Cellulose Fibres By The Liquid Permeability Method", Pulp & Paper Magazine of Canada, 50(13) 1, 1949.
69. **Sandberg, C., Nilsson, L., Nikko, A.**, "Fibre Fractionation - A Way To Improve Paper Quality", Proceedings, 1997 International Mechanical Pulping Conference, 1997.
70. **SCAN-Test Methods**, Scandinavian Pulp, Paper, and Board Testing Committee, 1998.
71. **Seifert, P., Long, K.J.**, "Fibre Fractionation - Methods And Applications", Tappi, 57(10), 69, 1974.
72. **Seth, R.S. and Chan, B.K.**, Tappi Journal 80(5), page 217, 1997.
73. **Smook, G.A.**, "Handbook of Pulp and Paper Terminology – A Guide to Industrial and Technological Usage", Angus Wilde Publications, 1990 Vancouver, B.C. Canada.
74. **Stephens, J.R., Pearson, A.J.**, "The Cleaning Of Eucalypt Groundwood By The Use Of The 623 Bauer Hydrocyclone", Appita 21(3), 79, 1967.
75. **Svarovsky, L.**, "Hydrocyclones", Technomic Publishing Co., Inc. 1984
76. **TAPPI**, TAPPI Test Methods, TAPPI Press Technology Park Atlanta, GA. Technical Association of the Pulp and Paper Industry, 1998-1999.
77. **Vollmer, H.**, "Fibre Fractionation for Quality Improvement of Multiply paper", Paper 3, PIRA 5th International Paper and Board Industry Conference Scientific and Technical Advances in Refining, Vienna, 1999.
78. **Welch, L.V.S.**, "Low Consistency Refining of Mechanical Pulps", PhD. Thesis, UBC Department of Chemical Engineering, April 1999.
79. **White, F.M.**, "Viscous Fluid Flow, 2nd Edition", McGraw Hill, New York, 1991, page 182.
80. **Wong, T.B.**, "The Hydrodynamics of Individual Fibres", Master of Applied Science Thesis, UBC Department of Mechanical Engineering, Oct. 2000.
81. **Wood, J.R.**, personal discussions, January 1994.

82. **Wood, J.R., Grondin, M., Karnis, A.**, "Characterization Of Mechanical Pulp Fines With A Small Hydrocyclone. Part I: The Principle And Nature Of The Separation", J. Pulp & Paper Science, 17(1), J1, 1991. See also Preprints 76th Annual Meeting, Technical Section, Canadian Pulp & Paper Association, Montreal pg. B137, 1990.
83. **Wood, J.R., Karnis, A.**, "Towards A Lint-Free Newsprint Sheet", Paperi ja Puu 59(10), 660, 1977.
84. **Wood, J.R., Karnis, A.**, "Distribution Of Fibre Specific Surface Of Papermaking Pulps", Pulp & Paper Canada, 80(4), T116, 1979.
85. **Wood, J.R., Karnis, A.**, "Linting Propensity Of Mechanical Pulps", Pulp & Paper Canada, 93(7), T191, 1992.